

**The role of Lysophosphatidic Acid
Acyltransferase beta (LPAAT- β)
inhibitors in Acute Myeloid Leukaemia
Cell Lines**

**A thesis submitted by
Hamed AL-Bakistani
For
The Degree of Doctor of Philosophy**

**University of Cardiff
Haematology Department
Cardiff
September 2005**

UMI Number: U487888

All rights reserved

INFORMATION TO ALL USERS

The quality of this reproduction is dependent upon the quality of the copy submitted.

In the unlikely event that the author did not send a complete manuscript and there are missing pages, these will be noted. Also, if material had to be removed, a note will indicate the deletion.



UMI U487888

Published by ProQuest LLC 2013. Copyright in the Dissertation held by the Author.
Microform Edition © ProQuest LLC.

All rights reserved. This work is protected against
unauthorized copying under Title 17, United States Code.



ProQuest LLC
789 East Eisenhower Parkway
P.O. Box 1346
Ann Arbor, MI 48106-1346

I love to express my warm thanks to the following people who provided me guidance,
support and invaluable help during of this work.

To

Dr. Ken Mills

Haematology Department, School of Medicine, University of Cardiff, who provided
me with excellent supervision, constant advice, encouragement and patience throughout
the research and subsequent completion of this thesis. His efforts and care are highly
appreciated.

Mandy and Val

Haematology Department, School of Medicine, University of Cardiff

For their invaluable kindness and excellent technique advice during this work

Dr. Lynn Bonham

Cell Therapeutic Inc, Seattle, USA.

For her kindness, support, and providing me the Immunohistochemistry data for this
work.

All the Members

Of the Haematology Department, School of Medicine, University of Cardiff.

For their help, kindness and excellent social support.

Abbreviations


Abbreviations

APL	Acute Promyelocytic Leukaemia
AML	Acute Myeloid Leukaemia
As₂O₃	Arsenic Trioxide
ATX	Autotoxin
BSA	Bovine Serum Albumin
CDK	Cyclin-Dependent Kinase
CL	Cardiolipin
CSF	Colony Stimulating Factors
CtBP/BARS	C-terminal-Binding Protein/Brefeldin A-ADP-Ribosylated Substrate
DAG	Diacylglycerol
DAG	Diacylglycerol
DAGK	Diacylglycerol -Kinase
dbEST	database of expressed sequence tags
DNA	Deoxyribose Nucleic Acid
dTTP	DeoxyThymidine TriPhosphate
dUTP	DeoxyUrine TriPhosphate
ECL	Enhanced ChemiLuminescence
EDTA	EthyleneDiamineTetraacetic Acid
EGFR	Epidermal Growth Factor Receptor
ER	Endoplasmic Reticulum
ERK	Extracellular-signal-regulated Mitogen Activated Protein Kinase
FAB	French-American-British
FACsort	Fluorescence activate cell sorter
FCM	Flow Cytometry

Abbreviations

FITC	Fluorescein-isothiocyanate
FSC	Forward scatter
G1	Growth phase 1
G2	Growth phase 2
GDP/GTP	Guanosine Diphosphate/Guanisine Triphosphate
GPCR	G-Protein Coupled Receptor
IL	Interleukin
LPA	Lysophosphatidic Acid
LPA₁ (Edg-2)	LPA1 receptor
LPAAT-α	Lysophosphatidic Acid Acyltransferase alpha
LPAAT-β	Lysophosphatidic Acid Acyltransferase beta
LPP	Lipid Phosphate Phosphatase
LysoPLD	lysophospholipase D
MHC	Major Histocompatibility Complex
mRNA	Messenger Ribose Nuclic Acid
mTOR	Mammalian Target of Rapamycin
NF-κB	Nuclear Factor- κ B
PA	Phospatidic Acid
PBS	Phosphate Buffered Saline
PC	Phosphatidylcholine
PCR	Polymerase Chain Reaction
PE	Phosphatidylethanolamine
PI	Phosphatidylinositol
PI	Propidium Iodide
PI3K	Phosphatidylinositol-3-Kinase

Abbreviations

PKB/Akt	Protein Kinase B
PKC	Proteinase C
PKC	Protein Kinase C
PLC	Phospholipase C
PLD	Phospholipase D
PPARγ	Factor-activated receptor- γ
PS	Phosphatidylserine
R1 	Region 1
R2	Region 2
RARα	Retinoic Acid Receptor alpha
RNA	Ribose Nucleic Aid
S1P	Sphingosine 1 Phosphate
SDS	Sodium dodecyl sulphate
SSC	Side scatter
TBS	Tris Buffered Saline
TBS-T	Tris Buffered Saline-Tween
TNF-α	Tumour Necrosis Factor- α
UV	Ultraviolet
WHO	World Health Organization

Abstract

Lysophosphatidic acid acyltransferase beta (LPAAT- β) is an enzyme that has been of growing interest in tumour research in the last few years. LPAAT- β is differentially expressed in normal cells and is highly expressed in a wide variety of tumour cells. LPAAT converts intracellular lysophosphatidic acid (LPA) to phosphatidic acid (PA). Apart from its counterpart LPA that is known as a stimulator of cell proliferation, migration and survival and whose role in tumorigenesis has been extensively examined, PA has emerged as another phospholipid important in cancer biology because its involvement in activation of a variety of signal transduction pathways.

Therefore, the aims of the present study was to examine inhibition of LPAAT- β in acute myeloid leukaemia cell lines (ATRA sensitive and resistant cell lines NB4, HL60 and NB4:R2 and HL60R respectively) by specific LPAAT- β inhibitors to determine their effect on cell proliferation, gene expression cell cycle progression and apoptosis in-vitro. This was achieved using a wide range of cellular and molecular techniques.

In this study, we found LPAAT- β inhibitor CT-32228, and its analogue PC020702 induced potent cytotoxicity in AML cell lines. Further our data indicates that PC020702 significantly inhibited LPAAT- β enzyme activity after 24 h of incubation, but had little toxicity after 1 hour. When differential gene expression was assessed by oligonucleotide array, gene ontology data indicated significant changes in expression of genes associated with the cell membrane and G-protein coupled receptors (GPCR). PC020702 was also shown to arrest cell cycle progression at G2/M phase and triggered apoptosis in AML cells via caspase-3 and annexin V. We focused on the potential therapeutic applications of inhibiting the production of PA, a lipid cofactor for the activation of raf and thus the Ras/Raf/MAPK pathway, for mTOR (mammalian target of rapamycin), a critical effector molecule downstream in the phosphatidylinositol-3-kinase (PI3K) pathway. Importantly, PC020702 neither inhibited mTOR nor Erk1/2 phosphorylation. However, PC020702 inhibited Akt phosphorylation a molecule which is not known as a target for PA.

The pharmacological action of LPAAT- β inhibitors, oligonucleotide array data and western blot analysis, have demonstrated that inhibition of PC020702 and CT32228 affects AML cell lines, the mechanism via which the inhibitor acts is still unclear. We speculate that the effects are mediated via LPA signal transduction pathways and not PA pathways, since known pathways associated with PA appear to be unperturbed by the presence of the inhibitors. However it is possible the production of PA by the targeted pathway may be compensated via the activity of other lipid associated enzymes (PLD,DAGK). The data presented indicates that inhibition of LPAAT- β activity in AML cells induces apoptosis and cell cycle arrest and is cytotoxic, and therefore may have potential as a therapeutic agent in AML and warrants further investigation. It will be important to overcome technical difficulties associated with availability of sample and determine the activity of this enzyme in clinical AML samples, the mechanism of action and pathways affected by these inhibitors as well as toxicity in normal blood and bone marrow samples.

CHAPTER 1

Introduction	1
1.1 Haematopoiesis	2
1.1.1 Normal Haematopoiesis.....	3
1.1.2 Stem cell and progenitor cells.....	3
1.2 Leukaemia	4
1.2.2 Acute myeloid leukaemia (AML).....	4
1.2.3 Acute promyelocytic leukemia (APL).....	6
1.2.4 Developmental Therapeutics in AML.....	6
1.2.4.1 Arsenic Trioxide (As ₂ O ₃).....	7
1.2.4.2 Cytokine.....	7
1.2.4.3 Cytotoxic drugs.....	8
1.2.4.4 Histone Acetylation.....	8
1.2.4.5 Drug-Induced Apoptosis in AML.....	8
1.3 Lysophosphatidic acid acyltransferase- β (LPAAT-β)	9
1.3.1 LPAAT- β in Phospholipid biosynthesis.....	9
1.3.2 LPAAT- β Molecular biology.....	11
1.3.2.1 Cloning and sequence analysis of human LPAAT cDNA.....	11
1.3.2.2 Conserved motifs in LPAAT sequences.....	11
1.3.2.3 Chromosomal localization of LPAAT- β	12
1.3.2.4 Membrane location of LPAAT.....	13
1.3.3 LPAAT- β and cytokines signalling responses.....	13
1.3.4 Tissue distribution of LPAAT- β	14
1.3.5 LPAAT- β and oncogenic mutation.....	14
1.3.6 LPAAT- β and cell signalling.....	15
1.3.7 LPAAT- β Inhibitors.....	17
1.4 Lysophosphatidic acid (LPA)	19
1.4.1 Introduction.....	19
1.4.2 Biochemistry of LPA.....	19
1.4.3 LPA production and degradation.....	19
1.4.4 LPA in tumorigenesis.....	20
1.4.5 The extracellular role of LPA.....	21
1.4.5.1 LPA receptors.....	21
1.4.5.2 G-protein signalling Pathways.....	21
1.4.6 LPA and Intracellular signalling.....	22
1.5 Aims of the study	24

CHAPTER 2

Material & Methods	26
2.1 Cell Culture and Cell line	27
2.1.1 General rules.....	27
2.1.2 Cell culture conditions.....	27
2.1.3 Long term liquid nitrogen storage of cell lines.....	27
2.1.4 Thawing of the cells.....	27
2.1.5 Cell line.....	28
2.1.6 Trypan blue exclusion cell counting.....	28

2.1.7 LPAAT-β inhibitors storage and preparation.....	29
2.1.8 Cell harvest and storage.....	29
2.2. LPAAT-β Assay.....	30
2.2.1 General rules for handling ¹⁴ C radioactive material.....	30
2.2.2 Principle.....	30
2.2.3 Data analysis.....	30
2.2.4 LPAAT-β Assay.....	30
2.3 Flow cytometry.....	33
2.3.1 Introduction.....	33
2.3.2 Apoptosis by Flow Cytometry.....	34
2.3.2.1 Annexin V Assay (Principle).....	34
2.3.2.2 Annexin V-FITC Staining Protocol.....	34
2.3.2.3 Experiment design and Flow cytometry analysis.....	35
2.3.3 Cell cycle analysis by Flow Cytometry.....	36
2.3.3.1 Propidium iodide Assay (Principle).....	36
2.3.3.2 Propidium iodide procedure.....	36
2.3.3.3 Data analysis and gating strategy.....	36
2.4 RNA analysis techniques.....	38
2.4.1 Introduction to RNA.....	38
2.4.2 RNA isolation.....	38
2.4.3 Methods.....	38
2.4.3.1 Rneasy Kit (Qiagen).....	38
2.4.3.2 RNA integrity and quantitation.....	39
2.5 Oligonucleotide Microarrays.....	40
2.5.1 The Principle.....	40
2.5.2 Methods.....	40
2.5.2.1 RNA isolation.....	41
2.5.2.2 First strand synthesis.....	41
2.5.2.3 Second strand synthesis.....	42
2.5.2.4 Cleanup of double stranded cDNA.....	42
2.5.2.5 In vitro transcription (IVT) cRNA synthesis.....	43
2.5.2.6 IVT cRNA cleanup.....	43
2.5.2.7 cRNA fragmentation.....	44
2.6 Real-Time PCR.....	45
2.6.1 The Principle.....	45
2.6.2 Methods.....	45
2.6.2.1 First strand synthesis.....	45
2.6.2.2 Primers designing.....	46
2.6.2.3 Optimising PCR reaction.....	46
2.6.2.4 DNA extraction and standard preparation.....	47
2.6.2.5 MgCl ₂ optimisation.....	47
2.6.2.6 Light Cycler PCR optimisation.....	48
2.7 Northern Blot.....	49
2.7.1 Principle.....	49
2.7.2 Methods.....	49
2.7.2.1 Electrophoresis.....	49

2.7.2.2 Blotting.....	49
2.7.2.3 Hybridisation.....	50
2.7.2.4 Post-Hybridisation.....	50
2.7.2.5 Striping the membrane.....	51
2.8 Western Blotting.....	52
2.8.1. Protein extraction and quantitation.....	52
2.8.2 Sodium Dodecyle Sulphate-Polyacrylamide Gel Electrophoresis (SDS-PAGE).....	52
2.8.3 Electro blotting.....	53
2.8.4 Blocking the membrane and antibody probing.....	53
2.8.5 Membrane stripping and re-probing.....	54
CHAPTER 3	55
Effect of LPAAT-β Inhibitors on AML LPAATβ Enzyme Activity and cell Proliferation.....	55
3.1 Introduction.....	56
3.2 Material and Methods.....	58
3.2.1 Cell lines and treatment.....	58
3.3. In cell LPAAT-β enzyme Assay.....	59
3.3.1 The effect of PC020702 inhibitor on LPAAT- β enzyme activity in AML cells.....	59
3.3.1.1 The effect of PC020702 inhibitor on LPAAT- β enzyme activity in NB4 cells.....	63
3.3.1.2 The effect of PC020702 inhibitor on LPAAT- β enzyme activity in NB4:R2.....	65
3.3.1.3 The effect of PC020702 inhibitor on LPAAT- β enzyme activity in NB4, NB4:R2, HL60 and HL60-R cells.....	67
3.4 AML cell proliferation and viability.....	71
3.4.1 The effect of LPAAT inhibitors (CT32228 and PC020702) on AML cell lines Proliferation.....	71
3.4.1.1 The effect of PC020702 on NB4 and NB4:R2 proliferation.....	72
3.4.1.2 The effect of PC020702 on HL60 and HL60-R proliferation.....	73
3.4.1.3 The effect of CT32228 on NB4 and NB4:R2 cell proliferation.....	74
3.4.1.4 The effect of CT32228 on HL60 and HL60-R proliferation.....	75
3.4.2 The effect of LPAAT inhibitors (CT32228 and PC020702) on AML cell lines viability.....	76
3.4.2.1 The effect of LPAAT- β inhibitor PC020702 on NB4 and NB4:R2 Viability.....	76
3.4.2.2 The effect of LPAAT- β inhibitor PC020702 on HL60 and HL60-R Viability.....	77
3.4.2.3 The effect of LPAAT- β inhibitor CT32228 on NB4 and NB4:R2 Viability.....	78
3.4.2.4 The effect of LPAAT- β inhibitor CT32228 on HL60 and HL60-R Viability.....	79
3.4.3 The effect of LPAAT inhibitors (CT32212 and PC020701) on AML cell lines proliferation and viability.....	80
3.5 Discussion.....	86
CHAPTER 4	88
Identification of molecular targets after LPAAT-β inhibitors induction in Acute Myeloid Leukaemia cell lines using oligonucleotide arrays and validation of selected genes using Real-Time PCR and Northern Blotting.....	88
4.1 Introduction.....	89
4.2 Material and Methods.....	91

4.2.1 Cell lines and treatment.....	91
4.2.2 Oligonucleotide Array Expression Analysis.....	91
4.2.3 Target Verification by RT-PCR Analysis.....	92
4.2.4 Real-time PCR	92
4.2.5 Northern Blotting.....	93
4.3 Oligonucleotide array.....	94
4.3.1 Image Analysis.....	95
4.3.2 Normalization.....	95
4.3.3 Filtering.....	96
4.3.4 Fold change and tree view.....	97
4.3.5 Venn Diagrams.....	99
4.3.6 Differentially expressed genes list.....	102
4.3.7 Data interpretation using Gene Ontology (GO).....	107
4.4 Validation of expression of selected genes.....	111
4.4.1 Real-time PCR.....	111
4.4.2 RT-PCR experimental preparation.....	112
4.4.3 Melting curves analysis (Tm).....	113
4.4.4 Real-time quantitative PCR.....	115
4.4.5 Verification of Caspase-5 expression.....	117
4.4.6 Verification of Cdc2.....	120
4.4.7 Caspase-5 verification by Northern blot.....	123
4.4.8 Cdc2 verification by Northern blot.....	126
4.5 Discussion.....	128
CHAPTER 5	132
The effect of LPAAT-β inhibitors on Apoptosis and Cell cycle.....	132
5.1 Introduction.....	133
5.2. Material and Methods.....	135
5.2.1 Cell lines and treatment.....	135
5.2.2 Annexin V-FITC.....	135
5.2.3 Propidium Iodide procedure.....	135
5.2.4 Immunoblotting.....	136
5.3 LPAAT-β inhibitors on programmed cell death activation.....	137
5.3.1 Cells culture and treatment.....	137
5.3.2 The effect of LPAAT- β inhibitors on NB4 and NB4:R2 apoptosis.....	138
5.3.3 The effect of LPAAT- β inhibitors on HL60 and HL60-R apoptosis.....	142
5.3.4 Apoptosis Triggered by PC020702 Is Mediated via Caspase-3.....	144
5.4 LPAAT-β inhibitors on cell cycle progression.....	148
5.4.1 Cell culture and treatment.....	148
5.4.2 Cell cycle progression on NB4 and NB4:R2 with LPAAT- β inhibitors.....	148
5.4.3 Cell cycle progression on HL60 and HL60-R with LPAAT- β inhibitors.....	152
5.5 Discussion.....	156

CHAPTER 6	159
The effect of LPAAT-β inhibitors on AML cell signalling.....	159
6.1 Introduction.....	160
6.2 Material and Methods.....	162
6.2.1 Cell lines and treatment.....	162
6.2.2 Immunoblotting.....	162
6.3 Effect of PC020702 on Akt/mTOR Activation.....	163
6.3.1 The effect of LPAAT- β inhibitors on Akt/mTOR pathways.....	163
6.3.1.1 LPAAT- β inhibitors overexpressed mTOR in NB4 and NB4:R2.....	163
6.3.2 LPAAT- β inhibitors downregulated Akt in NB4 & NB4:R2.....	167
6.4 Effect of PC020702 on raf/ERk Activation.....	173
6.4.1 LPAAT- β inhibitors on MAP kinase in NB4 and NB4:R2.....	173
6.5 Discussion.....	176
CHAPTER 7	179
Discussion, Main Findings and future work.....	179
7.1. Discussion.....	180
7.2. Main Findings.....	184
7.3 Future Works.....	189
References.....	191

CHAPTER 1

Introduction

1.1 Haematopoiesis

1.1.1 Normal Haematopoiesis

Haematopoiesis is a very sophisticated process involving many factors, including hormones, hormone receptors, signal transducers, transcription factors and cell cycle regulators. These factors are finely tuned by endogenous and exogenous signals during haematopoietic development. The haematopoietic system continuously maintains a cell population through a complex network of tissues, organs, stem cells, and controlling factors. This network is responsible for the maturation and division of undifferentiated cells into the operational cell lineages that perform immune function, transport oxygen and carbon dioxide, and maintain haemostasis, for example all cells derive from a pool of multipotential self renewing haemopoietic stem cells found in the bone marrow. Under the influence of factors such as colony stimulating factors (CSF) and interleukins (ILs), stem cells divide and differentiate to form the mature cellular elements of the blood. The haematopoietic system consists of the bone marrow, liver, spleen, lymph nodes, and thymus. All these tissues and organs are involved in the production, maturation, and destruction of blood cells. The entire process of haematopoiesis involves an intricate structure of tissues, organs, cellular elements, and factors which result in the maintenance and function of blood cells (Orkin 1995) (Figure 1.1).

1.1.2 Stem cell and progenitor cells:

A common primitive stem cell in the marrow has the capacity to self replicate and differentiates to increasingly specialized progenitor cells which, after many cell divisions within the marrow, form mature cells (red cells, granulocytes, monocytes, platelets and lymphocytes) of the peripheral blood.

An early lineage division is between progenitors for lymphoid and myeloid cells. The earliest recognizable granulocyte or monocyte precursor is a myeloblast.

Stem and progenitor cells cannot be recognized morphologically; they resemble lymphocytes. Progenitor cells can be detected by special *in vitro* assays in which they form colonies (e.g. colony forming units for granulocytes and monocytes, CFU-GM, or for red cells, burst forming units-erythroid, BFU-E and CFU-E). Stem and progenitor cells also

circulate in peripheral blood. The stromal cells of the marrow (fibroblast, endothelial cells, macrophages, fat cells) have adhesion molecules which react with corresponding ligands on the stem cells and maintain their viability (Howard & Hamilton 2002; Mehta & Hoffbrand 2000).

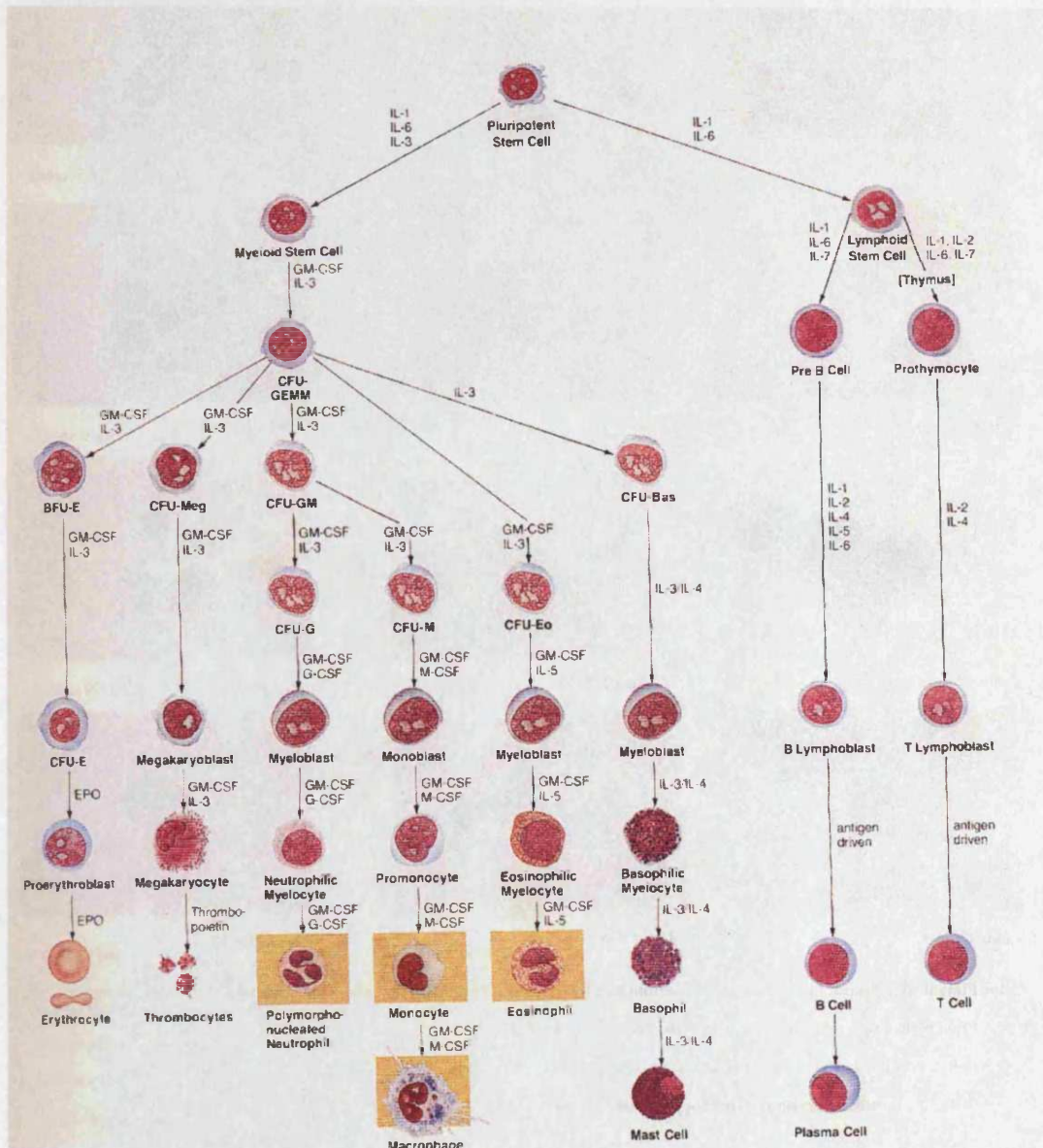


Figure 1.1. Regulation of haematopoiesis by colony stimulating factors (CSFs) and Interleukins. (Reprinted with permission from Essential Haematology book) (Hoffbrand, et al. 2001).

1. 2 Leukaemia

1.2.1 Leukaemia:

Leukaemia is a malignant disease of haematopoietic tissue, characterized by replacement of normal bone marrow elements with abnormal (neoplastic) blood cells. These leukaemic cells are frequently (but not always) present in the peripheral blood and commonly invade reticuloendothelial tissue including the spleen, liver, and lymph nodes. They may also invade other tissues, infiltrating any organ of the body. If left untreated, leukaemia eventually causes death. The ability of a cell to proliferate is related to its ability to differentiate, as each phenotype is determined by activation of separate programmers of gene expression. Disruption of the normal balance between proliferative and differentiative genetic programme is a characteristic of leukaemia and other neoplasia. In leukaemia, many of the features of normal haematopoiesis are retained. The disease can begin as a transformation of early haematopoietic progenitor stem cells to yield malignant populations which are clonal in each affected individual. A leukaemic stem cell gives rise to a single abnormal clone that eventually dominates the blood forming tissue. Some cells following normal patterns of maturation can usually be found in association with the acute myeloid leukaemia clones, but the dominant and defining feature is the presence of blast cells (McCulloch 1993).

1.2.2 Acute myeloid leukaemia (AML):

AML arises out of the malignant transformation of a myeloid precursor cell. Usually this occurs at a very early stage of myeloid development, although acute promyelocytic leukaemia (APL), a subtype of AML, involves proliferation of a more mature cell. AML is rare in childhood and the incidence increases with age. Cases may occur *de novo* or secondary to well-defined predisposing factors such as chemotherapy or a myelodysplastic syndrome- such cases are referred to as secondary AML.

The classification of AML is based upon the appearance of the leukaemic cells in a bone marrow aspirate. The French-American-British (FAB) group had described eight different variants of AML (Table 1.1). An experienced haematologist can often identify the subtype on microscopy, but certain types (e.g. AML M0) routinely require other test to establish a firm diagnosis (cytochemical, immunological, and cytogenetic criteria). In 2001 the World

Health organization (WHO) classification for tumours of haematopoietic and lymphoid tissues was proposed. In an attempt to define biologic homogenous entities that have clinical relevance, morphologic, immunophenotypic, genetic, and clinical features were incorporated into the classification of AML. The WHO classification of AML encompasses 4 major categories: (1) AML with recurring genetic abnormalities, (2) AML with multilineage dysplasia, (3) AML, therapy related, and (4) AML not otherwise categorized (Harris et al. 1999).

Type	Characteristics
M0	Undifferentiated, myeloid immunophenotype
M1	Little differentiation, >90% blast
M2	Myeloblastic with differentiation, 30-90% blasts
M3	Promyelocytic: intensely granular, variant form is microgranular.
M4	Myelomonocytic: both monocytic and myeloid differentiation.
M5a	Monocytic with differentiation
M5b	Monocytic, without differentiation
M6	Erythroleukaemia: dysplastic erythroblasts with multinucleation, cytoplasmic budding, vacuolation, and megaloblastoid changes.
M7	Megakaryoblastic: wide range of morphology, cytoplasmic projections sometimes present; electron microscopy or immunocytochemical stains necessary for diagnosis.

Table 1.1. FAB classification of Acute Myeloblastic Leukaemia (Hoffbrand, et al. 2001).

1.2.3 Acute promyelocytic leukaemia (APL)

Acute promyelocytic leukemia (APL) is always associated with chromosomal translocations involving the retinoic acid receptor alpha (RAR α) locus on chromosome 17 and one of five different partner genes. Each of these is associated with APL characterized by a block in differentiation at the promyelocyte stage of hematopoietic development. The most extensively studied, and the most common fusion gene in APL, is PML-RAR α associated with t(15;17). PML-RAR α is a dominant negative form of RAR that inhibits rather than stimulates expression of retinoic acid target genes due to recruitment of the co-repressor complex. Expression of PML-RAR α is associated with inhibition of differentiation and increased cell self-renewal. All-trans-retinoic acid (ATRA), a ligand for RAR α , is effective therapy for APL, especially when given in combination with conventional induction chemotherapy. The efficacy of ATRA in treatment of APL is related to the ability of ATRA to bind to the fusion protein, with resultant dissociation of the co-repressor complexes, engagement of co-activation complexes by the chimerical receptor and subsequent degradation of the fusion protein (Tallman et al. 2002). Promyelocytes are then able to undergo a normal hematopoietic differentiation program that ultimately results in apoptotic cell death. The ability of ATRA to reverse transcriptional repression by PML-RAR α by release of co-repressors suggested that inhibitors of histone deacetylase, a key component of the co-repressor complexes, might have therapeutic efficacy not only in APL but in other leukemias characterized by aberrant recruitment of the nuclear co-repressor complex, such as RUNX1-ETO and CBF β -MYH11 (Pandolfi 2001).

1.2.4 Developmental Therapeutics in AML

The development of resistance, as well as the presence of de novo resistant subtype of APL and AML, has forced the need to develop alternative mean of therapy for this leukaemia. The redundancy and complexity of the biological mechanisms of retinoic acid resistance made most approaches to overcome this resistance solely by ATRA unsuccessful. Therefore, the use of more than one therapeutic agent may be more effective for the treatment of patients with retinoic acid resistant APL and other AML.

1.2.4.1 Arsenic Trioxide (As₂O₃)

Arsenic has also been proven effective in the treatment of APL, probably through a mechanism separate from that of RA. A majority of patients with relapsed ATRA-resistant and chemotherapy-resistant APL had complete remission following arsenic treatment (Shen et al. 1997; Soignet et al. 1998). This response was associated with apoptosis rather than differentiation of leukaemic cells. In vitro, PML-RAR α relocalizes PML from nuclear bodies (NBs) into microspeckles, an effect which is reversed by arsenic. Arsenic treatment of cells in culture results in enhanced conjugation of PML to SUMO1 and PML and PML-RAR α recruitment to nuclear bodies, which is followed by degradation of both of these proteins (Zhu et al. 1997). Thus, arsenic seems to specifically target the PML portion of the fusion protein, whereas RA results in differentiation of APL cells, degradation of PML-RAR α by arsenic causes apoptosis (Shao et al. 1998). These differences may be the result of transcriptional activation by RA, in contrast to the effect of arsenic on NB proteins. However, research with PML null cells does not support the conclusion that arsenic solely targets PML and PML-RAR α for its effects. As₂O₃ and an organic arsenical also suppress growth in PML null cells and APL cells which no longer express PML-RAR α (Wang et al. 1998). Thus, the effects of arsenic on APL cells may be mediated by multiple pathways. Warrell et al. report clinical remission of APL following addition of the histone deacetylase inhibitor sodium phenylbutyrate to the ATRA treatment regimen in a single patient with ATRA-resistant APL, suggesting that inhibition of histone deacetylases may restore sensitivity to ATRA (Warrell, et al. 1998).

1.2.4.2 Cytokine

The effects of various cytokines on AML cell proliferation and viability have been extensively studied. Relatively few studies have examined effects of single cytokines, cytokine combinations, or cytokines plus vitamin-D₃ on differentiation of native AML blasts. AML blasts can be induced to differentiate in several myeloid directions, and the same differentiation response can often be induced by different cytokines. A certain cytokine or cytokine combination usually induces differentiation only for a subset of patients, and the direction of differentiation often varies between patients (Buhning et al. 1993; Gore et al. 1995; Howell et al. 1990).

1.2.4.3 Cytotoxic drugs

Anticancer agents (e.g., cytarabine, daunorubicin, 6-thioguanine) can induce differentiation in AML cell lines and in native AML blasts, and combinations of cytosine arabinoside or 6-thioguanine plus retinoic acid plus either hexamethylene or dimethylformamide seem to induce AML blast differentiation even for a majority of patients. This effect is observed at lower concentrations than are required for drug-mediated killing, and it probably involves drug-induced alterations in the cytokine responsiveness of AML cells (Bloch 1993; Hassan & Rees 1989; Tawhid & Rees 1990).

1.2.4.4 Histone Acetylation

Acetylation and deacetylation of histones are regarded as important for transcription activation and repression, respectively. Histone deacetylase inhibitors can induce differentiation in native AML blasts for a subset of patients, and they also cause a synergistic enhancement of ATRA-induced differentiation (Kosugi et al. 1999). These effects show no correlation with previous signs of differentiation (i.e., FAB classification). Butyrates are another group of drugs that seem to induce gene expression via histone hyperacetylation, and monosaccharide butyrate derivatives can also induce differentiation in native AML blasts for a subset of patients (Santini et al. 1998).

1.2.4.5 Drug-Induced Apoptosis in AML

In vitro studies have demonstrated that apoptosis can be induced in AML blasts by several cytotoxic drugs, including cytarabine (Balkham et al. 1999; Ibrado et al. 1996; Zhu et al. 1995), daunorubicin (Hu, et al. 1996), etoposide (Droin et al. 1998), and idarubicin (Ketley et al. 1997). Furthermore, clinical studies indicate that the expression of apoptosis-regulating molecules (bcl-2, Mcl-1, caspases) is important for the risk of relapse after chemotherapy (Estrov et al. 1998; Kaufmann et al. 1998). Taken together these data suggest that the susceptibility of AML blasts to drug-induced apoptosis is important for the outcome after intensive chemotherapy in AML.

1.3 Lysophosphatidic acid acyltransferase- β (LPAAT- β)

1.3.1 LPAAT- β in Phospholipid biosynthesis

Lysophosphatidic acid acyltransferase (LPAAT), also known as 1-acyl-sn-glycerol-3-phosphate acyltransferase, is the enzyme that converts lysophosphatidic acid (LPA) into phosphatidic acid (PA) in lipid metabolism. LPAAT activity was first described in the early 1960s, but the biochemical properties were not well defined due to the inability to solubilise and purify the enzymes (Kanfer & Kennedy 1963). Recent cloning of the different LPAAT isoforms has allowed for the expression of these enzymes in insect SF9 cells, with activities 250 times above background levels (West et al. 1997). Although solubilization and purification of active enzyme have not been possible, SF9 membrane preparations have allowed each isoform to be studied separately without interference from other acyltransferase activities.

In the endoplasmic reticulum (ER) membrane, LPA is formed from glycerol 3-phosphate through the action of glycerol-3-phosphate acyltransferase. LPA is then further acylated in the ER by LPAAT to yield PA, the precursor of all glycerolipids. The newly synthesized PA is a precursor for biosynthesis of major constituents of biological membranes that include Phosphatidylcholine (PC), Phosphatidylethanolamine (PE), and Phosphatidylserine (PS) through Diacylglycerol (DAG) as an intermediate, or for synthesis of anionic phospholipids including Phosphatidylinositol (PI) and cardiolipin (CL) through CDP-DAG as intermediate. Smaller quantities of PA can also be generated from PC by the action of PLD (Phospholipase D) and diacylglycerol (DAG) from DAG-kinase (DAGK) (Dowhan 1997).

PA has been shown recently to have targets implicated in neoplastic transformation and growth factor signal transduction pathways. These targets include phospholipase C γ , Ras-Gap, Raf-1 and a protein tyrosine phosphatase (Figure 1.2).

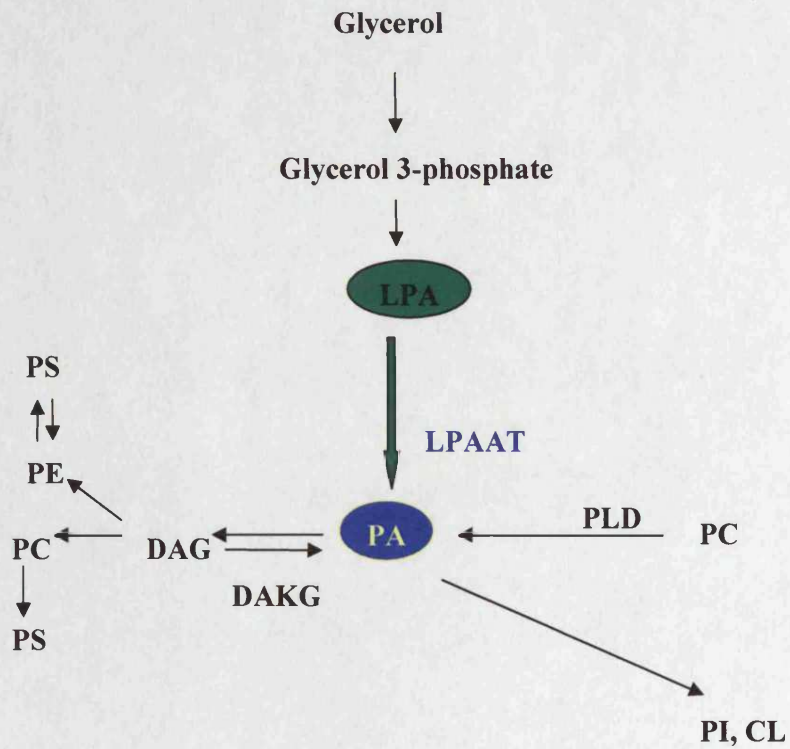


Figure 1.2. Phospholipid biosynthesis pathways. Lysophosphatidic acid (LPA) is acylated in the endoplasmic reticulum by LPAAT to yield phosphatidic acid (PA) (large green arrow), PA is also produced by other two enzymes such as phospholipase D (PLD) and diacylglycerol kinase (DAGK). Abbreviation: Phosphatidylcholine (PC), Phosphatidylethanolamine (PE), Phosphatidylserine (PS), Diacylglycerol (DAG) Phosphatidylinositol (PI), cardiolipin (CL)

1.3.2 LPAAT- β Molecular biology

1.3.2.1 Cloning and sequence analysis of human LPAAT cDNA

Human cDNAs coding for LPAAT were identified from GenBank database of expressed sequence tags (dbEST) based on the sequence homology (Altschul et al. 1997), with yeast (Nagiec et al. 1993) or certain plant (Knutzon et al. 1995) LPAAT protein sequences. Sequence comparison of these cDNA clone suggests the presence of at least two types of potential human LPAAT isoforms, designated here as LPAAT- α and LPAAT- β . The full length cDNAs for LPAAT- α and LPAAT- β encode a 283 and 278 amino acid polypeptide, respectively (West, et al. 1997). Other human proteins that are homologous to LPAAT have recently been designated as LPAAT- γ , - δ , and - ϵ . Two cytosolic protein, endophilin I (Schmid et al. 2003) and CtBP/BARS (Barr & Shorter 2000) (C-terminal-binding Protein/brefeldin A-ADP-ribosylated substrate) involved in, respectively synaptic and golgi membrane vesicle formation have also been found to have LPAAT activity. These two proteins do not have any primary sequence homology with LPAAT- α and LPAAT- β . LPAAT- α and LPAAT- β are probably responsible for the bulk of LPAAT activity in most cells, as the catalytic activity of LPAAT- γ , - δ , - ϵ , endophilin and BARS are relatively low, suggesting that these proteins may use other substrates yet to be identified (Barr & Shorter 2000; Leung 2001).

1.3.2.2 Conserved motifs in LPAAT sequences

Sequence alignment of the human LPAAT- α and LPAAT- β coding sequences with LPAAT coding sequences from other species shows that the regions around the amino acid sequences asparagine-histidine-serine-aspartic acid (Asn-His-Gln-Ser-X-X-Asp) and proline-glutamic acid-glycine-threonine-arginine (Pro-Glu-Gly-Thr-Arg) corresponding to amino acid 97-103 and 171-175 of LPAAT- β are the most conserved among all LPAAT species. These two short stretches of amino acid may represent a consensus sequence important for catalytic activity (Heath & Rock 1998; Lewin, et al. 1999). The residues in Pro-Glu-Gly-Thr-Arg may be partly involved in binding the substrate LPA (Lewin, et al. 1999).

1.3.2.3 Chromosomal localization of LPAAT- β

The location of the human LPAAT- β gene was mapped to band 9q34.3 near the q terminus of chromosome 9 (Eberhardt, et al. 1997), where as the human LPAAT- α gene was mapped to the chromosome band 6p21.3, at site of the human major histocompatibility complex (Aguado & Campbell 1998). A comparison of the sequences of LPAAT- α and LPAAT- β at exon/intron boundaries showed them to have similar coding exon sizes and hence similar genomic organization. Besides LPAAT- α and LPAAT- β , the chromosomal band 6p21.3 (MHC class III region) and 9q34 contain other gene family members that are present in both areas such as NOTCH-4, PBX-2, and TN-X in 6p21.3 and NOTCH-1, PBX-3, and TN-C in 9q34 suggesting these two regions may have arisen due to duplication of a primary common sequence (Aguado & Campbell 1998). The major biochemical and genetic properties of human LPAAT- α and LPAAT- β summarized in table 1.2. (Table 1.2).

	LPAAT- α	LPAAT- β
Chromosomal location	6p21.3	9q34.3
Tissue distribution	Uniformly expressed in all tissues	Differentially expressed in selective tissue
Tumour vs. matched normal tissues	Evenly expressed in both tissues	Overexpressed in selective tumour tissues
Protein type	Integral membrane protein	
Membrane topology	Catalytic domains on the cytoplasmic side of endoplasmic reticulum	
Molecular weight	31.7 kDa	30.9 kDa
Isoelectric point	9.66	8.80
Acyl donor	Acyl CoA	Acyl CoA
Acyl acceptor	1-acyl or 1-alkyl sn-glycerol-3-phosphate	
Size of mRNA	2.3 kb	1.7 kb

Table 1.2 The biochemical and genetic properties of human LPAAT- α and LPAAT- β

1.3.2.4 Membrane location of LPAAT

The proteins encoded by LPAAT- α and LPAAT- β have similar hydrophobicity profile. Four transmembrane stretches are predicted based on sequence comparison using the dense alignment surface method, suggesting that human LPAATs are integral membrane proteins. LPAAT- α fusion protein containing a short epitope-tagged at a carboxyl-terminus has been expressed in CHO cells (Aguado & Campbell 1998; Cserzo et al. 1997). Immunohistochemical analysis of the permeabilised cells expressing an epitope-tagged LPAAT- α showed LPAAT was expressed predominantly in the endoplasmic reticulum (ER). This model is consistent with the finding that the synthesis of glycerolipid intermediates occurs on the cytoplasmic side of the ER (Ballas & Bell 1980; Ballas & Bell 1981). LPAAT- α although its activity has been observed in mitochondria (Chakraborty et al. 1999). The tissue distribution and differential levels of expression of LPAAT- β compared to LPAAT- α suggest that LPAAT- β may play specialized roles distinct from LPAAT- α .

1.3.3 LPAAT- β and cytokines signalling responses

As a key enzyme involved in the second step of glycerophospholipid biosynthesis (Coleman 1992), LPAAT activity in cells can lead to the generation of PA. PA has been implicated in cytokine induced inflammatory responses and the modulation of numerous protein kinase involved in signal transduction (English, et al. 1996; Ghosh et al. 1996; Ghosh & Bell 1997; Honda et al. 1999). LPAAT- α and LPAAT- β overexpression in number of cytokine responsive cell lines, has led to increased synthesis of interleukin-6 (IL-6) and tumour necrosis factor- α (TNF- α) upon stimulation for 16 hours with IL-1 β . However, there is little effect on the basal level of cytokine release in these cell lines, suggesting that overexpression of LPAAT amplifies the cytokine signalling response but not steady state basal signals.

In addition Northern analysis of TNF and IL-6 mRNA levels was performed in ECV304 (bladder carcinoma) cells transfected with either LPAAT expression vectors or control vector at various times after IL-1 β stimulation. As compared to vector control cells, which show some induction of both TNF and IL-6 mRNA after IL-1 β stimulation, cells transfected with LPAAT- α expression vector showed an additional 8 to 12 fold increase in TNF mRNA level and a 4 to 6 fold increase in IL-6 mRNA level within the first few hours

after IL-1 β induction, with little variation in the mRNA level of a housekeeping gene (West, et al. 1997).

1.3.4 Tissue distribution of LPAAT- β

An association of LPAAT- β function with a disease phenotype was first identified by northern blot analysis of its expression pattern in mRNA from human tissues. This analysis showed an increase in expression of the LPAAT- β isoform in tumours of the uterus, fallopian tube and ovary compared to normal adjacent tissue, whilst the expression of the LPAAT- α isoform of this gene showed no significant differences in expression level (Leung 2001).

Immunostaining was carried out on number of multiple samples of 30 different types of normal human tissues and 13 tumour types by an LPAAT- β -specific monoclonal antibody raised to an epitope expressed by LPAAT- β but not LPAAT- α (Hsu, et al. 1981). This analysis showed a limited and select expression of LPAAT- β in normal tissues, which suggests a regulated and tissue-specific (as opposed to housekeeping) function. Expression in normal tissues was primarily limited to tissues responsive to estrogens (uterine glands, ovarian follicles, breast glands), endothelial and inflammatory cells. In contrast, LPAAT- β was expressed at very high levels in a significant proportion of epithelial tumours of the lung, colon, brain, cervix, mammary, ovary and prostate compared to normal tissues section of the same type (Bonham et al. 2003).

1.3.5 LPAAT- β and oncogenic mutation

A previous study indicates increased activity of LPAAT- β is associated with ras transformation, a report has examined endogenous activity of LPAAT- β in a genetically-defined immortalized rodent cell line. A Rat-1 fibroblast model of homologous recombination was used, which includes three related populations: an untransformed line, a clone containing a single copy of a Ha-ras oncogene that shows some evidence of low level transformation, and clone overexpressing that gene that is fully transformed and tumorigenic in nude mice (Finney & Bishop 1993). They also found that LPAAT level were 2-fold higher in the fully transformed cells and 1.2-fold higher in the partially transformed clone compared to the normal Rat-1, suggesting an association of increasing LPAAT levels with a continuum of transformation (Bonham, et al. 2003).

1.3.6 LPAAT- β and cell signalling

PA is implicated in numerous signal transduction pathways, including raf translocation (Ghosh, et al. 1996;Rizzo et al. 2000), epidermal growth factor receptor (EGFR) internalization (Shen, et al. 2001), mTOR activation (Fang et al. 2001), vesicle formation (Jones, et al. 1999), regulation of the non-receptor tyrosine kinase fibroblast growth receptor (FGR) (Sergeant et al. 2001), and association of PKC with membrane (Pawelczyk & Matecki 1999). PA may affect constituents of various signalling pathways through interaction with specific proteins or by locally altering the physical properties of membrane bilayers in a more generalized manner.

A previous study examined whether LPAAT- β activity could provide PA for one of these documented functions relevant to cell signalling, overexpression LPAAT- β , - α and inactive LPAAT- β mutant were tested for enhancement of ras and raf-mediated ras/raf/Erk pathway activation in frog oocyte germinal vessel breakdown. LPAAT- β , but not LPAAT- α or the R-175 inactive LPAAT- β mutant, accelerated germinal vessel breakdown when co-injected into frog oocytes with activated ras or raf. The data suggested that expression of LPAAT- β can cooperate with and enhance the signalling activity of mutant ras or raf (Bonham, et al. 2003). A further study used RNAi technology (Elbashir et al. 2001) to knockdown LPAAT- β expression with LPAAT- β -specific siRNA duplex in prostate cancer cells. The knockdown of LPAAT- β inhibits Erk phosphorylation and proliferation, suggesting that LPAAT- β played a role in the ras/raf/Erk pathway (Bonham, et al. 2003). The proposed role of LPAAT- β and PA in cell signalling is illustrated in figure 1.3 (**Figure 1.3**).

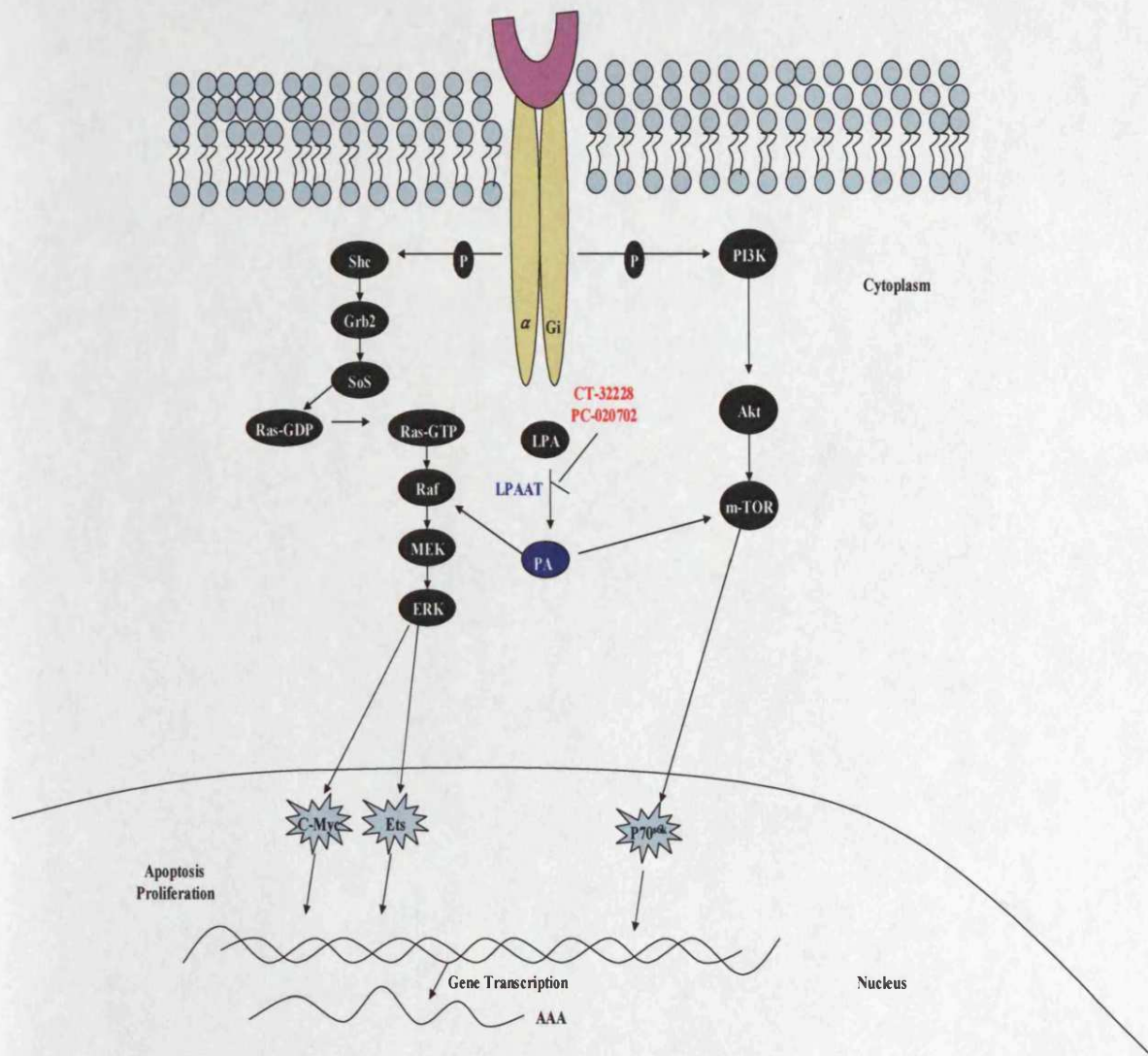


Figure 1.3. The proposed role of LPAAT-β in cell signalling.

The step involves the acylation of LPA at the sn-2 position of LPAAT to form PA. Besides being the precursor molecule for all glycerophospholipid biosynthesis, PA has also been identified as a phospholipids signalling molecule. The inhibition of overexpressed LPAAT-β enzyme activity will lead to down regulation of PA and subsequently down regulation of conjugate molecules. These molecules, including raf and mTOR and thus ras/raf/ERK and Akt/mTOR pathways respectively that have been the target of other drugs in development.

1.3.7 LPAAT- β Inhibitors

Understanding the role that LPAAT may play in functions critical to tumour cell growth and survival, a group of compounds that inhibit this enzyme has been developed. Cell Therapeutic Inc (CTI), screened of a diverse library of small molecules for their ability to inhibit LPAAT- β in cell-free, high-throughput assay led to the discovery of a group of isoform-selective inhibitors with IC_{50} (inhibitory concentration 50%) values at nanomolar concentrations. There are three groups of inhibitors developed by CTI.

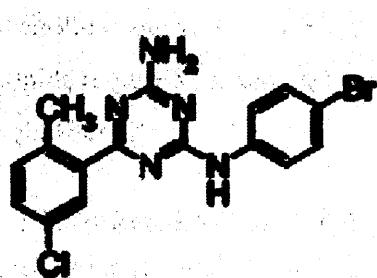
A group of 2,4-diamino- N^4 ,6-diaryltriazines has been reported as isoforms of a specific small molecule inhibitors of LPAAT- β (Figure 1.4A). This group is exemplified by CT-32228 (LPAAT- β IC_{50} =0.06 μ M) an effective antiproliferative agent toward a variety of tumour cell lines in vitro with IC_{50} s ranging from 0.025 to 0.5 μ M. These aryldiaminotriazines did not inhibit LPAAT- α at concentrations up to at least 40 μ M. CT32228 inhibited LPAAT- β in both the cell-free assay (IC_{50} = 60 nM) and the cellular assay measuring PM formation.

The structural specificity for both inhibition of LPAAT- β and antiproliferative activity within this group of compounds was clarified by comparison of activities of isomeric compounds CT32169 and CT32212. The para-chloro isomer CT32169 was both an effective inhibitor of LPAAT- β (cell-free IC_{50} = 50nM) and an antiproliferative agent (IC_{50} on tumour cell line proliferation ranging 150-400 nM). In contrast, the ortho-chloro isomer CT32212 was a weak LPAAT- β inhibitor (cell-free IC_{50} = 64 μ M) and weakly antiproliferative (IC_{50} > 3.7 μ M). This group of compounds were used in our study.

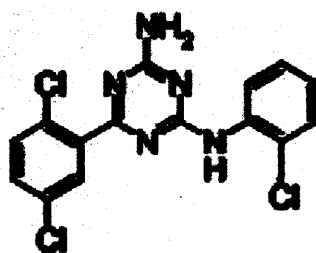
A second group of inhibitors synthesized are diamine-C,N-diarylpyrimidine analogue. A pyrimidine, possesses one less ring nitrogen than a triazine. The inhibitors examined for LPAAT- β inhibition by three possible pyrimidine positional isomers and proliferation of tumour cells in vitro. The 2,4-diamino- N^4 ,6-diarylpyrimidines positional isoform was found to be more potent for LPAAT- β inhibition and to be a highly effective antiproliferative agent compared with other isomers (Figure 1.4B).

A 2-arylbenzoxazole, a third group of inhibitors and its isoforms were synthesized and found to be weak LPAAT- β inhibitor (IC_{50} =1.7 μ M). These inhibitors represent a new class of LPAAT- β inhibitors, 2-arylbenzoxazole did not inhibit LPAAT- α up to at least 64 μ M (Gong et al. 2004a;Gong et al. 2004b).

Kinetic analysis of CT32228 showed uncompetitive inhibition of LPA binding and mixed noncompetitive inhibition of 18:1-CoA binding. Bonham et al (2003) reported that LPAAT- β binds LPA binding before it can bind the inhibitor. It has been suggested that the binding LPA to LPAAT- β induces a conformational change in the enzyme, exposing a site on the enzyme for the inhibitors to bind. CT32228 does not inhibit the ability of PLD1 or PLD2 to hydrolyze phosphatidylcholine. Initial biochemical studies have shown that LPAAT- β appears to have a preference for the transfer of oleoyl acyl chains over that of arachidonoyl acyl chains (Bonham, et al. 2003; Coon et al. 2003).

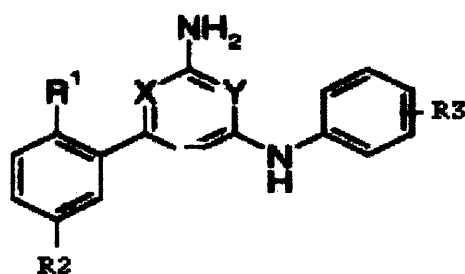


CT32228



CT32212

2,4-diamino- N^4 ,6-diaryltriazines (A)



2,4-diamino- N^4 ,6-diarylpyrimidines (B)

Figure 1.4 LPAAT- β Inhibitors compound structure.

1.4 Lysophosphatidic acid (LPA)

1.4.1 Introduction

Lipid molecules are insoluble in water but dissolve readily in organic solvents. They constitute about 50% of the mass of the most animal cell membranes, nearly all of the remainder being protein. The most abundant are the phospholipids. These have a polar head group and two hydrophobic hydrocarbon tails. The tails are usually fatty acids, and they can differ in length. One tail usually has one or more *cis*-double bonds (unsaturated), while the other tail does not (saturated) (Alberts 2002).

It is widely recognized that phospholipids play multiple roles in cell processes. Their primary function is to define the permeability barrier of cells and organelles by forming phospholipid bilayers. The endoplasmic reticulum (ER) membrane produces nearly all of the lipids required for the elaboration of new cell membrane, including both phospholipids and cholesterol.

1.4.2 Biochemistry of LPA

Lysophosphatic acid (LPA) is the common name for monoacyl-*sn*-glycero-3-phosphate, signalling phospholipids with numerous biological actions. The era of LPA research began around 1990 with the discovery that LPA is mitogenic for fibroblasts and signals via specific G-protein-coupled receptors (GPCR) (Moolenaar & van Corven 1990; van Corven et al. 1989). Serum is a rich source of LPA, as are other body fluids such as saliva, follicular fluid and malignant effusion. In serum, LPA binds tightly to albumin, and other as-yet-unidentified proteins (15 and 28 kDa protein) (Goetzl et al. 2000; Moolenaar 1995; Moolenaar, et al. 2004; van der Bend et al. 1992). The major serum LPA band consists of a mixture of LPA species with unsaturated and saturated fatty acid chains (Baker et al. 2000). LPA is more water soluble than long chain phospholipids because of its free hydroxyl and phosphate moiety (Jalink, et al. 1990).

1.4.3 LPA production and degradation

LPA can be generated in an activated cell by the hydrolysis of phospholipids preexisting in the cellular membranes. Although serum LPA can be generated from thrombin-activated platelets (Eichholtz et al. 1993), its production and release appears not to be restricted to platelets (Gaits et al. 1997). Recent data indicate that LPA may also be produced locally

within reproductive tissues. It has been suggested that LPA found within the ovary may be produced by the ovary itself, because LPA is present both in follicular fluid and in the ascites from ovarian cancer patients. Human follicular fluid contains an active lysophospholipase D (LysoPLD), an enzyme that may be responsible for the local production of LPA (Tokumura et al. 1999). In contrast, to the mechanism of LPA production in serum and plasma, the mechanisms of LPA production in cells are still ambiguous.

The degradation of LPA by lipid phosphate phosphatases (LPPs) and other enzymes also play a very important role in keeping LPA in check under physiological conditions. It has been demonstrated that the major mechanism of degradation of LPA by ovarian cancer cells is through a lipid phosphate phosphatase (LPP)-like activity. In ovarian cancer cell lines, LPP RNA level are lower than those in normal ovarian epithelium and immortalized ovarian epithelial cells (Tanyi et al. 2003). Overexpression of LPP in ovarian cancer cells decreases tumour growth and apoptosis in vitro and in vivo (Tanyi et al. 2003).

1.4.4 LPA in tumorigenesis

The first indication that LPA could contribute to tumorigenesis came from studies showing that LPA increases motility and invasiveness of cells (Fishman et al. 2001;Imamura et al. 1993;Jalink, et al. 1990;Stam et al. 1998;Zheng, et al. 2001). Many studies reported that autotoxin/ lysophospholipase D (ATX/LysoPLD) mediates its effects through the production of LPA, have implicated LPA in the pathophysiology of ovarian cancer, and several studies have indicated a role for LPA in the initiation or progression of prostate, breast, melanoma, head and neck, bowel, thyroid and other cancers (Eder et al. 2000;Fang et al. 2000;Fang et al. 2002;Fang et al. 2004;Furui et al. 1999;Goetzl et al. 1999;Hu et al. 2001;Schulte et al. 2001;Xu et al. 1995).

Ascites fluid is a potent mitogen for ovarian cancer cells in vitro and in vivo. A significant portion of this activity is mediated by LPA, which is present in ascites fluid at between 1 and 80 μ M, exceeding levels required to optimally activate LPA receptors. LPA is not produced at significant levels by normal ovarian epithelial cells, whereas ovarian cancer cells produce high levels of LPA. Prostate cancer cells also produce high levels of LPA.

1.4.5 The extracellular role of LPA

1.4.5.1 LPA receptors

The first extracellular action of LPA was reported by as early as the 1970s, when Tokumura et al described the effect of LPA on blood pressure (Tokumura, et al. 1978). However, clear evidence of LPA as an extracellular signalling molecule and molecular dissections of its signalling pathways came in the 1980s and early 1990s (Moolenaar et al. 1992;Moolenaar & van Corven 1990).

Based on the sequences homology, the LPA receptors belong to the so-called Edg (endothelial differentiation gene) subfamily of the GPCR superfamily of seven-transmembrane domain receptors. Candidate high-affinity LPA receptors were initially detected by photo-affinity labelling experiments (van der Bend et al. 1992); several years later the first LPA receptor gene was identified (LPA₁, previously Edg-2) (Hecht et al. 1996). This opened the way to the identification of two related LPA receptors, LPA₂ and LPA₃ (previously Edg-4 and Edg-7, respectively), and of five additional Edg family members that encode receptors for another lipid mediator, sphingosine-1-phosphate (S1P) (Anliker & Chun 2004).

Receptor gene targeting studies are beginning to reveal the normal physiological function of LPA. Mice lacking LPA₁receptors show partial lethality due to defect suckling which in turn is attributed to defect in olfaction (Contos et al. 2000); consistent with this, LPA₁ is expressed in the nasal cavity (McGiffert et al. 2002).

1.4.5.2 G-protein signalling Pathways

The great variety of cellular and biological action of LPA is explained by the fact that LPA receptors can couple to at least three distinct G proteins (G_q, G_i and G_{12/13}), which in turn feed into multiple effectors systems (Fang et al. 2000;Fang et al. 2000;Jalink et al. 1993;Kranenburg et al. 1999;Kranenburg & Moolenaar 2001;Kumagai et al. 1993;van Corven et al. 1993;van Dijk et al. 1998). LPA activate G_q and thereby stimulate phospholipase C (PLC), with subsequent phosphatidylinositol-bisphosphate hydrolysis and generation of multiple second messenger leading to protein kinase C (PKC) activation and changes in cytosolic calcium (van Corven et al. 1989). LPA also activates G_i, which lead to at least three distinct signalling routes: inhibition of adenyl cyclase with inhibition of cyclic AMP accumulation; stimulation of the Ras/MAPK cascade; and activation of PI3K, leading

to activation of the guanosine diphosphate/guanisine triphosphate (GDP/GTP) exchange factor TIMA1 and down stream RAC/GTPase, as well as to activation of the Akt/PKB anti-apoptotic pathway (Fang et al. 2000;Fang et al. 2000;Kranenburg & Moolenaar 2001;Takeda et al. 1999;van Corven, et al. 1989;van Corven, et al. 1993;van Leeuwen et al. 2003). Finally, LPA activates G_{12/13}, leading to activation of the small GTPase RHOA, which drives cytoskeletal contraction and cell rounding (Kranenburg et al. 1999).

By activating G_i, LPA triggers the Ras/MAPK cascade and thereby promote cell cycle progression and survival. LPA induced RAS activation presumably involves the ras-specific GEF,SOS, and intermediate protein. The role of LPA on RAS activation is still a matter of debate.

1.4.6 LPA and Intracellular signalling

A recurring theme in studies on lipid mediators is their possible signalling role inside the cell. However evidence for such a role is scant. Well established is the role of intracellular LPA as an intermediate in the early steps of phospholipids biosynthesis. This process occurs in the endoplasmic reticulum, where LPA is formed from glycerol-3-phosphate by acyl-CoA and then acylated to PA, the precursor for all glycerolipids. Since the rate of acylation of LPA to PA is very high, there is little or no accumulation of LPA at the site of biosynthesis.

A more interesting role for intracellular LPA as a signalling molecule has been suggested by the finding that LPA can compete with a synthetic ligand for binding to the nuclear transcription factor-activated receptor- γ (PPAR γ). PPAR γ normally bind fatty acid derivatives with rather low specificity to regulate gene involved in energy metabolism, cell differentiation, apoptosis and inflammation. Extracellular LPA induces PPAR γ -mediated gene transcription, seemingly in an LPA receptor-independent manner, since yeast deficient in the receptor still respond (McIntyre et al. 2003). In a rat carotid artery model, LPA-induced neointima formation is inhibited by a PPAR γ antagonist and only observed with unsaturated LPA species, which is incompatible with the LPA structure activity relationship for LPA GPCRs. Nevertheless, LPA induces neointima formation which must involve G-protein signalling as the effect is partially inhibited by pertussis toxin (Zhang et al. 2004). Another study also showed a requirement for unsaturated LPA in vascular

remodelling and suggested the involvement of a yet unidentified receptor specific for unsaturated LPA (Yoshida et al. 2003).

To date no studies have been found a link between LPA and AML pathophysiology. However, sphingosine 1 phosphate (S1P) which has a similar molecular structure to LPA phospholipids acts both intracellularly and extracellularly to cause pleiotropic biological responses. S1P was found protect HL60 cells from apoptosis intracellularly without acting on the Edg 1receptor (Van Brocklyn et al. 1998).

1.5 Aims of the study

Relapses and resistance occurring after a complete remission of APL can develop after a short time of therapy. Cytotoxic chemotherapy and improvement in supportive care have prolonged survival for patients with APL. Nevertheless, cytotoxic agents have several side effects, including a risk of secondary malignancy and death. Therefore, the research of modern drug development in oncology with therapeutic improvement will result from specific targeting of molecular alterations that occur during tumorigenesis. One strategy is to inhibit enzyme that produce cofactors critical to signalling and/or survival pathways specific to AML. LPAAT- β is differentially expressed in normal cells and is highly expressed in a wide variety of tumour cells. We propose that LPAAT- β is also overexpressed in AML. We focus on the potential therapeutic applications of inhibiting LPAAT- β enzyme and thus the production of PA, a required lipid cofactor for the activation of raf and thus the ras/raf/Erk pathway, for mTOR, critical effector molecules downstream in phosphatidylinositol-3-kinase (PI3K) pathway. These signalling molecules and their downstream effectors are involved in proliferation and/or survival of AML cells and have been independently targeted for anticancer drug development.

Therefore, the aims of the present study were to test this hypothesis by inhibition LPAAT- β by specific LPAAT- β inhibitors led to effect on apoptotic event in-vitro. Cells were evaluated (pre and post treatment), by flow cytometry for expression of apoptotic markers (Annexin V and propidium Iodide staining) and cell cycle progression. To measure inhibitors specificity on LPAAT- β , LPAAT- β enzyme activity was measured by radioenzymatic assay after long and short time of exposures to PC020702.

Also, we used Oligonucleotide array to examine gene expression before and after a short time of exposure to LPAAT- β inhibitors in both NB4 and NB4:R2 cells, in order to identify common genes differentially expressed in proliferation and apoptosis after inhibitor induction. Using gene analysis software including AtlasImage and GeneSpring, genes from Oligonucleotide array were analyzed and comparison of expression patterns within and between cell lines have been made possible. Quantitative real-time- PCR was used to confirm the involvement of these genes in the enzyme inhibition processes.

Involvement of PA in cell signalling was analyzed by measuring phosphorylated Erk1/2, mTOR and Akt by Western blotting using specific antibodies. PA has been implicated as playing either a direct or indirect role in activation of these signalling molecules. These results provide evidence for the identity of targets of these inhibitors that may play a role in the development of AML treatment.

CHAPTER 2

MATERIALS & METHODS

2.1 Cell Culture and Cell line

2.1.1. General rules

All cell culture work was handled in a Class II microflow laminar hood. 70% ethanol was used to wipe all surfaces and materials before it was brought into the hood. Pipettes, pipette tips, falcon tubes and syringes were sterilized by autoclaving or purchased sterile. Contaminated tips and pipettes were soaked in 10x actichlore solution for 24 hours before being discarded into autoclave bags in lidded autoclave bins.

2.1.2 Cell culture conditions

The haematopoietic cell lines NB4, NB4:R2, HL60 and HL60-R, were cultured in RPMI 1640 medium supplemented with L-glutamine medium (Sigma). The medium utilizes bicarbonate buffering system to maintain pH at 7.3-7.5. 10% Foetal Bovine Serum (FBS) was added to the medium. For HL60 and HL60-R, 100 units/ml penicillin and 100 µg/ml streptomycin were added to medium. All cell lines were maintained at 2.5×10^5 cell/ml, and split every 2 days. The cells were incubated at 37°C in 5% CO₂ and 98% humidity.

2.1.3 Long term liquid nitrogen storage of cell lines

Liquid nitrogen stocks of cell cultures were prepared by resuspending cells at $4-6 \times 10^6$ cells/ml in freezing media (normal culture medium with 20% FBS and 10% DMSO). Cells were aliquoted into 1.5 ml cryopreservation tubes. The cells were gradually frozen, as rapid freezing causes ice crystal to form inside the cell, which causes rupture. The tubes were placed into a polystyrene box, and placed into -70°C freezer for gradual freezing over 24 hours. The cryopreservation tubes were finally placed into liquid nitrogen for long term storage.

2.1.4 Thawing of the cells

When required, cells were removed from liquid nitrogen storage and thawed quickly at 37°C. Cells were slowly diluted by dropwise addition of 1 ml of fresh medium to the freezing vial. The cells were then transferred to a universal container (UC) and gradually diluted with 5 mls of fresh medium. Slow dilution prevents a dramatic osmotic shock. Cells were centrifuged and washed to remove residual DMSO, placed in tissue culture flasks in fresh medium and maintained as described above.

2.1.5 Cell line

All cell lines used in this study were derived from human myeloid leukaemia. These cell lines were blocked at different stages of differentiation. The work was done on four cell lines, which between them represent models of ATRA induced differentiation and resistance. These cell lines were summarized in the following table (Table 2.1):

Cell line	Descriptions	References
NB4	A leukaemia cells were optioned from 20 years old female with APL. Contains t(15:17) translocation. Maturation induced towards the granulocytic lineage after treatment with ATRA.	(Lanotte et al. 1991)
NB4:R2	A mutant leukaemia cell line (APL) resistant to ATRA This cell line was selected for resistance to retinoic acid by initially exposing wild type NB4 cells to long term treatment with retinoic acid.	(Duprez et al. 1992)
HL60	A leukaemia cell line derived from 36 years old female with acute myeloid leukaemia. Lack t(15:17) translocation. Induced to mature to neutrophils after treatment with ATRA and DMSO.	(Breitman, et al.1980;Collins, et al. 1977;Dalton, et al. 1988)
HL60-R	HL60-R subline was resistant to ATRA. This cell line was selected for resistance to retinoic acid by initially exposing wild type HL60 cells to low drug concentration and then step wise augmenting the drug concentration.	(Gallagher et al. 1985)

Table 2.1: Cell lines used in the study

2.1.6 Trypan blue exclusion cell counting

Trypan blue (Sigma) was purchased ready to use or prepared at a working solution of 0.1% PBS (w/v) and 10 ul mixed with 10ul of the cell suspension. Sample were loaded onto Neubauer haemocytometers and viable cells counted. Viable cells appeared clear whilst dead cells absorbed the blue dye. The viability was calculated according to the following formula:

$$\text{Viability (\%)} = (\text{total viable cells} / \text{total viable and dead cells}) \times 100.$$

2.1.7 LPAAT- β inhibitors storage and preparation:

LPAAT- β inhibitors: were purchased from Cell Therapeutic, Inc, as powder. They were active form (PC020702 and CT32228) and inactive form (PC020701 and CT32212). All LPAAT- β inhibitors were dissolved in absolute dimethylsulfoxide (DMSO) as a stock solution (10 mM) in a sterile UC, which was tightly capped, wrapped in foil and kept at -20°C for up to a three months. These drugs were added to the cell culture of AML cell lines in falcon flasks at 25 nM concentration. Cells were incubated for the period required at 37°C and 5% CO_2 .

2.1.8 Cell harvest and storage

At the end of each experiment and the completion of counts, and viability assessment, cells were harvested. The required number of cells were spun down at 1200 rpm for 5 minutes, washed with 1x PBS, pelleted and frozen immediately at -80°C . Cells were later used for RNA or protein extraction.

2.2. LPAAT- β Assay

2.2.1. General rules for handling ^{14}C radioactive material

Before work appropriate lab coat and double gloves must be worn before starting any experiment. A work area monitoring sheet was filled with name, date and time of entry and departure from the hot lab. A Geiger (Radio active monitor) counter was used to monitor the desk, sink and all equipments. If contaminated, the area and equipments were wiped with Deacon 90 solution (a radioactive decontaminated solution) and rechecked before use. A hot waste pot was prepared by filling with 10% Deacon solution, for disposal tips and tubes. During work the Geiger was left on and regularly used to check the gloves and working area.

After work, solid waste should be sealed in plastic bag with name, date and estimated activity of the waste and stored in the Perspex bin until collection. Liquid waste was discarded directly in a radioactive designated sink in the hot lab.

2.2.2 Principle

The principle of the assay is the ability of LPAAT- β to convert sn-1-oleoyl lysophosphatidylmethanol (LPM) into [^{14}C]-phosphatidylmethanol (^{14}C -PM) in the presence of [^{14}C]-Oleate. ^{14}C -oleate act as Acyl-CoA donor where LPM act as substrate. The end products of the reaction were separated by Thin Layer Chromatography (TLC) plate. The ^{14}C -PM spots intensity was exposed to a Phosphoscreen. Storm Imager was used to quantitate spots and the data analysed by ImageQuant software. The ^{14}C -PM production represents LPAAT- β enzyme activity (Coon et al. 2003;Hideshima et al. 2003;Saulnier-Blache et al. 2000).

2.2.3 Data analysis

The ^{14}C -PM spots percentage was calculated by the following equation:

$$^{14}\text{C-PM \%} = (^{14}\text{C-PM spots relative pixel volume} / \text{whole lane relative pixel volume}) \times 100.$$

2.2.4 LPAAT- β Assay

The AML cell lines were treated with LPAAT- β inhibitor for an appropriate time. At the day of labelling, one million cells were harvested from treated and untreated cells and resuspended in 0.48 ml of medium. 5 μM of LPM (from Avanti) and 25 nM of LPAAT- β inhibitor (PC020702) were added to appropriate tubes. Then the cells were incubated at 37 $^{\circ}\text{C}$ for 20 minutes. Further 10 μl of ^{14}C -labeled oleate (pre-prepared a

stocks (0.4 $\mu\text{Ci}/\mu\text{l}$) in 1x PBS and 20mg/ml fatty acid free bovine serum albumin (FAF-BSA) from Sigma was added to all cells and incubated at 37 °C for 30 minutes. The cells were washed thrice with 1.5 ml ice cold PBS. The reaction was stopped by addition 0.5 mL of ice cold pure methanol and 2 mL of ice cold pure chloroform followed by vigorous shaking and centrifugation. The reaction was separated into two phases by addition of 0.5 ml of 0.2 M of phosphoric acid, and then centrifuged for 2 minutes at 500 x g.

Lipids were extracted from cells after discarding the upper phase and drying the lower phase under nitrogen. The dried lipids were then resuspended in 100 μL of chloroform\methanol (ratio 2:1). A volume of 50 μl of lipids along with LPM and PM standard were spotted on silica gel 60 HP-TLC (Thin Layer Chromatography) plates from Analtech.

The plate was developed in mobile phase chloroform/methanol/ammonium hydroxide (65/30/4). The spots along with LPM and PM standard were visualized under UV light after sprayed with 0.05 % w/v Primulin to identify the position of LPM and PM. The TLC plate was exposed for 24 hours to Phosphor screen which records the image. Then the screen was analysed by the PhosphoImager which is capable of producing digital images of blots labelled with radioisotopes (**Figure 2.1**). The data were analysed by ImageQuant software.



Figure 2.1 PhosphorImager instrument.* (A) the PhosphorImager instrument was used to scan the Phosphor screen (B). Phosphor screen was used to records the image on TLC plate.

* Reproduced from website with slight modification (<http://www.oardc.ohio-state.edu>)

2.3 Flow cytometry

2.3.1 Introduction

The basic flow cytometer consists of a laser beam intersecting a stream of fluid containing single cells passing by sequentially. As the cells flow past a focused laser beam of appropriate wavelength, the probes fluoresce and the emitted light is collected and directed to appropriate detectors. These detectors, in turn, translate these light signals into electronic signals proportional to the amount of light collected. When the laser beam hits the edge of an individual cell, some of the photons of light are deflected slightly and the amount of this light, called “forward angle” light scatter is an indication of the cell size. Other photons may hit internal structures (granules, etc.) of the cell which causes them to be deflected on a wide angle. This light scatter is often called “side scatter” or “90 degree light scatter”. All of the fluorescent light (up to 8 - 12 colours in the state-of-the-art flow cytometer) and scattered light signals are measured, digitized and correlated particle by particle. The signals can then be converted into histograms for immediate results and/or stored as raw data for experimental analysis later.

Most flow cytometers are equipped with an argon laser tuned to 488nm wavelength since the most common fluorochrome, Fluorescein (FITC), is excited at this wavelength. Fortunately, many other fluorochromes are also excited by this wavelength, and it is possible to design a four-color flow cytometric experiment using this one laser.

Flow cytometers come in two different varieties: analyzers and analyzer/cell sorters. In cell sorters the flow stream is agitated and droplets are formed. If the desired cell is known to be in a particular droplet, it is charged negatively or positively when the droplet passes the charging collar. There are two deflection plates just beyond the charging collar, one of which is positively charged to deflect the negatively charged droplets while the other is negatively charged to deflect the positively charged droplets. The deflection is controlled in such a way that the cells land in a tube filled with medium. Because only the droplets with cells are sorted, the volume of cells plus sheath fluid is very small and the cells can be exposed to a high protein medium quickly. Another advantage with the electronic sorters is that you can sort two different types of cells simultaneously and, if desired, collect the unsorted cells (Ormerod 1999; Shapiro 1995)

2.3.2 Apoptosis by Flow Cytometry

2.3.2.1 Annexin V Assay (Principle)

Apoptosis is a normal physiologic process, which occurs during embryonic development as well as in maintenance of tissue homeostasis. Certain morphologic features, including loss of plasma membrane asymmetry and attachment, characterize the apoptotic programme. In apoptotic cells, the membrane phospholipids phosphatidyleserine (PS) is translocated from the inner to the outer leaflet of the plasma membrane, thereby exposing PS to the external cellular environment. Annexin V was initially discovered as a vascular protein with strong anticoagulant properties (Reutelingsperger, et al. 1985). It is a 35-36 kDa Ca^{2+} dependent phospholipid-binding protein that has a high affinity for PS, and binds to cells with exposed PS (Raynal & Pollard 1994). Translocation of PS to the external cell surface is not unique to apoptosis, but occurs also during cell necrosis. Therefore, staining cells with Annexin V labelled with fluorescence is typically used in conjunction with a vital dye such as Propidium Iodide (PI). PI is a standard flow cytometry viability probe and is used to distinguish viable from nonviable cells. Analysis can be carried out using fluorescence microscopy or flow cytometry. In this manner, viable, apoptotic and dead cells can be recognized easily. Cells that stain positive for Annexin V and negative for PI are undergoing apoptosis. Cells that stain positive for both Annexin V and PI are either in the end stage of apoptosis, are undergoing necrosis, or are already dead. Cells that stain negative for both Annexin V and PI are non-apoptotic cells and not undergoing measurable apoptosis (Vermes et al. 1995).

2.3.2.2 Annexin V-FITC Staining Protocol:

The cells were treated as necessary with inhibitors and at the day of labelling, 1×10^5 cells were harvested and washed twice with PBS, then cells were resuspend in 100 μl of binding buffer (10 mM Hepes/NaOH (PH 7.4), 140 mM NaCl, 2.5 mM CaCl_2), after that the amount of 5 μl (1 $\mu\text{g}/\text{ml}$) Annexin V-FITC and 5 μl of PI were added to the cells, then cells were incubated for 15 minutes at room temperature. Finally cells were resuspend in 400 μl binding buffer. The sample was analysed by Flow cytometry within 1 hour of staining.

2.3.2.3 Experiment design and Flow cytometry analysis

On the day of labelling, each untreated cell lines were divided into four tubes. The first tube was unstained (annexin V-/PI-). The second tube was stained with annexin V only, while the third tube was stained with PI. The fourth tube was stained with both annexin V and PI. This was done to adjust electronic compensation to eliminate bleed through of fluorescence (Figure 2.2). After adjustment the file was saved for future analysis.

For flow cytometric analysis, to quantitate the frequency of apoptotic cells, the cultures were incubated with FITC-labelled annexin V and harvested and analysed by flow cytometry. (Becton Dickinson, Sunnyvale, CA) (B-D). Excitation was done at 488 nm. A minimum of 10000 cells per sample were analysed and data stored in list mode.

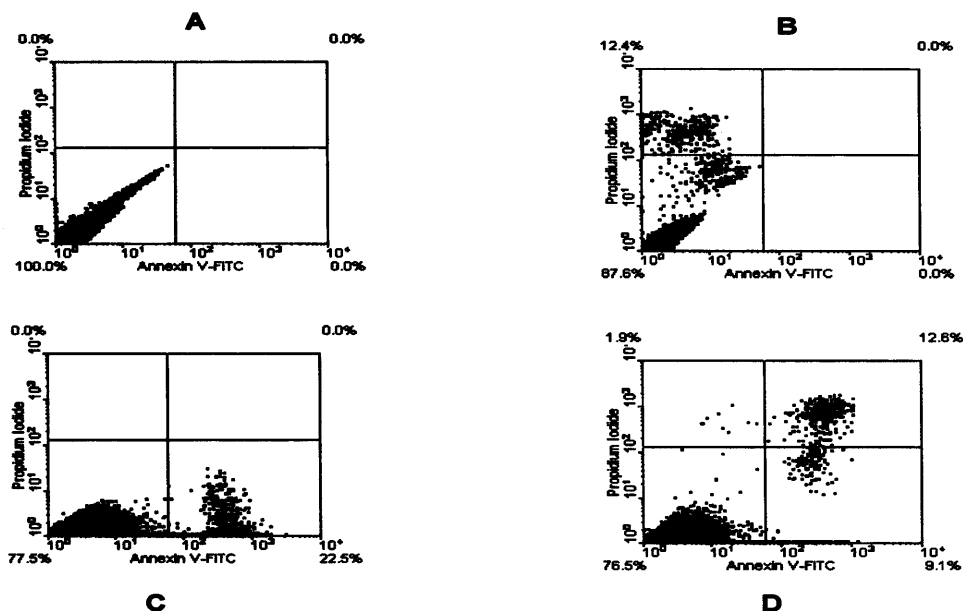


Figure 2.2 Annexin V gating strategy. This figure shows density-plot of FITC-Annexin V (x-axis)/Propidium Iodide (PI) (y-axis) two parameter flow cytometry. Figure (A) shows cells negative for both the annexin V-FITC binding and PI uptake. Figure (B) shows cells contain PI stain only. Figure (C) shows cells stained with annexin V-FITC only. Figure (D) shows cells stained with both PI and annexin V-FITC, due to a compensation error the region encompassing the apoptotic cells has been shifted.

2.3.3 Cell Cycle Analysis by Flow Cytometry

2.3.3.1 Propidium iodide Assay (Principle)

DNA content per cell was determined using the DNA-binding fluorochrome propidium iodide (PI) and flow cytometric analysis. PI stained nuclei emit fluorescent light and the FL2 detector of the flow cytometry was used to analyse the light emitted by stained cells. The fluorescence signal produced by excitation at 488nm was detected at around 585 nm and the level of fluorescence obtained is proportional to the amount of bound PI. Using markers to analyse the distribution of DNA content, the percentage of cells in each cell cycle phase G₁, S and G₂/M was determined. A region is created (on the density plot graph) by drawing polygonal “box” which would contain only the best representative population. Upon analysis, the plot of fluorescence values of that “gated” region would exclusively represent data of the gated population.

2.3.3.2 Propidium Iodide procedure:

After treatments, 2.5×10^6 of cells in tissue culture suspension were placed in 17x100 mm tube, centrifuged for 5 minute (300x g) at room temperature. The supernatant was aspirated and pellet resuspended in 5 ml of 1x PBS, centrifuge for another 5 minutes (300x g) at room temperature. The supernatant was aspirated and pellet resuspended in 200µl of PBS, and 500µl of ice-cold 70% ethanol in PBS were added. The samples were left on ice for 30 minutes or over night after which they were harvested by centrifugation at 300x g for 5 minutes. The samples were washed once and resuspended in 200µl of PBS, and 5µl of 5 µg/ml RNase A was added as well as 20µl of 50µg/ml propidium iodide. The samples were mixed vigorously and incubated at 37 °C for 30 minutes in the dark. The samples were analysed by flow cytometry within 1 hour. A total of 10,000 events were acquired and the data were saved for further analysis.

2.3.3.3 Data analysis and gating strategy.

After the samples were analysed by the flow cytometer and the data were stored in a file for further analysis. The data were further analysed by the WinMDI version 2.8 and Cylchred version 1.0.2 software. WinMDI density blots were applied and a gate (R1) was applied on the forward and side scatter density blot to exclude background noise. The second gate (R2) was applied on the FL2-Area and FL2-Width to exclude sub G₀/G₁ and apoptotic cells. After gating R1 and R2 were applied on a histogram plot and further saved with FCS file extension. The FCS file extension histogram was then analysed by Cylchred software (**Figure 2.3**). This software has the ability to detect the

different cell cycle phase simultaneously and the data can be saved as percentage in Excel file.

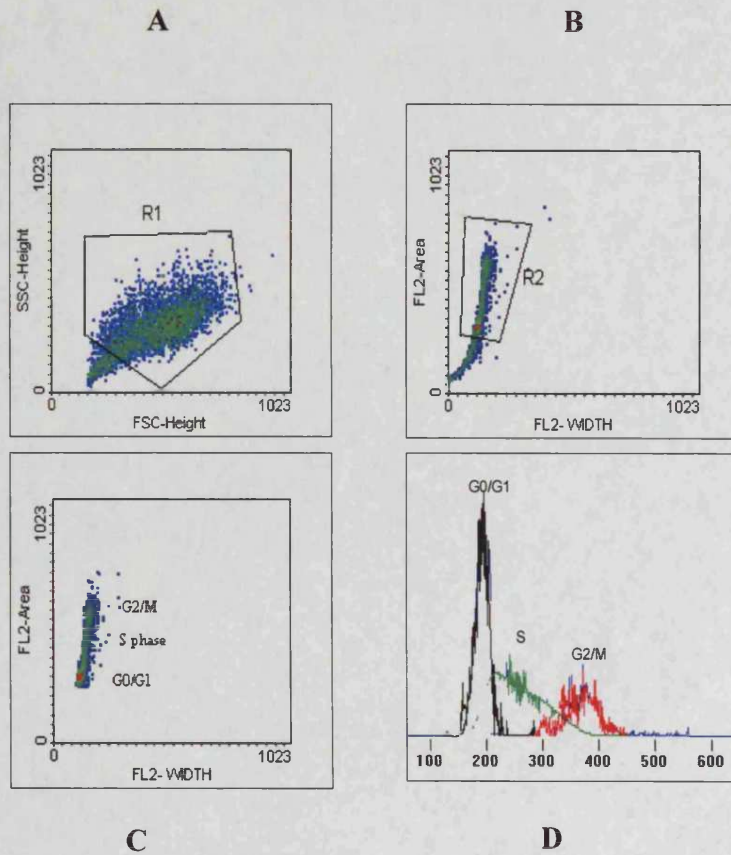


Figure 2.3 Cell Cycle gating strategy.

This figure shows typical density plot of WinMDI cell cycle analysis by propidium iodide and the gating strategy on typical non-treated NB4 cells. Figure A shows a gate region (R1) applied on forward and side scatter density plot graph for all events to exclude background noise. Figure B shows a gate region (R2) applied on the fluorescence from FL-2 width (FL2-W) versus FL2 area (FL2-A) showing the whole population of cells in cell cycle. Figure C shows different cell cycle phases after gating to exclude sub G₀/G₁ and apoptotic events. Figure D shows a typical histogram of Cylchred software cell cycle stained by PI after gating (black line = G₀/G₁, green line = S phase, and red line = G₂/M).

2.4 RNA analysis techniques

2.4.1 Introduction to RNA

Each mammalian cell contains about 10 pg of Ribonucleic Acid (RNA), made up of ribosomal RNA (rRNA) (80-85%), transfer RNA (tRNA) (10-15%) and messenger RNA (mRNA) (1-5%). For the sake of gene expression studies, it is the mRNA that is required. mRNA molecules initially synthesized in the nucleus from genomic Deoxyribonucleic acid (DNA) (nascent RNA) will contain several sequences, called introns that are not transcribed into protein. These are successively excised in the nucleus, leaving only coding sequences (exons) in the mRNA that migrates to the cytoplasm, to be translated at the ribosome.

2.4.2 RNA Isolation

RNA isolation is very critical in the success of any expression experiments, partly because of degradation during the extraction process due to the action of contaminating ribonucleases (RNase's), therefore inactivation of such enzyme is necessary, and partly because the rigorous treatment required dissociating the RNA from protein in ribosomes may fragment the polyribonucleotide strands. In this study, Qiagen Rneasy mini kit was used for total RNA extraction. This kit allows up to 100 ug of RNA longer than 200 bases to be purified. The cells are first lysed and homogenized in the presence of guanidine isothiocyanate (GITC) containing buffer, which immediately inactivates RNases to ensure appropriate binding conditions. Ethanol is added to provide appropriate binding conditions, and the sample is then applied to supplied columns where the total RNA binds to a silicon gel based membrane and contaminants are efficiently washed away. RNA is then eluted in RNase-free water.

2.4.3 Methods

2.4.3.1 Rneasy Kit (Qiagen)

After experimental treatment, 1×10^7 cells were harvested by centrifugation at $300 \times g$ for 5 minutes. The cell pellet was disrupted by adding 600 μ l of lysis buffer RLT, which contains β -mercaptoethanol. The sample was homogenized by passing the lysate through a 20G (0.9mm) needle fitted into a syringe. An amount of 600 μ l of 70% ethanol was added and mixed by pipetting several times. The sample was applied to an RNeasy spin column in a 2ml collection tube and centrifuged at $8,000 \times g$ for 15 seconds and the flow through was discarded. This step was repeated as necessary to allow all samples to pass through the column. A volume of 350 μ l of RW1 washing

buffer was added onto column and centrifuged as above. The flow through was discarded.

At this step RNA was DNase treated in order to completely remove any traces of DNA. DNA contamination may be a major source of false positive or negative findings in gene expression analysis. A solid DNase I was dissolved in 550µl RNase free water and stored in -20 °C as stock solution. 80µl of preprepared DNase I solution (10µl DNase I stock solution and 70µl of supplied RDD buffer) was added directly to column membrane. The column was incubated at room temperature for 15 minutes. A volume of 350 µl of RW1 washing buffer was added into the column, and centrifuged for 15 seconds at 8,000 x g. The spin column was placed into a new 2 ml collection tube and a volume of 500 µl of RPE washing buffer applied into the column and centrifuged as above. The flow though was discarded. An additional 500 µl of RPE washing buffer was added to the column, which was then centrifuged for 2 minutes at maximum speed and the flow through and column discarded. Finally the column was transferred to a new 1.5ml collection tube. For RNA elution, 30ul of RNase-free water was added directly onto the membrane of the column and centrifuged for 1 minute at 8,000 x g. the last step was repeated as necessary to elute more RNA.

2.4.3.2 RNA Integrity and quantitation

RNA purity and integrity is very important for effective use in RNA analysis. Such changes in RNA integrity and quantitation pattern need to be avoided for all reliable quantitative gene expression analysis, such as cDNA array analysis, quantitative RT-PCR, Northern blot or any related other technologies. Therefore immediate RNA extraction and quantitation after harvesting must be done to avoid RNA degradation. In addition, all apparatus and buffer used in the extraction and handling of RNA was either purchased as Rnase free components or treated with di-ethyl-pyrocabonate (DEPC) overnight at 37°C followed by autoclaving.

The eluted RNA was quantitated by UV spectrophotometric instrument. RNA was diluted 1:70 in RNase-free water and analysed in a GeneQuant from Amersham. The absorbance at 260nm (Ab_{260}) and 280nm (Ab_{280}) were recorded and RNA concentration calculated by the following formula:

$$\text{RNA concentration} = Ab_{260} \times 40 \times \text{Dilution factor}$$

Where Ab_{260} is the absorbance of the sample at 260nm and 40 is RNA correction factor. The purity of RNA can be estimated from the ration of the two wavelengths (Ab_{260}/Ab_{280}). Pure RNA has a ratio of 1.8-2.0.

2.5 Oligonucleotide Microarrays

2.5.1 The Principle

Microarray technology enables simultaneous gene expression analysis of thousands of genes. Two microarray technologies (platforms) are mainly used today for high throughput gene expression analysis: the spotted glass slide microarray technology and the Affymetrix GeneChip technology. Oligonucleotide probes on GeneChip T7-Oligo(dT) expression arrays are designed in the sense direction of corresponding transcript. In GeneChip expression analysis, sample amplification and labelling is used to produce biotinylated antisense targets for hybridisation to probes on the arrays.

The complete procedure involves hybridising a chimeric T7-oligo(dT) primer to the sample mRNA in the reverse transcription reaction for first strand cDNA synthesis, followed by second strand cDNA synthesis. The purified double-stranded cDNA containing a T7 promoter at its 5' end can now serve as a template in the *in vitro* transcription reaction that produces many copies of complementary RNA (cRNA) that has incorporated biotinylated nucleotides. The biotinylated cRNA targets are then fragmented and hybridised to GeneChip expression arrays.

2.5.2 Methods

1×10^7 cells of NB4 and NB4:R2 cells were untreated and treated with LPAAT- β inhibitors for 1 hour. After 1 hour the cells were harvested and centrifuged at high speed. The cells pellet was dried completely from media, and frozen at -80°C until needed. The basic steps in the Affymetrix assay are as follows:

1. RNA isolation
2. First strand cDNA synthesis
3. Second strand cDNA synthesis
4. Cleanup of double stranded cDNA
5. *In vitro* transcription (IVT) cRNA synthesis
6. Cleanup of biotin-labelled cRNA
7. Fragmentation
8. Hybridization
9. Staining
10. Scanning

RNA extraction was performed, the samples were then processed by Mrs Amanda Gilkes before analysis within CBS (Central Biotechnology Surfaces) University of Cardiff, School of Medicine.

2.5.2.1 RNA Isolation

RNA isolation for the Affymetrix system was different from the RNA isolation described previously in section (2.4.2). The cells were lysed with 1 ml of Trizol reagent, with gentle pipetting. The lysate were added to the pre-spun Phase Lock Gel-Heavy tube (PLG-H) and incubated for 5 minutes at 15-30 °C. Then, 0.2 ml of chloroform was added to the lysate and centrifuged at 12000 x g for 10 minutes at 2-8 °C. After centrifugation, the aqueous phase, which contains RNA was formed at the top of the PLG-H, and red phenol chloroform and cloudy interphase was below.

The upper phase was extracted into separate tube, isopropyl alcohol was added to the tubes and incubated at 15-30°C for 10 minutes. Then the sample was centrifuged at 12,000 x g for 10 minutes, to aid RNA precipitation.

The supernatant was decanted, 75% ethanol was added to RNA pellet. The sample was centrifuged at 7,500 x g for 5 minutes at 2-8 °C, to help remove the isopropyl alcohol. The supernatant were decanted and the tube was left opened to air dry RNA pellet. RNase-free water were added to RNA pellet and incubated at 65 °C for 5 minutes. Finally RNA concentration and purity was quantitated by Agilent chip.

2.5.2.2 First strand cDNA synthesis:

An amount of 7.5 µg of total RNA was mixed with water to get total volume of 10 µl and 2 µl of 100 pmol/µl T7 primer (Affy_T7 primer 5'-GGC CAG TGA ATT GTA ATA CGA CTC ACT ATA GGG AGG CGG TTT TTT TTT TTT TTT TTT TTT-3') was added to RNA.

The sample was incubated at 70 °C for 10 minutes for primer hybridisation. After brief centrifugation, the sample was kept on ice. Another tube, containing a master mix for all other components for 1st strand synthesis was prepared as follows:

5 x 1 st Strand Buffer	4 µl
0.1 M DTT	2 µl
10 mM dNTP	1 µl

After addition of a master mix the sample were mixed and centrifuged for a few seconds. The sample was then incubated at 40 °C for 2 minutes. After that, 1 µl per reaction of SuperScript II reverse transcriptase were added to the mix. Then the sample was mixed and incubated at 42 °C for 1 hour. After incubation the sample was kept in –80 °C for the second strand synthesis.

2.5.2.3 Second strand cDNA synthesis:

For the second strand synthesis the following master mix were added to the sample:

RNAse-free water	91 µl
5 x 2 nd Strand Buffer	30 µl
10 mM dNTP	3 µl
DNA Ligase	1 µl
DNA Polymerase I	4 µl
RNAse H	1 µl

After mixing and brief centrifugation the sample was incubated at 16 °C for 2 hours in DNA thermal cycler. The reaction was stopped by the addition of 10ul of 0.5M EDTA.

2.5.2.4 Cleanup of double stranded cDNA

A volume of 600 µl of cDNA binding buffer was added to the second strand reaction preparation. The mixture was vortexed for 3 second and a volume of 500 µl of sample were added to the cDNA Cleanup Spin Column sitting in a 2 mL collection tube. The column was centrifuged at $\geq 8,000 \times g$ for 1 minute. Then, the column was reloaded with the remaining mixture and centrifuged as above, after centrifugation, flow through and collection tube were discarded.

The column was transferred to a new collection tubes, and a volume of 750 µl of cDNA washing buffer was added to the column. The column was centrifuged at $\geq 8,000 \times g$ for 1 minute, and the flow through was discarded. The column was centrifuged for 5 minutes at $\leq 25,000 \times g$ to dry the membrane. The flow through and collection tube were discarded. The column was transferred to a new 1.5 mL collection tube, and a volume of 14 µl of cDNA Elution buffer was added to column and centrifuged for 1 minutes at maximum speed ($\leq 25,000 \times g$). This step will elute the cleaned up cDNA. The eluted cDNA were kept in –20 for IVT synthesis.

2.5.2.5 In vitro transcription (IVT) cRNA synthesis:

1 μ l from the sample was taken for Agilent bioanalyser analysis and the rest of the sample was used for IVT synthesis. All sample and solution were brought to room temperature except the enzymes. For IVT synthesis the following master mix was added to the sample to get total volume of 40 μ l:

RNAse-free water	11 μ l
10 x HY Buffer	4 μ l
10 x Biotin-labelled Ribonucleotides	4 μ l
10 x DTT	4 μ l
RNAse Inhibitor Mix	4 μ l
T7 RNA polymerase	2 μ l
Total	29 μ l + 11 μ l of the cleaned cDNA

After mixing and centrifugation, the sample was incubated at 37 °C for 6 hours with gentle mixing every 30-45 minutes.

2.5.2.6 IVT cRNA Cleanup:

IVT cRNA cleanup step is necessary to remove unincorporated NTPs, so that not interfere with cRNA quantification, as the biotinylated nucleotides interfere with the Ultra-Violet spectrophotometer. 60 μ l of RNAse-free water were added to IVT reaction and mixed by vortexing for 3 second. Then 350 μ l of IVT cRNA Binding Buffer was added to the sample and mixed by vortexing for 3 seconds. After that, 250 μ l of ethanol (96-100%) was added to the lysate, and mixed well by pipetting. IVT cRNA cleanup spin column sited in a 2 mL collection tube and 700 μ l of the mixture were added. After centrifuging for 15 second at $\geq 8,000 \times g$, the flow through and collection tube were discarded. The spin column was transferred to a new 2 mL collection tube, and 500 μ l of IVT cRNA Wash Buffer (96-100% of ethanol was added before use) was added to the spin column. After centrifuging for 15 seconds at $\geq 8,000 \times g$, the flow through was discarded. A volume of 500 μ l ethanol (80%) was added onto spin column. The column was centrifuged as above and the flow through was discarded. The column was centrifuged for 5 minutes at maximum speed to dry any residual ethanol from the membrane; the flow through and collection tube were discarded. The spin column was

transferred to a 1.5 collection tube. For elution of cleaned cRNA a volume of 11 µl of Rnase-free water was pipetted directly onto the membrane and centrifuged at maximum speed ($\leq 25,000$ g) for 1 minute. For the second elution another 10 µl of Rnase-free water was pipetted directly onto the membrane and centrifuged as above.

The cleaned IVT cRNA was quantitated before cRNA fragmentation step. For quantification of cRNA when using total RNA as starting material, an adjusted cRNA yield must be calculated to reflect carryover of unlabeled total RNA. UV spectrophotometer was used to estimate of percent carryover, the following formula was used to determine adjusted cRNA yield:

Adjusted cRNA yield = (amount of cRNA measured after IVT(ug)) – (amount of total RNA used in cDNA synthesis reaction) x (fraction of cDNA synthesis reaction used in IVT).

2.5.2.7 cRNA Fragmentation:

A total of 15µg cRNA was used in fragmentation; the reaction was performed in a microfuge tube.

cRNA	15ug (1-32µl)
5 x fragmentation buffer	8µl
DNase free water	To 40µl

The reaction was incubated at 94°C for 35 minutes then placed on ice. A volume of 1ul of fragmented cRNA was retained for analysis on an Agilent Bioanalyser and the rest was stored at -20°C until hybridisation.

As mentioned earlier the rest of steps, which include hybridisation, staining and scanning, were performed at Central Biotechnology Surfaces, in Cardiff University School of Medicine.

2.6 Real-Time PCR

2.6.1 The Principle:

Polymerase Chain Reaction (PCR) is a powerful techniques used for many applications in molecular genetics studies. Quantitative PCR using Real Time-PCR (Light Cycler) was used in this study to confirm gene expression pattern obtained from Affymetrix system.

The Light Cycler system has been designed to reduce time by simultaneously allowing amplification and monitoring of the PCR product. The system uses PCR temperature cycling using air, which allows faster control the temperature (accuracy of $\pm 0.3^{\circ}\text{C}$) than conventional heating methods. The PCR reaction takes place in a specially designed capillary, with a high surface area to volume ratio. The combination of using air for rapid thermal cycling and the high surface to volume ratio of the capillaries allows 30-40 cycles can be performed in 20-30 minutes.

The capillary ideally has been designed for use as cuvettes for the fluorescence measurements. The Light Cycler optical unit detects florescence from the tip of the capillary. The Florescence used with Light Cycler system is SYBR Green I dye (Roche). This dye binds only to the minor groove of double strand (dsDNA). During annealing the PCR primers hybridise to the target sequence, resulting in small parts of dsDNA to which SYBR green I dye can bind thereby increasing fluorescence intensity. At the end of elongation phase of the PCR, the more SYBR green I is bound which means the fluorescence increase as more PCR product is produced in the reaction.

The Light Cycler system is also capable of providing confirmation of the amplified product. The melting temperature (T_m), is defined as the temperature at which 50% of the DNA becomes single stranded, and 50% remains double stranded. Every PCR product is verified by a specific T_m , which provides accurate identification of the product, where as primer dimers and other small amplification artefacts melt at lower temperature.

2.6.2 Methods:

2.6.2.1 First strand synthesis

After experimental treatment, RNA was extracted as mentioned in section (2.4.3). RNA sample was converted into cDNA by an enzyme Murine Leukemia Virus (MuLV) Reverse Transcriptase from Applied Biosystem. The end product of the RT reaction was

further used by RT-PCR for the determination of the expression level of mRNA in the sample. The following master mix (19 μ l) was added to 1 μ l of RNA sample:

Master Mix	
25 mM MgCl ₂	4 μ l
10X PCR buffer II	2 μ l
dGTP	2 μ l
dATP	2 μ l
dTTP	2 μ l
dCTP	2 μ l
RNase inhibitor	1 μ l
MuLV Reverse Transcriptase	1 μ l
Random Hexamers	1 μ l
DEPC water	2 μ l

The sample was placed in thermal cycler machine. The sample was incubated at 37 °C for 1 hour, then at 75°C for 5 minutes and then at 4°C. The sample was stored in -20 °C until required.

2.6.2.2. Primers Designing

The primers were designed so that the GC content of the primer was not more than 60% and had a T_m between 55-60 °C. This was done to assure optimal performance and minimize formation of primer dimers. All primers were purchased from Oswel and diluted to 10 μ M and 50ng/ μ l. The primers were stored in aliquots in -20°C until required.

2.6.2.3 Optimising PCR reaction

The PCR optimisation using specific primers of the gene of interest was done on Cetus thermal cycler. The optimisation of PCR is required to give a product of the gene of interest, which will be used with light cycler analysis. The following reaction mix was used to optimise the PCR:

RT reaction (standard)	1.0 μ l
DEPC water	Up to 10 μ l

The reaction mixed was analysed by Light Cycler. The appropriate MgCl₂ concentration for every gene was further used in RT-PCR experiment.

Mg Cl ₂	2.5µl
10 x PCR buffer II	5.0µl
Primer (sense)	2.5µl
Primer (anti-sense)	2.5µl
Tag	0.625µl
RT reaction (from	12.5µl
DEPC water	To 50µl

The master mix shown above was incubated in thermal cycler. The sample was first denatured at 95°C for 5 minutes. Then the PCR cycle was started for denaturing, annealing and extension at 95°C for 1 minute, 60°C for 1 minute and 72°C for 1 minute respectively. At the end of PCR reaction the sample was soaked at 4°C.

2.6.2.4 DNA extraction and standard preparation

The PCR product, along with a ladder was run on 1.5% agarose gel stained with ethidium bromide. The band was visualized under UV light (the product size was compared with the marker lane). The bands were cut and DNA was extracted according to manufacturer's instruction using QIAquick gel extraction kit from Qiagen. The DNA was quantitated as mentioned in section (2.4.3.2), and stored in aliquots (5 ng/µl) at -20°C, these were called standard. The DNA was used later to prepare serial dilution for the standard curve.

2.6.2.5 MgCl₂ optimisation

The enzyme activity in PCR reaction depends on the specific MgCl₂ concentration. In RT-PCR each gene was optimised with MgCl₂ concentration range from 2 to 5 mM. The following reaction mixture was used in MgCl₂ concentration optimization:

MgCl ₂ 2mM/3mM/4mM/5mM	0.4µl /0.8µl /1.2µl /1.6µl
Primer sense (50ng/µl)	0.5µl
Primer anti-sense (50ng/µl)	0.5µl
Syber Green reaction mixture (LC/FS)	1.0µl
RT reaction (standard)	1.0µl
DEPC water	Up to 10µl

The reaction mixed was analysed by Light Cycler. The appropriate MgCl₂ concentration for every gene was further used in RT-PCR experiment.

2.6.2.6 Light Cycler PCR optimisation

The Real Time PCR reaction performed in a Light Cycler uses the optimised magnesium chloride concentration and the serial standard as mentioned above for each set of primers. Serial dilutions of standards varied from 10^{-2} to 10^{-7} copies of the target molecule per microlitre. The samples were repeated in duplicate and two independent sets of samples were analysed on Light Cycler, with a negative control (no template) was always run. The Light Cycler PCR mixture was prepared in a total volume of 9 μ l:

MgCl ₂	as determined by optimisation
Primer sense (50ng/ μ l)	0.5 μ l
Primer anti-sense (50ng/ μ l)	0.5 μ l
Syber Green reaction mixture (LC/FS)	1.0 μ l
DEPC water	variable

9 μ l of mix was aliquoted in a special designed capillary and 1 μ l of sample RT (prepared using random hexamers) was used in Light Cycler PCR reaction. The Light Cycler PCR run is divided into five steps. They include: hot start, denaturation, amplification, melting curve analysis and cooling. After the end of a run, the samples were soaked at 4°C. The Light Cycler PCR reaction for the housekeeping genes (S14) were generated in the same manner as the reaction for the sample.

2.7 Northern Blot

2.7.1 Principle:

Total RNA molecules are separated on agarose gel using electrophoresis, the separation is based on the size of RNA where the small molecules run faster than the large one. The separated RNA is transferred to a membrane (nylon filter), which allows repetitive use and easier accessibility. Once RNA is transferred on membrane, the target mRNA can be detected by hybridisation probe with a base sequence complementary to all, or a part, of the sequence of such mRNA. The technique provides semi-quantitative information about RNA. The location of a signal (binding between probe and its target) indicates the presence of the target sequence and the intensity of the signal, as well as reflects the activity or abundance of that target.

2.7.2 Methods:

2.7.2.1 Electrophoresis

After experimental treatment, RNA was extracted and quantitated, RNA was loaded on 1% agarose (0.66 formaldehyde) denaturing gel. The gel was prepared by dissolving 2g agarose in 170 ml DEPC water using a microwave. The boiled gel was left to cool slightly, an accurate amount of 10X MOPS, 40 % of formaldehyde and 1 mg/ml ethidium bromide were added to the gel. The gel was mixed gently and poured in a large tray (20x20 cm) in the fume hood. Once the gel was solidified, the tray was put in the tank and 1X MOPS with 1 mg/ml ethidium bromide were added (Running buffer). The 10 ug of RNA sample was prepared with loading buffer and heated at 55°C for 15 minutes. The loading dye (5 uL) was added to the sample. The mixed sample was loaded into gel along side with a DNA marker (pGEM® from Promega). The gel run at 60 volts for an hour to run the sample in the gel, followed by 30 volts overnight.

2.7.2.2 Blotting

The gel was observed under UV light to check run was acceptable and that RNA loading was equal. The gel was transferred to a Pyrex dish and rinsed twice with DEPC water for 20 minutes with gentle shaking (to remove excess formaldehyde) and the gel was equilibrated in 10x SSC buffer for 10 minutes. The blotting tools were prepared as follows. A platform was made in a Pyrex dish using four rubber bungs and a glass plate. The glass plate was covered with a 3MM Whatmann paper reached and touch down the base of the dish that it formed a wick. 500 mls of 10x SSC was poured on top of the paper. Air bubbles were removed by rolling a glass rod over the paper. The three

sheets of 3 MM Whatmann paper presoaked with 10x SSC buffer were placed on the top of the wick. The gel was positioned at the centre on the top of the paper, and the membrane (Hybond N, Amersham, UK) placed on top of the gel. Air bubbles were removed as mentioned above. Another 3 sheets of 3MM Whatmann paper were placed on the top of the membrane. A stack of absorbent paper towels were placed on top of the Whatmann paper, and saran wrap was placed up to each side of the gel to prevent liquid short circuit between the paper towels and the lower 3MM sheets. A glass plate was placed top of the towels, and compressed with a 500g weigh. Transfer was allowed to proceed overnight. The RNA was fixed onto membrane by heating at 80°C for 2 hours. Alternatively the filter was exposed to UV light cross linker. The filter was sealed in a plastic bag and stored at 4°C until required.

2.7.2.3 Hybridisation

The principle of hybridisation that DNA probe to be labelled is first denatured and then mixed with oligodeoxyribonucleotides of random sequence. These random oligomers anneal to random sites on the DNA and then serve as primers for DNA synthesis by a DNA polymerase. With labelled nucleotide(s) present during this synthesis, labelled DNA is generated. Each kit contains predispensed reaction mixes, which are compressed into a bead. Ready-To-Go DNA labelling beads (dCTP) from Amersham and [α -³²P]dCTP were used for labelling probes.

The membrane was placed in a hybridisation tube RNA side facing inwards. The filter was prehybridised by ULTRAhyb hybridisation buffer (Ambion, UK) at 42°C for 30 minutes. 25-50 ng of DNA template was diluted to 45 ul with Tris-EDTA (TE) buffer and denatured at 95-100 °C for 5 minutes. After incubation the denatured DNA was chilled in ice for 5 minutes. The reaction mixed bead was reconstituted with denatured DNA then 5ul of [α -³²P]dCTP was added to the reaction. The sample mix was placed at 37°C for 5-15 minutes. The probe was push through NucTrap purification column from Stratagene, to remove unincorporated nucleotides and reduce background noise. The process was performed according to the manufacturer's description. The probe was added in a hybridisation tube and incubated overnight.

2.7.2.4 Post-Hybridisation

The following day, the hybridisation buffer was discarded and the membrane was washed with washing buffer at several dilutions. The washing started from low stringency and gradually increased stringency. The membrane was washed twice for 5

minutes with 2X SSC, 0.1% SDS followed by two washes for 5 minutes with 1X SSC, 0.1% SDS. The membrane was further washed twice for 5 minutes with 0.1X SSC, 0.1% SDS. The membrane was carefully monitored in between washes to achieve the appropriate radioactive level (20-50 count per minute). The filter was sealed in a plastic bag and exposed to two films from Kodak over night or longer in -70°C . The films were developed and the band was verified through measurements of distance relative to the DNA marker and /or the ribosomal bands.

2.7.2.5 Striping the Membrane

The membrane striping removes probe and gives opportunity of using the filter for multiple hybridisation with different probes. The membrane was placed in pyrex dish and washed with boiling 0.5% SDS with agitation and allowed to cool to room temperature. The washing was repeated as necessary to make sure the filter was ready for reuse.

2.8 Western Blotting.

2.8.1. Protein extraction and quantitation

Following appropriate treatment, 5×10^6 cells were harvested by centrifugation at 1200 rpm for 5 min followed by three washes in 1x PBS and the pellet was stored at -80°C until use. The cells were resuspended in 200 μl of lysis buffer (100 mM NaCl, 10 mM Tris-HCL (pH 7.2), 2mM EDTA, 0.5% (w/v) sodium deoxycholate and 1% Nonidet P40) and pipetted up and down. Samples were sonicated for 10 seconds on ice to shear DNA and reduce sample viscosity. The lysate was centrifuged at 16,000 x g for 5 minutes at 4°C . The supernatant (protein) was transferred to a fresh microcentrifuge tube and kept on ice or stored at -70°C until use.

The protein concentration was determined using Bio-Rad DC protein assay kit (Bio-Rad Laboratories Ltd). The principle of the protein assay is based on a reaction between protein and copper in an alkaline medium, and followed reduction of folin reagent by the copper-treated protein. The colour formed was measured at absorbance of 750 nm. A brief description of the procedure, a "working reagent A" was prepared by adding 20 μl of reagent S to each ml of reagent A that would be required to complete the run. 5 μl of bovine serum albumin standard (ranging from 0–1000 $\mu\text{g}/\text{ml}$) or sample lysate was added to 25 μl of working reagent A. 200 μl reagent B was added followed by gentle mixing and incubation at room temperature for 15 minutes. Absorbance was determined at 750 nm within 1 hour.

2.8.2 Sodium Dodecyl Sulphate-Polyacrylamide Gel Electrophoresis (SDS-PAGE).

Electrophoresis was performed using the NuPAGE[®] electrophoresis system using XCell SureLock[™] Mini-Cell obtained from NOVEX (Invitrogen experimental technology, Frankfurt, Germany). This system is based upon a Bis-Tris-HCL buffered (pH 6.4) 10% polyacrylamide 10 mm gel run under reduced conditions with 3-(N-morpholino) propane sulphonic acid (MOPS) running buffer. Samples of protein lysate with equal protein concentrations were mixed with, 12.5 μl of 4X NuPAGE[®] LDS (lithium dodecyl sulphate) sample buffer and 5 μl NuPAGE[®] reducing agents to a final volume of 50 μl . The mixture was vortexed and then heated at 70°C for 10 minutes and centrifuged briefly before being placed on ice. The appropriate volumes of samples (20 μl) were loaded to each well of the gel 10% SDS PAGE gel using extra fine tips. Also molecular weight marker (magic mark) was loaded in one of the wells.

Electrophoresis was carried out and the proteins separated at 200V for 50 minutes using NuPAGE® SDS MOPS running buffer at room temperature.

2.8.3 Electro blotting

Once the electrophoresis was finished, the gel cassette was carefully opened and the gel allowed to rest on the larger plate. A pre-soaked filter paper was placed on top of the gel and the plate was turned over, the gel was then separated from the plate. The surface of the gel was wetted and a pre-soaked (in pure Methanol for 1h) polyvinylidene difluoride (PVDF) membrane put on the gel. Another pre-soaked filter paper was placed on top of the transfer membrane and air bubbles were removed using a glass rod. The gel membrane assembly was then placed on two soaked pads that were placed on the blot module. Another two pre-soaked pads were placed on top so that the gel-membrane assembly was sandwiched between the pads. The blotting assembly module was placed in XCell SureLock™ Mini-Cell tank and filled with NuPAGE™ transfer buffer until the gel-membrane sandwich was just covered with the transfer buffer. The outer chamber was filled with ultra pure water, and the gels were electroblotted at 30V for 60 minutes.

2.8.4 Blocking the membrane and antibody probing

PVDF membranes were washed twice with 20 ml of 1 x TBS-T washing buffer (24.2 g Tris base, 80g NaCl and 10% Tween-20) on rotary shaker before incubation in 10 ml blocking buffer (1 x TBS-T and 5% Bovine serum albumin) for 60 minutes. The membranes were then washed twice and incubated with primary antibodies diluted 1:1000 in 10ml blocking buffer overnight at 4⁰C. Thereafter, the membranes were washed three times, five minutes each in antibody washing buffer before were incubated for 30 minutes with secondary antibodies (anti rabbit-HRP or mouse-HRP) diluted 1:50000/or 1:100000 respectively. The membranes were washed three times, washing five minutes each in washing buffer before they were washed once with ultra pure water. The excess of water was taken from the membranes using filter paper before the membranes were developed using ECL advance detection kit according to the protocol supplied by Amersham. Finally, the chemiluminescence's signal was detected with KODAK X-ray photographic films (Amersham) that were exposed for 30 seconds to 5 minutes. The films were developed with 20% (v/v) developer and were fixed using fixing agents (Sigma). The films were dried and the bands for interest proteins were identified by comparison with molecular weight markers.

2.8.5 Membrane stripping and re-probing

In some circumstances membranes were stripped of antibody and re-probed. For efficient stripping, membranes were incubated in stripping buffer (15g glycine, 10% sodium azid, 100% HCL and 10% Tween-20) for 2 hours at 80°C with shaking. Stripping buffer was removed away by washing membrane thrice with washing buffer. Membranes were blocked for 1 hour with blocking buffer before re-probing with new antibodies.

CHAPTER 3

Effect of LPAAT- β Inhibitors on AML LPAAT β Enzyme Activity and cell Proliferation

3.1 Introduction

The coordination and balance between cell proliferation and apoptosis is crucial for normal development and tissue-size homeostasis in normal individuals. Cancer results when clones of mutated cells survive and proliferate inappropriately, disrupting this balance. One mechanism for maintaining size homeostasis is a requirement for factor-dependent signalling from the environment for cell survival (Raff 1992).

Cells that exhaust local supplies of these factors or that move to new locations away from the source will die. Although this mechanism of growth control is certainly part of the story, it is not sufficient to limit the expansion of clones that have a proliferation- or survival-promoting mutation. This is because either kind of mutation would be expected to cause an increase in the number of mutant cells relative to their normal neighbours (Guo & Hay 1999).

LPAAT- β is a family of intrinsic membrane enzymes that catalyse the de novo biosynthesis of PA, an essential component of a number of signal pathways as well as a critical intermediate in the synthesis of cell membranes. LPAAT- β may play a role in functions critical to tumour cell growth and survival. LPAAT- β mRNA was found to be elevated in many solid tumour cells including uterus, fallopian tube and ovary. LPAAT- β was also detected in myeloid cell lines THP-1, HL60, and U937 with mRNA levels remaining the same with or without phorbol-ester treatment (Coon et al. 2003; Leung 2001; Leung, et al. 1998). We hypothesise that this enzyme is also over expressed in AML and conversely, that inhibition of LPAAT- β activity may lead to effects on PA production and hence effect cell signalling particularly the ras/raf/Erk and PI3K/Akt/mTOR pathways. These two pathways are known to play roles in cell proliferation and apoptosis in AML.

Understanding the role that LPAAT- β may play in functions critical to tumour cell growth and survival has prompted us to use small molecular compound inhibitors (LPAAT- β inhibitors). These inhibitors were found to inhibit LPAAT- β in a cell-free and the cellular assay measuring PM formation (see explanation of assay in chapter 2), high-throughput assays led to the discovery of a group of isoform-selective inhibitors with IC₅₀ (inhibitory concentration 50%) values in the nanomolar concentration range. These inhibitors were found to inhibit proliferation of a large variety of tumour cell lines with IC₅₀ values at nanomolar concentrations (Bonham et al. 2003). The inhibitors used in our

study belong to diamino-diaryltriazines group. Exemplars of this group of compound were CT32228, CT32212, PC020701 and PC020702.

In this study, a radio enzymatic assay was used. This assay measures the production of ¹⁴C-labelled phosphatidylmethanol (PM) by the addition of ¹⁴C-labelled oleate and the pseudo substrate, lysophosphatidylmethanol (lysoPM). ¹⁴C-labelled PM production represents enzyme activity. Analogous experiments with the natural, preferred substrate for LPAAT, LPA, are not possible for two reasons: the doubly charged head group of LPA will not translocate across the membrane; and the action of lipid phosphate phosphatases rapidly metabolises lysoPA to monoacylglycerol (Waggoner et al. 1996). This “in cell” enzyme assay can detect PM formation in AML cell lines, suggesting that this assay might be used to monitor LPAAT-β enzyme activity.

In this chapter we are going to discuss in detail the effect of LPAAT-β inhibitors on AML LPAAT-β enzyme activity, and AML cell proliferation and viability.

3.2 Material and Methods

A detailed description of LPAAT- β enzyme assay can be found in section (2.2). Also a detailed description of cell counting can be found in section (2.1.6). The following sections will describe briefly the exact setting for these experiments.

3.2.1 Cell lines and treatment

Four different acute myeloid leukaemia cell lines were used in this study representing different responses to ATRA. The first cell line was NB4, which represent the AML/M3 according to FAB classification. NB4 differentiates to granulocytes upon ATRA treatment and maintain the PML/RAR α transcript. NB4:R2 cell line was the second cell line used in this study, they do not respond to ATRA and express a mutated form of PML/RAR α . The third cell line was HL60, which also represent the AML/M3. HL60 cells differentiate in response to ATRA and lacks the PML/RAR α translocation. The HL60-R cell line was the fourth cell line used in this study, these do not respond to ATRA.

For LPAAT- β enzyme assay, NB4 and NB4:R2 cells were used. Each cell line divided into three flasks, one for untreated (control) and two for treated (test). The tests flasks were treated for 24 and 48 hours with 25 nM of LPAAT- β inhibitor (PC020702). On the day of labelling, 1×10^6 cells were harvested and resuspended in 0.48 ml of fresh medium.

For 1 hour LPAAT- β enzyme assay, NB4, NB4:R2, HL60 and HL60-R cells were used. Each cell line divided into two flasks, one for untreated (control) and one for treated (test). The tests flasks were treated for 1 hour with 250 nM of LPAAT- β inhibitor (PC020702). On the day of labelling, 1×10^6 cells were harvested and resuspended in 0.48 ml of fresh medium.

For proliferation and viability experiments, NB4, NB4:R2, HL60 and HL60-R cells were used. Each cell line divided into five flasks, one for untreated (control) and four for treated (test). The four tests flasks were treated for 96 hours with LPAAT- β inhibitors (two with inactive form and two with active form). The cells were subcultured after 48 h. All five flasks for each cell line were gassed and incubated at 37°C and 5% CO₂.

3.3. In cell LPAAT- β enzyme Assay

3.3.1. The effect of PC 020702 inhibitor on LPAAT- β enzyme activity in AML cells

The ability of LPAAT- β to acylate LPA to form PA was tested by exposure NB4 and NB4:R2 cells to the 25nM of PC020702 inhibitor for 24 and 48 hours. In the presence of [14 C]-labeled oleate, as an Acyl-CoA donor, the LPAAT- β enzyme exhibits a high specificity for LPM as a substrate to produce PM and this was used to assay the LPAAT- β enzyme activity. To identify the products of the reaction, one-dimensional TLC was used to separate them (**Fig. 3.1 and 3.2**). 14 C-PM was interpreted as the results of the LPAAT- β enzyme activity after inhibitor induction.

Figure 3.1 and 3.2 shows lipids separation of treated and untreated NB4 and NB4:R2 cells respectively. Figure (A) left is for 24 hours and (B) right for 48 hours treatment. The untreated cells were done in replicates (0h and 24 h). The red arrow shows the spots of PM, which is consistent with standard PM spots visualized after sprayed with Primulin and exposed to Ultra Violet light as described in Material and Methods (data not shown). Small black arrow indicates a minor but unidentified spots that were observed. The upper spots co-migrating (large arrow at the top of the plate) with un-incorporated [14 C]-labeled oleate and LPM, that are consistent with standard LPM spots after sprayed with Primulin and exposed to Ultra Violet light (**Figure 3.3**). This upper lane was therefore named as (14 C)-labeled Neutral lipids.

Figure 3.3 (A) shows LPM standard after sprayed with Primulin (**Figure 3.3 (A)**). The LPM spot was migrated to the top of the plate which indicates the position of LPM after development. In the absence of LPM, no 14 C-PM was detected. The radioactive spot of non-incorporated [14 C]-oleate was found at the top of the plate with 14 C -neutral lipids (**Figure 3.3 (B)**). This indicates that LPM substrate is sensitive and specific to LPAAT- β enzyme.

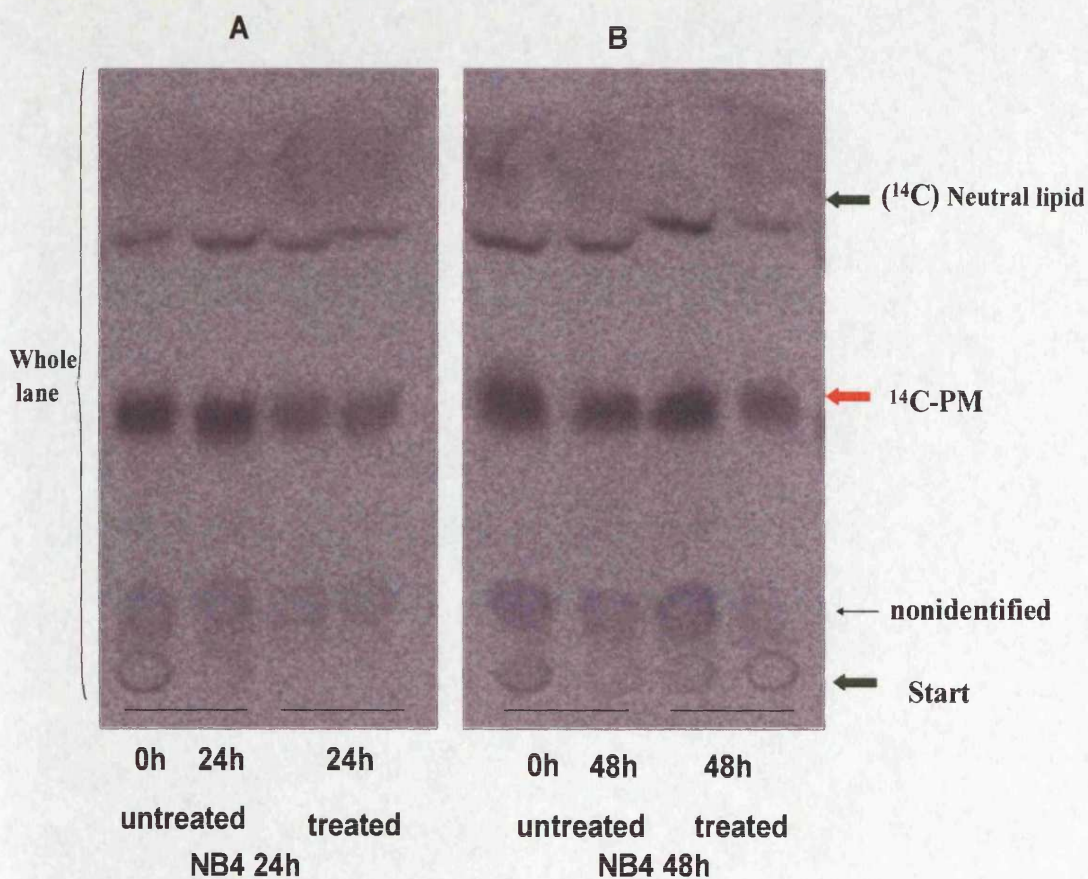


Figure 3.1. LPAAT- β acylation of LPM to form ^{14}C -PM. NB4 cells were treated for 24 h (A) and 48 h (B) with 25 nm of LPAAT- β inhibitor (PC020702). At the day of labelling, 10^6 cells were incubated for 20 minutes with 50 μM of LPM along with 25nM of LPAAT- β inhibitor. Then the cells were incubated for 30 minutes with 0.4 μCi of ^{14}C -oleate, as described in material and methods. One-dimensional TLC separated the products of the reaction and the Storm Imager as described in material and methods measured ^{14}C -PM intensities.

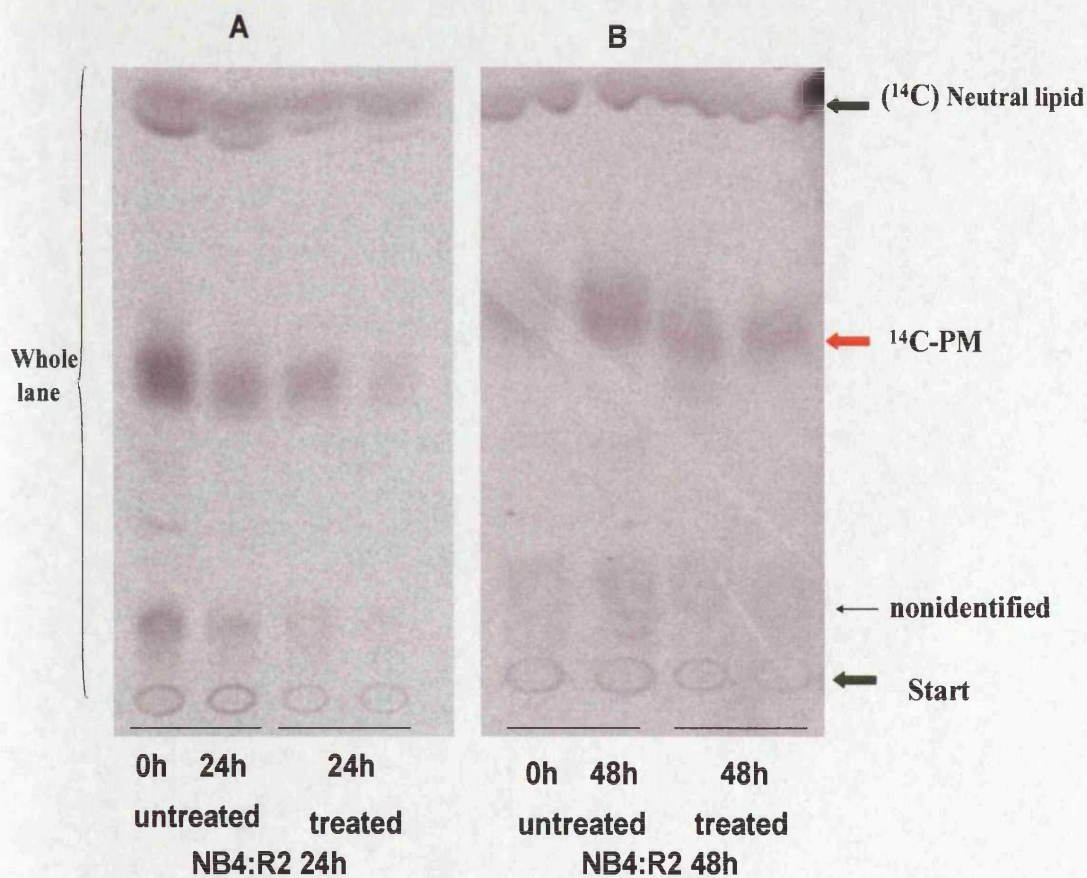


Figure 3.2 LPAAT-β acylation of LPM to form ¹⁴C-PM. NB4:R2 cells were treated for 24 h (A) and 48 h (B) with 25 nm of LPAAT-β inhibitor (PC020707). At the day of labelling, 10⁶ cells were incubated for 20 minutes with 50 uM of LPM along with 25nM of LPAAT-β inhibitor. Then the cells were incubated for 30 minutes with 0.4 μCi of ¹⁴C-oleate, as described in material and methods. One-dimensional TLC separated the products of the reaction and Storm Imager as described in material and methods measured ¹⁴C-PM intensities.

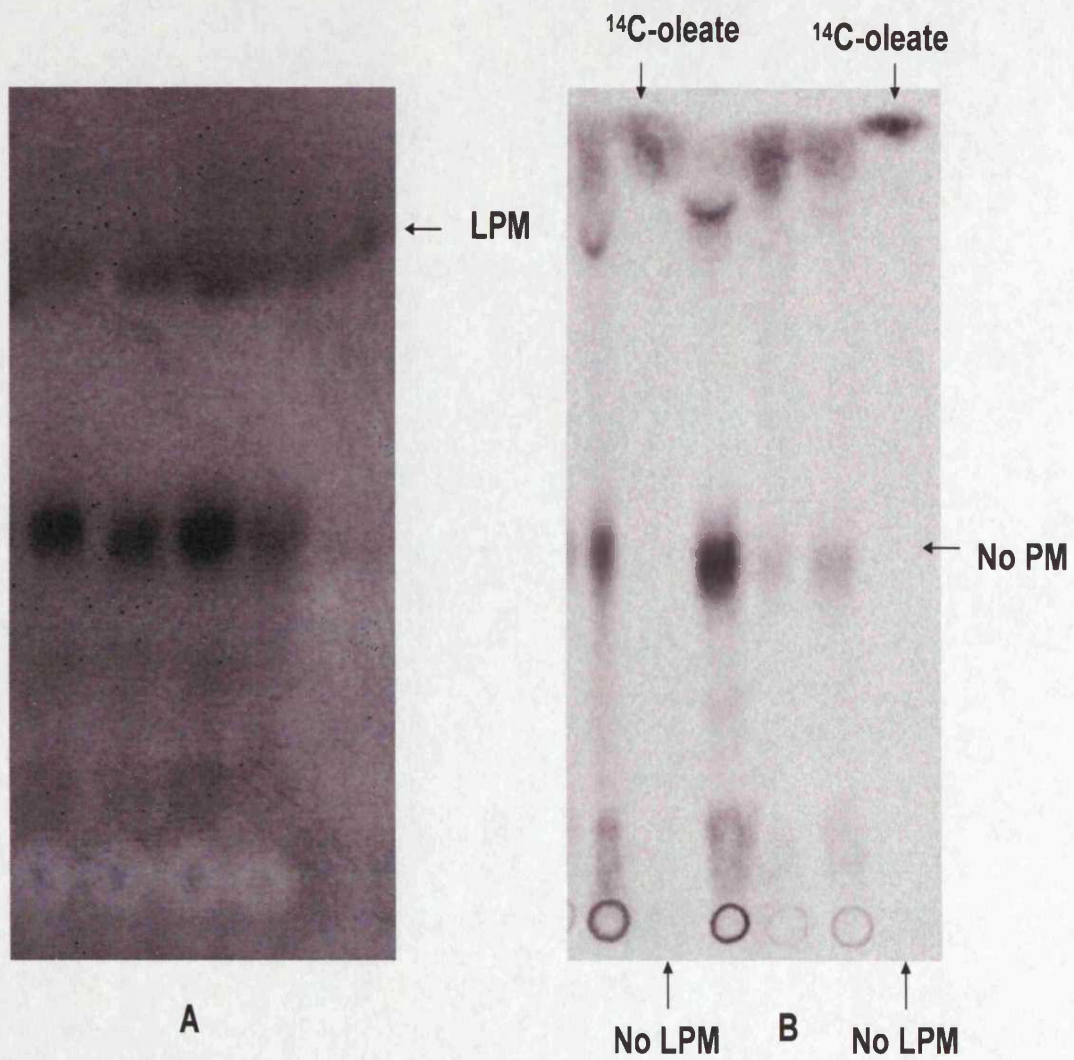


Figure 3.3 LPM spots position. Figure (A) shows LPM position after TLC plate was sprayed with Primulin and exposed to UV light. Figure (B) right shows no ^{14}C -PM production in the absence of LPM and the un-incorporated ^{14}C -oleate migrates to the top of the plate.

3.3.1.1 The effect of PC020702 inhibitor on LPAAT- β enzyme activity in NB4 cells

ImageQuant software was used to quantitating the relative pixel volume of the ^{14}C -PM bands. The software tools were used to outline ^{14}C -PM spots and whole line spots. Then the background was corrected by choosing "Local Median" (ImageQuant determines the median (middle value) of all the pixel values in the object outline and uses this value for the background). ImageQuant software was further saved relative pixel volume data in Excel file. The ^{14}C -PM spots percentage were calculated by the following equation:

$$^{14}\text{C-PM \%} = \left(\frac{^{14}\text{C-PM spots relative pixel volume}}{\text{whole lane relative pixel volume}} \right) \times 100$$

A slight but non significant difference was seen between 0h time ($P > 0.05$) and 24 hours and 48 hours in untreated cells, which may indicates LPAAT- β not changing during cell growth or at least at 24 hours and 48 hours compared with 0 hour. LPAAT- β activity showed a decreased in its activity in NB4 cell line after 24 hours of treatment, more than at 48 hours. The activity of the enzyme was inhibited to about 50 % and 15% after PC020702 induction for 24h and 48 h respectively. The results showed a statistically significant inhibition of enzyme activity between untreated and treated cell after 24 h of PC-020702 induction ($P = 0.034$), however no statistically differences were seen between untreated and treated after 48 h ($P > 0.05$) (Figure 3.4).

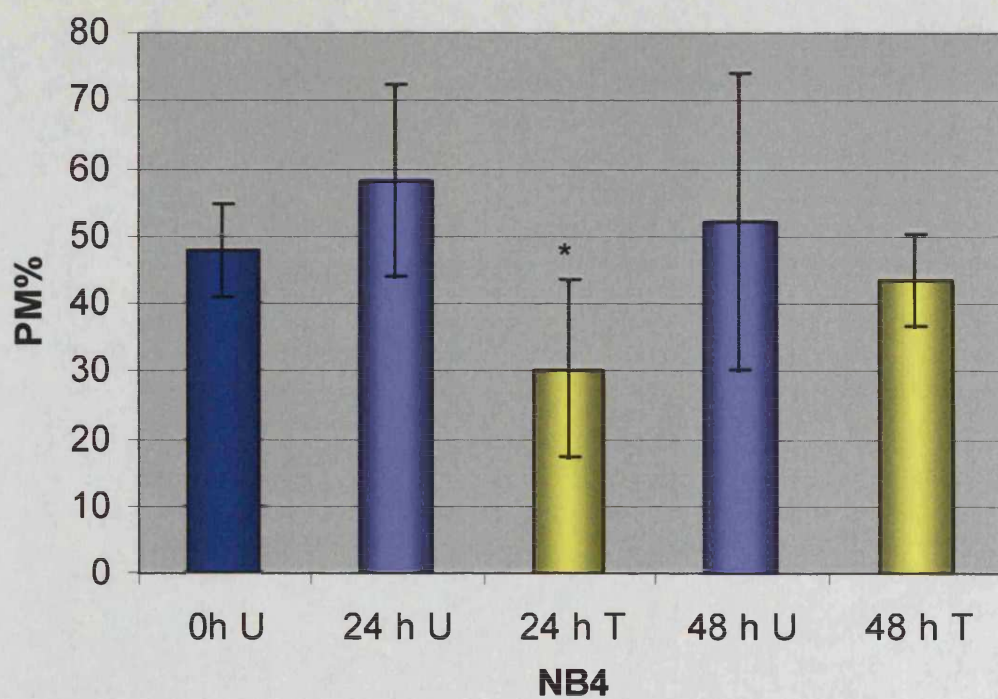


Figure: 3.4. The effect of LPAAT inhibitor on NB4 enzyme Activity. NB4 cell were treated with LPAAT- β inhibitor (PC020702) at 25 nM (2.5×10^{-8} M) for 24h and 48h. The enzyme activity was assayed by radioenzymatic assay. The student T-test was used to calculate P value, which $P=0.034$ for 24 h. The symbol (*) represents the P value for NB4 after 24h treatment. The results are given as a mean percentage of ¹⁴C-PM \pm Standard Deviation (SD). The label (U) is for untreated, (T) is for treated cells.

3.3.1.2 The effect of PC020702 inhibitor on LPAAT- β enzyme activity in NB4:R2 cells

NB4:R2 cell also showed a decreased in enzyme activity after LPAAT- β inhibitor induction for 24 hours and 48 hours. The activity of the enzyme was inhibited to about 45-39% and less than 15% after PC020702 induction for 24h and 48 h respectively. The results show a statistically significant inhibition of enzyme activity between untreated and treated cells after 24 h ($P= 0.044$), however no statistically significant inhibition was seen between untreated and treated after 48h ($P>0.05$) (Figure 3.5).

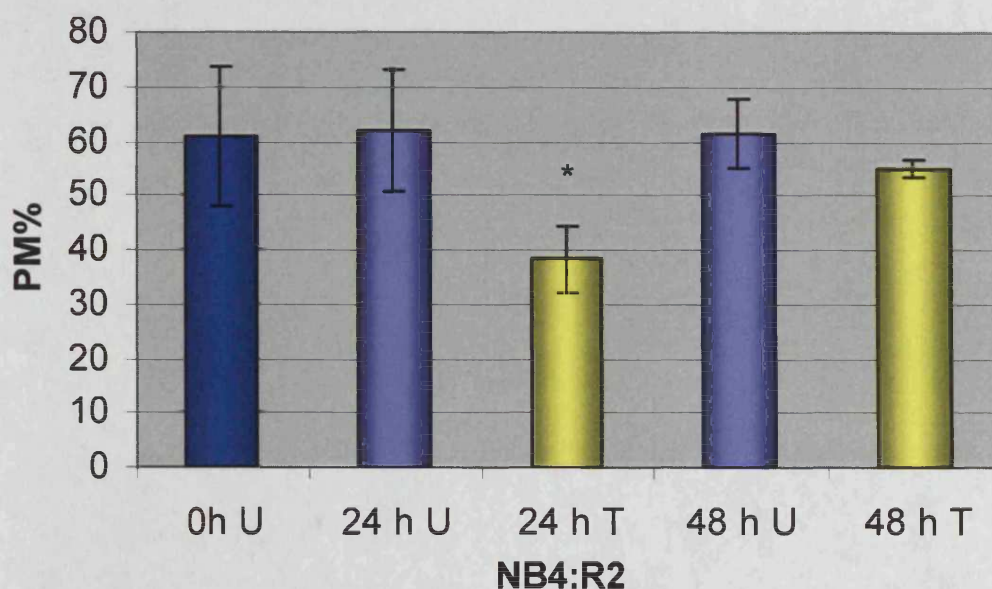


Figure: 3.5 The effect of LPAAT inhibitor on NB4:R2 enzyme Activity. NB4:R2 cell were treated with LPAAT- β inhibitor (PC020702) at 25 nM (2.5×10^{-8} M) for 24h and 48h. The results are given as a mean percentage of ¹⁴C-PM \pm Standard Deviation (SD). The enzyme activity was assayed by radioenzymatic assay. The student T-test was used to calculate P value, which $P= 0.044$ for 24 h. The symbol (*) represents the P value for NB4 after 24h treatment. The label (U) is for untreated, (T) is for treated cells

In order to correct for any possible difference in the amount of sample loading in different lanes, the whole lane were expressed as relative pixel volume. The whole lanes were affected with treatment after 24 h and 48h. This may indicate that long exposure of the drugs may affected cell uptakes to LPM and ^{14}C -oleate (**Figure 3.6 & 3.7**). Because of the 48 h results and the whole lane relative pixels volumes were affected compared with untreated to treated cells. Therefore we decide to see the effect of the LPAAT- β inhibitor on enzyme activity after 1 hour of treatment.

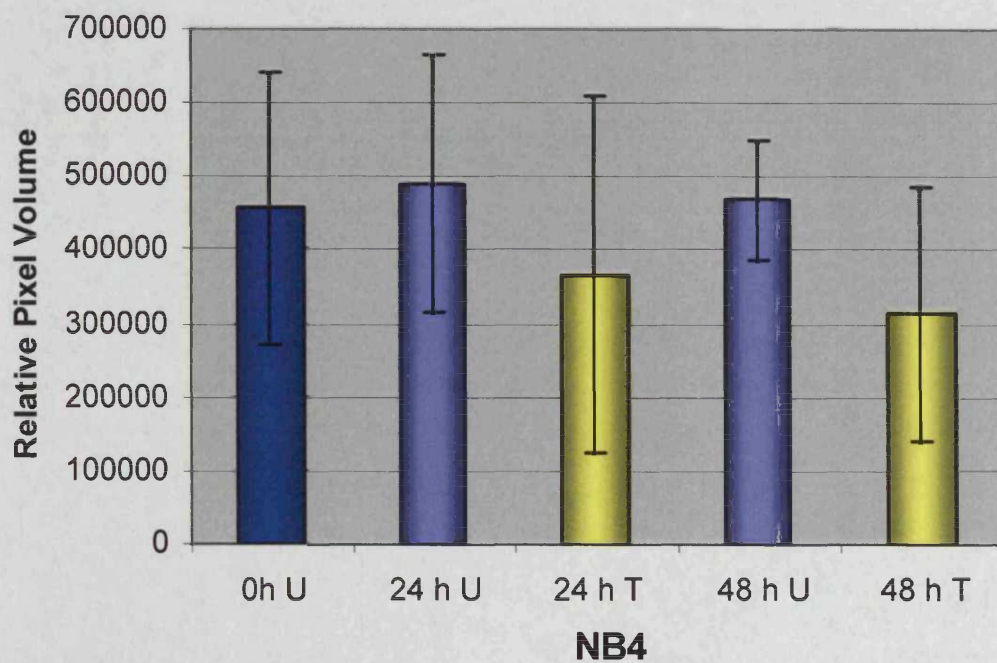


Figure 3.6 The whole lane expression in NB4 cells for the treated and untreated cell. The results are given as a mean of relative pixel volume \pm Standard Deviation (SD). The label (U) is for untreated, (T) is for treated cells

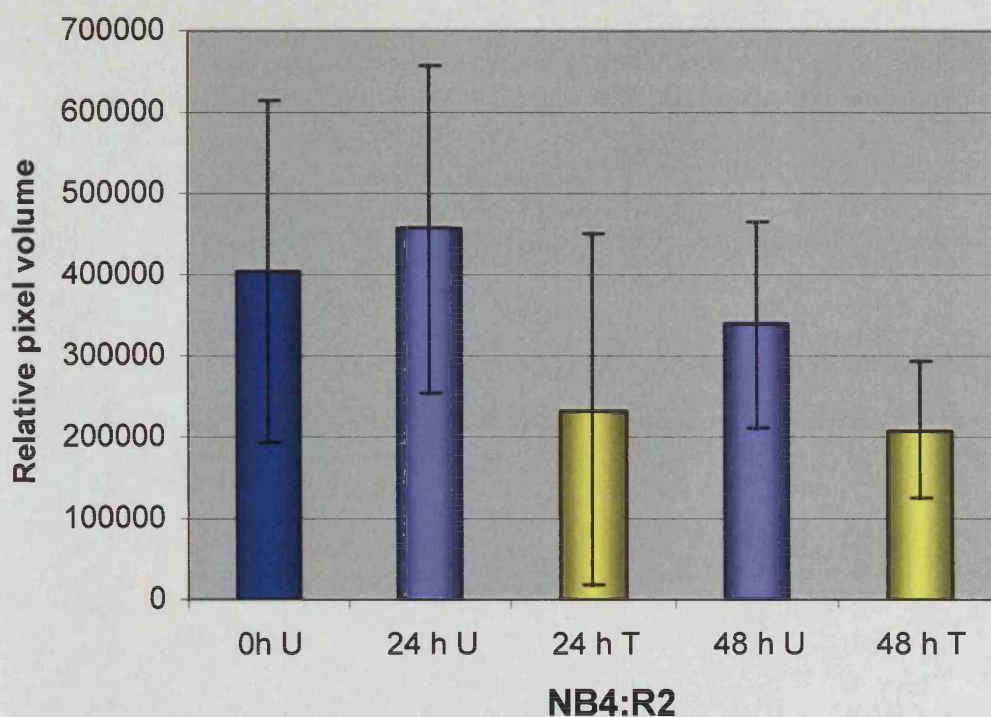


Figure 3.7 The whole lane expression in NB4:R2 cells for the treated and untreated cell. The results are given as a mean of relative pixel volume \pm Standard Deviation (SD). The label (U) is for untreated, (T) is for treated cells

3.3.1.3 The effect of PC020702 inhibitor on LPAAT- β enzyme activity in NB4, NB4:R2, HL60 and HL60-R cells

The cells sensitive and resistant to ATRA were treated with PC020702 for 1 hour. The TLC plate showed the same result as for the TLC plate for 24 h and 48 h (**Figure 3.8**). The activity of the enzyme was inhibited after incubation with 250 nM of PC020702 for 1 h in ATRA sensitive and resistant cells. 28 % and 15 % of the enzyme activities were inhibited in NB4 and NB4:R2 respectively. Where as HL60 and HL60-R cells showed about 15 %-10 % inhibition in enzyme activity after 1 hour of LPAAT- β inhibitor induction. This indicates that NB4 was more sensitive to inhibitor than NB4:R2 and HL60 was more sensitive to inhibitor than HL60-R. There were no statistical significant differences ($P > 0.05$) found between untreated and treated cells in all cell lines (**Figure 3.9**).

The relative pixel volumes of the whole lane were equally expressed in all cell line (**Figure 3.10**).

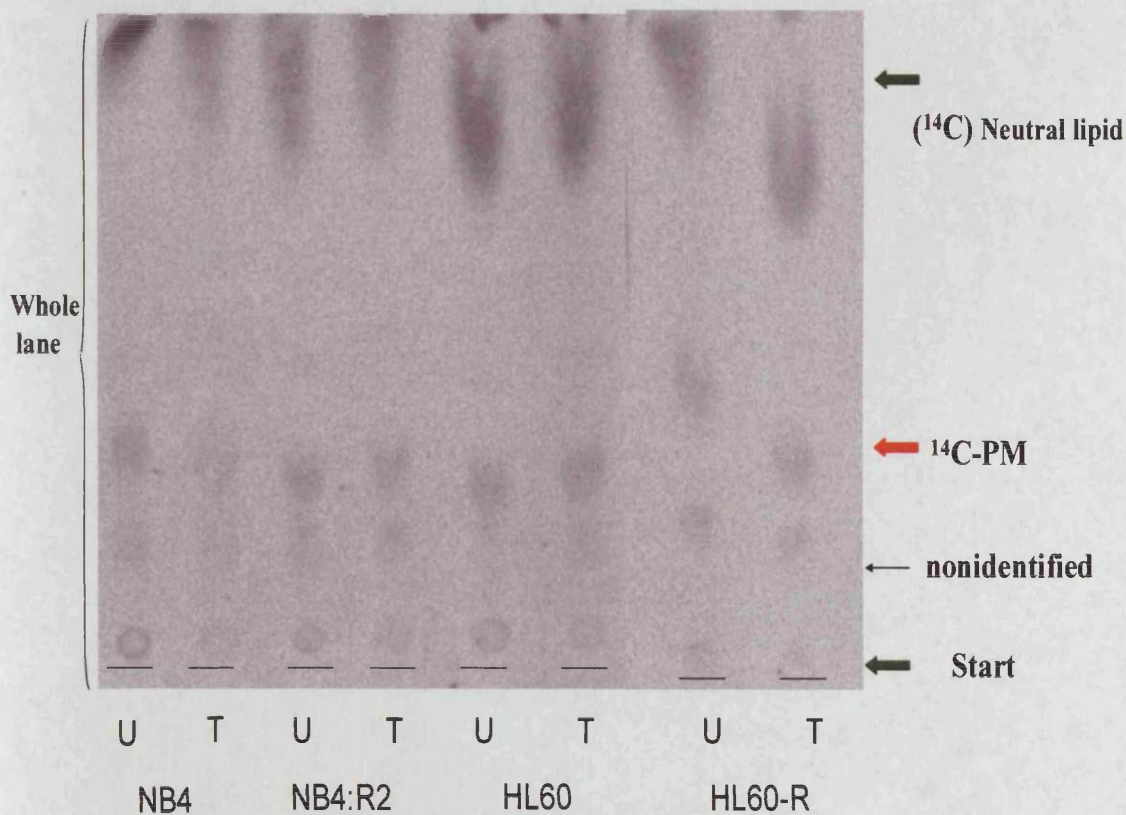


Figure 3.8 LPAAT- β acylation of LPM to form ^{14}C -PM. NB4, NB4:R2, HL60 and HL60-R cells were treated for 1 hour with 250 nM of LPAAT- β inhibitor (PC020707). At the day of labelling, 10^6 cells were incubated for 20 minutes with 50 μM of LPM along with 250 nM of LPAAT- β inhibitor. Then the cells were incubated for 30 minutes with 0.4 μCi of ^{14}C -oleate, as described in material and methods. One-dimensional TLC plate was used for phospholipid separation. Storm Imager was used to measure ^{14}C -PM intensities. The label (U) is for untreated, (T) is for treated cells.

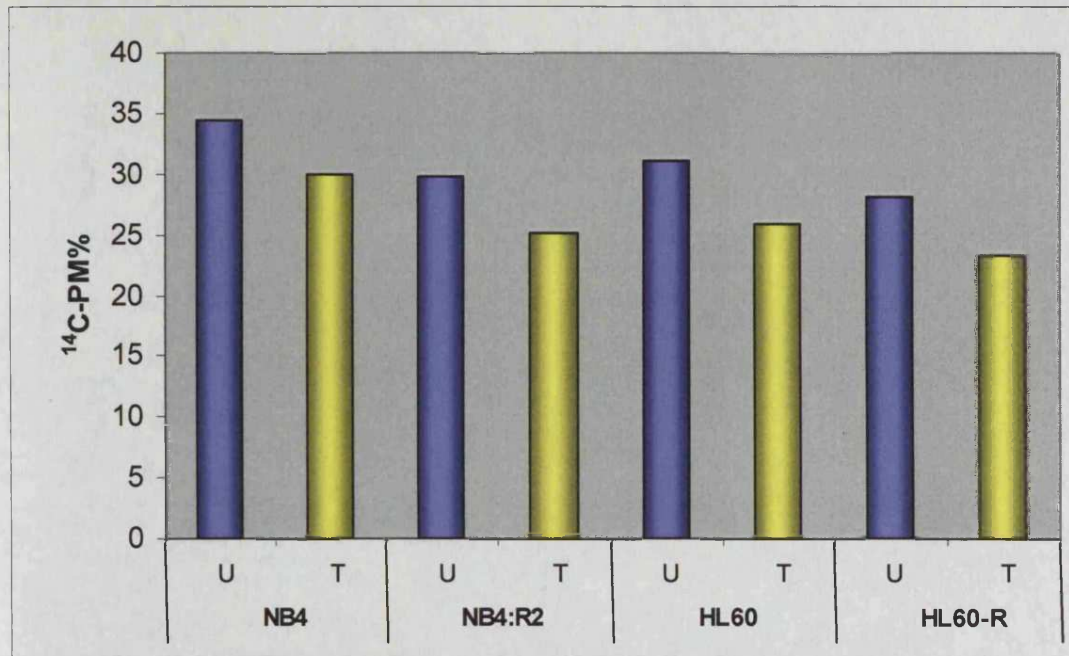


Figure: 3.9 The effect of LPAAT inhibitor on NB4, NB4:R2, HL60 and HL60-R enzyme Activity. Four AML cell lines (NB4, NB4:R2, HL60 and HL60-R) were treated with LPAAT- β inhibitor (PC020702) at 250 nM (25×10^{-8} M) for 1 hour. The results are given as a mean percentage of ¹⁴C-PM. The label (U) is for untreated, (T) is for treated cells

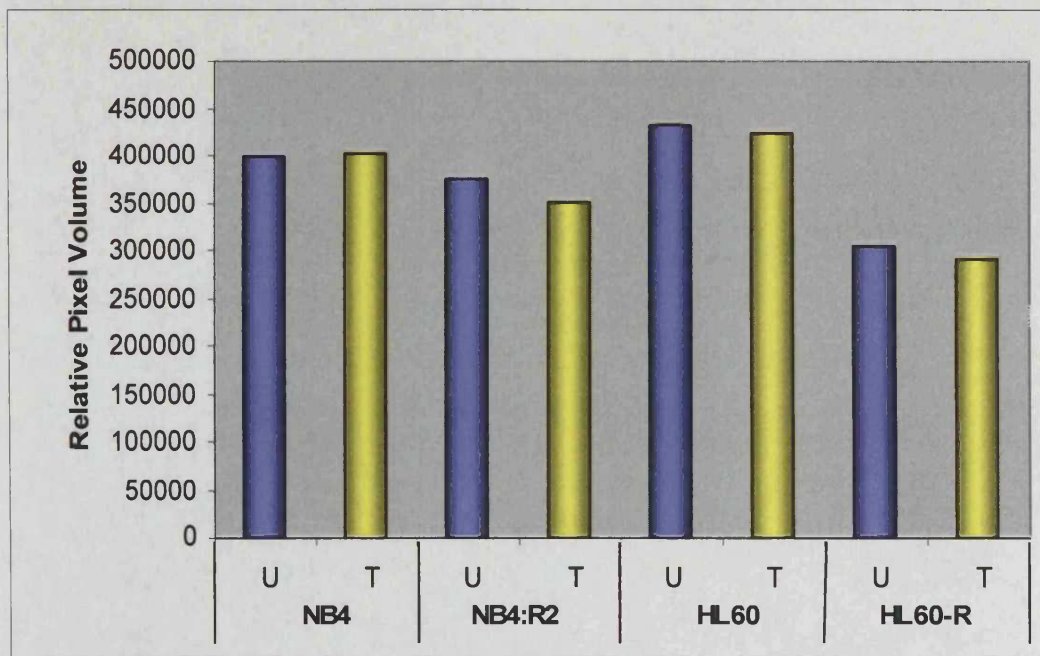


Figure 3.10 The whole lane expression in NB4, NB4:R2, HL60 and HL60-R cells for the treated and untreated cell. The results are given as a mean of relative pixel volume. The label (U) is for untreated, (T) is for treated cells

concentrations of LPAAT- β inhibitors (CT32228 and PC020702) were evaluated on ALL cells (NB4, NB4:R2, HL-60 and HL-60-R). All cells were exposed to the two inhibitors at different concentrations for 4 days. The following table summarizes cell lines and treatment used (Table 3.1 & 3.2)

No of flasks	NB4		NB4:R2	
	PC020702	CT32228	PC020702	CT32228
1	Untreated	Untreated	Untreated	Untreated
2	1 nM	50 nM	1 nM	50 nM
3	5 nM	100 nM	5 nM	100 nM
4	10 nM	250 nM	10 nM	250 nM
5	25 nM	500 nM	25 nM	500 nM

Table 3.1 the concentrations of the LPAAT- β inhibitors were used in proliferation and viability experiment in NB4 and NB4:R2.

No of flasks	HL60		HL60-R	
	PC020702	CT32228	PC020702	CT32228
1	Untreated	Untreated	Untreated	Untreated
2	1 nM	50 nM	1 nM	50 nM
3	5 nM	100 nM	5 nM	100 nM
4	10 nM	250 nM	10 nM	250 nM
5	25 nM	500 nM	25 nM	500 nM

Table 3.2 the concentrations of the LPAAT- β inhibitors were used in proliferation and viability experiment in HL60 and HL60-R.

3.4.1.1 The effect of PC020702 on NB4 and NB4:R2 proliferation

PC020702 at a low concentration of 10 nM started to inhibit proliferation and reached optimum inhibition at 25 nM by day four. The cell counts were less than 1×10^5 cells/ml compare to untreated control which were at 19×10^5 cells/ml by day 4 ($P = 0.014$).

PC020702 was shown to have a toxic effect on NB4:R2 cells as compared to untreated control. PC020702 started to inhibits cell proliferation at concentration 10 nM, with an optimum concentration of PC020702 at 25 nM compared to untreated control ($P=0.012$) (Figure 3.11).

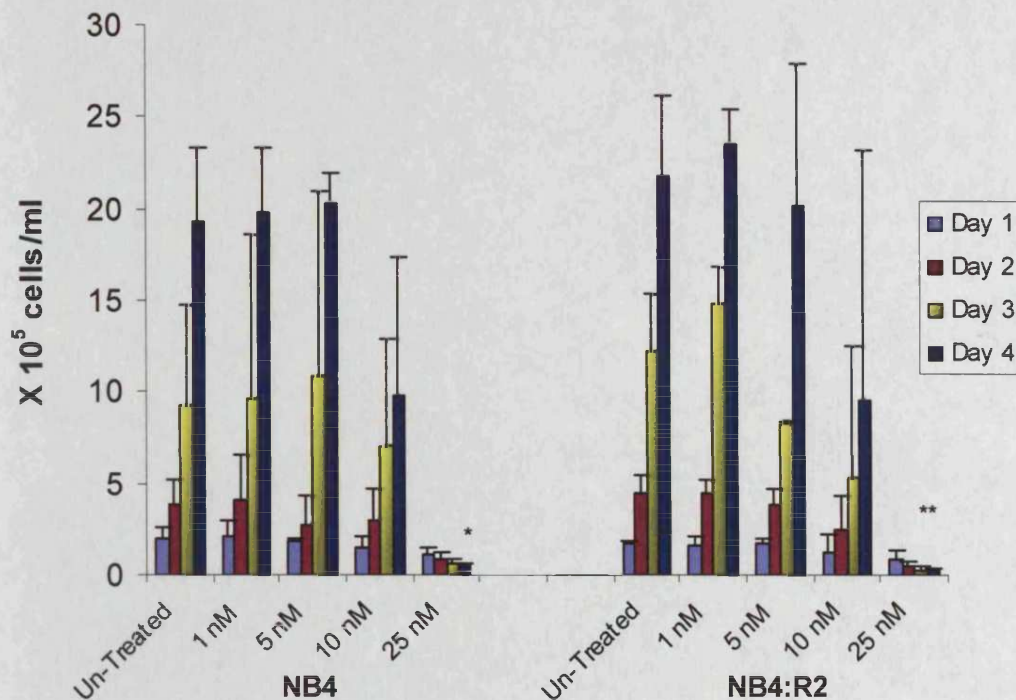


Figure 3.11 The effect of PC020702 on NB4 and NB4:R2 cell proliferation. NB4 and NB4:R2 cells were grown in RPMI medium with 10% FBS and incubated at 37°C with 5%CO₂, cells were treated for at least four days, at different concentrations of PC020702 LPAAT-β inhibitor. The proliferation of cells was measured every 24 hour by cell counting. The student T-test was used to calculate P value (* and **), which $P=0.014$ and 0.012 for NB4 and NB4:R2 respectively. Data are expressed as mean values + standard deviation obtained from at least three independent experiments.

3.4.1.2 The effect of PC020702 on HL60 and HL60-R proliferation

PC020702 at the optimum concentration 25 nM was sufficient to inhibit proliferation significantly by day 4 (with cell count of 5×10^5 cell/ml compared to 30×10^5 cells/ml of untreated HL60 ($P = 0.018$)). HL60-R cell proliferation was significantly inhibited at this concentration ($P=0.004$). For HL60-R the cell count was 2.5×10^5 cells/ml compared to 30×10^5 cells/ml for untreated HL60-R by day four. These results suggest that PC020702 had a toxic effect on sensitive and resistant cell lines in a time and dose dependent manner (Figure 3.12).

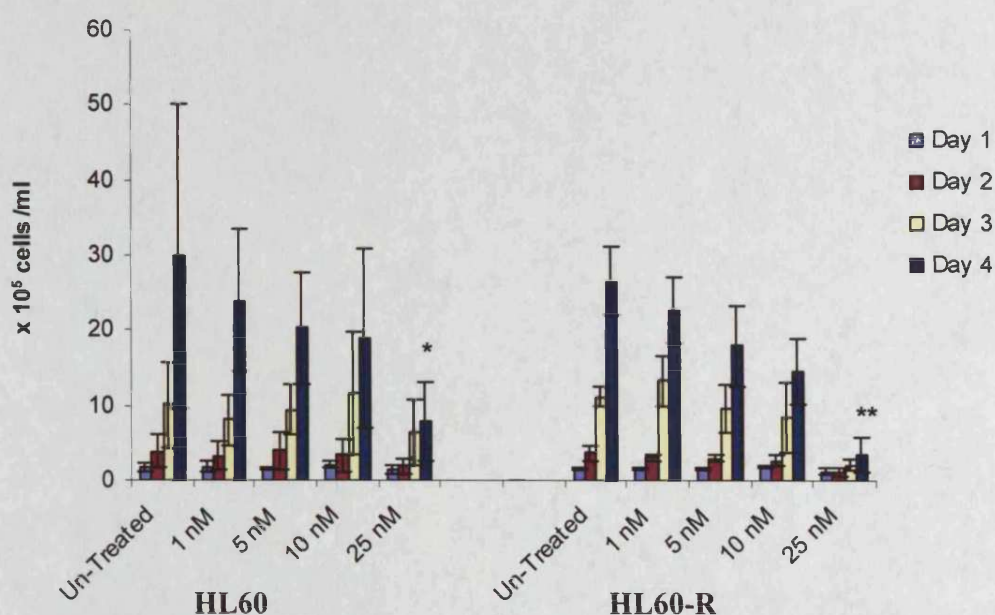


Figure 3.12 The effect of PC020702 on HL60 and HL60-R cell proliferation. HL60 and HL60-R cells were grown in RPMI medium with 10% FBS and incubated at 37°C with 5%CO₂, cells were treated for at least four days, at different concentrations of PC020702 LPAAT-β inhibitor. The proliferation of cells was measured every 24 hour by cell counting. The student T-test was used to calculate P value (* and **), which $P=0.018$ and 0.004 for HL60 and HL60-R respectively. Data are expressed as mean values + standard deviation obtained from at least three independent experiments.

3.4.1.3 The effect of CT32228 on NB4 and NB4:R2 cell proliferation

LPAAT- β inhibitor (CT32228) isoform is structurally different from PC020702. It was used for AML cell line treatment. CT32228 inhibited NB4 and NB4:R2 cell proliferation at different concentration. CT32228 at a concentration 50 nM was sufficient to inhibit NB4 cell proliferation by day 4. On day four, NB4 cell proliferation was significantly inhibited at concentration 100 nM ($P=0.037$). CT32228 was toxic to NB4:R2 cells also compared to untreated control. It was started to inhibits cell proliferation at concentration of 50 nM, and with maximal inhibition with CT32228 at 250 nM compared to untreated control ($P=0.031$) (Figure 3.13).

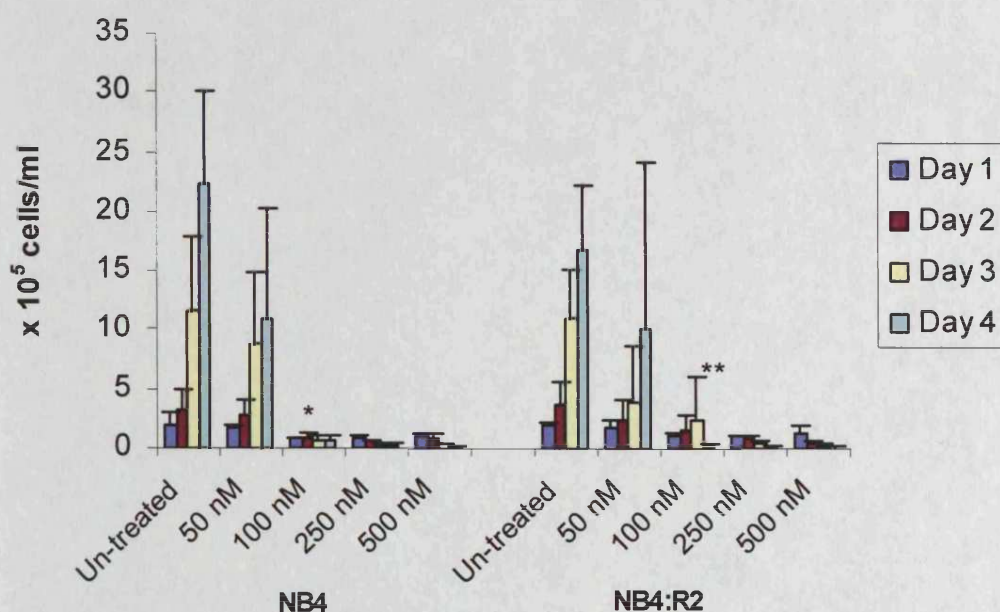


Figure 3.13 The effect of CT32228 on NB4 and NB4:R2 cell proliferation. NB4 and NB4:R2 cells were grown in RPMI medium with 10%FBS and incubated at 37°C and 5%CO₂, cells were treated for at least four days, with different concentrations of CT32228 LPAAT- β inhibitors. The proliferation of cells was measured every 24 hour by cell counting. The student T-test was used to calculate P value (* and **), $P=0.037$ and 0.031 for NB4 and NB4:R2 respectively. Data are expressed as mean values + standard deviation obtained from at least three independent experiments.

3.4.1.4 The effect of CT32228 on HL60 and HL60-R proliferation

LPAAT- β inhibitor CT32228 exhibited significant growth inhibition after 96 hours at a concentration of 100 nM in all HL60 and HL60-R cell lines tested ($P=0.0014$ and $P=0.005$ for HL60 and HL60-R respectively). CT32228 exhibited maximal inhibition at concentration of 250 nM (25×10^{-8} M) in both HL60 and HL60-R. Using 100 nM LPAAT- β inhibitor CT32228, HL60 and HL60-R cell proliferation decreased to $<10\%$ at 4 days compared with control cells (untreated). These results suggest that inhibitors of the LPAAT- β isoform were antiproliferative in ATRA sensitive and resistant AML cell lines *in vitro* (Figure 3.14).

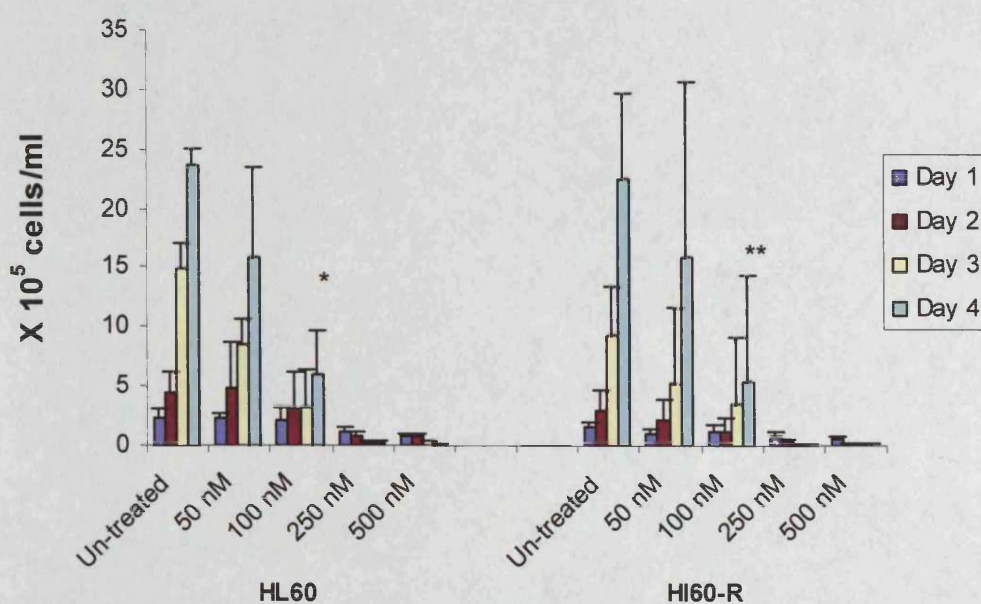


Figure 3.14 The effect of CT32228 on HL60 and HL60-R cell proliferation. HL60 and HL60-R cells were grown in RPMI medium with 10%FBS and incubated at 37°C with 5%CO₂, cells were treated for at least four days, with different concentrations of CT32228 LPAAT- β inhibitors. The proliferation of cells was measured every 24 hour by cell counting. The student T-test was used to calculate P value (* and **), which $P=0.0014$ and 0.005 for HL60 and HL60-R respectively. The results shown as mean + SD of cell count $\times 10^5$ cells/ 5 ml of three independent experiments.

3.4.2 The effect of LPAAT inhibitors (CT32228 and PC020702) on AML cell lines viability.

3.4.2.1 The effect of LPAAT- β inhibitor PC020702 on NB4 and NB4:R2 Viability

A breakdown in membrane integrity determined by the uptake of a dye to which the cell is normally impermeable. Dead cells and debris could not exclude the dye and were stained dark blue, whereas live cells were clear. NB4 and NB4:R2 cell lines induced with various concentrations of PC020702, for at least four days, NB4 and NB4:R2 cells were seeded at about 2.5×10^5 on day 1, the viability of these cells were determined every 24 hours. Untreated control NB4 and NB4:R2 shows a great viability by day four (97% and 98% respectively), while treated NB4 and NB4:R2 with PC020702 represented a decrease in viability by day four after induction with 10 nM concentration of the inhibitor. The optimal concentration (25 nM) of PC020702 showed 30 % and 25 % viability by day 4 for NB4 and NB4:R2 respectively (**Figure 3.15**).

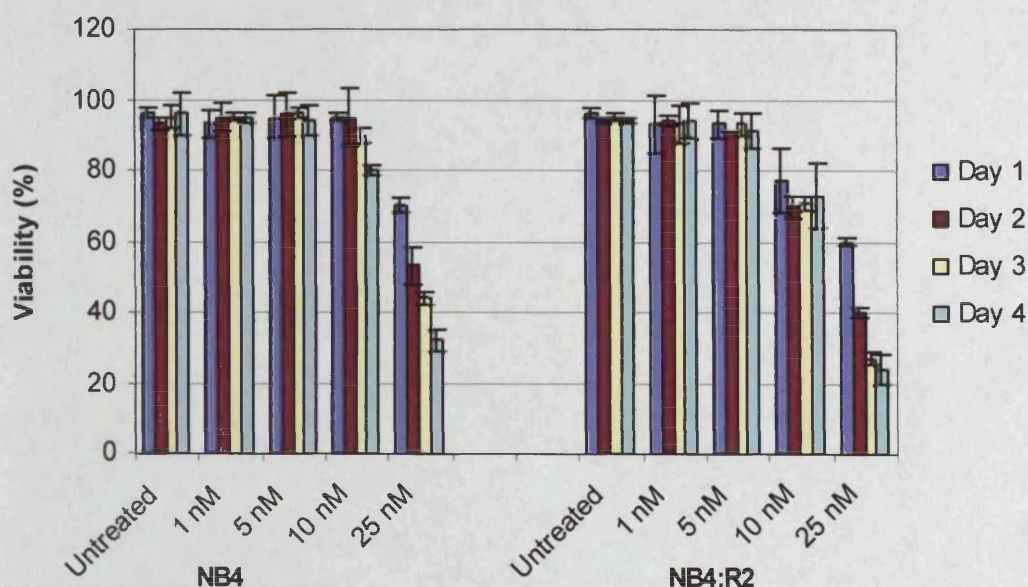


Figure 3.15 The effect of PC020702 on NB4 and NB4:R2 cell viability. NB4 and NB4:R2 were grown in RPMI medium and 10% FBS, cells were induced with different concentrations of PC020702, incubated at 37 °C in the presence of CO₂, cells stained with Trypan blue every 24 h to measure viability of cells during four days of induction. The results are shown mean \pm SD of percentage of three independent experiments.

3.4.2.2 The effect of LPAAT- β inhibitor PC020702 on HL60 and HL60-R Viability

Treated HL60 with different concentrations of PC020702 characterized an inhibition in viability by day four (65%) after treatment with 25nM with PC020702. Treatment of HL60-R cells with PC020702 resulted in greater than 50% inhibit of proliferation. These results suggest this LPAAT- β isoform inhibitor may be toxic and that ATRA resistant cells may be more sensitive to the effect of the inhibitor (Figure 3.16).

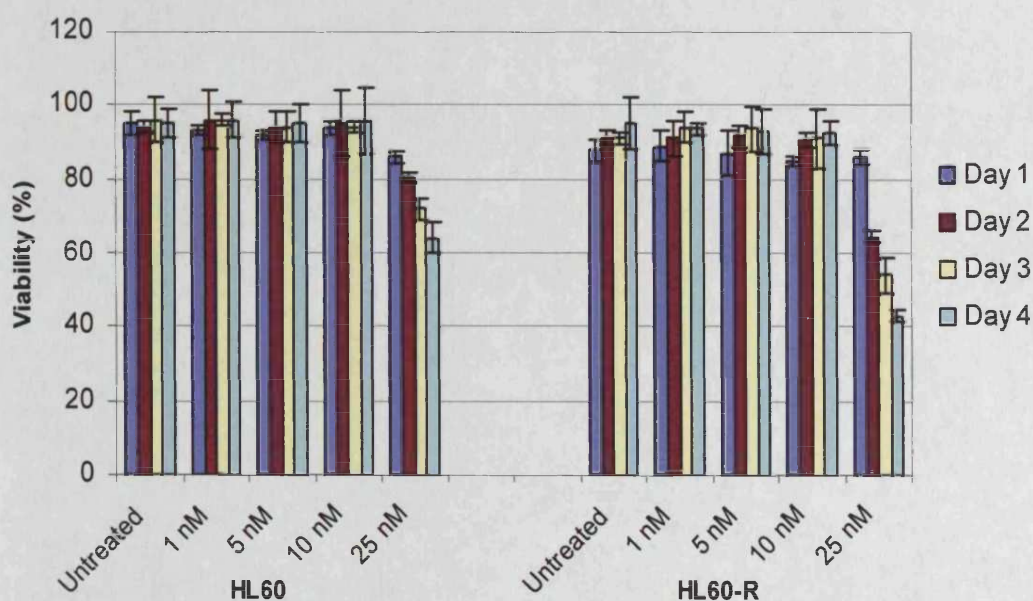


Figure 3.16 The effect of PC020702 on HL60 and HL60-R cell viability. HL60 and HL60-R were grown in RPMI and 10% FBS, cells were treated with different concentrations of PC020702. Details are as given for Fig. 3.15.

3.4.2.3 The effect of LPAAT- β inhibitor CT32228 on NB4 and NB4:R2 Viability

Untreated NB4 and NB4:R2 cells exhibited good viability more than 90% of the cells. The viability of the cells was decreased as the concentration increased with CT32228 in both NB4 and NB4:R2. The toxicity of the inhibitors started at 50 nM and less than 10% viability was seen after 500 nM by day four in both sensitive and resistant cells (**Figure 3.17**).

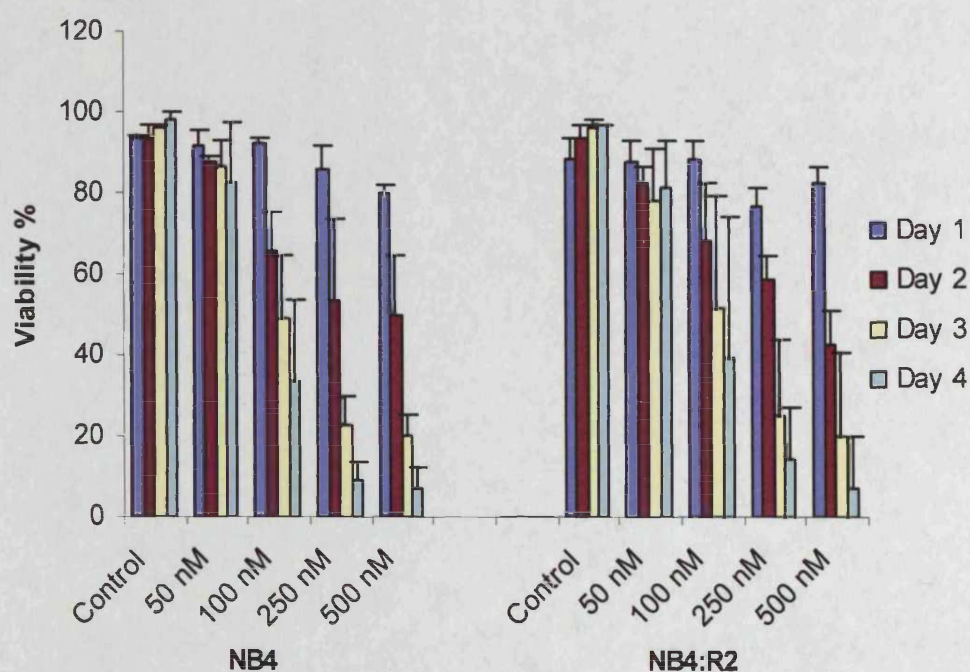


Figure 3.17 The effect of CT32228 on NB4 and NB4:R2 cell viability. The viability percentage of NB4 and NB4:R2 cells after treated with CT32228 at different concentration. The viability was assed by Trypan blue. The results are shown mean + SD of percentage of three independent experiments.

3.4.2.4 The effect of LPAAT- β inhibitor CT32228 on HL60 and HL60-R Viability

CT32228 exhibited less toxicity in HL60 cells than HL60-R, the viability in HL60-R decreased after treatment with CT32228 at concentration of 50 nM, while the viability decreased at concentration of 100 nM in HL60 cells (Figure 3.18).

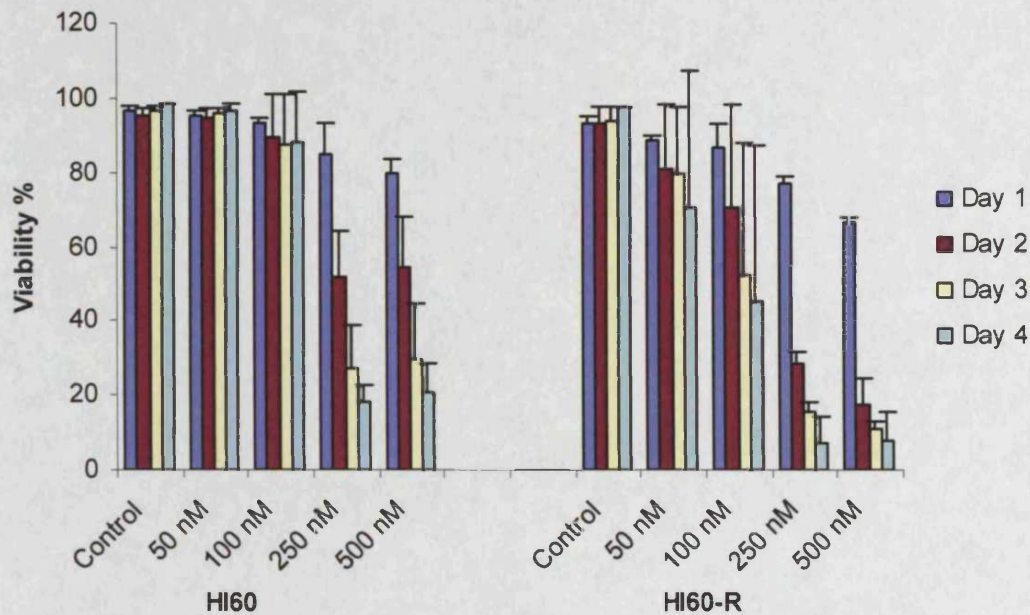


Figure 3.18 The effect of CT32228 on HL60 and HL60-R cell viability. The viability percentage of HL60 and HL60-R cells after treated with CT32228 at different concentration. The viability was assed by Trypan blue. The results are shown of mean + SD of percentage of three independent experiments.

3.4.3 The effect of LPAAT inhibitors (CT32212 and PC020701) on AML cell lines proliferation and viability.

The PC020701 compound is structurally similar to PC020702, and CT32212 compound is structurally similar to CT32228. These two inhibitors were also tested on cell proliferation and viability in NB4, NB4:R2, HL60 and HL60-R AML cells. The following table summaries cell lines and treatment used (Table 3.3 & 3.4)

No of flasks	NB4		NB4:R2	
	PC020701	CT32212	PC020701	CT32212
1	Untreated	Untreated	Untreated	Untreated
2	1 nM	50 nM	1 nM	50 nM
3	5 nM	100 nM	5 nM	100 nM
4	10 nM	250 nM	10 nM	250 nM
5	25 nM	500 nM	25 nM	500 nM

Table 3.3 the concentrations of the LPAAT- β inhibitors were used in proliferation and viability experiment in NB4 and NB4:R2.

No of flasks	HL60		HL60-R	
	PC020701	CT32212	PC020701	CT32212
1	Untreated	Untreated	Untreated	Untreated
2	1 nM	50 nM	1 nM	50 nM
3	5 nM	100 nM	5 nM	100 nM
4	10 nM	250 nM	10 nM	250 nM
5	25 nM	500 nM	25 nM	500 nM

Table 3.4 the concentrations of the LPAAT- β inhibitors were used in proliferation and viability experiment in HL60 and HL60-R.

PC020701 inhibitor showed insignificant ($P>0.05$) cell growth inhibition at concentration 25 nM by day four, in all cell lines tested. PC020701 at concentration of 25 nM exhibited an insignificant antiproliferative effect in NB4 and NB4:R2 cells by day four. Also viability, treated cells at 25 nM displayed good viability by day four in all cell lines tested. Treated HL60-R cells were shown to have no more than 20% of dead cells at concentration 25 nM by day four with PC020701. The CT32212 inhibitor did not show any toxicity on all in the cell lines tested. Treated cells were viable even at high concentration of inhibitor (500 nM) CT32212. These results suggest that the analogues form of LPAAT- β inhibitors (PC020701 and CT32212) were not toxic to any of the four AML cell lines used, therefore, these inhibitors were used as negative control (**Figures 3.19, 3.20, 3.21 and 3.22**).

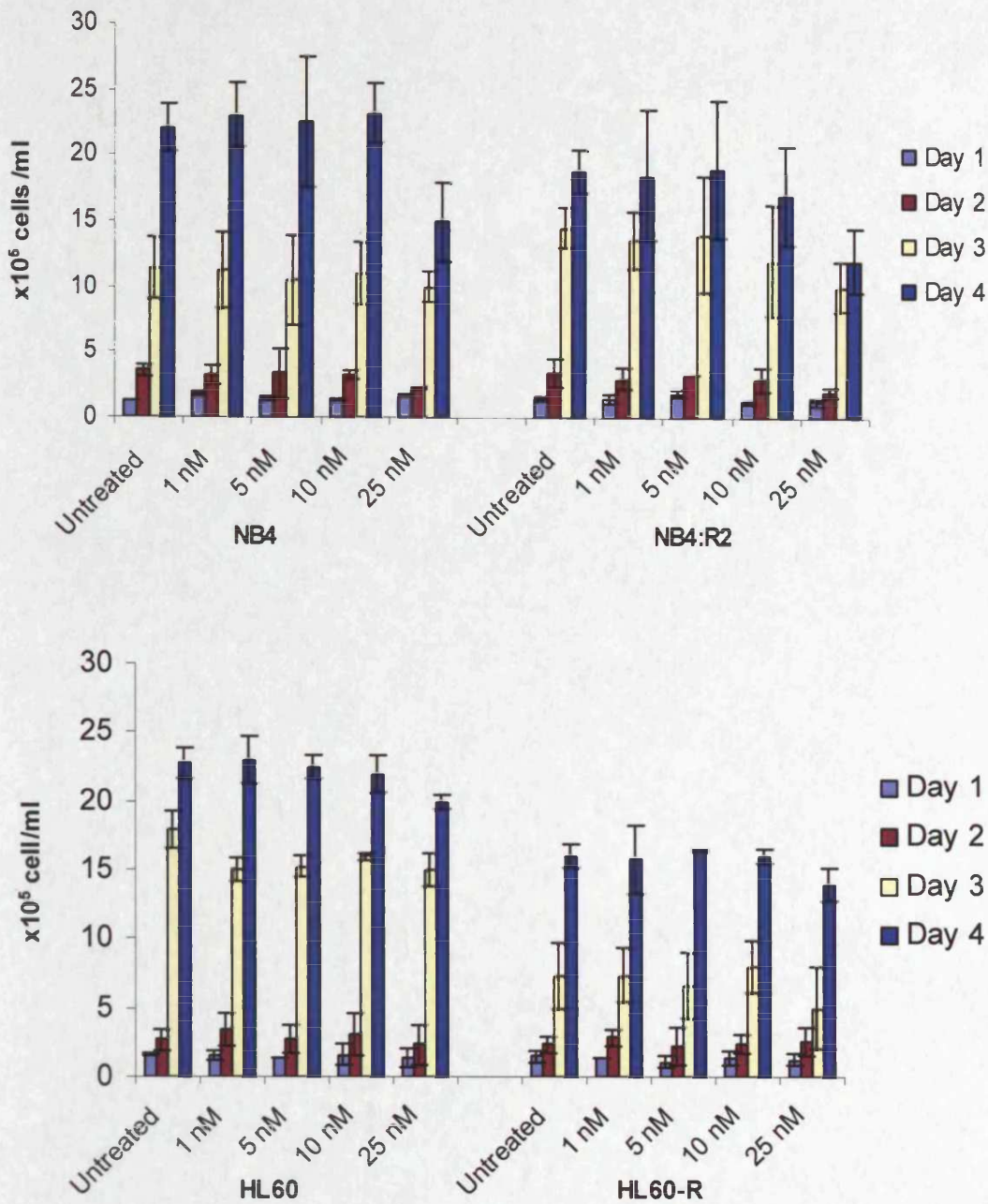


Figure 3.19 The effect of PC020701 on NB4, NB4:R2, HL60 and HL60-R cell proliferation. NB4, NB4:R2, HL60 and HL60-R cells were grown in RPMI medium with 10% FBS and incubated at 37°C and 5%CO₂, cells were treated for at least four days, with different concentrations of PC020701 LPAAT-β inhibitors. The proliferation of cells was measured every 24 hour by cell counting. The results are shown of mean + SD of percentage of three independent experiments.

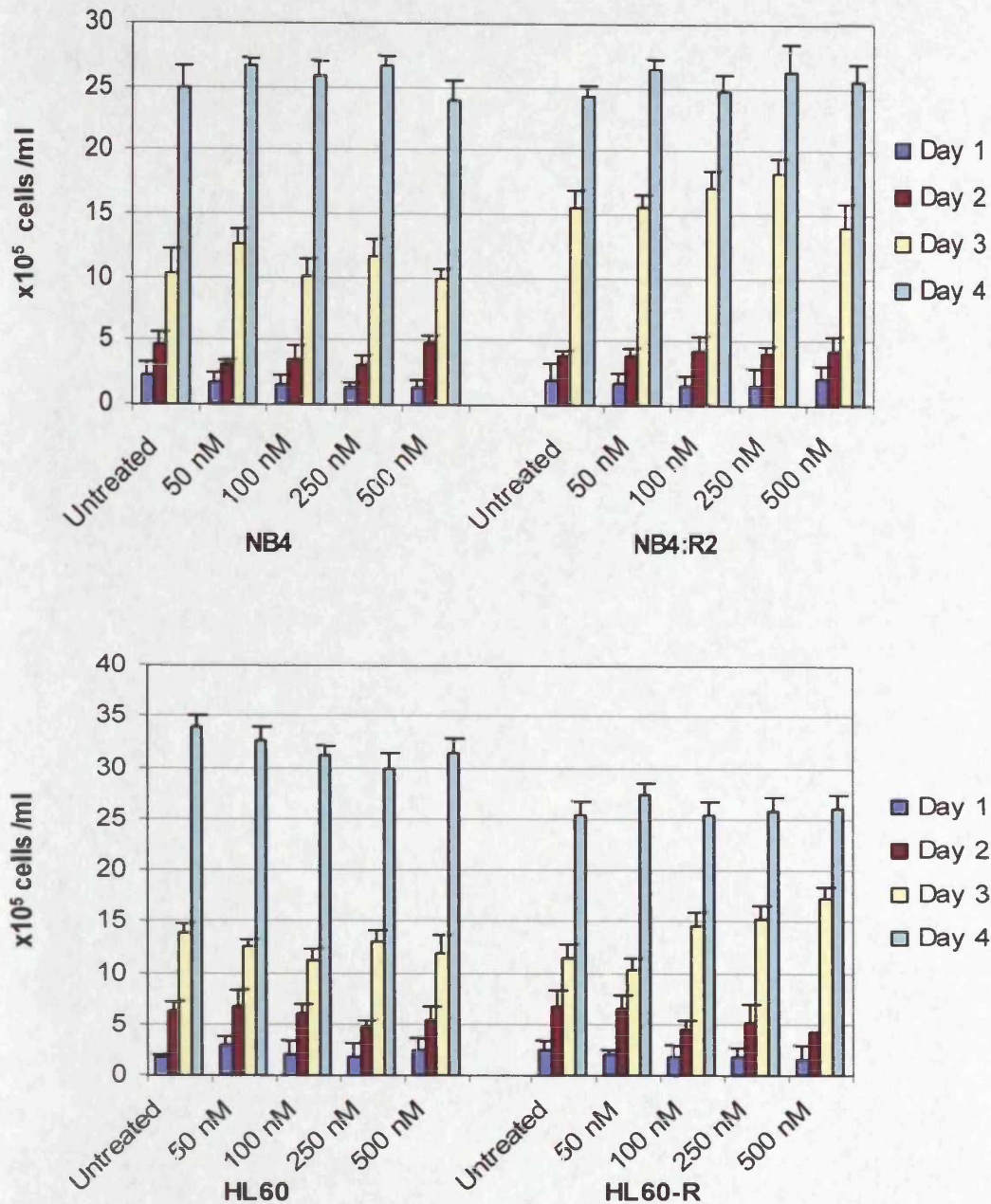


Figure 3.20 The effect of CT32212 on NB4, NB4:R2, HL60 and HL60-R cell proliferation. NB4, NB4:R2, HL60 and HL60-R cells were grown in RPMI medium with 10% FBS and incubated at 37°C and 5%CO₂, cells were treated for at least four days, with different concentrations of CT32212 LPAAT-β inhibitors. The proliferation of cells was measured every 24 hour by cell counting. The results are shown of mean + SD of percentage of three independent experiments.

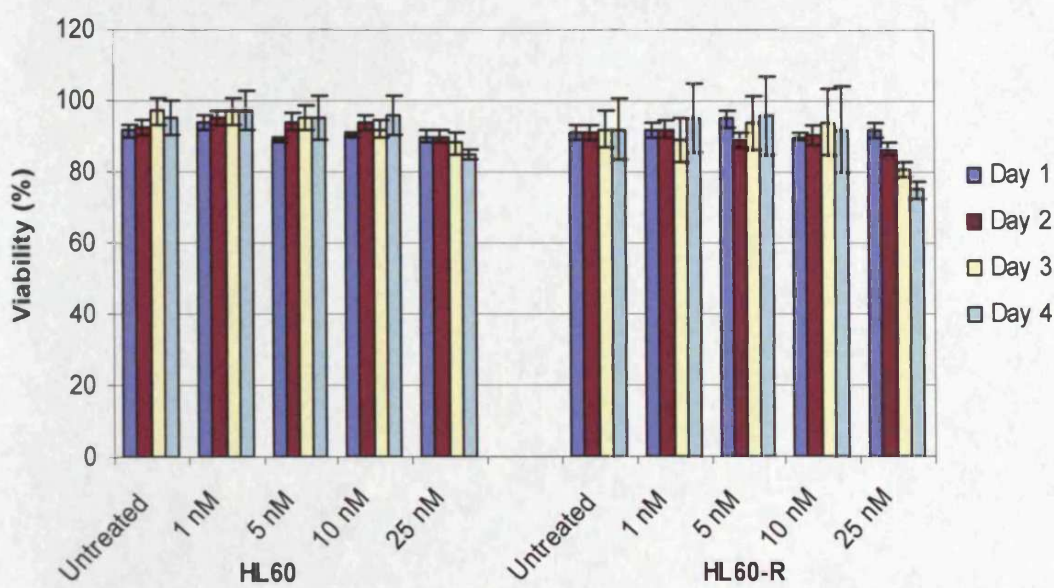
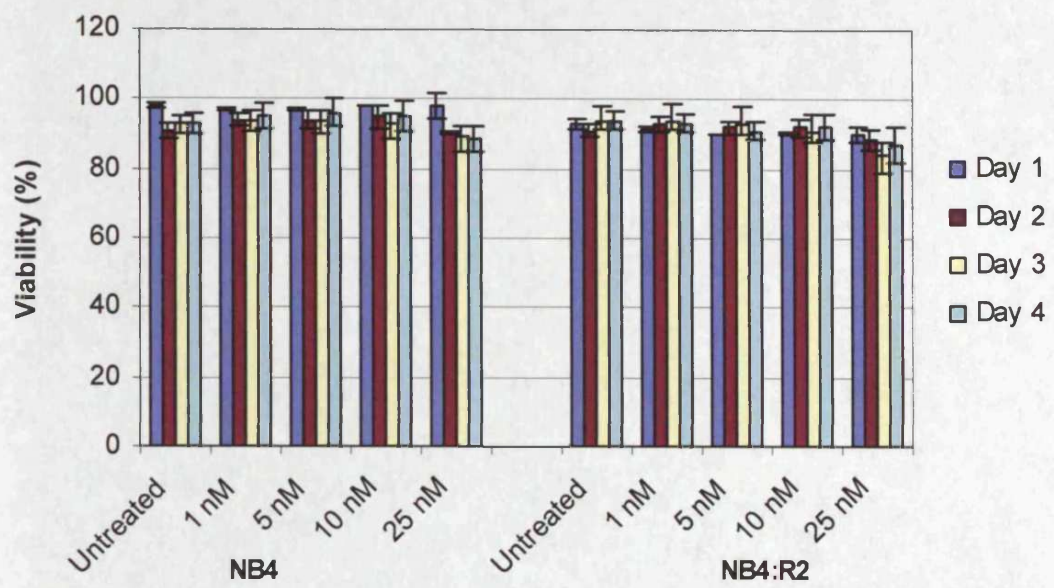


Figure 3.21 The effect of PC020701 on NB4, NB4:R2, HL60 and HL60-R cell viability. Cells were grown in RPMI medium and 10% FBS, cells were induced with different concentrations of PC020701, incubated at 37 °C in the presence of CO₂, and cells stained with Trypan blue every 24 h to measure viability of cells during four days of induction. The results are shown mean ± SD of percentage of three independent experiments.

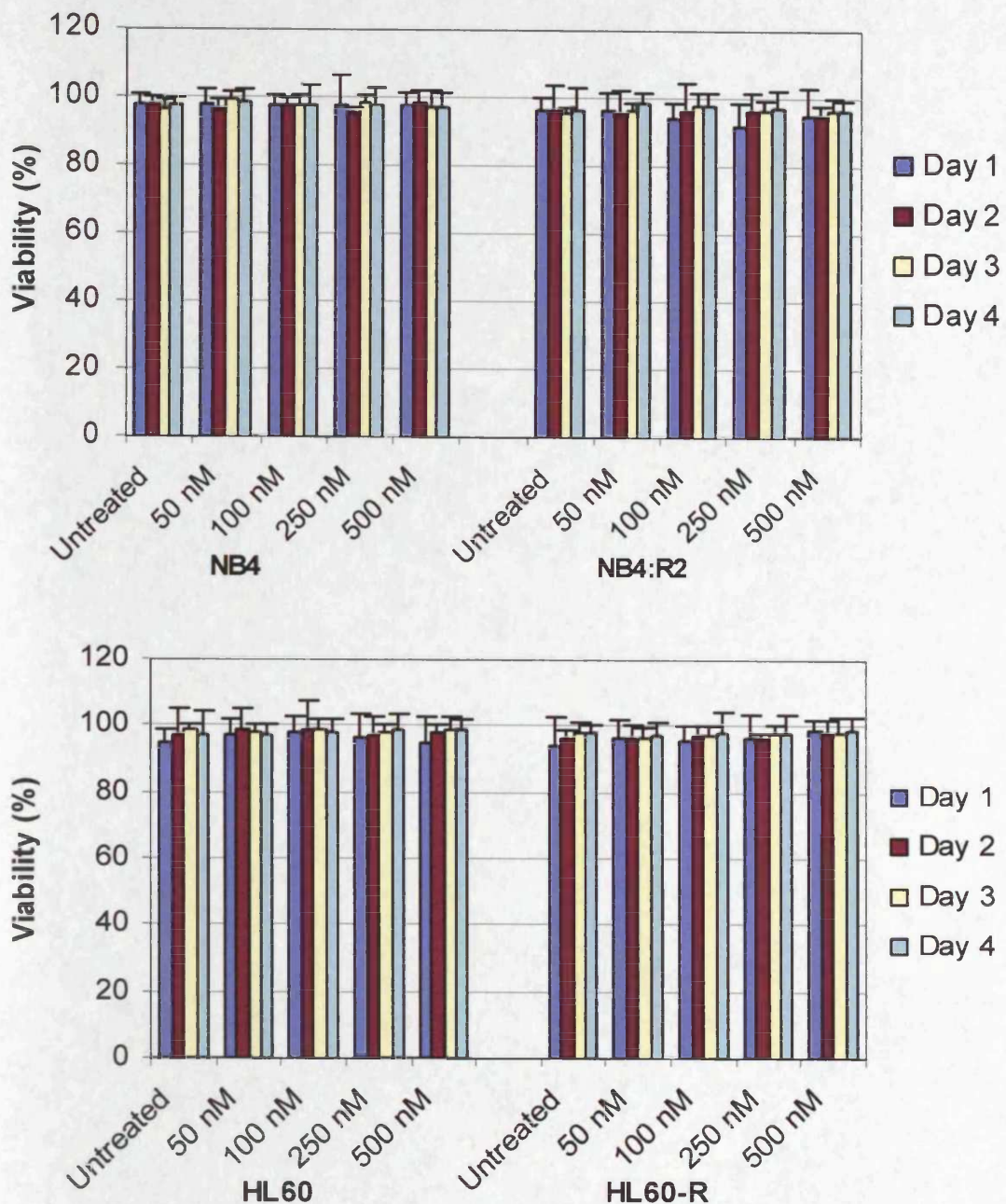


Figure 3.22 The effect of CT32212 on NB4, NB4:R2, HL60 and HL60-R cell viability. Cells were grown in RPMI medium and 10% FBS, cells were induced with different concentrations of CT32212, incubated at 37 °C in the presence of CO₂, and cells stained with Trypan blue every 24 h to measure viability of cells during four days of induction. The results are shown mean ± SD of percentage of three independent experiments.

3.5 Discussion

Inhibition of the LPAAT- β isoform has been shown to have antiproliferative effect on haematopoietic cell lines. The inhibition of the LPAAT- β enzyme using nanomolar concentration of aryldiaminotrizine compounds has been previously shown to result in significant inhibition of cell proliferation *in vitro* in Epstein Barr virus-transformed B non-Hodgkin's lymphoma, T cell leukaemia, chronic myeloid leukaemia, acute myeloid leukaemia (HL60), and Burkitt's lymphoma (Bonham et al. 2003;Pagel et al. 2005). Hideshima et al (2003), also showed that LPAAT- β inhibitors had antiproliferative effect in multiple myeloma cells at concentration of <200 nM (Hideshima et al. 2003). Consistent with these prior studies, we hypothesised that LPAAT- β is overexpressed in AML. Therefore, inhibition of LPAAT- β in AML could lead to downregulation of its end product PA and affect signalling pathways important in apoptosis and cell cycle regulation. To examine specificity of LPAAT- β inhibitors on LPAAT- β enzyme activity we used a radio enzyme assay. The biological effect of these compounds on AML cells, however, had not been previously characterized.

In this chapter the LPAAT- β enzyme activity was assayed at different time points; 48 h, 24h and 1 h on AML ATRA sensitive and resistant cell lines after LPAAT- β inhibitor treatment. In the presence of ^{14}C -Oleate as an Acyl-CoA donor and LPM as a substrate, the LPAAT- β enzyme activity was quantitated.

The LPAAT- β inhibitor (PC020702) showed a significant inhibition ($P=0.034$) of the enzyme activity after 24 hours in both ATRA sensitive and resistant cell lines, NB4 and NB4:R2 (50% and 39% inhibition respectively) indicating that NB4 may be more sensitive to the inhibitor than NB4:R2 cells.

However inhibition was insignificant in both NB4 and NB4:R2 following 48 hours incubation. The relative pixel volume of the whole lane shows a decrease in the treated cells compared to untreated, which may indicate that long term of inhibitor induction had affected on the cell uptakes for the LPM and ^{14}C -Oleate and as a result of that the whole cell line was also affected.

For that reason we decided to examine the effect of the inhibitor after short term exposure. The results show the activity of the enzyme was inhibited after PC020702 treatment for 1 hour in NB4, NB4:R2, HL60 and HL60-R, with little change seen in whole lane pixel volume analysis.

In a recent study from another group, LPAAT- β activity was quantified on Multiple Myeloma cell lines after treated with different LPAAT- β and LPAAT- α inhibitors, and they found the enzyme activity to be inhibited between (65-70% and 15-20%) respectively (Hideshima, et al. 2003).

In this current study, we found that cell growth of human AML cell lines was inhibited up to 10-fold following incubation with LPAAT- β inhibitors PC020702 compared with untreated cells. By day four a significant decrease ($P=0.014$ and $P=0.012$ of NB4 and NB4:R2 respectively) in cell proliferation was observed. Also significant decreases in proliferation were observed in HL60 and HL60-R ($P=0.018$ and $P=0.004$ respectively). It would appear that the inhibitor has a more toxic effect on the HL60-R cells than the wild type HL60. PC020702 has been shown to be antiproliferative at 10 nM and 25 nM in all cells. CT32228 has been shown to be antiproliferative in all ATRA sensitive and resistant cell lines studied at 50 nM and 100 nM.

The analogous compounds PC020701 and CT32212 to PC020702 and CT32228 respectively were also tested on AML cell lines. These inhibitors did not exhibit an antiproliferative effect on any of the cell lines tested, consistent with previous studies (Bonham, et al. 2003). CT32212 and PC020701 were named as inactive form and were, therefore, used as a negative controls.

To further elucidate the mechanism of the antiproliferative effects mediated by LPAAT- β inhibitors. The following two chapters will examine in detail the effect of LPAAT- β inhibitors on gene expression using oligonucleotide arrays and on signaling pathways important in cell cycle progression and apoptosis.

CHAPTER 4

**Identification of molecular targets following
LPAAT- β inhibitor treatment in Acute Myeloid
Leukemia cell lines using oligonucleotide
arrays and validation of selected genes using
Real-Time PCR and Northern blotting**

4.1 Introduction:

DNA microarrays can measure expression of thousands of genes simultaneously, providing extensive information on gene interaction and function. Microarray technology is a powerful tool for identifying novel molecular drug targets and for elucidating mechanisms of drug action. Furthermore, microarrays can monitor the large-scale profile of gene expression in response to specific pharmacologic agents, providing information on drug efficacy and toxicity. DNA microarrays are divided into two groups mainly cDNA microarrays and oligonucleotide arrays.

cDNA microarrays consist of long cDNA fragments (200-600 bp), either produced from cDNA libraries or PCR products generated from gene specific primers, which are printed onto nylon membrane. It can easily be used in the laboratory without expensive additional equipment.

The Affymetrix oligonucleotide array system uses a single colour fluorescent label, where experimental mRNA is enzymatically amplified, biotin-labelled for detection, hybridized to the wafer, and detected through the binding of a fluorescent compound. The current generation of photolithographic arrays have 250,000-400,000 probes arranged in pairs – a perfect match (PM) probe that is complementary to a 25-base pair segment of mRNA and a mismatch (MM) probe that is complementary to the same mRNA segment except for the 13th nucleotide. A collection of 16 to 20 probe pairs, called a *probe set*, is used to represent a gene (McGall & Fidanza 2001).

The oligonucleotide arrays, developed by the Affymetrix system were used in our study. Data is obtained by examining the signals of fluorescence, analyzed and compared by computer software, particularly GeneSpring version 7.1. To date no other studies have analysed the gene expression profile using cDNA microarray or oligonucleotide array after LPAAT- β inhibitors treatment in AML cells.

In the previous chapters, we assayed LPAAT- β enzyme activity using a radioenzymatic assay technique. The LPAAT- β inhibitors were active after 24 hours and 1 hour of treatment. The inhibitors were found to be anti-proliferative and induced toxicity in all four cell lines tested. The reason we decided to examine the effect of gene expression after 1h was to avoid disturbance of all signalling after 24h or 48 h due to the toxicity of the drug.

Many studies have recommended repeating hybridization as a means of filtering and confirming the data. It was recommended that at least three replicates be used in designing experiments using microarray (Lee et al. 2000). In our study, eight arrays were hybridized and each one was repeated once. In addition, prior to oligonucleotide array experiments, all procedures including RNA extraction, sample loading, probe labelling, hybridization, staining and washing were standardized for all experiments. Repeating the experiment is costly, and there are still inherent limitations of consistency. Therefore, the assay was performed in duplicate for all conditions examined but genes found to be differentially expressed between samples required confirmation by other methods.

Real-time PCR and Northern Blotting techniques were used as the methods of choice for confirming genes differentially expressed in our oligonucleotide array experiment. Real-time PCR and Northern Blotting provide a quantitative estimate of RNA/DNA concentration in different samples. Like oligonucleotide array experiments, Real-time PCR and Northern Blotting measure gene expression at mRNA level.

In this chapter we use Real-time PCR and Northern blotting to verify the expression of genes found to be differentially expressed using oligonucleotide array. There were two genes selected from those differentially expressed (2 fold higher) by oligonucleotide array to be validated with the two methods mentioned above. These two genes were caspase-5 and cdc2 that regulated apoptosis and cell cycle progression respectively.

The following chapter will discuss in detail oligonucleotide array techniques used to assess the gene expression profile of NB4 and NB4:R2 cell lines following treatment with PC020701, PC020702 and CT32228 for 1 hour versus untreated cells. All experiments were performed in duplicate. The use of real-time PCR and northern blot for validation of selected differentially expressed genes will also be discussed.

4.2 Material and Methods

A detailed description of oligonucleotide array material and methods can be found in section (2.5). For real-time PCR and Northern blotting materials and methods were mentioned in sections 2.6 and 2.7 respectively.

4.2.1 Cell lines and treatment

Two different acute myeloid leukaemia cell lines were used in this study representing different responses to ATRA. The first cell line was NB4, represents the AML/M3 according to FAB classification. NB4 cells differentiate to granulocytes upon ATRA treatment and maintain the PML/RAR α transcript. NB4:R2 cell line was the second cell line used in this study, these do not respond to ATRA and express a mutated form of PML/RAR α .

NB4 and NB4:R2 cells were seeded at 2.5×10^5 cells/ml in RPMI-1640 medium supplemented with 10% FBS. Each cell line was divided into four flasks, one for untreated (control) and three for treated samples (tests). The three test flasks were treated with 250 nM PC020701 (inactive), PC020702 and CT32228 (active) of LPAAT- β inhibitors respectively. All four flasks for each cell line were gassed and incubated in 37°C, 5% CO₂ for 1 hour. After one hour the cells were harvested and total RNA was extracted as described previously in section (2.5.3) using Trizol reagent.

4.2.2 Oligonucleotide Array Expression Analysis:

In brief, total RNA was extracted with Trizol reagent and was used to create cDNA with a T7-polyT primer and the reverse transcriptase, Superscript II. Approximately 1 μ g of cDNA was subjected to in vitro transcription in the presence of biotinylated UTP and CTP. A total of 15 μ g of cRNA was fragmented. Target cRNA was hybridized to a set of oligonucleotide arrays (Affymetrix) containing 22283 probe sets of human genes. Expression data was analyzed by GenSpring version 7.1. As mentioned in material and methods chapter (section 2.5) the procedure was completed with assistance from Mrs A Gilkes and staff at Central Biotechnology Surfaces, Cardiff University, School of Medicine.

4.2.3 Target Verification by RT-PCR Analysis.

Two genes were selected for validation by Northern blotting and real-time PCR. Different RNA samples were used for the oligonucleotide array measurements, and RT-PCR analysis. The RNA extraction method used in RT-PCR and Northern blot was different from that used with oligonucleotide arrays. The detail of RNA extraction can be found in section (2.4.2).

All primers used in this study were purchased from Oswel and diluted to 10 μ M and 50ng/ μ l (Table 4.1).

Gene	Primer 1 (5'-3')	Primer 2 (5'-3')
Caspase5	CACAGCCAGGGATATGGAGT	GCCTGGACAATGATGACCTT
Cdc2	CCAGCAAGTGTTTAGCACGA	CAGCCTTTGAGTAGGGTCCA

Table 4.1 Caspase 5 and Cdc2 Primer sequences used for RT-PCR analysis

After RNA extraction, a total 2 μ g of RNA were converted into cDNA by reverse transcription in a total volume 20 μ l according to manufacturer's protocol. DNA standards were prepared for all genes under the following thermal PCR conditions: 95°C for 5 minutes, 95°C for 1 minute, 60°C for 1 minute, 72°C for 1 minute for 35 cycle and soaked at 4°C. PCR product analysed on 1.5% agarose gel, and the bands of interest were cut, and DNA was extracted according to the manufacturer's protocol.

4.2.4 Real-time PCR

The real-time PCR mixture contained 1.0 μ l of the RT sample, 0.5 μ l (50ng/ μ l) of each primers, 1.0 μ l SYBR Green I, variable amounts of MgCl₂ (final concentration, 4 mM), and PCR-grade sterile water. Up to 32 samples were run in parallel by performing an initial 600

seconds denaturation step at 95°C followed by 40 cycles of repeated denaturation (3 seconds at 95°C), annealing (5 seconds at 60°C), and extension (12 seconds at 72°C). In the final cycle the melting curves for the samples were determined by initially heating the mixture to 95°C, cooling it to 40°C. All results were normalized to the expression of S14, a house keeping gene.

4.2.5 Northern Blotting

Differentially expressed genes were validated by northern blot techniques. RNA were reverse transcribed into cDNA as mentioned above, bands of interest were cut from agarose gel, and used as probes for Northern blotting. A total of 10 µg of RNA sample was prepared with loading buffer and heated at 55°C for 15 minutes. The mixed sample was loaded into 1% agarose gel and separated by electrophoresis. The RNA was blotted on a membrane as detailed in section (2.7.2.2).

The membrane was hybridised with 25-50 ng of cDNA probe that was denatured and labelled by [α -³²P] dCTP. The membrane was washed, sealed in a plastic bag and exposed to two films from Kodak over night or longer in -70°C. The films were developed and the band size verified through measurements of distance relative to the DNA marker and /or the ribosomal bands.

4.3 Oligonucleotide array

Microarray data is characterized by a large number of measurement values per sample. Therefore the challenge is to distinguish between random and significant patterns of gene expression. For this reason a systematic approach in data management with detailed planning and documentation is strongly recommended to keep an overview with microarray analysis in a clinical setting. Oligonucleotide array studies generate vast quantities of data. Several steps have to be performed before the raw data are in any shape for a biological evaluation (**Figure 4.1**).

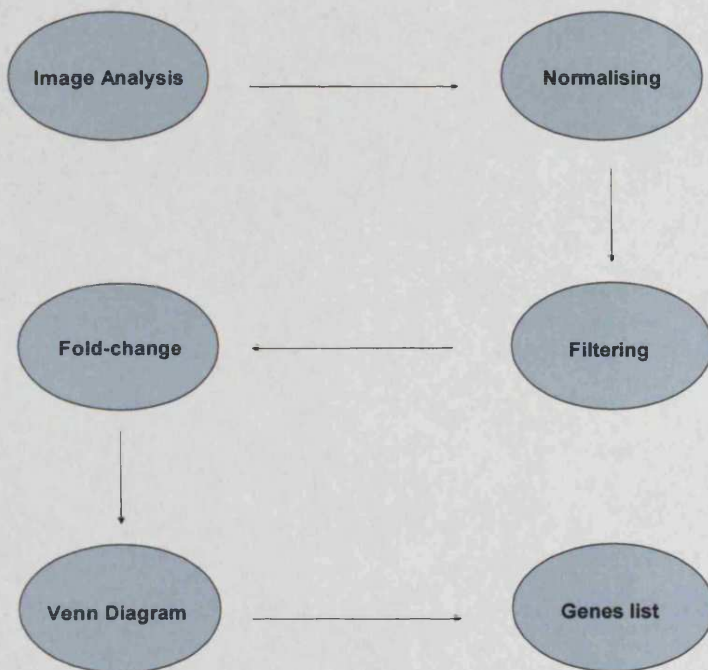


Figure 4.1 Overview of GeneSpring data analysis

4.3.1 Image Analysis

First, one should always look at the raw data, i.e. scanned chip images, to identify artefacts. After image processing, the first analysis step is to produce a large number of quantified gene expression values. These values represent absolute fluorescence signal intensities as a direct result of hybridization events on the array surface. It is also possible to qualitatively rate gene expression as absent/present detection call calculations.

4.3.2 Normalization

Before analyzing the data it is a routine procedure to normalize the raw data. This is a mandatory step in the data extraction process in order to appropriately compare the measured gene expression levels. Normalization is defined as the removing slide/chip effect, background intensities and other sources of systematic errors.

There are many methods for normalization of array data in GeneSpring. These methods are dependent on many factors such as the type of experiment being carried out and the type of data set being used. This means normalization procedures allow microarray data to be in as much of a linear format as possible. It will be evident from certain normalization procedures that certain data will have unusual bends or curves. Normalization aims to avoid this and produce as much a linear distribution as possible. In our study, one per-chip normalization together with one per-gene normalization was performed. Per-chip normalization is extremely useful to help eliminate minor differences in probe preparation, hybridization conditions, washing, or other microarray production imperfection. Usually, the adjustments are made to set the average fluorescence intensity to some standard value, so that all the intensities on the chip go up or down to a similar degree. This approach makes sense if the samples are all similar, e.g. all from the same types of cells or tissues.

The goal of microarray experiments is to identify the genes whose expression is changed under different conditions. Per-gene normalization is necessary to compare the gene expression profiles of genes that may be expressed at very different levels. Figure 4.2 shows a window of GeneSpring software used in normalization (Figure 4.2).

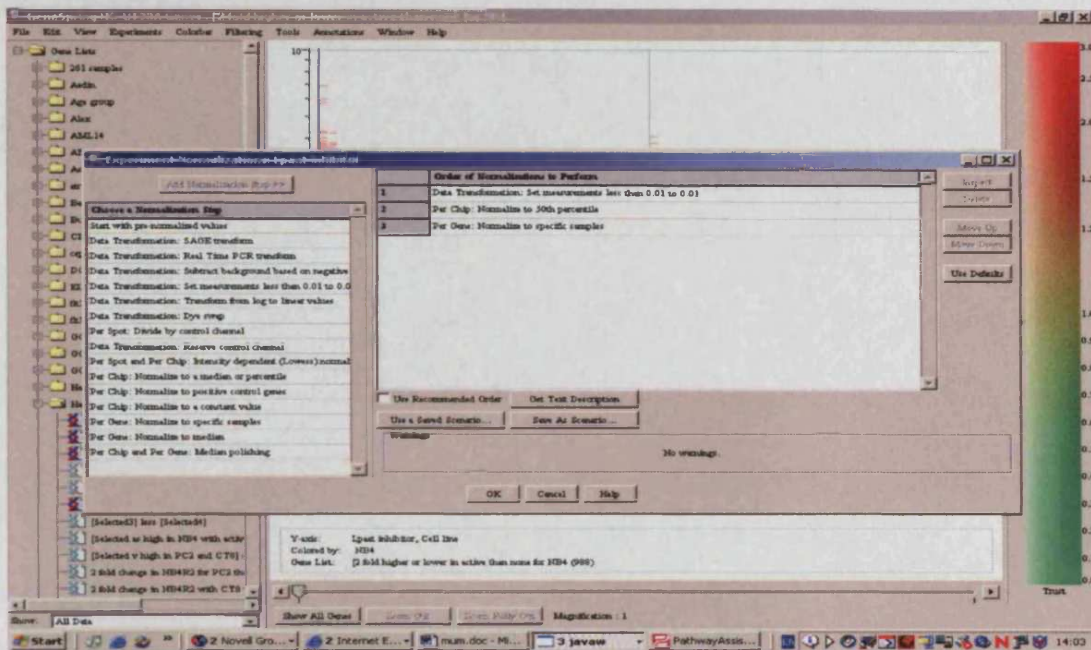


Figure 4.2 The normalized window displayed - GeneSpring

4.3.3 Filtering

All gene lists imported into GeneSpring at this stage include all genes displayed on each array (22,283/array). After normalization the data was filtered, eliminating genes that were not changed or that were expressed at background levels and a source of noise. There are two principal sources of noise in oligonucleotide array experiments: biological noise and technical noise. Biological noise consists of variation among patients and tumor locations, variation in the cellular composition of tumours, heterogeneity of the genetic material within tumor due to genomic instability. Technical noise consists of differences in sample preparation and experiment variables which include nonspecific cross hybridization, differences in the efficiency of labelling reactions and production differences between oligonucleotide arrays.

The filters include factors such as quality control, expression level constraints. Genes were removed that were absent in all samples, returning the availability of genes to 12941. Then genes that changed to less than 2-fold in all samples (non-changing) were identified (9335 gene). The genes that then remained in the present and changing list totalled 3606 (the

differences of gene lists present and less than 2-fold (12941-9335=3606)). This list was saved and further analyzed.

4.3.4 Fold change and tree view

A natural first step in extracting this information is to examine the extremes, e.g., genes with significant differential expression in two individual samples or in a time series after a given treatment. This simple technique can be extremely efficient, for example, in screens for potential tumour markers or drug targets. A natural basis for organizing gene expression data is to group together genes with similar patterns of expression.

To detect groups of correlated genes and tissues we used a clustering approach to the data set. Clustering can be thought of as forming a phylogenetic tree of genes or cells. Genes are near each other on the "gene tree" if they show a strong correlation across experiments, and cell lines are near each other on the "cells tree" if they have similar gene expression patterns (Eisen et al. 1998).

Figure 4.3 shows cluster analysis of all samples using the present and changing genes. The analyses were performed in duplicate. Untreated NB4 and NB4:R2 cells were grouped together showing similar gene expression patterns but different from the treated group. The second group shows treated NB4 cells with the active and inactive form of inhibitors were grouped together, suggesting equal gene expression pattern, different from the untreated NB4. The gene expression pattern of active form PC2 and CT8 from untreated was not surprising; however the surprising outcome was from the inactive form which shows different expression from untreated. This may be due to the fact that the inactive form was shown to be toxic at higher concentrations.

The third major group shows NB4:R2 treated with inactive (PC1) and active (PC2 and CT8) grouped together, while NB4:R2 untreated grouped separately as mentioned above with untreated NB4. The third group shows similar gene expression pattern as NB4 treated cells. However the gene expression of the treated NB4:R2 shows a difference from treated NB4, which indicate that the inhibitors had some what different effects between the two cell lines. This may be due to NB4 being more sensitive to the inhibitors than NB4:R2 (Figure 4.3).

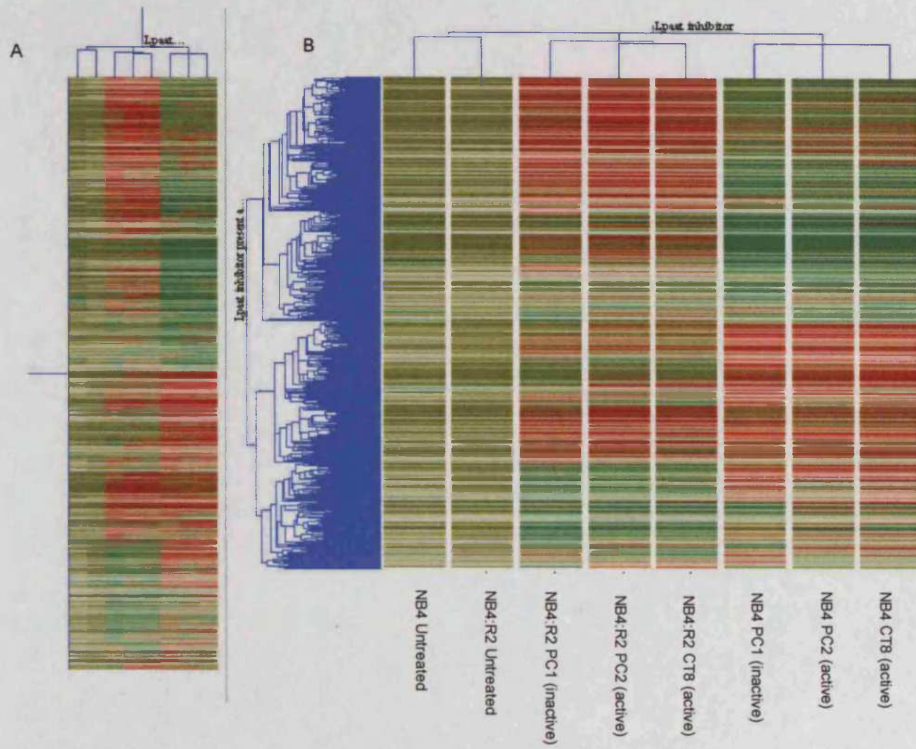


Figure 4.3 Cluster analysis of combined AML cell lines treated and untreated.

NB4 and NB4:R2 cells were incubated with or without LPAAT- β inhibitors PC020701 (inactive) and PC020702 and CT32228 (active) for 1 hour. Total RNA was extracted and analysed by oligonucleotide array as mentioned in the material and methods. The entire clustered image is shown in (A), the detail clustered image is shown in (B). In figure (B) the branches on the top represent clustering of the cell lines, while branches on the left represent clustering of genes. Up regulated genes are shown in red, while down regulated genes are shown in green. The expression level of each gene is represented by colour intensity. The higher the expression the brighter colour displayed and vice versa.

4.3.5 Venn Diagrams

After normalizing the data to eliminate random variations, and cluster analysis to have an overall visualization of the data, we next attempted to further assess the gene list created. The Venn diagram is an intuitive way of comparing gene lists, showing how many genes are in common. As we mentioned earlier, one of the main aims of this study was to look for marker genes for different cellular responses to LPAAT- β inhibitor treatment in ATRA sensitive and resistant cells. Therefore we looked at common gene lists within the two active forms of inhibitors (PC2 and CT8) compared with untreated (control) in both NB4 and NB4:R2. Figure 4.4 shows an example of a Venn diagram.

Figure 4.4 down shows a Venn diagram of NB4 and NB4:R2 cells, the left Venn diagram shows gene number in NB4 cells when treated with PC2 and CT8 for 1h. A total of 2240 genes with two fold higher or lower expressing after CT8 treatment, and 2165 genes were expressed after PC2 treatment, 988 genes were in common. The common genes list was saved for further analysis.

The same Venn diagram analysis was created for NB4:R2 cells (right figure). A total of 1928 genes 2-fold higher or lower expression after CT8 treatment, and 2092 genes were expressed after PC2 treatment, 803 genes were in common. The common gene list was saved for further analysis (Figure 4.4).

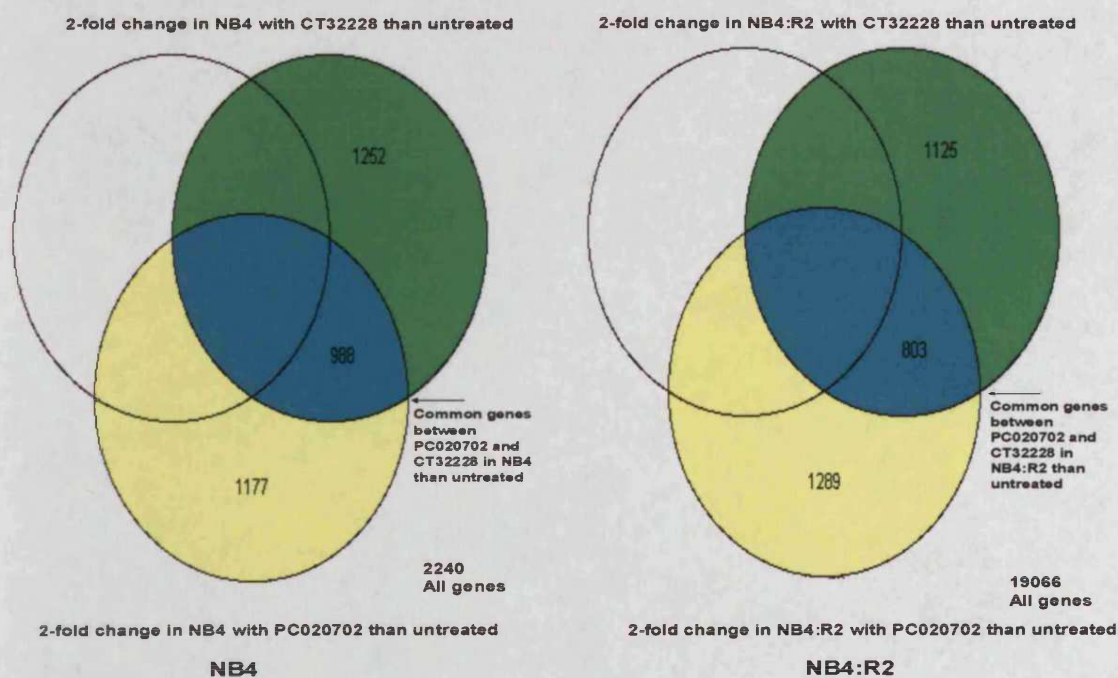


Figure 4.4. Venn diagram representing expression patterns of genes in NB4 and NB4:R2 cells after LPAAT- β inhibitor treatment. The circles represent a time point with the numbers of the genes present in each sample (2 fold change). Numbers in the outer portion of each circle are specific to that sample. The number in the innermost portion of the diagram represents genes expressed following both treatments. Likewise, the numbers in the portions of the diagram shared by two circles represent common genes expressed in those samples.

From the Venn diagram figure 4.4 we were created a Venn diagram 4.5 which shows common genes were expressed after active form treatment in both cell lines. A total of 122 genes sets were found common in both NB4 and NB4:R2 after PC020702 and CT32228 treatment compared with the control (Figure 4.5). These 122 genes were two fold higher or lower changed in both NB4 and NB4:R2 than untreated. The common list was saved for further analysis.

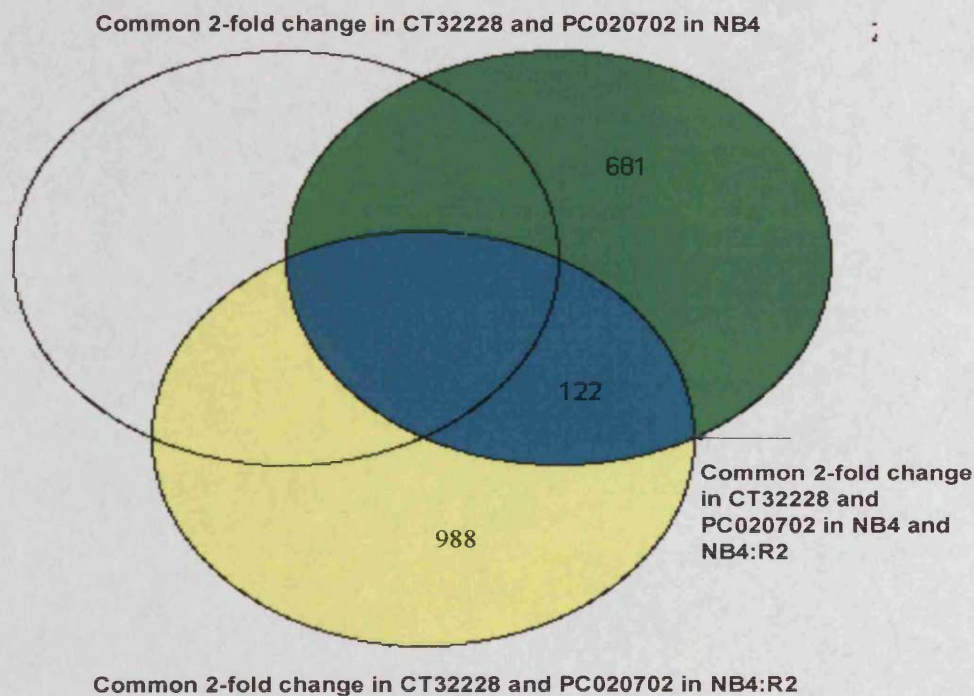


Figure 4.5 A Venn diagram created to produce common genes expressed in both NB4 and NB4:R2 cells after PC020702 and CT32228 treatment. The yellow circle represents genes expressed in NB4. The green circle represents genes expressed in NB4:R2. The common genes in both cell lines are in the grey area.

4.3.6 Differentially expressed genes list

The next step is to examine the common genes up- and down regulated in both cell lines, we found 122 common genes expressed after PC020702 and CT32228 inhibitor treatment in both NB4 and NB4:R2 cells. The reason for this step was to look for similar patterns of expression within these cell lines after treatment with PC020702 and CT32228. This is because PC020702 and CT32228 are from the same group of inhibitors (diaryltriazines) and PC020702 was found to inhibit LPAAT- β (see chapter 3) after 1 hour of treatment. CT32228 in a previous study was found also inhibit LPAAT- β enzyme activity (Bonham et al. 2003). Out of 122 genes, 30 genes were over expressed and 92 genes were down regulated in both cell lines.

Table 4.2 & 4.3 shows genes differentially expressed in both NB4 and NB4:R2 cells after 1 hour of treatment. These genes were found to be higher lower in both cells after PC020702 and CT32228 (active form) treatment. I had expected to see genes that related more to apoptosis, cell signalling pathways or cell cycle progression, and the phosphatidic acid signalling pathways, especially ras/raf/Erk and PI3K/Akt/mTOR pathways, as the inhibitors have a major effect on these biological phenomena. This may be due to short exposure of these inhibitors on these cell lines. The two tables lists showed that most of the genes expressed were integrated to cell membrane. However, this is not surprising as the inhibitors block LPAAT- β enzyme activity that converts lysophosphatidic acid to phosphatidic acid (PA). In addition to the role of PA in cell signalling, it has been implicated in lipid biosynthesis that is important to membrane function and structure.

Table 4.2 Common Up-regulated selected genes were differentially expressed in NB4 and NB4:R2 after treatment with PC2 and CT8 for 1 hour.

GeneBank Accession	Description
NM_007347	adaptor-related protein complex AP-4 epsilon
AI337584	NCI_CGAP nuclear mitotic apparatus protein 1
NM_018110	FLJ10488; docking protein 4 (DOK4)
Y13710	macrophage specific
AF020774	hair and skin epidermal-type 12-lipoxygenase-related protein
BE675337	NCI_CGAP_CLL1 Homo sapiens gelsolin
NM_016734	B-cell lineage specific activator protein
L07335	putative; Homo sapiens SRY (sex determining region Y)-box 2
BC004857	Homo sapiens, clone IMAGE:3690478, mRNA, partial cds.
NM_004347	Caspase 5, apoptosis-related cysteine protease
AI344141	member RAS oncogene family
AK023111	Homo sapiens cDNA FLJ13049
NM_002968	HSAL1; DNA binding sal-like 1 (Drosophila) (SALL1)
AF068220	sarco-/endoplasmic reticulum Ca-ATPase 3 (ATP2A3)
AK024214	Homo sapiens cDNA FLJ14152
NM_016608	X chromosome, 1
NM_005823	megakaryocyte potentiating factor
NM_004196	cyclin-dependent kinase-like 1 (CDC2-related kinase)
NM_017757	zinc finger protein 407 (ZNF407)
AA018923	Soares retina phosphodiesterase 6A
NM_014124	PRO0255 protein
AI146308	activated Cdc42-associated kinase 1
NM_025009	hypothetical protein FLJ13621
NM_001463	frizzled-related protein (FRZB), mRNA.
NM_002590	protocadherin 8 (PCDH8)
NM_002922	regulator of G-protein signalling 1 (RGS1), mRNA.

Table 4.3 Common down-regulated selected genes were differentially expressed in NB4 and NB4:R2 after treatment with PC2 and CT8 for 1 hour.

213172_at	KIAA0227 gene tetratricopeptide repeat domain 9
207750_at	Hypothetical protein PRO1866
207252_at	ubiquitin-activating enzyme E1
219858_s_at	Homo sapiens FLJ20160 protein (FLJ20160)
219973_at	Homo sapiens hypothetical protein FLJ23548 (FLJ23548)
220850_at	microrchidia,
211265_at	prostaglandin E receptor 3 (subtype EP3)
209988_s_at	Homo sapiens achaete-scute complex-like 1 (Drosophila)
207166_at	guanine nucleotide binding protein (G protein), gamma transducing activity polypeptide 1 (GNGT1)
220402_at	p53-regulated apoptosis-inducing protein 1 (P53AIP1)
206418_at	NADPH oxidase 1 (NOX1)
215957_at	Homo sapiens unknown mRNA, sequence.
204671_s_at	ankyrin repeat domain 6
214920_at	Soares placenta Nb2HP
221101_at	Hypothetical protein FLJ20034
210121_at	beta 1,3-galactosyltransferase, polypeptide 2
205908_s_at	SLRR2C; osteoadherin; Homo sapiens osteomodulin (OMD)
222322_at	Homo sapiens cDNA clone IMAGE:1011110
211523_at	gonadotropin-releasing hormone receptor
221057_at	spermatogenesis associated protein 1
219895_at	hypothetical protein FLJ20716 (FLJ20716)
206675_s_at	SNO; ski-related oncogene snoN;
211468_s_at	DNA helicase recQ5 gamma
215386_at	Homo sapiens cDNA clone MAMMA1002758 3'
217504_at	Soares_pregnant_uterus_NbHPU
206717_at	myosin, heavy polypeptide 8, skeletal muscle
204704_s_at	aldolase B, fructose-bisphosphate

216039_at	postmeiotic segregation increased 2-like 6
217050_at	Human early lymphoid activation protein (EPAG)
219255_x_at	interleukin 17 receptor B (IL17RB)
208279_s_at	CMT1A duplicated region transcript 1 (CDRT1)
220907_at	Homo sapiens hypothetical protein FLJ22684 (FLJ22684)
206116_s_at	tropomyosin 1 (alpha) (TPM1)
206624_at	fat facets-like; ubiquitin specific protease 9,
221868_at	; Homo sapiens mRNA for KIAA1155 protein
207103_at	voltage-sensitive potassium channel
206543_at	SWI/SNF related, matrix associated, actin dependent regulator of chromatin, subfamily a, member 2 (SMARCA2
216586_at	H.sapiens UNG2 pseudogene.
216329_at	H.sapiens partial cDNA for homologue of mPOU homeobox protein.
210066_s_at	hAQP4; Homo sapiens mRNA for aquaporin, complete cds.; aquaporin 4
220736_at	member of the folate transporter gene family
209807_s_at	nuclear factor I/X (CCAAT-binding transcription factor)
220336_s_at	H platelet glycoprotein VI-3
206964_at	putative N-acetyltransferase Camello 2 (CML2), mRNA.
221683_s_at	monoclonal antibody 3H11 antigen
210917_at	v-yes-1 Yamaguchi sarcoma viral oncogene homolog 1
211078_s_at	serine/threonine kinase 3
208450_at	galactoside-binding, soluble, 2 (galectin 2)
213067_at	myosin, heavy polypeptide 10, non-muscle
216464_x_at	orphan G protein-coupled receptor GPR44 (GPR44) gene
216817_s_at	olfactory receptor, cell line LG2.
209978_s_at	Human plasminogen
206909_at	four transmembrane domain protein;
211213_at	C terminal truncation;

215077_at	collagen, type III, alpha 1
215774_s_at	GTP-specific succinyl-CoA synthetase beta subunit,
208359_s_at	potassium inwardly-rectifying channel, subfamily J, member 4 (KCNJ4),
206466_at	very long-chain acyl-CoA synthetase
208220_x_at	amelogenin, Y-linked (AMELY)
216307_at	diacylglycerol kinase beta 90k
207747_s_at	docking protein 4 (DOK4)
219815_at	galactose-3-O-sulfotransferase 4 (GAL3ST4)
203780_at	epithelial V-like antigen 1 (EVA1)
214251_s_at	nuclear mitotic apparatus protein 1
210834_s_at	prostaglandin E receptor 3 (subtype EP3)
205234_at	monocarboxylate transporter 4
204400_at	embryonal Fyn-associated substrate (EFS), transcript variant 1
203838_s_at	activated Cdc42-associated kinase 1
210155_at	myocilin, trabecular meshwork inducible glucocorticoid response
220842_at	Abelson helper integration site (AHI1)
205767_at	epiregulin (EREG)
218694_at	ALEX1 protein (ALEX1), mRNA.
201451_x_at	Ras homolog enriched in brain
210000_s_at	suppressor of cytokine signaling 1 (SOCS1)
219414_at	calsyntenin 2 (CLSTN2)
220771_at	melanoma antigen (LOC51152)
217524_x_at	phosphodiesterase 6A, cGMP-specific, rod, alpha
210194_at	phospholipase A2 receptor 1, 180kDa
202563_at	chromosome 14 open reading frame 1 (C14orf1), mRNA.
218541_s_at	chromosome 8 open reading frame 4 (C8orf4)
207928_s_at	glycine receptor, alpha 3 (GLRA3)

4.3.7 Data interpretation using Gene Ontology (GO)

One of the most important tools for the representation and processing of information about gene products and functions is the Gene Ontology (GO). The GO Consortium is a joint project of three model organism databases: FlyBase, Mouse Genome Informatics (MGI) and the Saccharomyces Genome Database (SGD). The goal of the Consortium is to produce a structured, precisely defined, common, controlled vocabulary for describing the roles of genes and gene products in any organism (Harris et al. 2005;Boyle et al. 2004).

GeneSpring software has ability to auto accesses to the Gene Ontology databases. Gene Ontology stores a dynamic controlled vocabulary organized on molecular function, cellular component, and biological process that can be applied to all organisms.

Molecular function describes activities, such as catalytic or binding activities, at the molecular level. GO molecular function terms represent activities rather than the entities (molecules or complexes) that perform the actions, and do not specify where or when, or in what context, the action takes place. The cellular component attributes were used to search for genes that were either extracellular (secreted) or transmembrane molecules as potential biomarkers. A biological process is accomplished by one or more ordered assemblies of molecular functions. Examples of broad biological process terms are cell growth and maintenance or signal transduction (Ashburner et al 2000;lomax 2005).

In this study we ran GO to extract the information and biological characteristics common to groups of genes of interest. We ran the GO analysis on this data set using two criteria, either an increase (fold change = 2 and $p < 0.05$) or decrease (fold change = 2 and $p < 0.05$) in gene expression after 1 hour treatment. We used this analysis for demonstration because of the large number of differences in gene expression observed in the list. The proportion of genes in the oligonucleotide array data that link to GO terms was increased as more GO terms and gene associations were added.

Table 4.4 shows the list of biological process, cell component and molecular function terms significantly increased and decreased at the one hour time point. The list shows GO of 122 genes found to be 2 fold higher or lower after PC020702 and CT32228 treatment for 1 hour in both NB4 and NB4:R2 cells. GO terms that had P value more than 0.05 were removed from the list.

Using the criterion for a significantly increased gene-expression change, GO analysis primarily identified GO terms involved in the cell membrane. Notable GO terms include the cell component “integral membrane” (12.3% of 122 genes, P-value 0.004) and “nuclear membrane and voltage-gated potassium channel complex” (each 1.6% of 122 genes, P-value 0.008 and 0.046 respectively).

GO terms include biological processes “G-protein coupled receptor protein signalling pathway” (4.9% of 122 genes, P-value 0.01) and “transcription DNA-dependent, cell death, regulation of cell growth, proton transport and cell differentiation” (each 1.6% of 122 genes P-value 0.001, 0.007, 0.025, 0.039 and 0.044 respectively). The GO terms included molecular function “function prostaglandin E receptor activity and legend-dependent nuclear receptor activity” (each 1.6% of 122 genes, P-value 0.00158 and 0.00339 respectively) (**Table 4.4**).

GO biological process	GO overlapping	
	genes	p-value
transcription, DNA-dependent	2	0.00104
cell death	2	0.00758
G-protein coupled receptor protein signaling pathway	6	0.0104
morphogenesis	1	0.0109
polysaccharide metabolism	1	0.0163
response to biotic stimulus	1	0.0163
FADH2 metabolism	1	0.0217
NADPH metabolism	1	0.0217
odontogenesis	1	0.0217
regulation of cell growth	2	0.0253
bone mineralization	1	0.0271
enzyme linked receptor protein signaling pathway	1	0.0271
monocarboxylic acid transport	1	0.0324
negative regulation of blood coagulation	1	0.0324
proton transport	2	0.039
cell differentiation	2	0.0441
B-cell activation	1	0.0482
GO cell component		
integral to membrane	15	0.00403
nuclear membrane	2	0.00887
cilium	1	0.0163
muscle thin filament tropomyosin	1	0.0271
voltage-gated potassium channel complex	2	0.0468

Continued,

GO molecular function	GO overlapping genes	p-value
prostaglandin E receptor activity	2	0.00158
ligand-dependent nuclear receptor activity	2	0.00339
reduced folate carrier activity	1	0.0109
Wnt-protein binding activity	1	0.0109
glucan 1,4-alpha-glucosidase activity	1	0.0163
gonadotropin-releasing hormone receptor activity	1	0.0163
plasmin activity	1	0.0163
catalytic activity	1	0.0217
epidermal growth factor receptor ligand activity	1	0.0217
superoxide-generating NADPH oxidase activity	1	0.0217
voltage-gated proton channel activity	1	0.0217
interleukin receptor activity	1	0.0271
structural constituent of tooth enamel	1	0.0271
thrombin activity	1	0.0271

Table 4.4 Gene ontology list of 122 genes. The GO include biological processes, cell components and molecular function of 2 fold higher or lower of 122 common genes expressed after PC2 and CT8 treatment for 1 hour in both NB4 and NB4:R2 cells. The list contains a significant increase and decrease GO data (P-value ≤ 0.05).

4.4 Validation of expression of selected genes

Despite to these differences in genes expression, there were some genes found to have 2 fold changes in expression or more linked to the apoptosis and cell cycle progression. The genes selected from the data obtained were caspase5 and Cdc2. These two genes were found either higher or lower in both cell lines after LPAAT- β inhibitors (active form). These two genes were selected for validation by real-time PCR and Northern blot.

4.4.1 Real-time PCR

A big advantage of this approach is quantitation of the initial amounts of target sequence in contrast to the other methods which detect the final amount of the amplified product. The unique part of this system is the use of fluorescent dye (SYBR Green I) which emits signals increasing in a direct proportion to the PCR product during each cycle. In order for the method to be precise, the quantitative data is collected in the exponential phase of amplification when a reaction proceeds at a constant rate and the first significant increase in the amount of PCR product is observed. The DNA specific dye SYBR Green binds to double stranded DNA and upon excitation emits light. During the elongation step an increasing amount of dye binds to DNA (**Figure 4.6**). After binding, its fluorescence increases over 100-fold. Fluorescence is measured at the end of the elongation step of every PCR cycle and thus product accumulation is monitored. This method has however one disadvantage; the dye binds to double stranded DNA of any origin, including primer dimer and nonspecific products. Therefore a precise optimization of PCR conditions is of major importance.

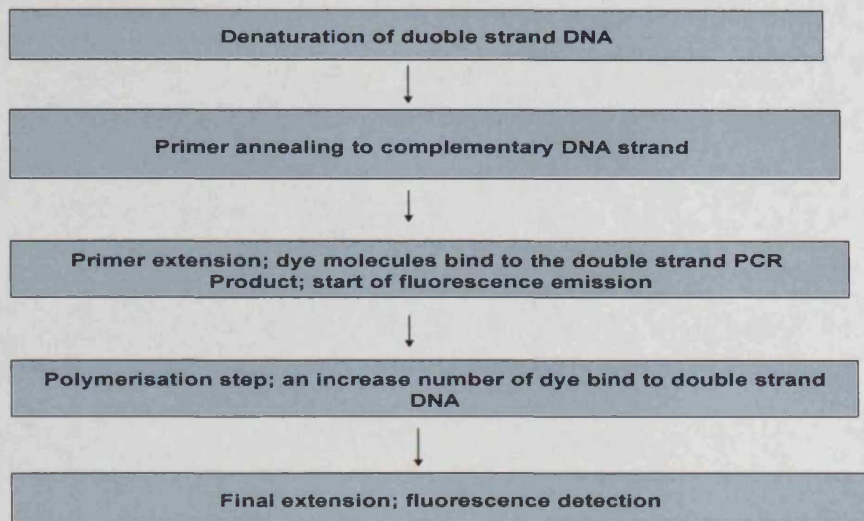


Figure 4.6 A diagram demonstrating one PCR cycle of the SYBR Green I dye in real-time PCR.

4.4.2 RT-PCR experimental preparation

The optimized PCR (as prepared in material and method section 2.6.2.3) was run on agarose gel. The bands of two genes were cut and DNA was purified. Upon preparation of DNA for standards, they were used as templates to optimize $MgCl_2$ concentration. The $MgCl_2$ concentration was used subsequently with the samples. In RT-PCR each gene was optimized with $MgCl_2$ concentration range from 2 to 5 mM. Finally, samples RTs were run using the optimized $MgCl_2$ concentration. Each assay included duplicate reactions for each sample and was repeated three times. The mean concentration of S14 was used to control for input RNA because it is considered a stable housekeeping gene. The mean S14 concentration was determined once for each cDNA sample and used to normalize all other genes tested from the same cDNA sample. Figure 4.10 shows the image displayed for quantification analysis. After the run was completed, a graphical displayed of fluorescence vs. cycle number was prepared (**Figure 4.7**).

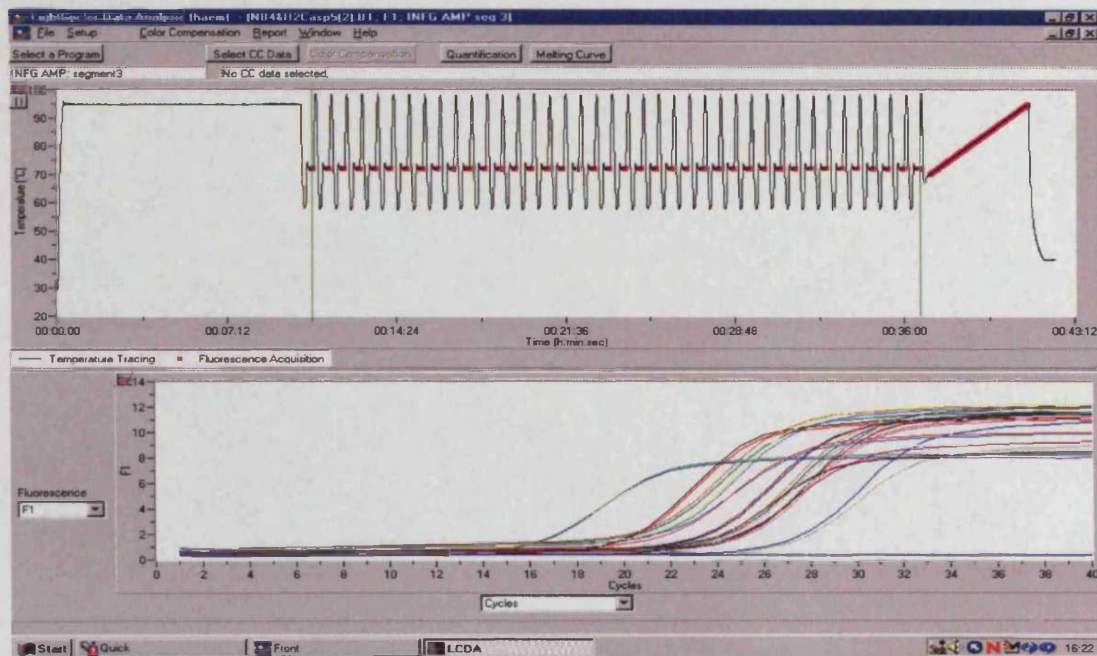


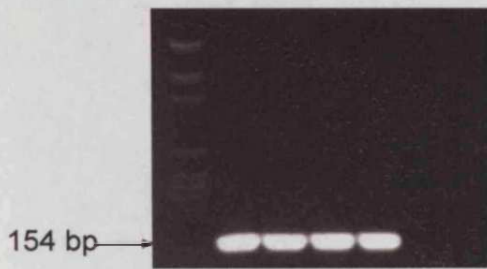
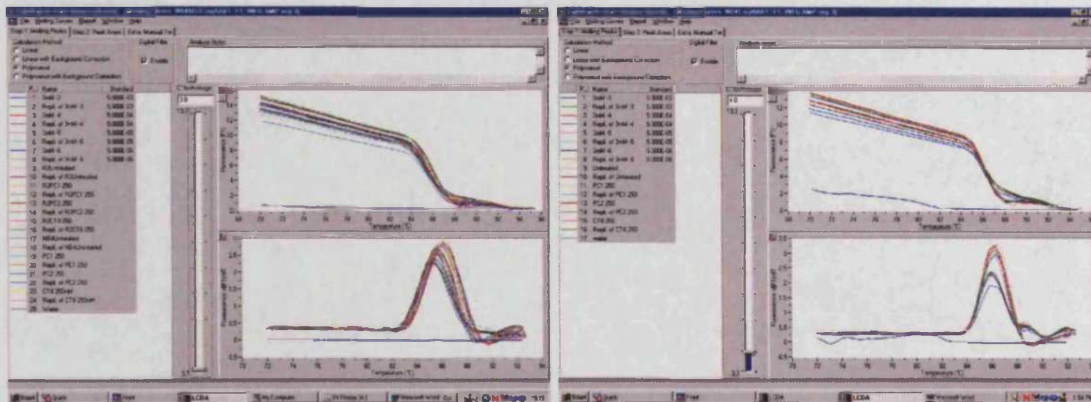
Figure 4.7 RT-PCR graphic displayed by Light Cycler data analysis. The top figure illustrates the run data as temperature vs. time graph. Each peak shows a cycle of different sample. The final step of run, a melting temperature (T_m) figure was displayed (the slope line). The lower figure represents fluorescence accumulation during the different cycles.

4.4.3 Melting curves analysis (T_m)

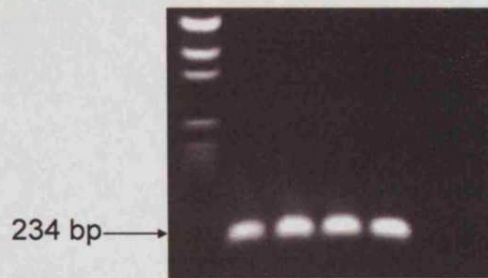
PCR products were analyzed by using the LightCycler melting curve analysis. The melting curve process involves the continuous acquisition of fluorescence as the temperature is steadily increased from 40 to 95°C. The melting temperature (T_m) can be used to determine the specificities of the PCR products. The presence of two products or primer dimer in the sample causes the probe to separate at a different temperature from the product of interest. Recently some paper mentioned that Agarose gel electrophoresis or melting curve analysis may not always reliably measure PCR specificity. The combination of both can always reveal PCR specificity (**Figure 4.8**).

Cdc2

Caspase-5



A



B

Figure 4.8. A melting curve and gel picture of Caspase-5 and *cdc2*. A figure (A) upper right showing a window melting curve for Caspase-5 displayed by lightCycler software and lower right post PCR product after run on agarose gel. A figure (B) is for Cdc2. Note the sharp narrow peaks (Upper window) and single sharp bands of the correct size for caspase5 (234bp) and Cdc2 (154bp).

4.4.4 Real-time quantitative PCR

A typical amplification curve of PCR can be divided into three phases. The first is the background phase, which lasts until the signal of the amplified product exceeds the background signal. The second is the exponential growth phase (the log phase), which finally ends in the plateau phase. The amount of product can be determined from the log phase. The log phase begins when sufficient product has accumulated to be detected above background, and ends where the reaction enters the plateau phase and the reaction efficiency falls.

For data analysis, we followed the recommendations provided by the manufacturer of the detection system. Data are produced as sigmoidal-shaped amplification plots (when using a linear scale), in which the fluorescence is plotted against the number of cycles.

There are two different methods of calculating crossing points: the fit point and the second derivative maximum method. The second method was used in quantification of differentially expressed gene by real-time PCR.

The second derivative maximum method is defined as the point at which the maximal increase of fluorescence within the maximum log-linear phase takes place, it is calculated by determining the second method: derivative maxima of the amplification curves. The software calculates at which cycle number this point is reached. Unlike the Fit Point method, the second derivative maximum method does not require defining the log linear segment of each curve, nor does it require setting a noise band. Also, we found this method to consistently produce reproducible results (**Figure 4.9**).

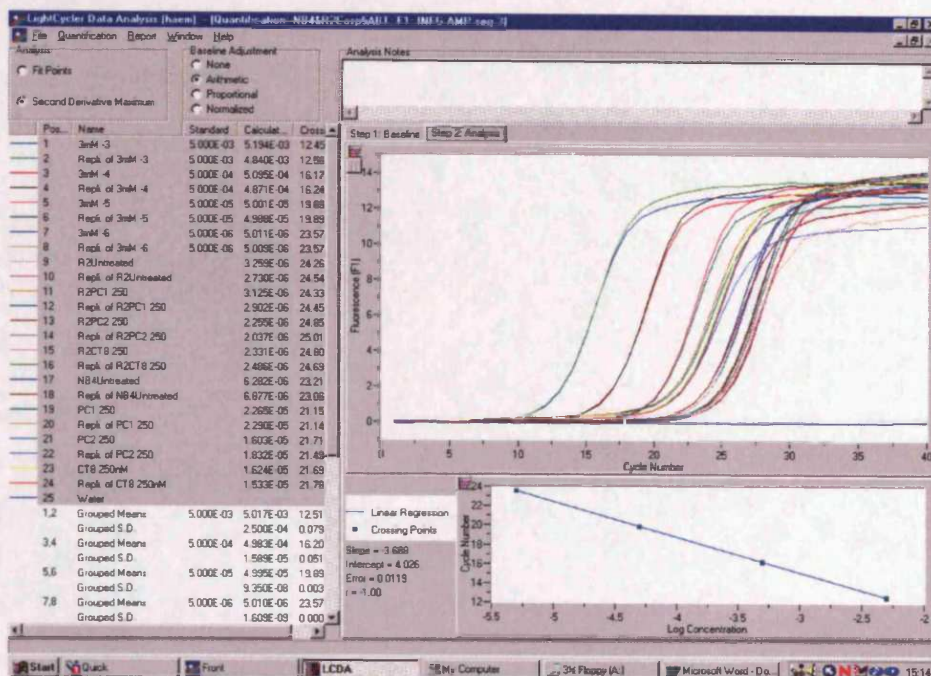


Figure 4.9 A window displayed during quantification. The screen displayed during quantification analysis. After selection of baseline and method of analysis the software displays a curve of fluorescence vs. cycle number. Five standard curves used for every experiment and they were prepared so their concentrations would cover the entire range of the sample concentration. On the left hand side, the screen shows standard “concentration and sample” labels together with the calculated concentration of all samples. On the right hand side top, the screen displays the analysis of the samples and standard. The right bottom shows the standard curve. All standards/samples were done in duplicates and average values were taken for further analysis

4.4.5 Verification of Caspase-5 expression

The expression of two genes was selected from gene list (Appendix 2.2) that were found 2-fold over expressed after PC2 and CT8 in both NB4 and NB4:R2 compared with untreated cells. Caspase-5 one of the gene was subjected for validation with real-time PCR and Northern blotting. Caspase-5 expression was validated with real-time PCR that showed similar expression with normalized oligonucleotide array. Figure 4.10 shows Caspase-5 gene expression in NB4 and NB4:R2 cells after treatment with LPAAT- β inhibitors for 1 hour. The figure shows a graphical representation of adjusted intensities of caspase-5 gene expression in our cell line captured by GeneSpring software. The figure shows an overexpression of caspase-5 after treatment with PC2 and CT8 active form in both NB4 and NB4:R2. The expression of caspase-5 by PC2 is more sensitive to NB4 than NB4:R2 cells, while CT8 shows an equal caspase-5 expression in both cell lines. The expression of caspase-5 with PC1 (inactive) was down regulated in NB4 while over expressed in NB4:R2 (Figure 4.10).

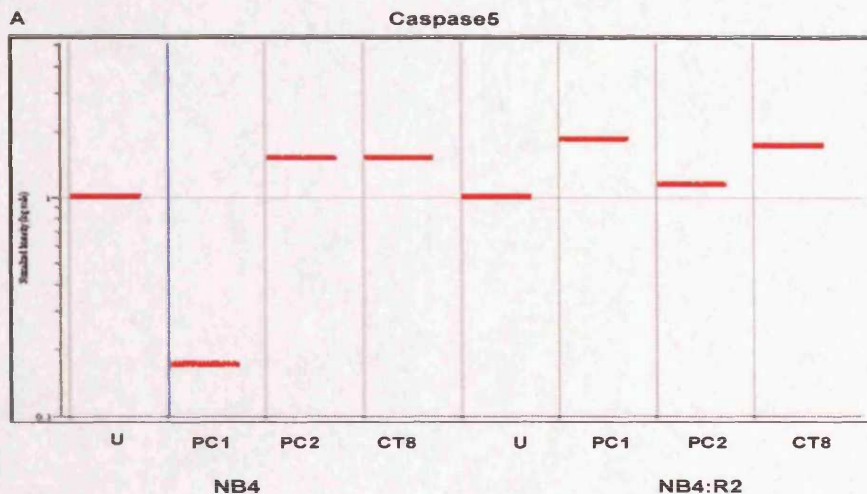
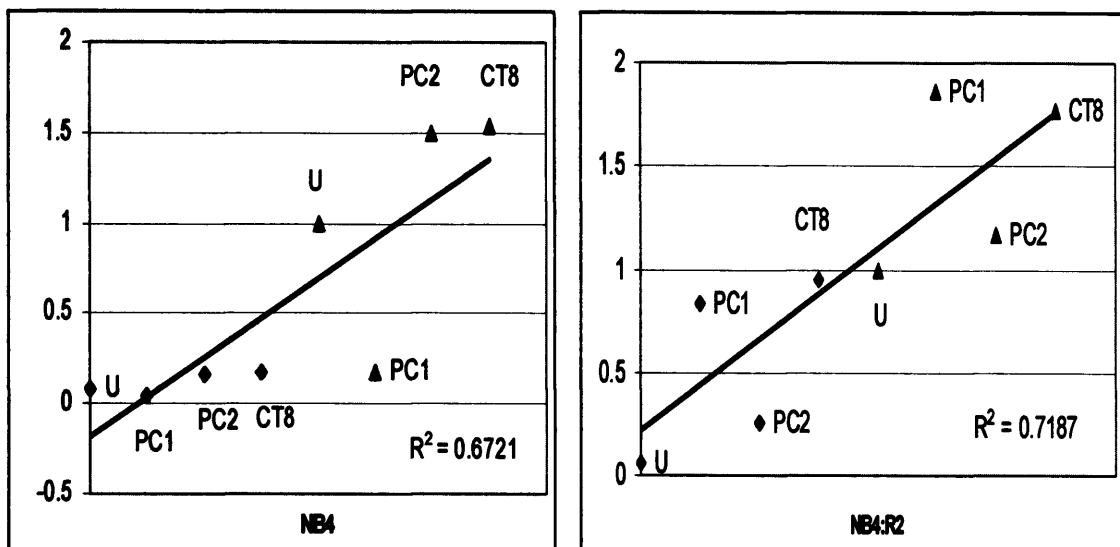


Figure 4.10 Caspase-5 gene expression in NB4 and NB4:R2 cells after treatment with LPAAT- β inhibitors for 1 hour. Figure shows a graphical representation of adjusted intensities of caspase-5 gene expression in our cell line. Note overexpression of caspase-5 after treatment with PC2 and CT8 active form in both NB4 and NB4:R2. The expression of caspase-5 with PC1 (inactive) was down regulated in NB4 while over expressed in NB4:R2. The figure is an image capture from GeneSpring software.

Figure 4.11 shows real time PCR of normalized caspase-5 and normalized oligonucleotide array. The figure represents similar caspase-5 gene expression in both techniques (Figure 4.11).

Lin et al found that caspase 5 (in high salt), 4, and 1 cleaved pro-caspase-3 with equivalent efficiencies. This was not the case with pro-IL-1 β as substrate, because caspase-1 cleaved pro-IL-1 β efficiently, caspase-4 cleaved pro-IL-1 β weakly, and caspase-5 had virtually no activity on this substrate (Lin et al. 2000). Although caspases 4 and 5 induced apoptosis when over expressed in cells (Faucheu et al. 1995;Faucheu et al. 1996c;Munday et al. 1995) there is no evidence that they play crucial roles in apoptosis, as do, for example, caspases 3, 8, and 9 (Wolf & Green 1999)



NB4	Normalized oligonucleotide array	Normalized Real-time PCR
Untreated	1	0.081±0.01
PC1 (inactive)	0.172	0.04±0.01
PC2 (active)	1.497	0.165±0.015
CT8 (active)	1.541	0.178±0.014
NB4:R2		
Untreated	1	0.062±0.007
PC1 (inactive)	1.866	0.83±0.0034
PC2 (active)	1.164	0.25±0.007
CT8 (active)	1.77	0.95±0.025

Figure 4.11 Normalized Caspase-5 expression by oligonucleotide array (▲) and real-time PCR (◆) in NB4 and NB4:R2. Oligonucleotide array data obtained from duplicate analysis where real-time PCR data was performed at three independent experiments ± SD. The real-time PCR samples were normalized by S14 housekeeping gene.

4.4.6 Verification of Cdc2

The other gene subjected to validation was Cdc2. The key cell-cycle regulator cyclin-dependent kinase Cdk 1 (also known as Cdc2) belongs to a family of cyclin-dependent kinases (Cdk) in higher eukaryotes. Cdc2 forms a complex with Cyclin B. Phosphorylation of Cdc2 at tyrosine and threonine inhibits its activity thus causing G₂ arrest. Once Cdc2 becomes activated, by dephosphorylation via Cdc25 phosphatases, the cell can progress into M phase (Gotoh et al. 2001;Masui 1992). Furthermore, cyclin B and cdc2 are also apoptotic regulators. Apoptosis occurs in response to DNA damage during haematopoiesis and lymphopoiesis (King & Cidlowski 1995). The figure (4.12) shows a graphical representation of adjusted intensities of Cdc2 gene expression in our cell line captured by GeneSpring software. NB4 cells show an overexpression of Cdc2 gene after treatment with CT8 active. The expression of Cdc2 by PC2 is more sensitive in NB4:R2 than NB4 cells, while CT8 shows an equal Cdc2 expression in both cell lines. The expression of Cdc2 with PC1 (inactive) was down regulated in NB4 while over expressed in NB4:R2 (Figure 4.12).

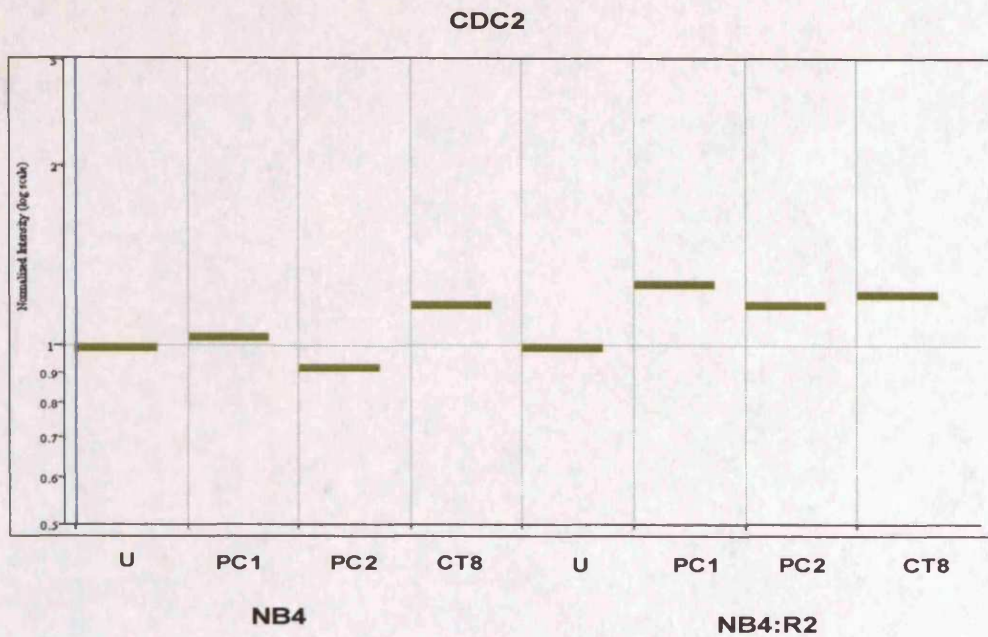
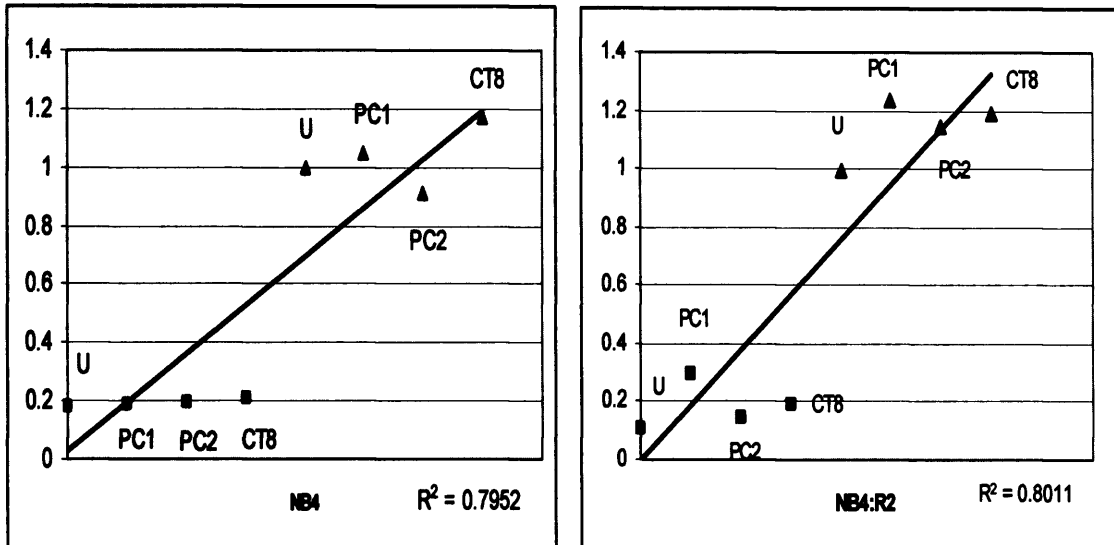


Figure 4.12 Cdc2 gene expression in NB4 and NB4:R2 cells after treatment with LPAAT- β inhibitors for 1 hour. Figure (A) top shows a graphical representation of adjusted intensities of Cdc2 gene expression in our cell line. Note over expression of Cdc2 after treatment with CT8 active form in both NB4 and NB4:R2. The expression of Cdc2 with PC1 (inactive) was down regulated in NB4 while over expressed in NB4:R2. The figure is an image capture from GeneSpring software.

Cdc2 expression was validated with real-time PCR that showed similar expression with normalized oligonucleotide array (Figure 4.13).



NB4	Normalized oligonucleotide array	Normalized Real-time PCR
Untreated	0.999	0.178±0.014
PC1 (inactive)	1.048	0.185±0.013
PC2 (active)	0.912	0.193±0.036
CT8 (active)	1.167	0.205±0.012
NB4-R2	Normalized oligonucleotide array	Normalized Real-time PCR
Untreated	0.99	0.105±0.025
PC1 (inactive)	1.237	0.293±0.015
PC2 (active)	1.147	0.145±0.031
CT8 (active)	1.191	0.190±0.026

Figure 4.13 Normalized Cdc2 expression by oligonucleotide array (▲) and real-time PCR (■) in NB4 and NB4:R2. Oligonucleotide array data obtained from duplicate analysis where real-time PCR data was performed at three independent experiments ± SD. The real-time PCR samples were normalized by S14 housekeeping gene.

4.4.7 Caspase-5 verification by Northern blot.

Northern blots were performed according to standard procedures as mentioned in material and method section (2.7). For caspase-5, complete cDNA was used as probes. To assess the relative amounts of RNA loaded into each lane, the same filter was stripped and hybridized with a PCR product for β -actin genes that remain essentially constant among samples. Hybridized filters were exposed sequentially to x-ray films. Figure 4.14 shows verification of caspase-5 gene expression by Northern blotting. The top figure as mentioned earlier represents gene intensity captured by GeneSpring software. The lower figure (B) shows the Northern blotting of caspase-5 expression. Caspase-5 expression in NB4 was up regulated at 1 hour after PC020702 (PC2) treatment; the expression was more clearly upregulated with PC2 compared with CT32228 (CT8). The expression of caspase-5 with northern blotting was similar to the data for real-time PCR.

The effect of inhibitors on NB4:R2 cell was more toxic and induced caspase-5 activation even by inactive form PC020701 (PC1). CT8 and PC2 showed similar effect on NB4:R2 cells compared with untreated cells (Figure 4.14).

The densitometry of the caspase 5 and CDC2 gene expression was quantitated using UVITec instrument (UVI Tec limited, UK). Caspase5 and CDC2 bands were analysed by UVIDOC software. The molecular weight of each band was measured according to the manufacture's instruction. We proposed caspase5 gene expression of untreated be designated as 1%. The densitometry of caspase5 in treated cells was calculated by the following formula:

$$\text{Caspase5 gene expression} = \frac{\text{molecular weight of treated}}{\text{molecular weight of untreated}}$$

However, the densitometry of caspase5 band of Northern blot demonstrated that caspase5 was not down regulated after PC1 treatment in NB4 cell which is different from the oligonucleotide array and real time PCR data. Also the densitometry shows no significant differences between untreated and treated cells in both NB4 and NB4:R2. this is may be because the Northern blot technique is less sensitive than Real time analysis (Figure 4.15).

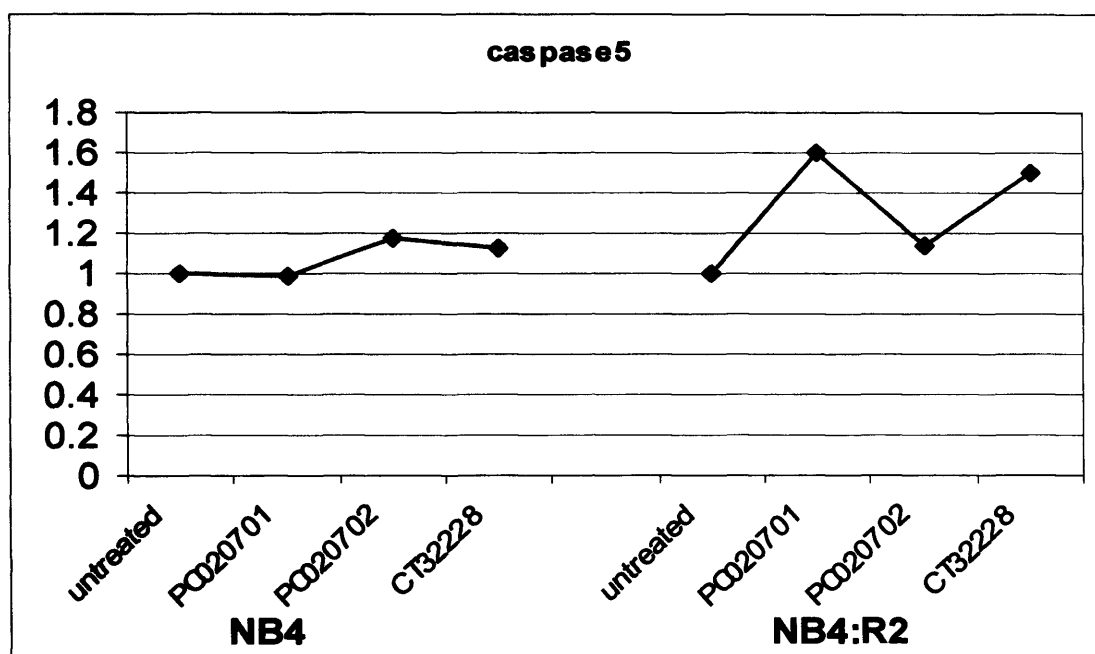


Figure 4.15: Caspase5 gene expression densitometry in NB4 and NB4:R2. Caspase 5 band of Northern blot were quantitated using UVIDOC software.

4.4.8 Cdc2 verification by Northern blot.

Figure 4.16 shows verification of Cdc2 gene expression by Northern blotting. The top figure as mentioned earlier represents gene intensity captured by GeneSpring software. The lower figure (B) shows the Northern blotting of Cdc2 expression. Cdc2 expression in NB4 was up regulated at 1 hour after CT8 induction, the expression was more clearly with CT8 compared with untreated, PC1 and PC2. These results may suggest CT8 may act on the Cdc2 gene more than PC2. The active PC2 showed different change in Cdc2 gene expression in NB4 and NB4:R2. On the other hand NB4:R2 cells showed an expression of all inhibitors for Cdc2 compared with untreated. This may suggest that Cdc2 expression act different in NB4 than NB4:R2 cells after LPAAT- β inhibitors treatment (Figure 4.16).

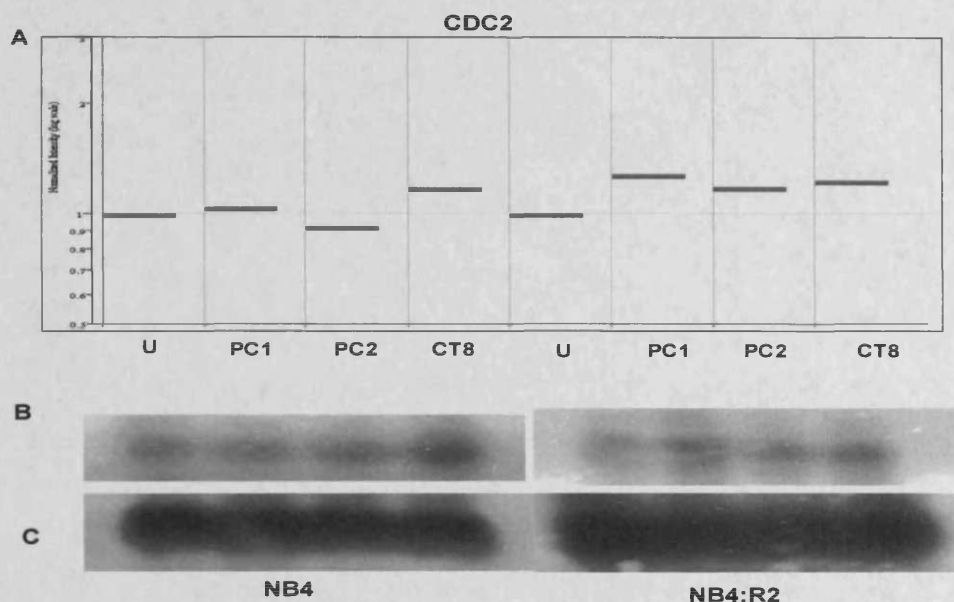


Figure 4.16 Northern blot analysis of CDC2. Northern blotting analysis of CDC2 gene expression in NB4 and NB4:R2 after 1 hour of LPAAT- β inhibitors treatment. Figure (A) top shows a graphical representation of adjusted intensities of CDC2 gene expression in our cell lines. (B) Total RNA was isolated from NB4 and NB4:R2 cells induced as described above and subjected to Northern analysis. RNA was isolated from untreated NB4 and NB4:R2 and cells treated for 1 hour after LPAAT- β inhibitors. Detail given in figure 4.1

The densitometry analysis of Northern blotting analysis showed no significant changes between untreated and LPAAT inhibitor treatment in NB4 and NB4:R2, which may indicate that Cdc2 was not affected by the drug which is inconsistent with oligonucleotide array and real time PCR (Figure 4.17).

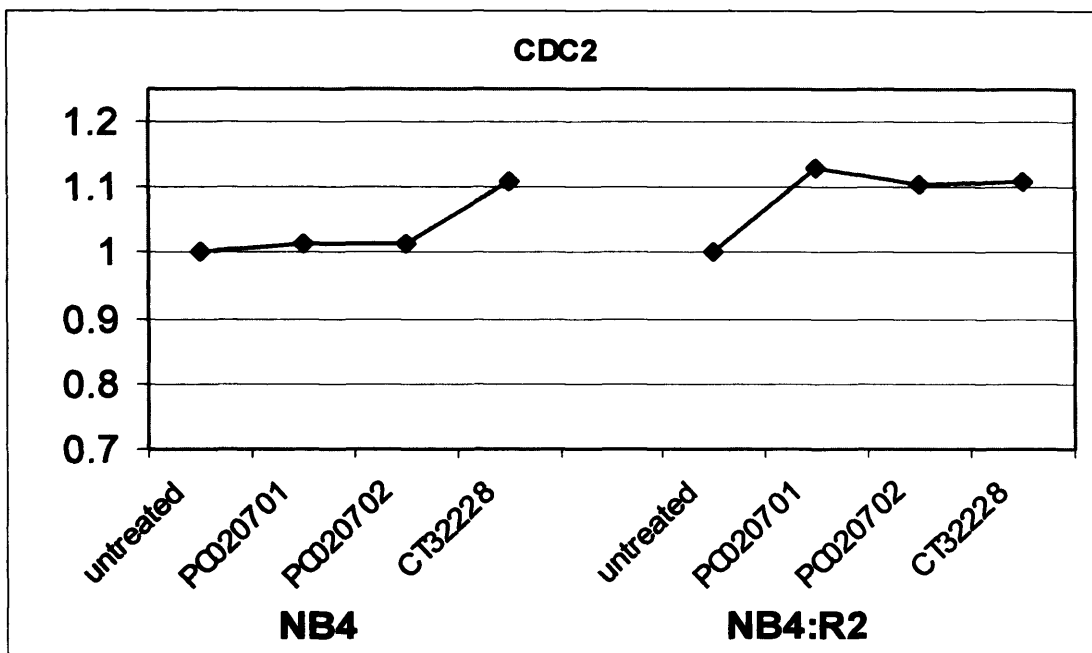


Figure 4.17: CDC2 gene expression densitometry in NB4 and NB4:R2. Cdc2 band of Northern blot were quantitated using UVIDOC software.

4.5 Discussion

In this study, oligonucleotide microarrays were used to provide information on the gene expression in NB4 and NB4:R2 cells after LPAAT- β inhibitor treatment. Information obtained from this analysis will aid in identifying genes regulated by LPAAT- β inhibitors and may provide insight in the identification of signalling pathways activated or inhibited in these cells.

It is important to note that the analysis was done after 1 hour of treatment to LPAAT- β inhibitors. Therefore the genes analyzed were differentially regulated at that time. To date no literature has reviewed gene expression or analysis by microarray after LPAAT- β inhibitor treatment.

The Gene Ontology (GO) analysis showed that when compared to the untreated, the NB4 and NB4:R2 cells after LPAAT- β inhibitor treatment, the differentially expressed genes were over-represented in the GO groups of “cell membrane integration” and “G-protein coupled receptor protein signalling pathway”.

Examination of the up and down regulated gene list (Table 4.2 & 4.3) also showed that genes related to cell membrane function or receptors were present. These may have a role in cell signalling, membrane fission activity or Ca⁺ release and may have been directly or indirectly effect by LPAAT- β inhibitors or phosphatidic acid (the end product of the enzyme activity). The expression of these genes may also suggest more complicated pathways in which these inhibitors may act. Unexpectedly we did not observe genes related to apoptosis, cell cycle and /or cell signalling especially those related to cell proliferation and apoptosis. These may be due to inhibitors after only 1 hour of induction at 250 nM being insufficient to trigger cell cycle or apoptosis pathways. Also we expected to see activation of the genes related to raf/ras/Erk and PI3K/Akt/mTOR pathways particularly as phosphotadic acid has a direct activation effect on to these two pathways, which is discussed in more detail in chapter 6.

Here we are going to discuss some of the selected genes that we found had a relation to LPAAT- β enzyme and phosphatidic acid. From the table 4.2 and 4.3, adaptor-related protein complex *AP-4* epsilon is localized to approximately 10-20 discrete dots in the perinuclear region of the cell, AP-4 functions as a vesicle coat component in different membrane traffic pathways (Hirst et al. 1999). The association of AP-4 with membranes is

regulated by the small GTPase. GTPase have been found to play a role in vesicle coat fission that is very important in endocytosis. No evidence was found for involvement of LPAAT in vesicle formation. However, Endophilin I which found have LPAAT activity, is more likely to be involved in fission formation (Schmidt et al. 1999). It seems more likely that direct insertion of LPAAT into the bilayer would have more dramatic consequences on membrane properties.

The second gene found over to be expressed, Docking protein 4 (*DOK4*). It is substrates of tyrosine kinases and function in the recruitment and assembly of specific signal transduction molecules. Cai et al recently reported *DOK4* maintaining in vivo metabolic homeostasis, insulin binds and activates insulin receptors present on insulin-responsive cells (Cai et al. 2003). No literature has reported of a relation of this gene with LPAAT- β enzyme activity or phosphatidic acid.

Sarco-/endoplasmic reticulum Ca-ATPase 3 (*ATP2A3*) is alternatively spliced transcripts of the human sarcoplasmic (or endoplasmic) reticulum Ca^{2+} -ATPase (SERCA3) gene. SERCA3 was found to be involved in pumping of Ca^{2+} into the endoplasmic reticulum (ER). Cell Ca^{2+} signalling is a dynamic process regulating a variety of important cellular functions such as secretion, contraction, metabolism, neuronal plasticity, and gene transcription (Berridge et al. 2000). (SERCA)-3 have been implicated in the possible dysregulation of Ca^{2+} homeostasis that accompanies the pathology of hypertension and diabetes.

Protocadherin 8 (*PCDH8*) is a gene belonging to the protocadherin gene family, a subfamily of the cadherin superfamily. The gene encodes an integral membrane protein that is thought to function in calcium dependent cell-cell adhesion.

One of the genes belonging to apoptosis pathways was found to be down regulated, *p53AIP1* gene, a novel target for the p53 tumour suppressor, generates three transcripts (α , β , and γ) by alternative splicing, encoding peptides of 124, 86, and 108 amino acids, respectively. Because *p53AIP1 α* and *p53AIP1 β* are localized at mitochondria, they are likely to regulate mitochondrial membrane potential. Expression of this gene is inducible by phosphorylated p53 in response to severe DNA damage, and evidence gathered to date suggests that *p53AIP1* is essential for p53-dependent apoptosis to occur (Oda et al. 2000). Matsuda et al reported that *p53AIP1* can induce apoptosis of various cancer cells regardless

of their p53 status, which means p53AIP1 triggers apoptosis directly (Matsuda et al. 2002). Cell-cycle arrest and induction of apoptosis generally have been considered the two most important functions of the p53 gene product (Levine 1997). Coon et al 2003 found that most tumour cell lines arrest and die by apoptosis irrespective of their p53 status, suggesting that p53-dependent G₂ checkpoint mechanisms are largely unaffected by LPAAT- β inhibition (Coon et al. 2003). Here we found that the gene is down regulated in both cell lines which indicate that the inhibitors did not affect the p53 status. As the over expression of such gene triggers p53 induces apoptosis.

An other gene found down regulated belongs to Suppressor of cytokine signalling (*SOCS*) 1. It was initially identified as an intracellular negative feedback regulator of the JAK-STAT signal pathway. Recently, it has been suggested that *SOCS1* affects signals of growth factors and hormones (Starr et al. 1997).

In addition, the global gene-expression profile presented by gene ontology shows that the changes observed were related to cell membrane integration and G-protein coupled receptor protein signalling pathway, these will be put in the context of other regulatory and developmental processes such as cell cycle, apoptosis and PI3K signalling which will be discussed in detail in chapters 5 and 6. This will help in explaining the role of LPAAT- β inhibitors that may act on these AML cell lines

Nevertheless, the gene intensity data cannot rule out that the caspase-5 activation found in these cell lines with active PC2 and CT8 may have a functional role in apoptosis because of the increase expression in NB4 and NB4:R2. Real time PCR results showed an over expression of caspase-5 compared with untreated in both cell lines. This may also indicate that caspase-5 may have a role in cell apoptosis. In all cases, the real-time PCR confirmed the oligonucleotide array results indicating up-regulation by LPAAT- β inhibitors (PC2 and CT8) in NB4. As shown in Fig. 4.11, Caspase-5 followed a similar pattern of expression to that of the known target gene. However, Northern blotting analysis showed different expression of caspase5 after PC1 treatment in NB4 cell from that of oligonucleotide array and real time PCR.

Caspase-5 is closely related to caspase-1 and is a constituent of the caspase-1-like subfamily (Faucheu et al. 1996b). Like caspase-1, caspase-4 and caspase-5 both cleave pro-caspase-3 to its active form, caspase-3 (Kamada et al. 2005). Further, caspase-4 and

caspase-3 are processed after Fas stimulation and can trigger the cell to apoptose (Kamada et al. 1997).

The other gene subjected for validation was Cdc2 a cell cycle regulator. The oligonucleotide microarray results showed the Cdc2 in NB4 were insignificant over expressed by CT8 and insignificant down regulated expression by PC2. The case was different with NB4:R2, Cdc2 was over expressed following treatment with all inhibitors active and inactive. Cdc2 gene expression was further validated with real time PCR and northern blotting. Cdc2 was insignificantly upregulated by PC2 and CT8 compared with untreated cell in NB4 and NB4:R2.

Previous studies have reported that Cdc2 was hypophosphorylated at protein level following treatment with LPAAT- β inhibitors in many cell lines tested. Coon et al (2003) indicated that Cdc2 was hypophosphorylated following treatment with CT32228 at 300 nM for 18 hours in HL60, Daudi (Burkitt's lymphoma), IM-9 (Lymphoblastoid) and Jurkat (T-cell leukaemia) cells (Coon et al. 2003). Recently, Hideshima et al found that Cdc2 was down regulated in Multiple Myeloma resistant cell line (DHL-4) after treatment with LPAAT- β inhibitor (CT-32615) at 200 nM for 12, 24, 36 and 48 hours (Hideshima et al. 2005). The analyses of Cdc2 in these articles were at the protein level. These results were unexpected as the cells were blocked at the G2/M phase in cell cycle analysis.

Our gene analysis results would suggest that caspase-5 may have an effect on apoptosis, as LPAAT- β inhibitors may initially induce caspase-5 gene activation. However, real time PCR and northern blotting analysis show that Cdc2 could not be triggered at 1 hour of treatment which is inconsistent with the gene array data, this may be due to either the lower level of significance in the gene arrays studies or due to the relative sensitivities of the different assays.

The next chapter we are going to discuss in detail the effect of LPAAT- β inhibitors on cell cycle and apoptosis using flow cytometry and western blotting techniques.

CHAPTER 5

The effect of LPAAT- β inhibitors on Apoptosis and Cell cycle

5.1 Introduction

The last two chapters (3 and 4) have examined the effect of LPAAT- β inhibitors on AML cell line LPAAT- β enzyme activity and gene expression respectively. The enzyme activity was measured using radioenzymatic assay. The PC020702 was found to significantly and insignificantly inhibited enzyme activity after 24 hours and 1 hour respectively. Genes differentially expressed were analyzed by oligonucleotide array (Affymetrix System). The gene ontology data showed most of the genes expressed were integrated to cell membrane, G coupled protein pathways, prostaglandin E receptor, and nuclear membrane. Despite to these result, we found caspase-5 was significantly upregulated with active form PC2 and CT8.

Apoptosis is a genetically controlled, energy-dependent process which removes unwanted cells from the body. Because of its orderly progression, apoptosis is also known as programmed cell death or cell suicide. Once initiated, apoptosis is characterized by a series of biochemical and morphological changes involving the cytoplasm, nucleus and cell membrane. Cytoplasmic changes include cytoskeletal disruption, cytoplasmic shrinkage and condensation; prominent changes in the nucleus include peripheral chromatin clumping and inter-nucleosomal DNA cleavage (DNA ladder formation); and membrane changes include the expression of phosphatidylserine on the outer surface of the cell membrane and blebbing (resulting in the formation of cell membrane-bound vesicles or apoptotic bodies). These events allow the cell to digest and package itself into membrane-bound packets containing autodigested cytoplasm and DNA, which can then be easily absorbed by adjacent cells or phagocytes (Darzynkiewicz 1995;Leist & Nicotera 1997;Osborne 1996).

Caspases, a family of proteases, are a central part of the apoptotic machinery (Thornberry & Lazebnik 1998). Caspases are expressed as precursors that are activated in a cascade following a proapoptotic stimulus. This cascade begins with autocatalytic activation of initiator caspases, which process and activate the effector caspases that, in turn, disassemble a cell. Each initiator caspase mediates a subset of proapoptotic signals. Caspase-3 cleavage is a hallmark of apoptosis triggered by many proapoptotic caspases one of which is caspase-9. The caspase-9 bound to the apoptosome is able to efficiently cleave and activate downstream executioner caspases such as caspase-3 (Rodriguez & Lazebnik 1999). These executioner caspases subsequently cleave many important intracellular substrates, leading

to characteristic morphological changes in apoptosis such as chromatin condensation, nucleosomal DNA fragmentation, nuclear membrane breakdown, externalization of phosphatidylserine, and formation of apoptotic bodies (Hengartner 2000).

Many therapeutically active anticancer treatments exert their effect by the induction of apoptosis and necrosis. Several methods exist for the detection of apoptosis using features of the cell as it undergoes the various stages leading to the death of the cell. One of the commonest uses of flow cytometry was the detection of annexin V. Understanding of the basic mechanisms that underlie apoptosis will point to potentially new targets of therapeutic treatment of diseases that show an imbalance between cell proliferation and cell loss (Jeong S, et al 2004).

Cell cycle control is a complex process by which cells decide whether to proliferate or to stay quiescent. Many different proteins are involved in this process. Basically, the engine that produces cell cycle progression is represented by a family of protein kinases (Sherr & Roberts 1995; Morgan 1995). Proliferation is characterized by cells crossing continuously, and generally in an asynchronous way the different cycle phases. S and G₂ phase durations are relatively constant, whereas the duration of G₁ phase can considerably vary according to the cell types.

The term 'cell-cycle checkpoint' refers to mechanisms by which the cell actively halts progression through the cell cycle until it can ensure that an earlier process, such as DNA replication or mitosis, is complete. There are three main checkpoints involved in controlling cell cycle progression. Checkpoint 1 drives G₁ progression and S-phase entry; checkpoint 2 governs the completion of S-phase and entry into mitosis; checkpoint 3 controls spindle formation and M-phase exit. Generally, checkpoints slow or even stop definite steps of the cycle, to furnish time for correction of molecular errors. When errors are excessive, and repair is thus impossible, the cell is eliminated by apoptosis.

This chapter investigates the effects of LPAAT- β inhibitors active (PC020702 and CT32228) and inactive (PC020701 and CT32212) on the apoptosis and cell cycle of ATRA sensitive (NB4 and HL60) and resistant (NB4:R2 and HL60-R) cell lines, these biological events can be assessed by propidium iodide, Annexin V and propidium iodide respectively. We also examine the effect of LPAAT- β inhibitors on cleaved caspase-3 activity.

5.2. Material and Methods

The full details of apoptosis, cell cycle and Western blotting analysis were outlined in chapter 2 (section 2.3.2, 2.3.3 and 2.8 respectively). Here we will give a brief description of these analyses.

5.2.1 Cell lines and treatment

Four different acute myeloid leukaemia cell lines were used in this study representing different responses to ATRA. NB4, NB4:R2, HL60 and HL60-R cells were seeded at 2.5×10^5 cells/ml in RPMI-1640 medium supplemented with 10% FBS. Each cell line was divided into five flasks, one for untreated (control) and four for treated (test). The four tests flasks were treated for 24 hours with 25 nM of LPAAT- β inhibitors (two with inactive form and two with active form). All five flasks for each cell line were gassed and incubated at 37°C and 5% CO₂. These treatment strategies were applied on Annexin V and cell cycle analysis.

The treatment strategy for Cleaved caspase-3 analysis was different from cell cycle and annexin V analysis. NB4 and NB4:R2 cell lines were used in this analysis. Each cell line was divided into six flasks, one for untreated (control) and five for treated (test). The five tests flasks were treated for 3, 6, 9, 12 and 24 hours with 25 nM of LPAAT- β inhibitor (active form only (PC020702)). All six flasks for each cell line were gassed and incubated at 37°C and 5% CO₂.

5.2.2 Annexin V-FITC:

The cells were treated as necessary with inhibitors and at the day of labelling, 1×10^5 cells were harvested and washed twice with PBS, then cells were resuspend in 100 μ l of binding buffer, after which 5 μ l (1 μ g/ml) Annexin V-FITC and 5 μ l of PI were added to the cells, cells were incubated for 15 minutes at room temperature. Finally cells were resuspended in 400 μ l binding buffer. The sample was analyzed by Flow cytometry.

5.2.3 Propidium Iodide procedure:

One millions cells were harvested and washed in PBS by centrifugation. Cells were resuspended in 200 μ l PBS, and 400 μ l ice-cold 70% ethanol in PBS was added. They were left on ice for 30 minutes (or overnight) after which they were harvested by centrifugation. Then they were washed twice and resuspended in 100 μ l of cocktail (1 x PBS, 100 μ g/ml

RNase and 50µg/ml of propidium iodide). The mixture was incubated at 37 °C for 30 minutes protected from light. The samples were analyzed within 1 hour by flow cytometry. Data was analyzed by WinMDI programme and Cyclchord software (details data analysis and gating strategy were found in section 2.4.2).

5.2.4 Immunoblotting

NB4 and NB4:R2 cells were cultured in the presence or absence of PC020702 inhibitors and then harvested, washed, and lysed. Cells were lysed with lysis buffer (20mM Tris(pH 8.0), 150 mM NaCl, 2mM EDTA, 1% NP40). The protein content of these cell lysate was determined using the Bio-Red protein assay kit. Each extract (20 ug protein) was fractionated by polyacrylamide-SDS gel electrophoresis, and then transferred to PVDF membrane (Amersham, UK). The membrane was incubated for 1 hour in blocking buffer TBS/Tween-20 (1xTBS/ 0.1%Tween-20) containing 5% BSA. After having been washed 3 times with 0.1% Tween 20 in TBS, the membrane was incubated overnight at 4 °C with each antibody (anti-cleaved caspase-3 (cleaved 19 and 17 kDa) antibody, anti-caspase-3 (35 kDa) antibody (Cell Signalling Technology, USA), and anti β-actin antibody (Sigma-aldrich, USA)) in blocking buffer. After 3 washes with the TBS/Tween-20 buffer, the membrane was incubated for 1 hour at room temperature with anti-rabbit or mouse IgG antibody linked to Horseradish Peroxidase (Amersham Biosciences, UK). Immunoreactive proteins were detected by the advanced ECLTM detection system. The membrane was exposed to Kodak film and protein position was measured compared to magicmarkTM XP Western protein standards.

5.3 LPAAT- β inhibitors on programmed cell death activation

In order to determine whether the toxicity of the LPAAT- β inhibitors had promoted any level of apoptosis or had caused an immediate death to AML cell lines. We attempted to assess an early stage of apoptosis by detecting annexin V in sensitive and resistant cells to ATRA with induction with an active and inactive form of LPAAT- β inhibitors.

To quantitate the frequency of apoptotic cells, the cultures were incubated with FITC-labelled annexin V, harvested and analyzed by flow cytometry. Apoptotic cells appeared in the annexin V +/PI – fraction, whereas dead cells appeared in annexin V+/PI+ fraction. Viable cells remained negative for both parameters (Benz J & Hofman, A; 1997). A few apoptotic cells after 24h culture without induction can be visualized in bivariate annexin V-FITC/PI analysis using WinMDI programme.

5.3.1 Cells culture and treatment

NB4, NB4:R2, HL60 and HL60-R cells seeded at 2.5×10^5 cell/ml at day 0. Each cell line was divided into 5 flasks and were incubated for 24h at concentration 50 nM with CT-32212 and CT-32228 and 25 nM with PC020701 and PC020702 (Table 5.1). On the day of labelling cells were harvested and assessed by the annexin V/PI method.

No. of Flask	NB4	NB4:R2	HL60	HL60-R
1	Untreated	Untreated	Untreated	Untreated
2	50 nM CT32212	50 nM CT32212	50 nM CT32212	50 nM CT32212
3	50 nM CT32228	50 nM CT32228	50 nM CT32228	50 nM CT32228
4	25nM PC020701	25nM PC020701	25nM PC020701	25nM PC020701
5	25nM PC020702	25nM PC020702	25nM PC020702	25nM PC020702

Table 5.1 A summary of treatment of AML cells lines for Annexin V assay

5.3.2 The effect of LPAAT- β inhibitors on NB4 and NB4:R2 apoptosis

As shown in **figure 5.1**, the untreated cells (control) of NB4 and NB4:R2 cells are scored viable due to absence of annexin V-FITC and propidium iodide uptake (lower left quarter (R1)). The lower right quarter (R3) represents apoptotic cells which still showed an intact cytoplasmic membrane, as indicated by annexin V staining only. The upper right quarter (R2) shows the dead cells (necrotic cells), as indicated by dual staining of annexin V- FITC and PI uptake. NB4 and NB4:R2 cells after 24h induction of inactive form CT-32212 and PC020701 (designated by CT12 and PC1 respectively) showed no increase in the number of apoptotic cells and dead cells compared with the untreated cells (control). However the active form CT-32228 and PC020702 (designated by CT8 and PC2 respectively) resulted in an increase in the apoptotic and dead cells compared with both untreated cells and the inactive form. As mentioned in material and methods (section 2.3.2.3), due to compensation error the region surrounding the apoptotic cells has been shifted (**Figure 5.1**).

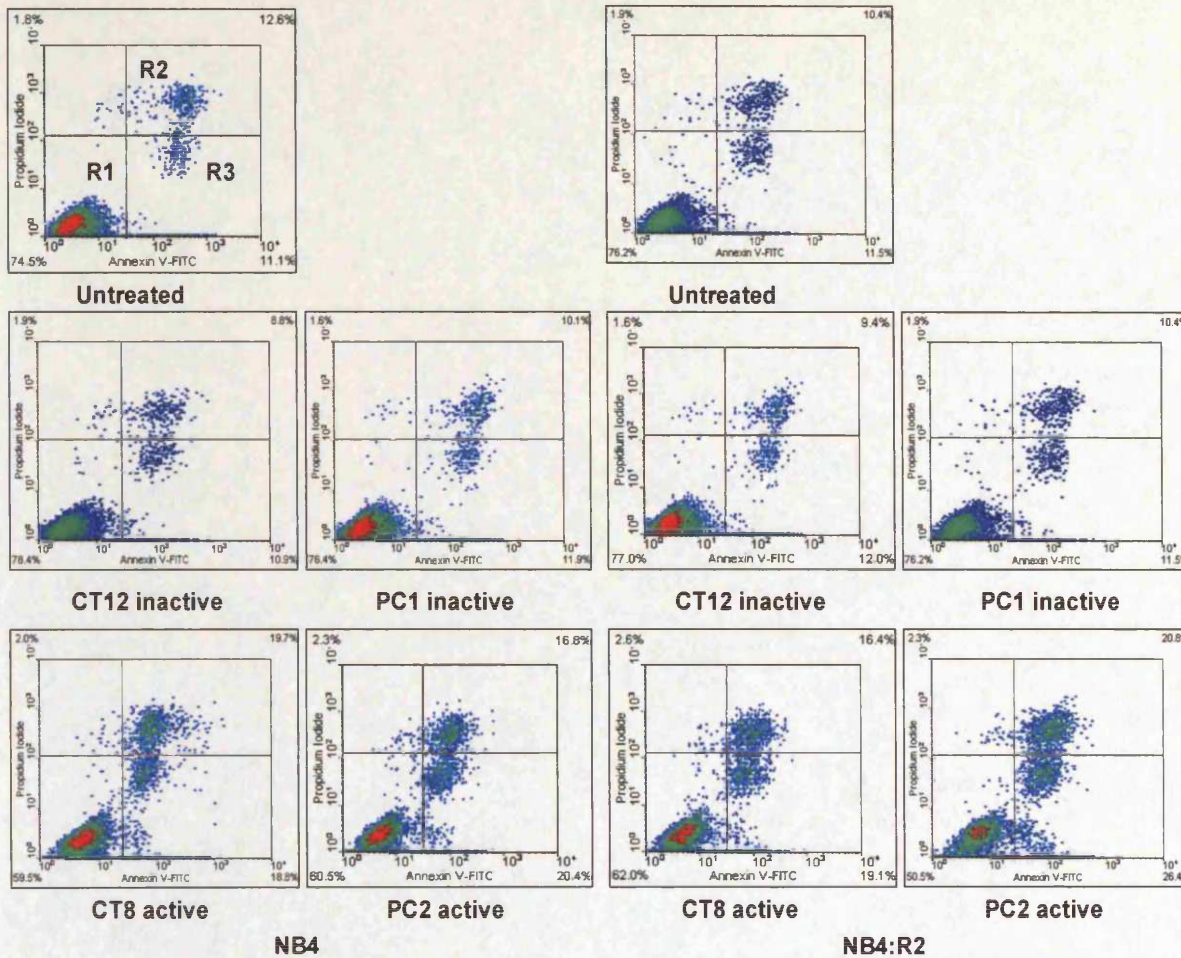


Figure 5.1 Induction of apoptosis by LPAAT- β inhibitors. NB4 and NB4:R2 cells were seeded at 2.5×10^5 cell/ml for 24h with or without LPAAT- β inhibitors (CT-32212, CT-32228, PC020701 and PC020702). After 24h cells were resuspended in diluted binding buffer and cell density was adjusted to 2×10^5 /ml. $5 \mu\text{l}$ of annexin V-FITC and $5 \mu\text{l}$ of PI were added to the cells and incubated for 15 minutes at room temperature in the dark. 400 μl of binding buffer was added and samples analyzed by flow cytometry. Data was analyzed using WinMDI ver 2.8 software programme. The lower left quadrant (R1) of each density plot shows viable cell (Annexin V-/PI-). The upper right quadrant (R2) of each density plot shows necrotic cells that were (Annexin +/PI+). The lower right quadrant (R3) shows apoptotic cells that were not necrotic (Annexin V+/PI-).

The figure below shows no difference in apoptotic cells number between untreated and inactive form PC1 and CT12 of LPAAT- β inhibitors after 24h. The same result was also found with viable and dead cells. The incubation of NB4 cells with PC2 and CT8 caused an increase in the number of apoptotic cells compared with untreated. CT32228 increased apoptotic cells from 10% to 19% in NB4 cells. While PC020702 exhibited an increase in apoptotic cells from 10% (untreated) to 24% (treated) after 24 hours. NB4 cells are more sensitive to PC2 than CT8 as we can see from increase in the mean percentage value of the apoptotic cells. (Figure 5.2).

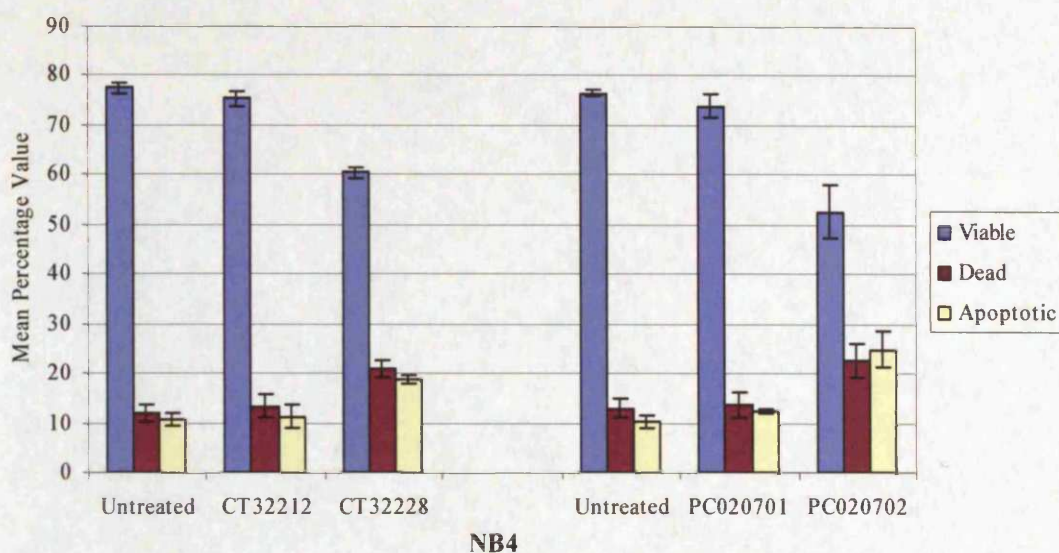


Figure 5.2 The effect of LPAAT inhibitors on apoptosis of NB4 cells. NB4 cells were seeded at 2.5×10^5 /ml. The cells were divided into 5 flasks. The first flask was untreated, the second and the third flasks were treated with 50 nM of CT32212 and CT32228 (inactive and active respectively) of LPAAT- β inhibitors. The fourth and the fifth flasks were treated with 25 nM of PC020701 and PC020702 (inactive and active respectively) of LPAAT- β inhibitors. The cells were incubated for 24h, then harvested and labelled with annexin V. The blue bars represent the viable cells, red bars represent the dead cells and yellow bars represent the apoptotic cells. Data are expressed as mean percentage value obtained from at least three independent experiments \pm SD.

NB4:R2 cells showed a similar response to NB4 cells. No differences were found between untreated and inactive form of these inhibitors. Whereas PC2 and CT8 showed an increase in the apoptotic cell number compared with untreated. Treatment of NB4:R2 cells for 24 hours with 50 nM (CT32228) lead to an increase in apoptotic cells from 10% (untreated) to 20%. While NB4:R2 cells treated with 25 nM (PC020702) exhibited an increase in apoptotic cells from 10% (untreated) to 26%. The dead cell were also increased in the NB4:R2 cells after treatment with the active form compared with untreated and inactive form of LPAAT- β inhibitors (**Figure 5.3**). These results suggest that LPAAT- β inhibitors were able to induce apoptosis in AML sensitive and resistant cells to ATRA.

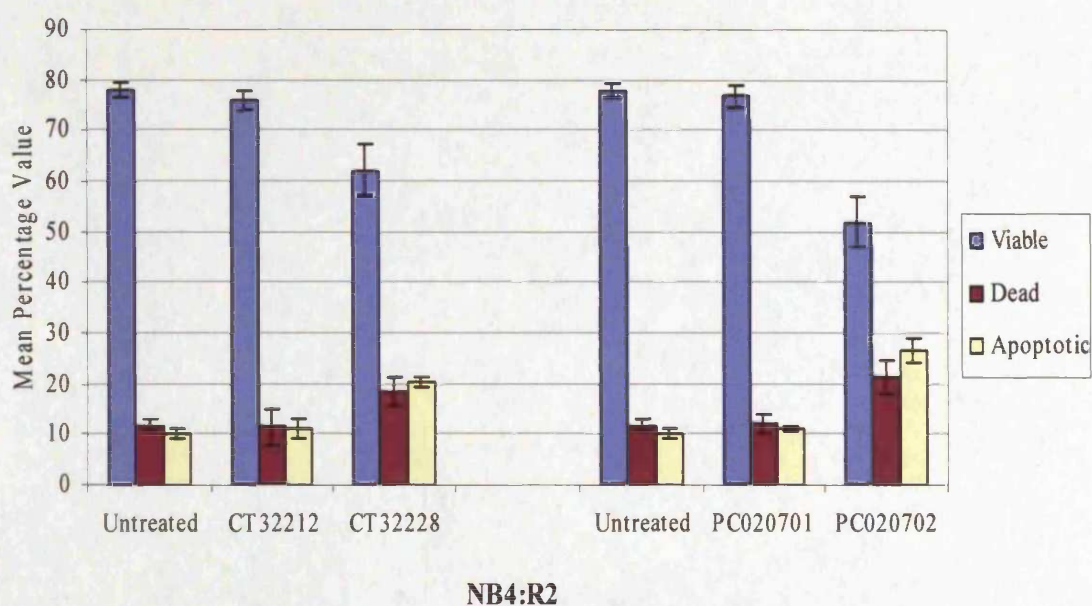


Figure 5.3 The effect of LPAAT inhibitors on apoptosis of NB4:R2 cells. NB4:R2 cells were seeded at 2.5×10^5 /ml. The cells were divided into 5 flasks. The first flask was untreated, the second and the third flasks were treated with 50 nM of CT32212 and CT32228 (inactive and active respectively) of LPAAT- β inhibitors. The fourth and the fifth flasks were treated with 25 nM of PC020701 and PC020702 (inactive and active respectively) of LPAAT- β inhibitors. Details are as given in **Figure 5.2**.

5.3.3 The effect of LPAAT- β inhibitors on HL60 and HL60-R apoptosis

Incubation of HL60 and HL60-R with 50 nM CT32212 and 25 nM PC020701 (inactive form) resulted in no significant increase in apoptotic cells compared with untreated cells. HL60 cells treated for 24 hours with 50 nM (CT32228) showed an increase in apoptotic cell number from a 8% (untreated) to 15%. While HL60 cells treated with 25 nM (PC020702) demonstrated an increase in apoptotic cells from 9% (untreated) to 18%. HL60 and HL60-R show less sensitivity to CT8 and PC2 active forms compared to NB4, NB4:R2 cells at the same concentration after 24h (Figure 5.4).

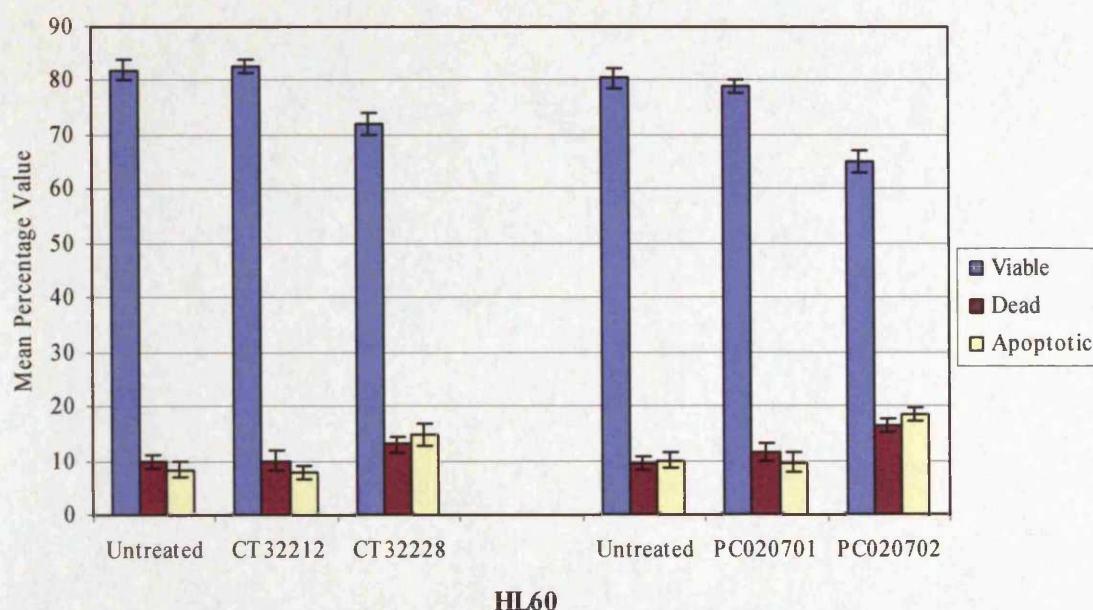


Figure 5.4 The effect of LPAAT inhibitors on apoptosis of HL60 cells. HL60 cells were seeded at 2.5×10^5 /ml. The cells were divided into 5 flasks. The first flask was untreated, the second and the third flasks were treated with 50 nM of CT32212 and CT32228 (inactive and active respectively) of LPAAT- β inhibitors. The fourth and the fifth flasks were treated with 25 nM of PC020701 and PC020702 (inactive and active respectively) of LPAAT- β inhibitors. Details are as given in Figure 5.2.

HL60-R cells exhibited an increase in apoptotic cells after treatment with CT32228 and PC020702. Treated HL60-R cells after 24 hours with 50 nM (CT32228) showed an increase in apoptotic cells from a 11% (untreated) to 17%. While HL60-R cells treated with 25 nM (PC020702) demonstrated an increase in apoptotic cells from 11% (untreated) to 20%. There was also an increase in dead cell number seen after PC020702 treatment (Figure 5.5)

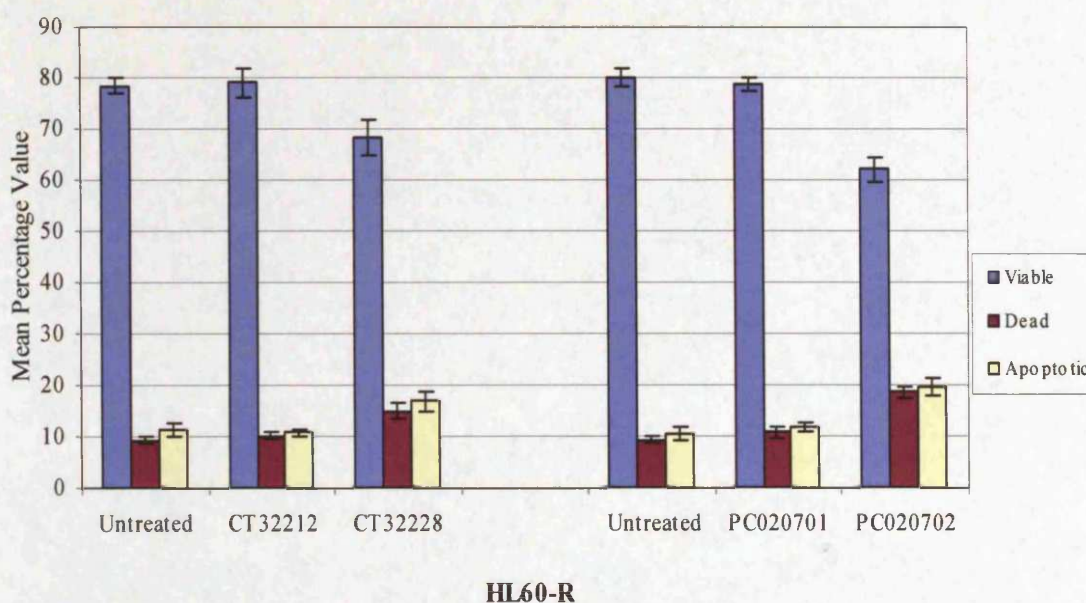


Figure 5.5 The effect of LPAAT inhibitors on apoptosis of HL60-R cells. HL60-R cells were seeded at 2.5×10^5 /ml. The cells were divided into 5 flasks. The first flask was untreated, the second and the third flasks were treated with 50 nM of CT32212 and CT32228 (inactive and active respectively) of LPAAT- β inhibitors. The fourth and the fifth flasks were treated with 25 nM of PC020701 and PC020702 (inactive and active respectively) of LPAAT- β inhibitors. Details are as given in Figure 5.2.

5.3.4 Apoptosis Triggered by PC020702 Is Mediated via Caspase-3

The induction of apoptosis was examined by LPAAT- β inhibitor through annexin V. Apoptosis triggered by LPAAT- β inhibitor (PC020702) was further characterized by examining cleavage of caspase-3 with a molecular weight (19 & 17 kDa). NB4 cells were treated with 25 nM of PC020702 and PC020701 for 0, 3, 6, 9, 12 and 24 hours were subjected to Western blotting to assess cleavage of caspase-3. In a time course experiment of PC2 (25 nM) treatment of NB4 cells, caspase-3 were cleaved within 3 h. Over time increased the level of caspase-3 cleavage were increased. At the same time the endogenous total caspase-3 decreased. For equal loading, the membrane was stripped and re-probed by β -actin (Figure 5.6).

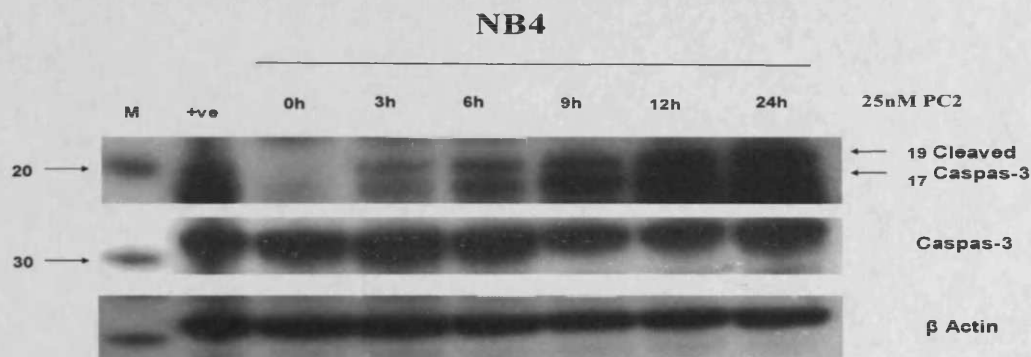


Figure 5.6 PC020702 induces caspase-3 cleavage in NB4. NB4 cells were cultured with 25 nM PC020702 for 0, 3, 6, 9, 12 and 24 h. Cells were then harvested, lysed, and subjected to Western blotting for detection of cleavage of caspase-3 using specific Abs. The membranes were striped and re-probed for total caspase-3 (middle panel). A band of β -actin, demonstrating equal protein loading, is presented as a loading control (lower panel). The sign M and +ve represent to protein marker and positive control protein respectively.

NB4:R2 cells represented cleaved caspase-3 was detected after PC020702 treatment after 3 hours. The total caspase-3 showed a decreased in there size as the time increased with treatment, for equal loading, membrane was re-probed with β -actin (**Figure 5.7**). Caspase - 3 cleavage is a hallmark of apoptosis triggered by proapoptotic proteins including caspase-9. Taken together, these results (annexin V expression and cleavage of caspase3) indicate that PC020702 and CT32228 induced apoptosis in both ATRA sensitive and resistant AML cell lines.

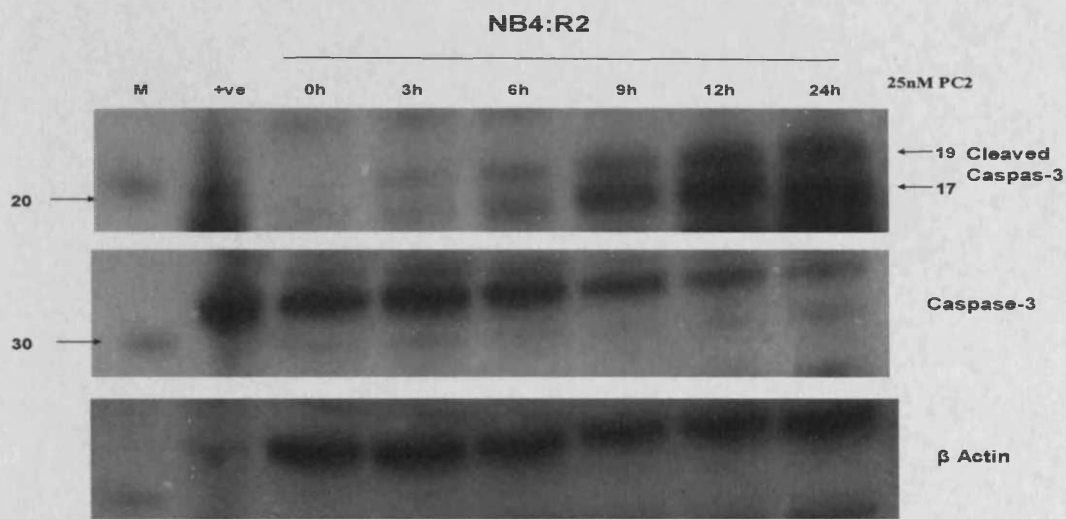


Figure 5.7 PC020702 induces caspase-3 cleavage in NB4:R2. NB4:R2 cells were cultured for 0, 3, 6, 9, 12 and 24h in the presence of 25 nM PC020701. Cells were then harvested, lysed, and subjected to Western blotting for detection of cleavage of caspase-3 using specific Abs. The membranes were striped and re-probed for total caspase-3 (middle panel). A band of β -actin, demonstrating equal protein loading, is presented as a loading control (lower panel). The sign M and +ve represent to protein marker and positive control protein respectively.

The densitometry of the cleaved caspase 3 (17 & 19 kDa) western Blotting was quantitated using UVITec instrument (UVI Tec limited, UK). Caspase 3 bands were analysed by UVIDOC software. The molecular weight of each band was measured according to the manufacture's instruction. We proposed cleaved caspase 3 activation of untreated be designated as 0%. The densitometry of cleaved caspase 3 in treated cells was calculated by the following formula:

$$\text{Caspase5 gene expression} = \frac{\text{molecular weight of treated}}{\text{molecular weight of untreated}}$$

the densitometry of caspase 3 band of western blot demonstrated that caspase 3 was Activated after PC2 treatment in NB4 cell Also the densitometry shows similar activation of cleaved caspase 3 in NB4:R2 after PC2 incubation. The data suggest an activation of cleaved caspase 3 at dose/time dependent manner after PC2 treatment in both NB4 and NB4:R2 cell lines (Figure 5.8 and 5.9)

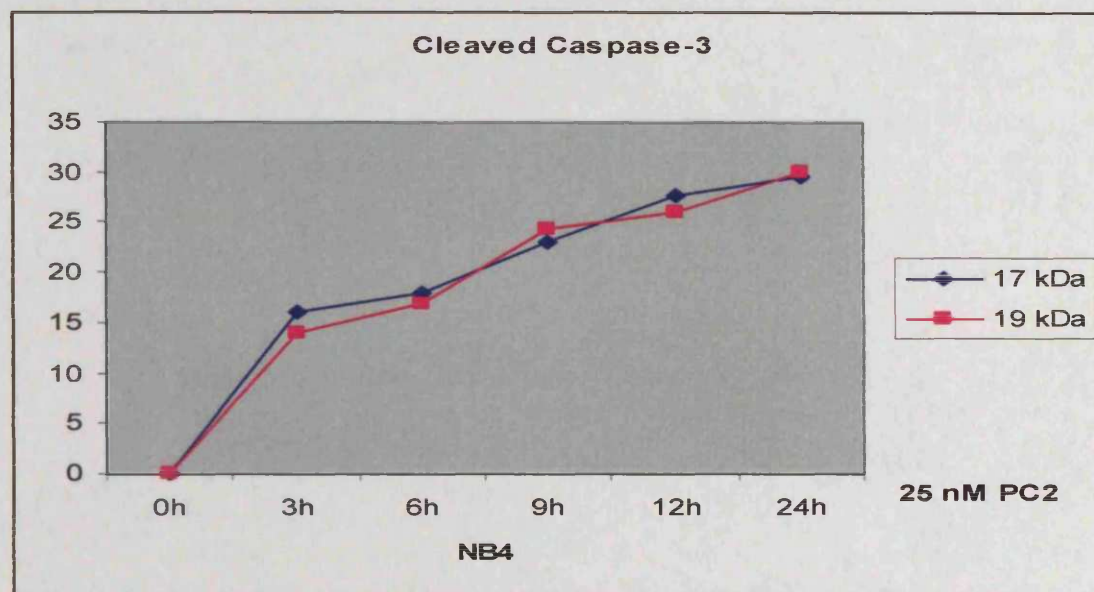


Figure 5.8 Quantitation of cleaved caspase 3 in NB4 cells. After treatment with PC020702 at the time indicated NB4 cells were thawed, washed, harvested by centrifugation and lysed in RIPA buffer. 100 ug of cell lysate was loaded on SDS-PAGE gel and analyzed by western blotting. The cleaved caspase 3 bands (17 & 19 kDa) were quantitated using UVIDOC software.

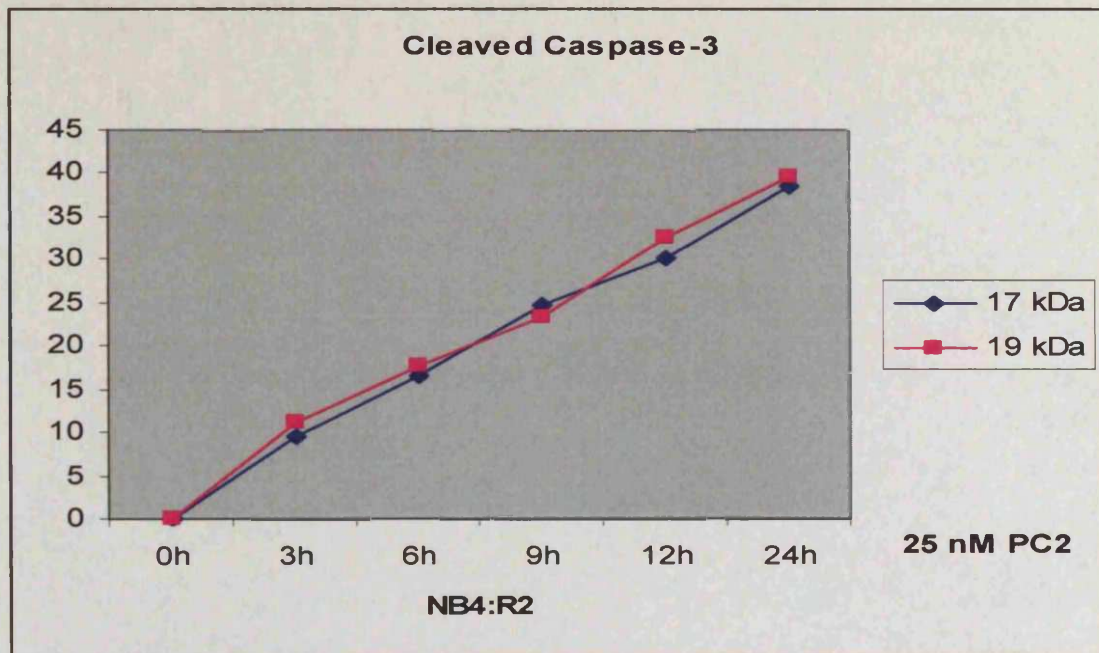


Figure 5.9 Quantitation of cleaved caspase 3 in NB4:R2 cells. After treatment with PC020702 at the time indicated NB4:R2 cells were thawed, washed, harvested by centrifugation and lysed in RIPA buffer. 100 ug of cell lysate was loaded on SDS-PAGE gel and analyzed by western blotting. The cleaved caspase 3 bands (17 & 19 kDa) were quantitated using UVIDOC software.

5.4 LPAAT- β inhibitors on cell cycle progression

The regulation of cell cycle progression is one of the most intensively studied fields in contemporary cell biology. In a typical animal cell cycle of about 24h, G₁, S, G₂ and M last for about 12, 6, 6 and 1 h, respectively. This section shows the effect of LPAAT- β inhibitors on NB4 and NB4:R2 cell cycle progression. DNA content per cell was determined using the DNA-binding fluorochrome propidium iodide (PI) and flow cytometric analysis. PI stained nuclei emit fluorescent light and the FL2 detector of the flow cytometry was used to analyse the light emitted by stained cells. The fluorescence signal produced by excitation at 488nm was detected at around 585 nm and the level of fluorescence obtained is proportional to the amount of bound PI. Using markers to analyse the distribution of DNA content the percentage of cells in each cell cycle phase G₀/G₁, S and G₂/M was determined. The flow cytometric analysis and gating strategy was given in **Section 2.4**. Data analysis was performed in WinMDI version 2.8 and Cylchred version 1.0.2 software.

5.4.1 Cell culture and treatment

Cell culture and treatment are as given in **Table 5.1**.

5.4.2 Cell cycle progression on NB4 and NB4:R2 with LPAAT- β inhibitors

Figure 5.8 shows typical histogram of cell cycle stained by PI method. The black marker lines represents different cell cycle phase. The black lines in the figures exhibited different cell cycle phases during cell proliferation (G₁, S and G₂/M phase). The G₁ Phase represents to G₀/G₁ phase where the cells accumulate proteins, grow in size and decide from exogenous and endogenous signals whether to progress to S phase (for synthesis) or become arrested. The S phase represents the duplication of cellular DNA content and synthesis of histones to package the newly synthesized DNA into chromatin. The G₂/M phase represents where G₂ is to assure that DNA replication is completed before chromosome segregation takes place. Finally M phase represents to the G₂ period precedes cell division which takes place during M phase (for mitosis) (Mullner, E et al 1996; Marks, P et al 1996; Yen, A 1985).

NB4 and NB4:R2 cells were treated with or without LPAAT- β inhibitors. The histogram shows no differences in cell cycle progression between untreated and treated with inactive form PC020701 and CT32212 after 24h of treatment. Treatment with the active forms of these drugs gave use to extensive apoptosis as demonstrated by the increase in the preparation of the cells with a sub G0/G1 DNA content. Since these cells may be apartming from any point in the cell cycle, then may be the interpretation of this data very difficult; for example the analysis cannot distinguish viable cells in S phase from cells that have undergone apoptosis in G2/M and have subsequently reduced this DNA content as a result of the apoptotic process. However, the data would indicate that these inhibitors do promote a degree of G2/M arrest (Figure 5.10).

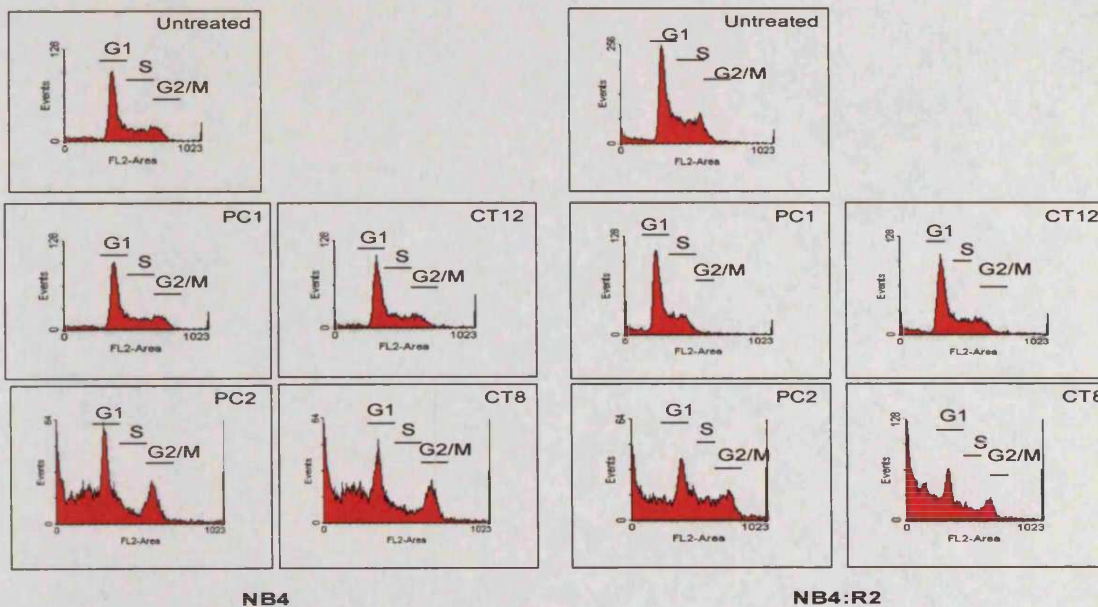


Figure 5.10 Cell cycle phases of NB4 and NB4:R2 using Propidium Iodide (PI) method. NB4 and NB4:R2 cells were seeded at 2.5×10^5 cell/ml for 24h with or without LPAAT- β inhibitors (CT-32212 (CT12), CT-32228 (CT8), PC020701 (PC1) and PC020702 (PC2)). The cells were resuspended at concentration of $1-2 \times 10^5$ cells in PBS. The cells were fixed in ice cold ethanol for at least 30 minutes. Then the cells were washed with PBS and resuspended in 400 μ l. A volume of 100 μ l of cocktail (100 μ g/ml Rnase, 50 μ g/ml probidium iodide, and 1x PBS) were added to the samples and incubated at 37 $^{\circ}$ C for 30 minutes. The samples were analyzed by flow cytometry. The markers, represent to G0/G1 phase, S phase and G2/M phase respectively.

Exposure of NB4 cells to active form PC020702 and CT32228 shows a different cell cycle phase pattern than inactive and untreated cells. Both cell lines started to be arrested at S phase with slight arrest in G2/M phase as well. PC020702 at optimal concentration (25 nM) ceased cellular proliferation of NB4 by increased the percentage of cells at S phase and G2/M phase reached 38 % and 16% respectively, and decreased cells on G0/G1 phase to 48% after 24 hours. This means that the active forms PC2 and CT8 of LPPAT- β inhibitors at 25nM and 50nM respectively started to exhibit some inhibitory effect on the cell cycle as early as 24h. However, the analysis was performed by Cylchred software which cannot differentiate between cells goes into apoptosis and that arrested in G2/M phase. Therefore it is literally that many events recorded in S phase and G1 are actually cells which have undergone apoptosis in G2/M phase (**Figure 5.11**).

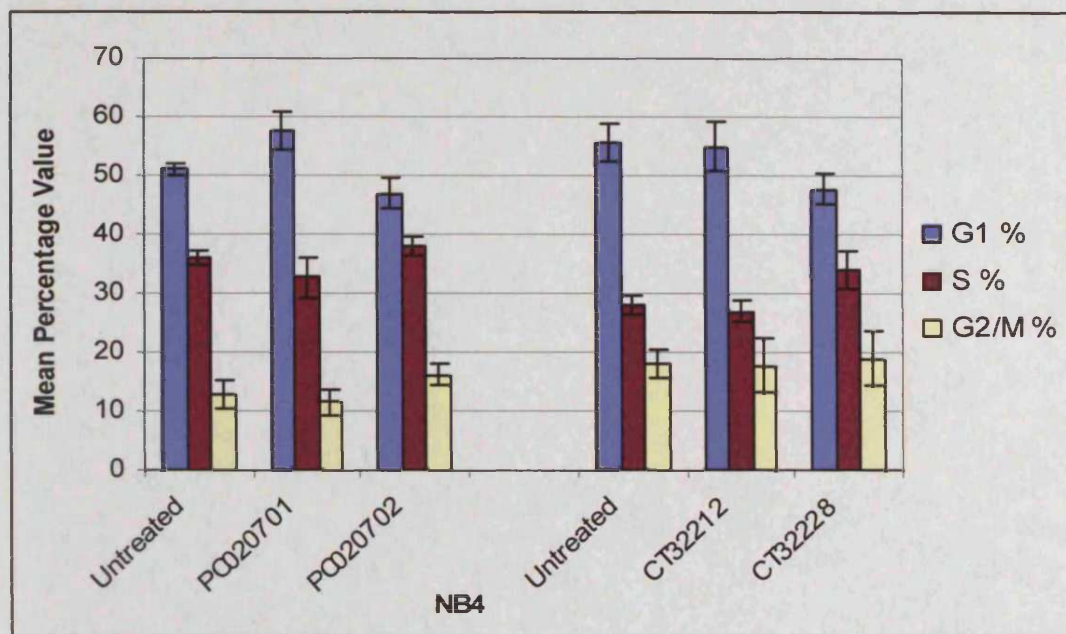


Figure 5.11 Cell cycle phases of NB4 cells after LPAAT- β inhibitor induction using the propidium iodide method. NB4 cells were treated with and without LPAAT- β inhibitors for 24h. On the day of labelling, $1-2 \times 10^5$ cells were harvested and fixed in ice cold ethanol for 30 minutes. After washing, a cocktail of (100 μ g/ml Rnase , 50 μ g/ml PI and 1x PBS) was added to samples and incubated at 37°C for 30 minutes. Data are expressed as mean percentage value obtained from at least three independent experiments \pm SD.

NB4:R2 cells showed an increased in S phase (from 35% to 40%) and G2/M phase (from 11% to 15%), and decreased cells on G0/G1 phase (from 55% to 48%) after PC020702 treatment. CT32228 exhibited arrest in G2/M phase (from 17% to 19-20%) and S phase (from 30% to 34%) and decreased cells on G0/G1 (from 54% to 48%). NB4:R2 cells showed very similar response to these event as NB4 cells. The events recorded in S phase was cells undergone into apoptosis from G2/M phase (Figure 5.12).

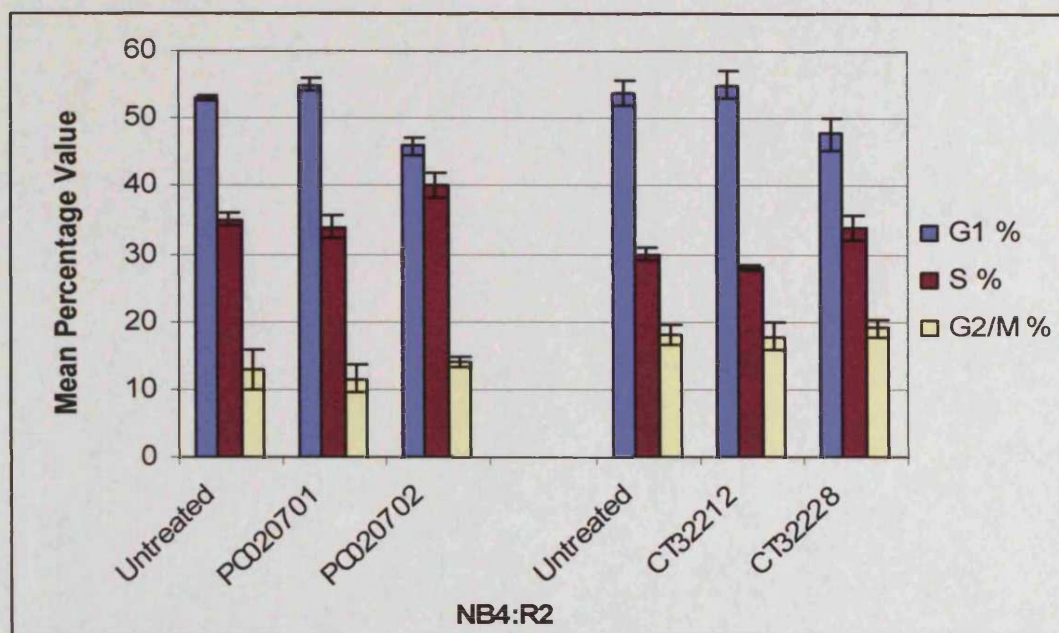


Figure 5.12 Cell cycle phases of NB4:R2 cells after LPAAT- β inhibitor induction using the propidium iodide method. NB4:R2 cells were treated with and without LPAAT- β inhibitors for 24h. On the day of labelling, $1-2 \times 10^5$ cells were harvested and fixed in ice cold ethanol for 30 minutes. After washing a cocktail (100 μ g/ml Rnase , 50 μ g/ml PI and 1x PBS) was added to samples and incubated at 37°C for 30 minutes. Data are expressed as mean percentage value obtained from at least three independent experiments \pm SD.

5.4.3 Cell cycle progression on HL60 and HL60-R with LPAAT- β inhibitors

The changes in the cell cycle distribution following treatment with 25 nM and 50 nM PC020702 and CT32228 respectively followed by a 30 min pulse label with PI on 24h. On day of labelling HL60 cells showed an accumulation of the cells in G2/M phase and no effect of the inactive form. HL60-R cells showed very similar events as HL60, NB4 and NB4:R2 after 24h of treatment (**Figure 5.13**).

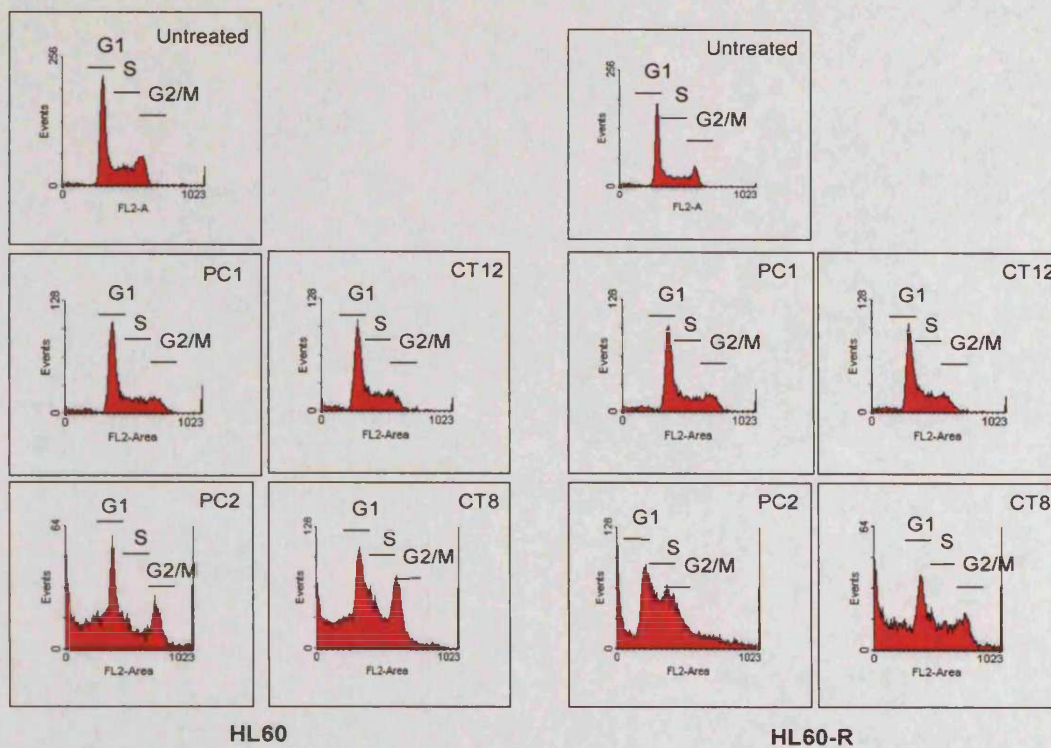


Figure 5.13 Cell cycle phases of HL60 and HL60-R using Propidium Iodide (PI) method. HL60 and HL60-R cells were seeded at 2.5×10^5 cell/ml for 24h with or without LPAAT- β inhibitors (CT-32212 (CT12), CT-32228 (CT8), PC020701 (PC1) and PC020702 (PC2)). The cells were resuspended at concentration of $1-2 \times 10^5$ cells in PBS. The cells were fixed in ice cold ethanol for at least 30 minutes. Then the cells were washed with PBS and resuspended in 400 μ l. A volume of 100 μ l of cocktail (100 μ g/ml Rnase , 50 μ g/ml PI and 1x PBS) was added to the samples and incubated at 37 $^{\circ}$ C for 30 minutes. The samples were analyzed by flow cytometry. The black markers represent to G1 phase, S phase and G2/M phase respectively.

HL60 cell cycle shows as we expected, an arrest in G2/M phase after 24h of treatment with the active forms and was accompanied by a reciprocal decrease in the G0/G1 phases. Cell cycle of HL60 treated with PC020702 at its effective dose (25 nM) started to exhibit some inhibitory effect on cell cycle after 24 hours i.e., 58% in G₀/G₁ phase, and 8% in G2/M phase in untreated, and was at 52 % at G₀/G₁ and 15% at G2/M phase after treatment. Cell cycle of HL60 treated with CT32228 at its effective dose (50 nM) started to exhibit some inhibitory effect on cell cycle after 24 hours i.e., 59% in G₀/G₁ phase, and 8% in G2/M phase in untreated, and reached to 49 % at G₀/G₁ and 19% at G2/M phase after treatment. As mentioned earlier (section 5.4.2), the analysis of the data was performed by Cylchred software which cannot differentiate DNA content in the S phase and the actual cells gone to apoptosis in G2/M phase, therefore a slight accumulation of HL60 cells in S phase were observed.

This means that the active form of inhibitors is also cell cycle blocking agent, which can block the cells at G2/M phase and stop the cells from cycling (**Figure 5.14**).

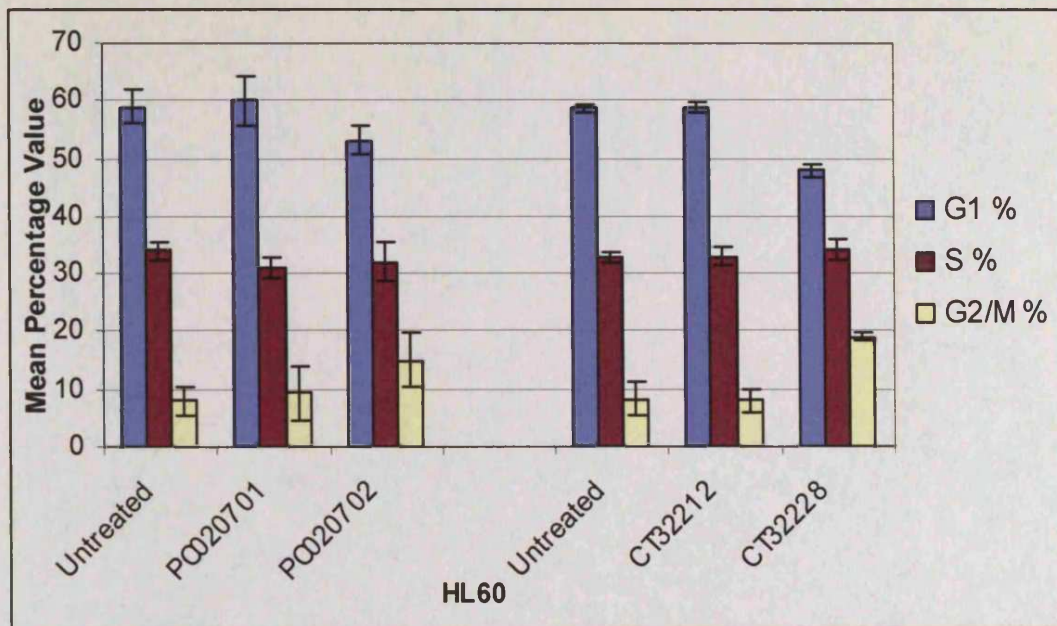


Figure 5.14 Cell cycle phases of HL60 cells after LPAAT- β inhibitor induction using the propidium iodide method. HL60 cells were treated with and without LPAAT- β inhibitors for 24h. On the day of labelling, $1-2 \times 10^5$ cells were harvested and fixed in ice cold ethanol for 30 minutes. After washing a cocktail (100 $\mu\text{g/ml}$ Rnase , 50 $\mu\text{g/ml}$ PI and 1x PBS) was added to samples and incubated at 37°C for 30 minutes. Data are expressed as mean percentage value obtained from at least three independent experiments \pm SD.

HL60-R cell cycle showed an accumulation in S and G2/M phase similar to HL60, NB4 and NB4:R2 cells. As seen with NB4 and NB4:R2 the inactive form shows no effect on cell cycle progression in HL60 and HL60-R (Figure 5.15).

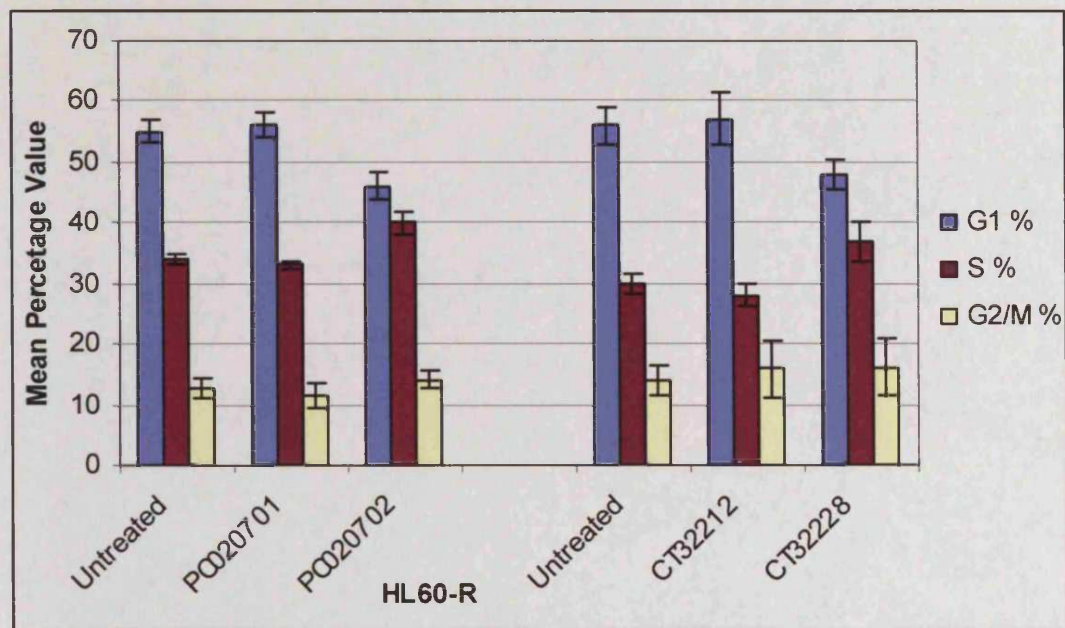


Figure 5.15 Cell cycle phases of HL60-R cells after LPAAT- β inhibitor induction using the propidium iodide method. HL60-R cells were treated with and without LPAAT- β inhibitors for 24h. On the day of labelling, $1-2 \times 10^5$ cells were harvested and fixed in ice cold ethanol for 30 minutes. After washing a cocktail (100 μ g/ml Rnase , 50 μ g/ml PI and 1x PBS) was added to samples and incubated at 37°C for 30 minutes. Data are expressed as mean percentage value obtained from at least three independent experiments \pm SD.

5.5 Discussion

This chapter examined the effect of LPAAT- β inhibitors on the apoptosis and cell cycle arrest on ATRA sensitive and resistance cells after 24h of treatment. The previous chapter 3 indicates that the enzyme activity was inhibited after 24 h and as early as 1 hour. Also the active form of LPAAT- β inhibitors induced antiproliferative effect on AML cell lines at nanomolar concentration. Chapter 4 examined the affect of LPAAT- β inhibitors on genes expression after 1h of treatment. There were varied large number of genes expressed which made the analysis difficult, with unexpressed expected genes related to raf/ras/Erk and PI3K/Akt/mTOR pathways .However, the Gene Ontology data showed significant involvement of cell membrane and its receptors genes expression.

This chapter discusses the affect of LPAAT- β inhibitors on cell cycle progression and apoptosis by probidium iodide and Annexin V-FITC staining along with PI respectively. Induction of apoptosis is tested also by caspase 3 cleavage using western blotting. The inactive forms of LPAAT- β inhibitors (PC020701 & CT32212) have no effect in increasing the proportion of apoptotic cells, with the number of viable and dead cells remaining almost the same as untreated cells in both ATRA sensitive and resistant cells. The active form CT32228 and PC020702 caused an increase in apoptotic cells in both NB4 and NB4:R2 cells compared with untreated cells

HL60 and HL60-R cells were less sensitive to CT8 than PC2 after 24h. We observed that PC020702 and CT32228 were induced apoptosis by increasing annexin V in both HL60 and HL60-R.

Importantly Western blot data showed that PC020702 triggered activation of cleaved caspase-3 in a time- and dose-dependent fashion in both NB4 and NB4:R2 cells, NB4:R2 cells triggered cleavage of caspase-3 at a slightly slower rate than NB4 cells.

At cell cycle level, these inhibitors showed cells accumulation at G2/M phase after 24h in NB4, NB4:R2, HL60 and HL60-R. As mentioned earlier, the Cylchred data analysis presented in figures (5.11, 5.12, 5.14 and 5.15) suggest an accumulation of cells observed in S phase and G2/M phase. However, in the treated cell lines, it is latterly that many event recorded in S phase are actually cells which have undergone apoptosis in G2/M. Therefore, taking the consideration of the WinMDI analysis presented in figures (5.10 and 5.13) suggest an accumulation of the cells in G2/M phase.

Studies have shown the anti-proliferation activity of LPAAT- β inhibitors to be associated with a block in the G2/M phase of cell cycle in human myeloid leukaemia cells lines sensitive or resistant to ATRA. The apoptosis inducing activity of LPAAT- β inhibitors appear to be via the mitochondria-dependent caspase cascade through activation caspase-3 that results in release of cytochrome c.

In common with our data, Coon et al (2003) reported that treatment with CT32228 resulted in Caspase-3 activation in many tumour cells tested (including HL60 cells), this was accompanied by a 24% increase in Annexin V positive cells after 24h. The cell cycle analysis showed a block in G2/M phase, the data also showed an increase in mitotic index. Also, treatment of IM-9 cells (lymphoblastoid cells) with 300 nM of CT32228 resulted in the expression and activation of Type I receptosome complexes by the activation of Caspase-8. Additionally, Type II pathways were activated as Bax expression was increased and Caspase-9 was activated (Coon et al. 2003).

Another report, found that apoptosis was triggered by LPAAT- β inhibitors (CT32615) in Multiple Myeloma cells (MM) mediated via caspase-3, caspase-7, caspase-8 and poly (ADP-ribose) polymerase (PARP) cleavage. The cell cycle analysis showed that CT32615 arrested cells at G2/M phase in a dose dependent manner (Hideshima et al. 2003). The same author, further tested LPAAT- β inhibitor (CT32615) on a resistant DHL-4 multiple myeloma (resistant to PS-341 (bortezomib, VelcadeTM)). CT32615 inhibited DHL-4 growth in a time and dose dependent manner, and without caspase/PARP cleavage activation, suggesting necrotic responses (Hideshima et al. 2005).

Recently, Pagel et al (2005) reported that LPAAT- β inhibitor (CT32228) alone or in combination with anti-CD20 monoclonal antibodies (Rituximab) induced caspase-mediated apoptosis at 50 to 100 nM in up to 90% of non-Hodgkin's lymphoma cells. The combination of LPAAT- β inhibitors and Rituximab resulted in a 2-fold increase in apoptosis compared with either agent alone, using the Annexin V technique (Pagel et al. 2005).

From our study and examining the previous studies, we suggest that LPAAT- β inhibitors activate many signalling pathways that results in activation of type I and type II apoptotic pathways. The inhibitors were found to induce a necrosis response in some resistant cells. Previous studies were also found that treatment cells with LPAAT- β inhibitors blocked cell

progression at G2/M phase. This was consistent with our result, our cells showed an increase in G2/M phase. These results may suggest that the LPAAT- β inhibitors may act on central factors that may activates all these signalling pathways. To elucidate these multiple signalling pathway activations, therefore, in the next chapter we examined the effect of these inhibitors on phosphatidic acid signalling pathways using western blotting technique. These pathways are ras/raf/ERK and PI3K/Akt/mTOR pathways.

CHAPTER 6

The effect of LPAAT- β inhibitors on AML cell signalling

6.1 Introduction

The last two chapters (4 and 5) have examined the effect of LPAAT- β inhibitors on AML cell lines gene expression and cell cycle and apoptosis respectively. Genes differentially expressed were analyzed by oligonucleotide array (Affymetrix System). Most of the genes expressed were integrated to cell membrane and G coupled protein pathways. Despite the unexpected result, we found caspase-5 was upregulated with active forms PC2 and CT8. Chapter 5 discussed cell cycle progression and apoptosis activation in AML cell lines. The ATRA sensitive and resistant cells were significantly blocked at G2/M phase with PC2 and CT8. The cells were further entered into apoptosis with increased annexin V+ cells and caspase-3 expression. It has been suggested that the inhibition of LPAAT- β by small-molecule inhibitors results in multiple pathways of cell growth being suppressed during LPAAT- β inhibition, including ras/raf/Erk and mTOR (Bonham et al. 2003;Coon et al. 2003). The suppression of these pathways by inhibitors results in an inhibition of PA production which acts as a second messenger on these pathways.

PI3 kinase is a lipid kinase that is regulated in response to multiple hematopoietic cytokines and chemokines. Many of the downstream effects of PI3 kinase are mediated through the serine-threonine kinase protein kinase B (PKB/Akt)(Coffer & Woodgett 1992). Akt interacts with a many of downstream effectors, which, in various cell types, lead to regulation of cell proliferation, cell growth, and cell survival. One of these downstream targets is mTOR (mammalian target of rapamycin), which regulates both nutrient sensing and protein translation through phosphorylation of its substrates, p70 S6 kinase and 4EBP-1 (Gingras, Raught, & Sonenberg 2001). Numerous studies have implicated activation of Akt in carcinogenesis (Vivanco & Sawyers 2002), and recently report involving primary cells from patients with AML have shown constitutive activation of the PI3 kinase mediator Akt. Inhibition of PI3 kinase in a short-term culture system found decreased growth in most AML samples and was associated with the induction of apoptosis in these cells (Xu et al. 2003).

A known LPAAT enzyme end product is phosphatidic acid (PA) which act as a second messenger and may play an important role in a number of cell signaling. One of these implications is an effect on mTOR. PA directly interacted with the domain in mTOR that is targeted by rapamycin, and this interaction positively correlated with mTOR's ability to activate downstream effectors (Fang et al. 2001). The phosphorylation/activation of another

molecule important for cell survival, Akt, is diminished by the LPAAT- β inhibitors in vascular smooth muscle (Bonham et al. 2003).

The second pathway, ras/raf/Erk was suggested to be down regulated by LPAAT- β inhibitor. The protein kinase cRaf-1 is one of the main targets of the small GTPase Ras. cRaf-1 is phosphorylated in serine, threonine and tyrosine residues by specific enzymes, and these phosphorylation reactions appear to be essential for the activation of the kinase . The idea that PA is a regulator of the Erk phosphorylation cascade was first proposed by Ghosh et al. in 1996, who reasoned that, since cRaf-1 must interact with the membrane in order to be activated, then the interaction with specific phospholipids may contribute significantly to the stabilization of cRaf-1–membrane complexes (Ghosh & Bell 1997).

It has been suggested that the inhibition of LPAAT- β can down regulate Ras/Raf/Erk and PI3K/Akt signal transduction pathways. In tumor cells, treatment with CT32228 results in accumulation of cells in G2/M followed by mitotic catastrophe and apoptosis while most normal cells simply arrest or become quiescent (Coon, Ball, Pound, Ap, Hollenback, White, Tulinsky, Bonham, Morrison, Finney, & Singer 2003).

In this chapter we discuss in detail the effect of LPAAT- β inhibitors on the Ras/Raf/Erk and PI3K/Akt signal transduction pathways in ATRA sensitive and resistant AML cell lines at protein level using Western blotting.

6.2 Material and Methods

The full details of Western blotting analysis were found in chapter 2 (section 2.8). Here we give a brief description of these two analyses.

6.2.1 Cell lines and treatment

NB4 and NB4:R2 cells were seeded at 2.5×10^5 cells/ml in RPMI-1640 medium supplemented with 10% FBS. Each cell line was divided into six flasks, one for untreated (control) and five for treated (test). The five test flasks were treated for 3, 6, 9, 12 and 24 hours with 25 nM of LPAAT- β inhibitor. All six flasks for each cell line were gassed and incubated at 37°C and 5% CO₂.

6.2.2 Immunoblotting

NB4 and NB4:R2 cells were cultured in the presence or absence of PC020702 inhibitor and then harvested, washed, and lysed. Cells were lysed with lysis buffer (20mM Tris(pH 8.0), 150 mM NaCl, 2mM EDTA, 1% NP40). The protein content of these cell lysate was determined using the Bio-Red protein assay kit. Each extract (20 ug protein) was separated by polyacrylamide-SDS gel electrophoresis, and then transferred to PVDF membrane (Amersham, UK). The membrane was incubated for 1 hour with blocking buffer TBS/Tween-20 (1xTBS/ 0.1%Tween-20) containing 5% BSA. After having been washed 3 times with 0.1% Tween 20 in TBS, the membrane was incubated overnight at 4 °C with each antibody (anti-phospho ERK1/2 (p⁴²/p⁴⁴) antibody, anti-ERK1/2 antibody, anti-phospho Akt antibody (S⁴⁷³), anti-Akt antibody, anti-phospho mTOR (S²⁴⁴⁸) antibody, anti-mTOR antibody (Cell Signalling Technology, USA), and anti β -actin antibody (Sigma-aldrich, USA)) in blocking buffer. After 3 washes with the TBS/Tween-20 buffer, the membrane was incubated for 1 hour at room temperature with anti-rabbit or mouse IgG antibody linked to Horseradish Peroxidase (Amersham Biosciences, UK).

Immunoreactive proteins were detected by the advanced ECLTM detection system.

6.3 Effect of PC020702 on Akt/mTOR Activation

6.3.1 The effect of LPAAT- β inhibitors on Akt/mTOR pathways

Because inhibition of LPAAT- β inhibitors by CT32228 and PC020702 was cytotoxic to NB4 and NB4:R2 cells, and induced apoptosis by activating annexin V and caspase3, we wanted to investigate effects on Akt/mTOR survival pathway. In NB4 and NB4:R2, PC020702 is potently antiproliferative at 25nM (see chapter 3). NB4 and NB4:R2 were treated with PC020702 (25nM) at 0, 3, 6, 9, 12 and 24 hours. The reason we selected this pathway was that the PA has been reported to activate mTOR (Ser²⁴⁴⁸) directly and this interaction was positively correlated with mTOR's ability to activate downstream effectors (Fang et al. 2001). Therefore the blocking of LPAAT- β will results in PA blocking and inactivation of mTOR and downstream protein.

6.3.1.1 LPAAT- β inhibitors resulted in overexpression of mTOR in NB4 and NB4:R2

When 25nM of PC020702 was added to NB4 cells, the representation phosphorylated mTOR protein overexpressed over time, starting from 3 hours after the administration. The expression was further down regulated after 9 hours and upregulated after 12 and 24 hours (**Figure 6.1**, upper panel (A)). Expression of total mTOR in NB4 was upregulated after 3, 6, 12 and 24 hours of treatment (**Figure 6.1**, middle panel (A)). Variation in phosph-mTOR expression was not a technical artefact as stripping and re-probing for β -actin showed equal levels of loading in all lanes.

A similar picture was seen in NB4:R2, phosphorylated-mTOR (Ser²⁴⁴⁸) was dramatically down regulated after 9h and then upregulated after 12 and 24 h (**Figure 6.1 (B)**).

These figures may indicate that the inhibition of LPAAT- β leading to overexpression of mTOR by PA rather to downregulated, which may indicate of down regulation of PA was overcome by another enzyme or molecular pathways. At the same time this indicates that LPAAT- β inhibitors may affect on different pathways other than PA.

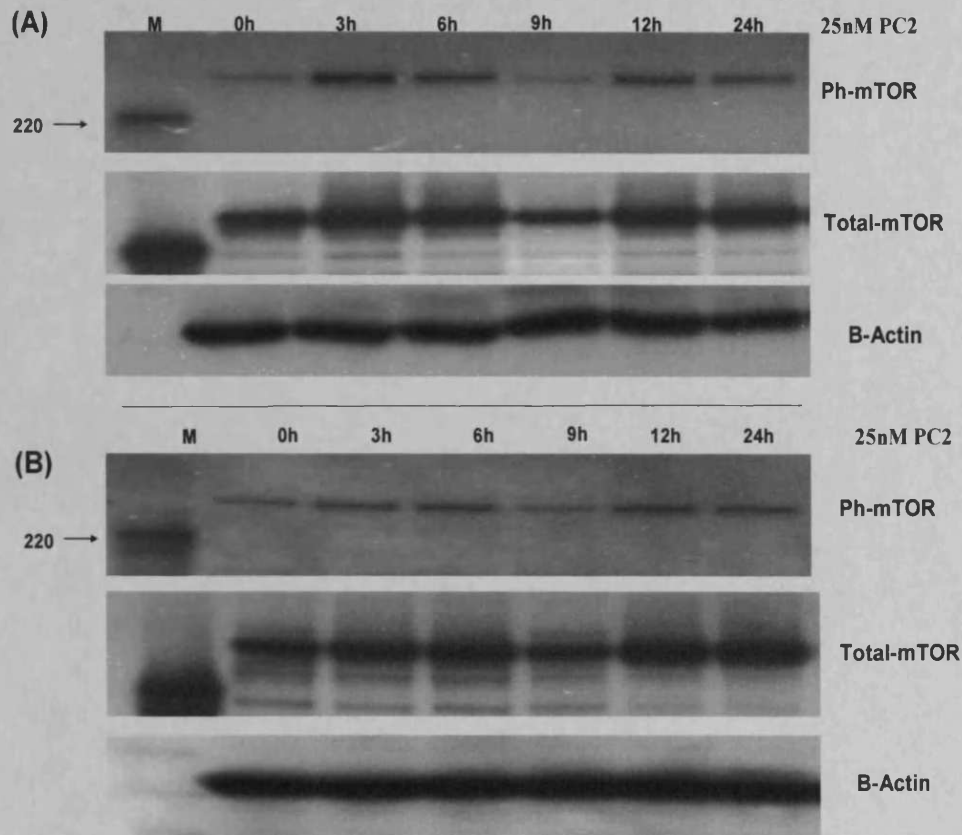


Figure 6.1 mTOR phosphorylation in NB4 and NB4:R2 cells. After treatment with PC020702 at the time indicated NB4 (A) and NB4:R2 (B) cells were thawed, washed, harvested by centrifugation and lysed in RIPA buffer. 100 ug of cell lysates were loaded on SDS-PAGE gel and analyzed by western blotting. Blots were probed with phospho-mTOR antibody (top panel) and then stripped and re-probed with total mTOR antibody (middle panel). As a loading control, blots were stripped and re-probed with β -actin (lower panel).

Phosphorylated mTOR band was quantitated using UVITec instrument (UVI Tec limited, UK). The instrument has ability to capture an image of Western film, which can be saved on floppy disc. The images were analyzed by UVIDOC software. The molecular weight of each band was measured. We proposed the phosphorylated mTOR at 0 time (untreated) be designated 100 %. The phosphorylated mTOR percentage in treated cells was calculated by the following formula:

mTOR phosphorylation (%)= (molecular weight of treated/molecular weight of 0 time) x 100.

From the quantitation curve, we observed that an increase in mTOR phosphorylation in NB4 and NB4:R2 cells after 3 and 6 hours of treatment, mTOR was dephosphorylated after 9 hours and upregulated again after 12 hours, that may indicate that the inhibitor disturb the PA production, or the inhibitor may directly or indirectly activated other enzymes that act as a backup for PA production and this was clearly seen after 9 hours of treatment, where the phosphorylated mTOR was upregulated again after it was dephosphorylated (**Figure 6.2**).

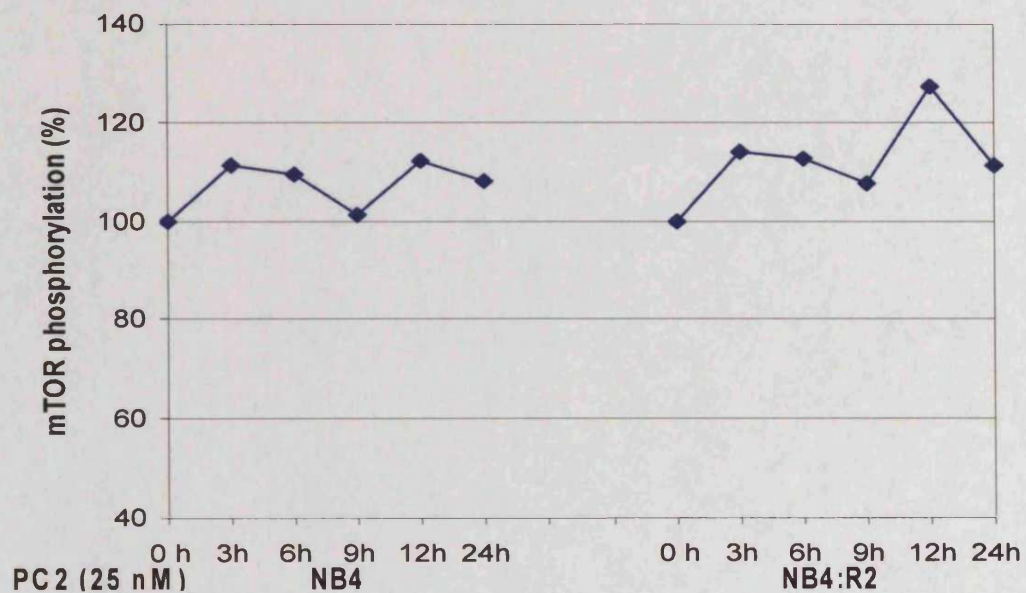


Figure 6.2 mTOR phosphorylation in NB4 and NB4:R2 cells. After treatment with PC020702 at the time indicated, NB4 and NB4:R2 cells were thawed, washed, harvested by centrifugation and lysed in RIPA buffer. 100 μ g of cell lysates were loaded on SDS-PAGE gel and analyzed by western blotting. The phosphorylated mTOR bands were quantitated using UVIDOC software. The results show mTOR phosphorylation percentage.

6.3.2 LPAAT- β inhibitor downregulates Akt in NB4 & NB4:R2

Here we want to investigate whether PA had an affect on PI3K/Akt pathway by detecting phosphorylated Akt. Pretreatment NB4 with PC020702 attenuated phosphorylation of Akt (S⁴⁷³) after 3 hours of induction (**Figure 6.3**, upper panel (A)). Expression of total AKT in NB4 cells declined as shown when the blot was stripped and re-probed with antibody for total Akt protein (**Figure 6.3**, middle panel (A)). Variation in AKT expression was not a technical artifact as stripping and re-probing for β -actin showed equal levels of loading in all lanes. This experiment demonstrated that PC020702 inhibited Akt phosphorylation in NB4 cells after 3h of treatment, while phosphorylated Akt in NB4:R2 was upregulated after 3 and 6 hours of treatment and then down regulated after 9 hours. Expression of total Akt in NB4:R2 was upregulated after 3 and 6 hours of treatment (middle lane (B)). This was inconsistent with densitometry blots. It is not clear what role PA play in the activation of Akt. These results suggest that LPAAT- β plays a role in the initiation of this signalling pathway, perhaps by blocking effective receptor internalization or by directly inhibiting early steps in the pathway (**Figure 6.3**).

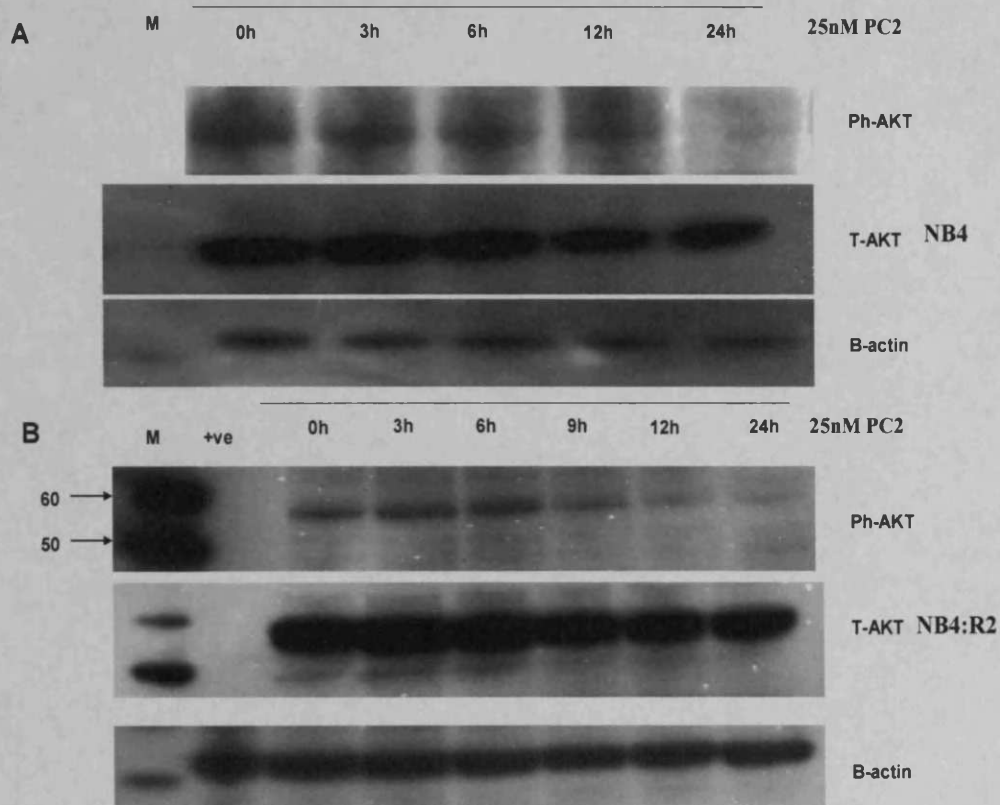


Figure 6.3 Akt phosphorylation in NB4 and NB4:R2 cells. After treatment with PC020702 at the time indicated NB4 (A) and NB4:R2 (B) cells were thawed, washed, harvested by centrifugation and lysed in RIPA buffer. 100 ug of cell lysates were loaded on SDS-PAGE gel and analyzed by western blotting. Blots were probed with phosphor-Akt (S^{473}) antibody (top panel) and then stripped and re-probed with total Akt antibody (middle panel). As a loading control, blots were stripped and re-probed with β -actin (lower panel). The symbol M and PC2 represent marker and PC020702 respectively.

In contrast to phospho-mTOR, phosphorylated Akt was dephosphorylated continuously after 9 hours in NB4:R2 cells and Akt dephosphorylated in NB4 cells after 3 hours of treatment as assessed by densitometry. NB4 cells treated with PC020702 (25 nM) exhibited a decrease in Akt phosphorylation during 24 hours of treatment. Treatment of NB4 cells with inhibitors caused a 50% inhibition in phospho-Akt at 24 hours. Akt dephosphorylated in NB4 cells started as early as 3 hours of treatment, while phospho-Akt in NB4:R2 cells was inhibited after 9 hours of treatment. Treatment of NB4:R2 cells with PC020702 (25 nM) resulted in 40% inhibition in phospho-Akt after 24 hours. These results may suggest that LPAAT- β inhibitor had diminished Akt phosphorylation in ATRA sensitive cells faster than in the resistant cells. Also it suggests the down stream pathway of Akt could be independent of mTOR protein. At the same time the role of PA on Akt is not documented, and may suggest an alternative role, the inhibitors may act in ways other than PA pathway (Figure 6.4).

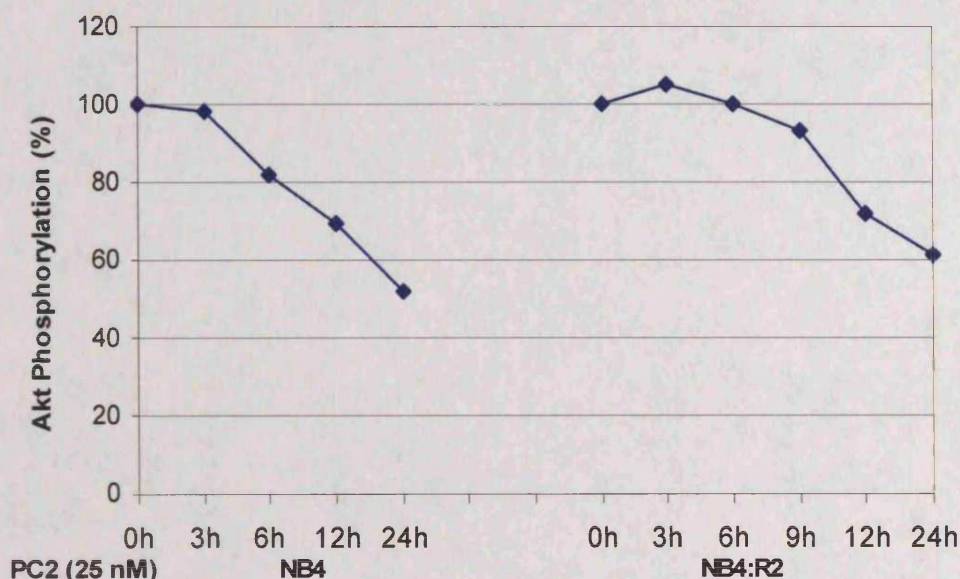


Figure 6.4 Akt phosphorylation quantitation in NB4 cells. After treatment with PC020702 at the times indicated NB4 cells were thawed, washed, harvested by centrifugation and lysed in RIPA buffer. 100 ug of cell lysate was loaded on SDS-PAGE gel and analyzed by western blotting. The phosphorylated Akt bands were quantitated using UVIDOC software. The results show mTOR phosphorylation as a percentage compared to control.

Consistent with western blotting data, the immunocytochemistry (ICC) data also showed an inhibition of phosphor-Akt in both NB4 and NB4:R2 cells after treatment with PC020702 for 96 hours. The data also showed an activation of caspase 3 in both cell lines. The percentage of positive expression was based on count of 100 cells.

The preparation of paraffin embedded cell suspension from tissue cultures was used for immunocytochemistry (ICC).

The preparation of paraffin embedded cell suspension blocks were held in Department of Histopathology, University Hospital of Wales with the help of Dr. Morgan. The material and methods for preparation of paraffin embedded cell suspension from tissue cultures can be found in Dr Morgan's publication. In summary, NB4 and NB4:R2 were seeded at 2.5×10^5 cells/ml. Each cell line was divided into three flasks. The first flask was untreated. The second flask treated for 96 hours with 10nM of LPAAT- β inhibitors PC020702. The third flask treated for 96 hours with 25 nM of LPAAT- β inhibitors PC020702. The paraffin embedded blocks protocol were performed according to Dr. Morgan's protocol (Morgan J M 2001). Then the blocks were sent to Dr. Bonham (Cell Therapeutic Inc, Seattle, USA). The cells were examined using Immunohistochemistry stain for activated caspase-3 and phosphorylated Akt. NB4 and NB4:R2 treated for 96 hours resulted in an increase of activated caspase 3 and decrease in Akt phosphorylation which may indicate that NB4 and NB4:R2 cell lines undergone apoptosis. Although, Akt dephosphorylation triggered by LPAAT- β inhibitor (Figure 6.5 and 6.6).

However, NB4:R2 cell western blotting data showed that caspase-3 cleavage (see chapter 5 section 5.3.4) was activated before Akt phosphorylation which downregulated after 6 hours (figure 6.3 and 6.4) of treatment, while caspase 3 activated after 3 hours. This may indicates that Akt dephosphorylation is not the pathway responsible for apoptosis in NB4:R2 cell line. NB4 cells showed similar event as NB4:R2

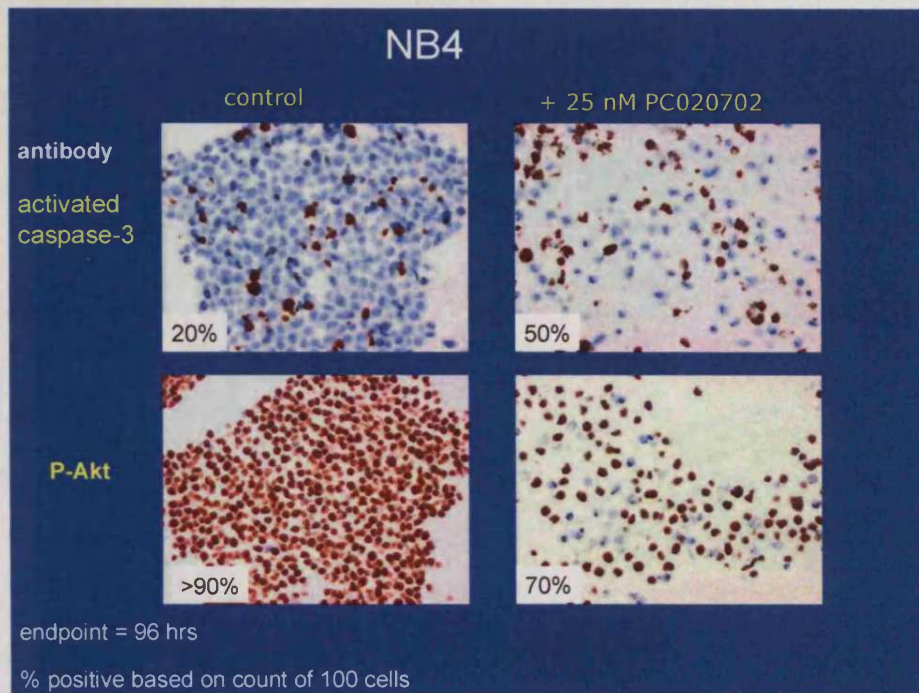


Figure 6.5 The expression of caspase-3 and phospho-Akt proteins in NB4. Upper left figure shows the untreated cells with 20 % activated caspase-3, while with LPAAT- β inhibitors (PC020702) at 25 nM after 96 hours the activity was increased to 50% (upper right). Lower left figure shows the untreated cells with > 90% of phosphorylated Akt expression and after treatment the expression was 70% (Lower right). The percentage of positive expression was based on count of 100 cells.

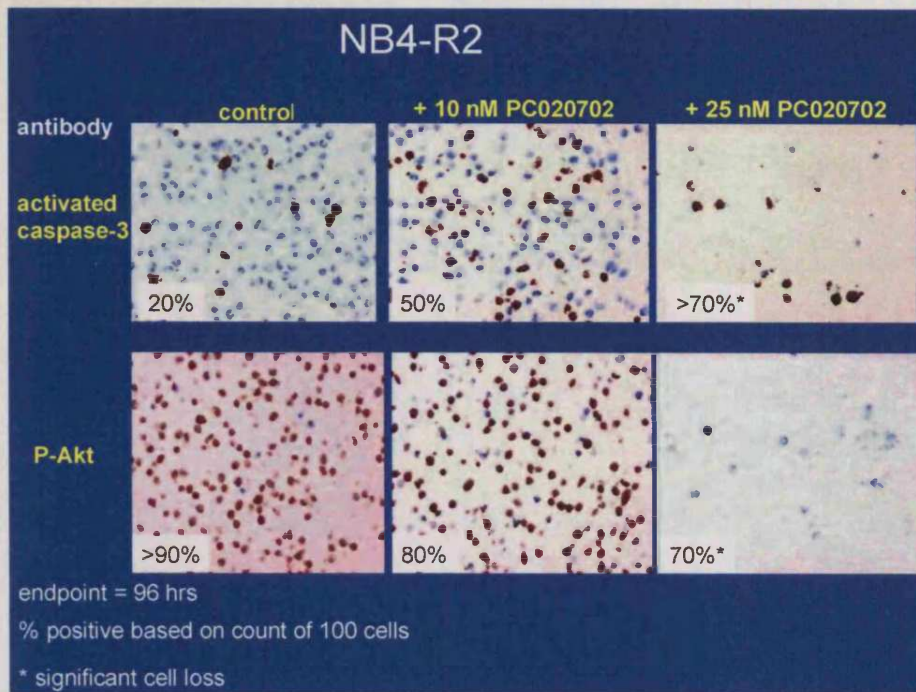


Figure 6.6 The expression of caspase-3 and phospho-Akt proteins in NB4:R2. Upper left figure shows the untreated cells with 20 % activated caspase-3, while with LPAAT- β inhibitors (PC020702) at 10 nM and 25 nM after 96 hours, the activity of caspase-3 was increased to 50% and > 70% respectively (upper middle and right). Lower left figure shows the untreated cells with > 90% of phosphorylated Akt expression, and after treatment the expression was decreased to 80% and 70% (Lower middle and right). The percentage of positive expression was based on count of 100 cells.

6.4 Effect of PC020702 on raf/ERk Activation

We wanted to determine whether PC020702 could block additional signaling pathways in NB4 and NB4:R2. Many reports have described activation of MAP kinase proteins in AML. Several reports suggests that the majority of AML blasts may depend on MEK activation for survival as incubation of the cells with pharmacologic MEK inhibitors leads to an increase in spontaneous and chemotherapy induced apoptosis (Milella et al. 2001; Towatari et al. 1997).

Translocation of raf from the cytosol to membrane is a necessary step before its activation and this translocation has been shown to be dependent on PA. We examined the Ras/Raf/Erk pathway in AML cells to more clearly define LPAAT- β inhibitor function.

6.4.1 LPAAT- β inhibitors on MAP kinase in NB4 and NB4:R2

NB4 and NB4:R2 were treated with PC020702 (25nM) at 0, 3, 6, 12 and 24 hours. Translocation of raf from the cytosol to membrane was examined by measuring downstream phosphorylated ERK1 and 2 (P44/42). Pretreatment NB4 and NB4:R2 with PC020702 at the time indicated did not attenuate phospho-Erk1 / 2. Treatment of NB4 cells resulted in no changes in MAPK phosphorylation, while in NB4:R2 cells there was an increase in MAPK phosphorylation after treatment (**Figure 6.7**).

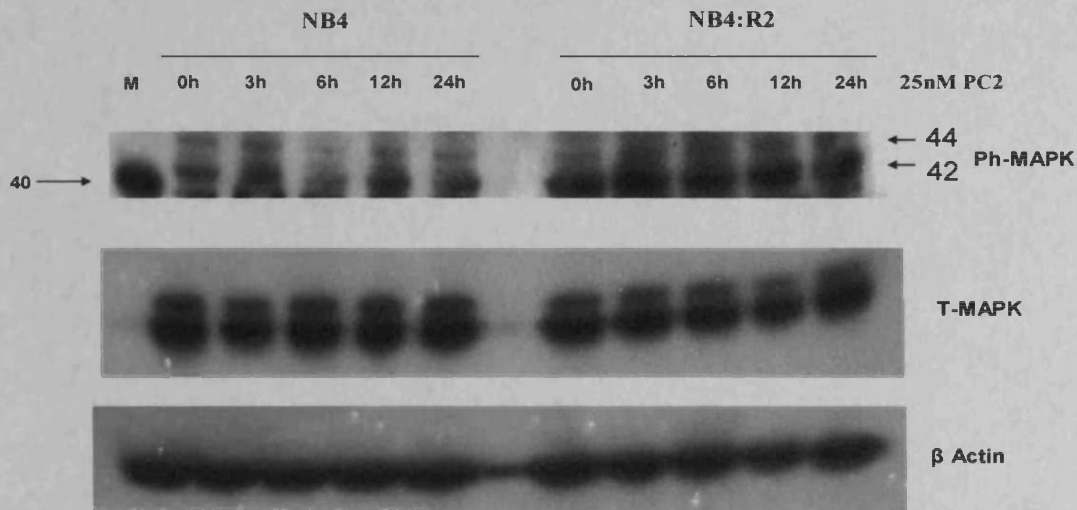


Figure 6.7 ERK1/2 phosphorylation in NB4 and NB4R2 cells. After treatment with PC020702 at the time indicated NB4 and NB4:R2 cells were thawed, washed, harvested by centrifugation and lysed in RIPA buffer. 100 ug of cell lysates were loaded on SDS-PAGE gel and analyzed by western blotting. Blots were probed with phospho-Erk1/2 (p44/42) antibody (top panel) and then stripped and re-probed with total Erk1/2 antibody (middle panel). As a loading control, blots were stripped and re-probed with β -actin (lower panel). The symbol M and PC2 represent for marker and PC020702 respectively.

From the quantitation curve, we observed that phospho-ERK1&2 in NB4 cells was not changed over time with treatment, while a slight inhibition was observed at 24 hours of treatment. NB4:R2 cells showed an increase in MAPK phosphorylation. The expected result of dephosphorylation of raf/ERK by LPAAT- β inhibitors was not observed in these cell lines. These results may suggest that the inhibitor had no effect on this pathway in NB4 and NB4:R2 cells or the PA production was over come by another source, most likely by phospholipase D and diacylglycerol Kinase enzymes. Alternatively, the action of these inhibitors relies upon different pathways other than PA pathway. (**Figure 6.8**).

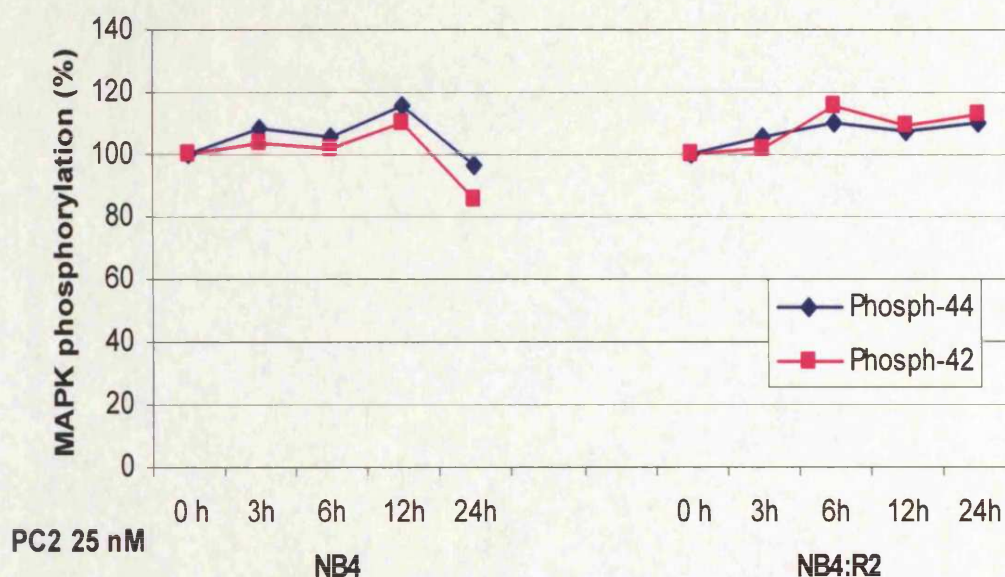


Figure 6.8 Quantitation of Phospho-MAPK in NB4 and NB4R2 cells. After treatment with PC020702 at the time indicated NB4 cells were thawed, washed, harvested by centrifugation and lysed in RIPA buffer. 100 ug of cell lysate was loaded on SDS-PAGE gel and analyzed by western blotting. The phosphorylated Akt bands were quantitated using UVIDOC software. The results show percentage of phospho-ERK1 and 2 (P42 & 44).

6.5 Discussion

PA is relatively unexplored molecule and LPAAT- β has not previously been recognized as a target for AML therapy. Manipulation of the levels of PA, now recognized as an important regulator of multiple tumour growth function LPAAT- β , may allow for AML therapy that is effective in shutting down these multiple paths and at the same time inhibits a gene upon which a tumour has become dependent for survival during its evolution. Such as among the signalling pathways used in our study was PI3K/Akt/mTOR and Ras/Raf/MAPK. These two pathways were found had an antiproliferative and apoptotic role in AML, as well as these pathways, some model systems have been shown to require PA for activation.

To further probe the role of LPAAT- β in AML cell signalling at the protein level, we used LPAAT- β inhibitor PC020702. Akt/mTOR was initially described as an oncogene and is activated by a variety of growth factors through a PI3K dependent pathway. Activation of Akt is known to deliver a survival signal that inhibits apoptosis induced by growth factor withdrawal. Activation of Akt ultimately lead to inhibition of caspase activity and protection from apoptotic cell death (Datta et al. 1997; Dudek et al. 1997). When NB4 and NB4:R2 cell line were treated with PC020702, mTOR phosphorylation was not inhibited but Akt phosphorylation is blocked, suggesting that LPAAT- β may not be the only source of PA required for mTOR activation. In other word PLD and DAGK other sources of PA production act as back-up for PA production. Also it is possible down stream activation of Akt could be through molecules other than mTOR. It is not clear what role PA plays in the activation of Akt. However, mTOR has been reported to require PA for its activation. Thus PA, the end product of LPAAT- β may not be the substrate which acted on the PI3K/Akt/mTOR pathway after inhibitor incubation (Table 6.1 & 6.2).

	0hours	3 hours	6 hours	9 hours	12 hours	24 hours
P-mTOR	++	+++	+++	++	+++	++
P-Akt	+++	++	+		+	+

Table 6.1 A summary of the effect of LPAAT- β inhibitor (PC020702) on phosphorylated mTOR and Akt activation in NB4 cells.

	0hours	3hours	6 hours	9 hours	12 hours	24 hours
P-mTOR	++	+++	+++	++	++++	+++
P-Akt	+++	+++	++++	+	+	+

Table 6.2 A summary of the effect of LPAAT- β inhibitor (PC020702) on phosphorylated mTOR and Akt activation in NB4:R2 cells.

The recruitment of Raf to membranes in some model systems has been shown to require PA (Rizzo et al. 2000) and this process is associated with oncogenesis. Activation of Raf involves two distinct steps; translocation as a multi subunit complex to the membrane (Wartmann & Davis 1994) followed by its activation by Src and Src-like kinases, Ras, and perhaps others (Morrison & Cutler 1997). Ras/Raf/MAPK pathway is one of the major pathways involved in the proliferation and apoptosis in AML. We used PC020702 to investigate the contribution from LPAAT- β to the PA requirement for Ras/Raf/MAPK recruitment by measure down stream phospho-Erk1/2 (42/44). Erk phosphorylation was not inhibited by PC020702 in NB4 and NB4:R2 which dose not support the idea that LPAAT- β exerts an inhibitory effect on Raf signalling via PA (Table 6.3). it is possible of PA is produced from other enzymes mainly PLD and DAGK contribute in it production. Alternatively, the action of these inhibitors may take different pathways other than PA pathway. Thus the antiproliferative action of LPAAT- β inhibitors may affect signalling pathways other than Ras/Raf/MAPK. This will suggests another role for LPAAT- β inhibitor in inducing antiproliferative and survival in these cell lines.

	Phosph-ERK				
	0 hours	3hours	6 hours	12 hours	24 hours
NB4	+++	+++	++	+++	++
NB4:R2	++	++	+++	+++	+++

Table 6.3 A summary of the effect of LPAAT- β inhibitor (PC020702) on phosphorylated ERK activation in NB4 and NB4:R2 cells.

Therefore so far our data demonstrated that the original hypothesis of the study that LPAAT- β inhibitors affect both LPAAT- β enzyme activity and the end product PA that act as a second messenger in addition to a role in lipid biosynthesis, is not supported. These will open other pathways LPAAT- β inhibitor may play in the antiproliferative and apoptotic role in AML. Along with our data and pharmacology of LPAAT- β inhibitors, the possibility is raised that LPAAT- β inhibitors block LPA signalling pathways and induce apoptosis but not the PA pathway, this will be discussed in detail in Chapter 7.

CHAPTER 7

Discussion, Main Findings and future work

7.1. Discussion

Acute myeloid leukemias are phenotypically characterized by the accumulation of clonal haematopoietic precursors blocked at specific stages of development. Genetically, they are associated with chromosomal translocations resulting in the generation of chimeric genes and fusion proteins, which can be directly or indirectly involved in blocking normal development. Acute promyelocytic leukemia (APL) is one of the commonest subtypes of AML and has been of particular interest given that it is a disease for which molecularly targeted therapies in the form of all-trans-retinoic acid (ATRA) have been successfully developed, yielding substantial improvement in clinical outcome. Relapses and resistance occurring after a complete remission of APL can develop after a short time of therapy. Cytotoxic chemotherapy and improvement in supportive care have prolonged survival for patients with APL. Nevertheless, cytotoxic agents have severe side effects, including a risk of secondary malignancy and death. Therefore, the research of modern drug development in oncology will result from specific targeting of molecular alterations that occur during tumorigenesis. One strategy is to identify and inhibit enzyme(s) that produce cofactors critical to signaling and/or survival pathways specific to neoplastic cells.

We have investigated whether LPAAT- β is a valid target for AML therapy. First, LPAAT- β catalyses the transfer of acyl groups to lysophosphatidic acid (LPA) to form phosphatidic acid (PA). LPAAT- α has a uniform tissue distribution and is apparently not upregulated in tumour cells, suggesting a housekeeping role for this enzyme. First, as an indicator of an association with tumorigenesis and progression, increased LPAAT- β expression level in several tumour types have been found compared to normal tissues of the same types, as well as high uniform levels of LPAAT- β in tumour cell lines that correlate with relatively high functional activity (Leung 2001; Bonham et al. 2003). Niesporek, et al (2005), reported expression of LPAAT- β mRNA as well as LPAAT- β proteins in vivo and in vitro in ovarian carcinomas and in benign ovarian tissues. They found that LPAAT- β mRNA was expressed in all ovarian tissue samples and all ovarian cell lines examined. On the protein level, LPAAT- β was expressed in most ovarian samples. The overexpression of LPAAT- β was correlated with tumour grading and prognosis (Niesporek et al. 2005).

The production of lysophosphatidic acid and phosphatidic acid have been shown to be important for cell survival because these lipid mediators play key roles in cell cycle

regulation due to their growth factor-like effects (Moolenaar et al. 1997; Tigyi et al. 1994; Tigyi & Parrill 2003). The suppression of phosphatidic acid biosynthesis by small compounds that inhibit the interleukin 2 receptor-associated JAK/signal transducers and activators of transcription signalling pathway have been shown to result in complete suppression of malignant T-cell lymphoma growth (Wasik et al. 1998). Phosphatidic acid has also been shown to be involved in the downstream activation of *raf* protein as a part of the *ras/raf/extracellular* signal-regulated Kinase signalling pathway. Because PA is an important cofactor in signaling pathways, we investigated a potential role for LPAAT- β in ATRA sensitive and resistant AML cell lines. To aid understanding the role that LPAAT- β may play in functions critical to tumour cell growth and survival, small molecule inhibitors were used. The LPAAT- β inhibitors used in our study were two active forms designated as CT32228 and PC020702 and two inactive forms CT32212 and PC020701.

In our study, the active forms were found to be very toxic to all ATRA sensitive and resistant cell lines in a dose/time dependent fashion. The active form PC020702 was more sensitive to AML cell lines than CT32228. The cell growth was significantly inhibited (75-99%) at concentration of 50 nM for CT32228. While PC020702 inhibited cell growth at 25 nM. The inhibition was more obvious in HL60-R than HL60 cells and overall inhibition was seen in NB4 and NB4:R2 (M3 FAB classification) than HL60 and its resistant form HL60-R (M2). However no growth inhibition was seen with the inactive forms. These results indicate that the active inhibitors were very toxic to AML type M2 and M3 and their ATRA resistant mutants. The effect was some how antiproliferative and blocked cell cycle progression resulting in increased in apoptosis these AML cell lines.

In our study, we wanted to measure intracellular inhibition of LPAAT- β activity and correlate the effects of its activity with physiological changes. This assay measures the production of ^{14}C -labelled PM by addition of ^{14}C -labelled oleate and the substrate, lysoPM. PC020702 significantly inhibited LPAAT- β activity (50 % inhibition) after 24 h, whereas 48 h showed minimal effects (10–20% inhibition). The enzyme activity was further inhibited after 1h of PC020702 incubation in all cell lines tested. This indicates that the inhibitor was specific to this enzyme activity. This is consistent with previous study of enzyme activity after incubation with LPAAT- β inhibitors in Multiple Myeloma and frog

oocytes, the LPAAT- β inhibitors significantly inhibited enzyme activity in a time and dose dependent manner (Coon et al. 2003;Hideshima et al. 2003).

Also in this study, our aim was to investigate differentially expressed genes after 1 hour treatment with LPAAT- β inhibitors. Analyzing the molecular events taking place after LPAAT- β inhibitor treatment in these cell lines elucidated the effect of LPAAT- β inhibitors in AML cells types and their resistant form.

The up and down regulated genes found were related to cell membrane function or receptors that have a role in cell signalling, membrane fission activity or Ca^{+} release. This may be a direct or indirect effect of the LPAAT- β inhibitors on phosphatidic acid, the end product of the enzyme activity. The expression of these genes may suggest more complicated pathways in which these inhibitors act. We expected to see expression of genes related to cell signalling especially those related to PA such as raf/ras/Erk and PI3K/Akt/mTOR. However, gene ontology data showed that the inhibitor action produced gene expression changes linked to cell membrane and cell membrane receptors. Closer observation of gene ontology data was not surprising for the effect of LPAAT- β that initially identified as an intermediate in lipid biosynthesis pathway. This observation both supports the critical nature of pathways inhibited and hints of an alternative pathway other than PA molecules as target of LPAAT- β inhibitor action.

In our study, we wanted to investigate the effect of LPAAT- β inhibitors on cell cycle progression and apoptosis. Proliferation is under the control of factors that regulate the transition between cell cycle stages at two main check points (Bell & Dutta 2002). The first one is at the G1/S phase transition for initiation and completion of DNA replication in S phase (Ho & Dowdy 2002;Obaya & Sedivy 2002). The second checkpoint is at the G2/M phase transition and controls mitosis and cell division (Smits & Medema 2001). When compared with untreated cells, treated cells increased the proportion of cells in G2/M phase of the cell cycle, as evidenced by flow cytometric analysis (chapter 5). These data, coupled with results indicated that LPAAT- β inhibitors block cells at G2/M phase in multiple myeloma and other cancer cell lines, suggest that LPAAT- β plays a role in the signalling pathways critical for the initiation and /or maintenance of the G2 checkpoint. Furthermore, treatment with LPAAT- β inhibitors results in giant, multinucleated cells and an increase in mitotic bodies. These data, coupled with results that indicate that some normal cells are

resistant to the pro-apoptotic effects of LPAAT- β inhibitors, suggest that LPAAT- β plays a role in the signalling pathways critical for cell cycle progression and survival. Many tumour cells have disregulated G2 checkpoint mechanisms and fail to control early or mistimed entry into M phase (Coon et al. 2003; Bonham et al. 2003; Hideshima et al. 2003; Hideshima et al. 2005). Therefore, it appears that LPAAT- β inhibitors may play a variety of roles in several signalling pathways, including those critical for proliferative responses, survival and the initiation/maintenance of cell cycle arrest. It is likely that the various roles played by LPAAT- β involve both direct and indirect associations with signalling constituents, and the pathways affected could vary dependent on the initiating signal, cell type and the duration and timing of the signal.

We also investigated whether PA generated from LPAAT- β contributes to signalling pathways, especially Ras/Raf/MAPK and PI3K/Akt/mTOR by measurement phospho-Erk1/2 and phospho-mTOR respectively. PA was found directly to act on these two pathways especially by acting on raf translocation and mTOR activation. Neither phospho-MAPK nor phospho-mTOR was downregulated after LPAAT- β inhibitor incubation. In contrast, phospho-Akt was attenuated after treatment with LPAAT- β inhibitors, suggesting alternative target exist other than PA pathways. Thus with LPAAT- β inhibitors, we cannot rule out the possibility that CT32228 and PC020702 have additional targets which may account for some of the findings reported here. This will be discussed in detail in the main findings (section 7.2).

7.2. Main Findings

Gene ontology and gene lists allows the gene-expression changes observed for cell membrane integration and cell membrane receptors such as G-protein coupled receptor to be put in the context of other regulatory and developmental processes such as cell cycle, apoptosis and study of Akt/mTOR and ERK signalling pathways elicited of LPAAT- β inhibitors action. From my studies a new hypothesis of the effect of these inhibitors on AML is proposed. Along with our data and pharmacology of LPAAT- β inhibitors raise the possibility that LPAAT- β inhibitors block LPA signalling pathways and not PA pathways. The main findings are summaries in the following points:

1. Bonham et al (2003) reported that kinetic analysis of LPAAT- β inhibitors showed uncompetitive inhibition of LPA (with fatty acid chain sn-1-18:1) binding and mixed noncompetitive inhibition of 18:1-CoA binding. The third possibility that LPAAT- β binds LPA binding before it can bind the inhibitor. It is tempting to speculate that the binding of LPA to LPAAT- β induces a conformational change in the enzyme, exposing a site on the enzyme for the inhibitor to bind. The pharmacological role of LPAAT- β inhibitors show that in all three possibilities of the inhibitors action, LPA is involved as a common substrate in the blocking mechanism.
2. In order to measure intracellular inhibition of LPAAT- β enzyme activity with physiological changes, a model was constructed using LPM (Lysophosphatidyle methanol) in the presence of ^{14}C -labelled oleate, due to the difficulty of measurement PA and LPA activity in the cells. This was due two reason: the doubly charged head group of LPA will not translocate across the membrane: and the action of lipid phosphate phosphatases rapidly metabolizes LPA to monoacylglycerol (Waggoner et al. 1996). There are two disadvantages of this assay, first the LPM (LPA) possesses range of biological activities similar to growth factors. These include stimulation of cellular proliferation, platelet aggregation, smooth muscle contraction, and tumour cell invasion (Fang et al. 2000;Goetzl et al. 2000;Goetzl & An 1998;Weiner & Chun 1999). LPM introduction in the cell will activate LPAAT- β activity even if it is in resting position. Therefore, introduction of the LPM substrate will switch on LPAAT- β enzyme activity and PM production, once inhibitor was introduced the PM was down regulated. In another word this enzymatic assay will measure enzyme activity even if not overexpressed. The second disadvantage, the

enzyme activity measurement depends on ^{14}C -labelled PM production, which is quite different from real cell PA that also produced from other enzymes mainly phospholipase D (PLD) and phosphorylation of diacylglycerol (DAG) by DAG Kinases (DAGK) (Athenstaedt & Daum 1999) . Therefore the inhibition of LPAAT- β measured does not necessarily correlate to PA inhibition. On the basis of the use of inhibitor of PLD, it has been suggested that PA produced by PLD is involved in numerous signalling-related events, such as inhibition of p38 (MAPK) activity but not Erk1/2 in activated promyeloblasts (Bechoua & Daniel 2001), hydrogen peroxide-induced apoptosis in rat pheochromocytoma cells (Lee et al. 2000). Although the principle function of DAGK in signaling pathways, however, appear to be attenuation of signalling propagated by the secondary messenger DAG rather than through effect of PA (Jones et al. 2002;Topham & Prescott 2001). Therefore the role of PA produced by other enzyme mainly PLD and DAGK appear to be more complicated than we expected. However, each of these studies depends on the use inhibitors of limited specificity and has not been confirmed by genetic techniques such as knockout and knockdown, thus leaving open the possibility that some of the effect ascribed to these sources of PA may in fact be associated with other enzymes. Nevertheless, logically a PA produced by PLD and DAGK could be the same PA produced by LPAAT- β enzyme. This is the LPAAT- β act on the tail of LPA (at carbon 2 (sn-2)) substrate to produce PA, while the synthesis of the other phospholipids from PA by the other enzyme are at the head (carbon 3 (sn-3)) of the phospholipids. Therefore the backup PA produced by PLD and DAGK could be the same type of PA produced by LPAAT- β .

3. PC020702 LPAAT- β inhibitor which suppressed proliferation of the AML cells was used to elucidate the role of LPAAT- β in signalling pathways. Translocation of raf from the cytosol to the membrane is a necessary step prior to its activation, and its translocation has been shown to be dependent upon PA (Andresen et al. 2002). Inhibition of LPAAT- β activity in AML cell lines resulted in no attenuation of phosphorylated Erk1/2 which is down stream from raf. These results indicate the possibility of the PA production from other sources mentioned above. Ras/Raf pathway is also activated by LPA which indicates this pathway is common in both LPA and PA. Nevertheless, Baudhuin et al (2002) reported, phospho-Akt activation induced by LPA requires both Mitogen activated protein kinase kinase (MEK) and p38 Mitogen-Activated protein kinase (p38 MAPK) but not

Erk1/2 in ovarian cancer cells and breast cancer cell lines. This resulted in a decreased caspase-3 activity in a PI3K/Mek/p38-dependent manner (Baudhuin et al. 2002). However Fang et al (2000) reported that LPA promoted cell survival largely via G couple protein-mediated activation of ERK1/ERK2, or other MAPK family (Fang et al. 2000). Therefore, LPA activates Ras/raf/Erk pathway relatively different from PA. In addition PA was found to act directly on raf translocation while LPA more likely through G couple protein receptors. Thus LPA acting on Erk1/2 may depend on type of cells and treatment used.

4. The PI3K/Akt pathway acts primarily as a survival pathway, and inhibition of this pathway is known to be pro-apoptotic. PC020702 was found attenuating this pathway was dephosphorylated-Akt after 6 hours of treatment (Chapter 6). As well, apoptosis was measured by cleaved caspase3 that was found overexpressed (chapter 5). Caspase3 is a hallmark of down stream of mitochondrial apoptotic pathway. It is not clear what role PA participate in the activation of Akt. Nevertheless, LPA has been shown to protect against apoptosis in number of cell types including ovarian cancer cells, intestinal epithelial cells, fibroblasts, osteoblasts, hepatocytes (Sautin et al. 2001), Schwann cells (Contos et al. 2002; Weiner & Chun 1999) macrophages, T cells, and renal proximal tubular cells. The primary signaling mechanisms that appear to be involved in this protection involved G coupled receptor, PI3K, Akt. In addition, a role for Rho in cell survival has been suggested in studies with ovarian cancer (Baudhuin et al. 2002). Recently Hu X et al reported, LPA protects B-cell Burkitt lymphoma cell line (BJAB), B-CLL like cell line (I-83) and primary CLL cells but not normal B-cells from fludarabine- and etoposide-induced apoptosis. Furthermore, LPA prevented spontaneous apoptosis in primary CLL cells. The LPA₁ (LPA receptor) expression was found to be increased in primary CLL cells compared with normal B-cells correlating with LPA prevention of apoptosis. Treatment of primary CLL cells with the LPA receptor antagonist, diacylglycerol pyrophosphate, reverses the protective effect of LPA against apoptosis, and down-regulation of the LPA₁ blocked LPA-mediated protection against spontaneous apoptosis in primary CLL cells. The protective effect of LPA was inhibited by blocking activation of the PI3K/AKT signalling pathway (Hu et al. 2005). In contrast, LPA protection against apoptosis in fibroblast cells is mediated by the mitogen-activated protein kinase (MAPK) signalling pathway (Fang et al. 2004). In addition, LPA activated transcription factors, such as NF_κB, that can lead to increased expression of anti-

apoptotic proteins and cell survival (Palmetshofer et al. 1999;Shahrestanifar et al. 1999). Therefore, LPAAT- β inhibitors block LPA that act on several GPCR that may activate different pathways. This may explained why treatment of tumour cells with LPAAT- β inhibitors compound results in type 1 and 2 apoptosis in a remarkably wide variety of tumours types (Bonham et al. 2003;Coon et al. 2003;Hideshima et al. 2003;Hideshima et al. 2005).

5. Although phosphorylated mTOR that has been shown to be dependent upon PA was not attenuated by LPAAT- β inhibitors. This also supports a possibility of PA produced by other enzymes and at the same time probable of LPA as alternative for LPAAT- β inhibitors action. In addition, Kam et al (2004) reported that LPA was found to activate PI3K by a PLD-dependent pathway. The reduction in PLD activity in Rat-2 fibroblast cells impaired the effect of LPA on mTOR signaling (Kam & Exton 2004). These results support the hypothesis that LPA activates protein translation through the action of PLD1-generated PA on mTOR. Therefore inhibition of LPA by LPAAT- β inhibitors resulted in activation of PLD that was act as a backup for PA production and as a result of that increase mTOR phosphorylation.

6. The Gene Ontology data showed an involvement of cell membrane and its receptor such as GPCR after short exposure of inhibitor incubation. Taking the consideration of GO data and the previous points mentioned earlier (points 1,3, 4 and 5) a question is raised; how dose the inhibition of LPAAT- β enzyme (which is intracellular transmembrane enzyme) by LPAAT- β inhibitor can activate these receptor and down stream signalling pathways (See chapter 1 section 1.4.5) which is normally be activated by extracellular LPA?. First, we grown our cell lines in RPMI and 10% Foetal Bovine Serum (FBS), and serum is one of the source of LPA production which can be produced by thrombine-activated platelets (Eichholtz et al. 1993). All the experiments were done in our study including oligonucleotide arrays had the same condition which is 10% FBS. Second, if the pharmacology of LPAAT- β inhibitors acts on LPA substrate which may indicate that the inhibitor abrogated extracellular LPA and thus effect its receptors and down stream signalling pathways. Therefore this is may explain an involvement of cell membrane and GCRP after the inhibitors incubation. Thus in the future beginning work is to measure intracellular and extracellular LPA after inhibitor incubation.

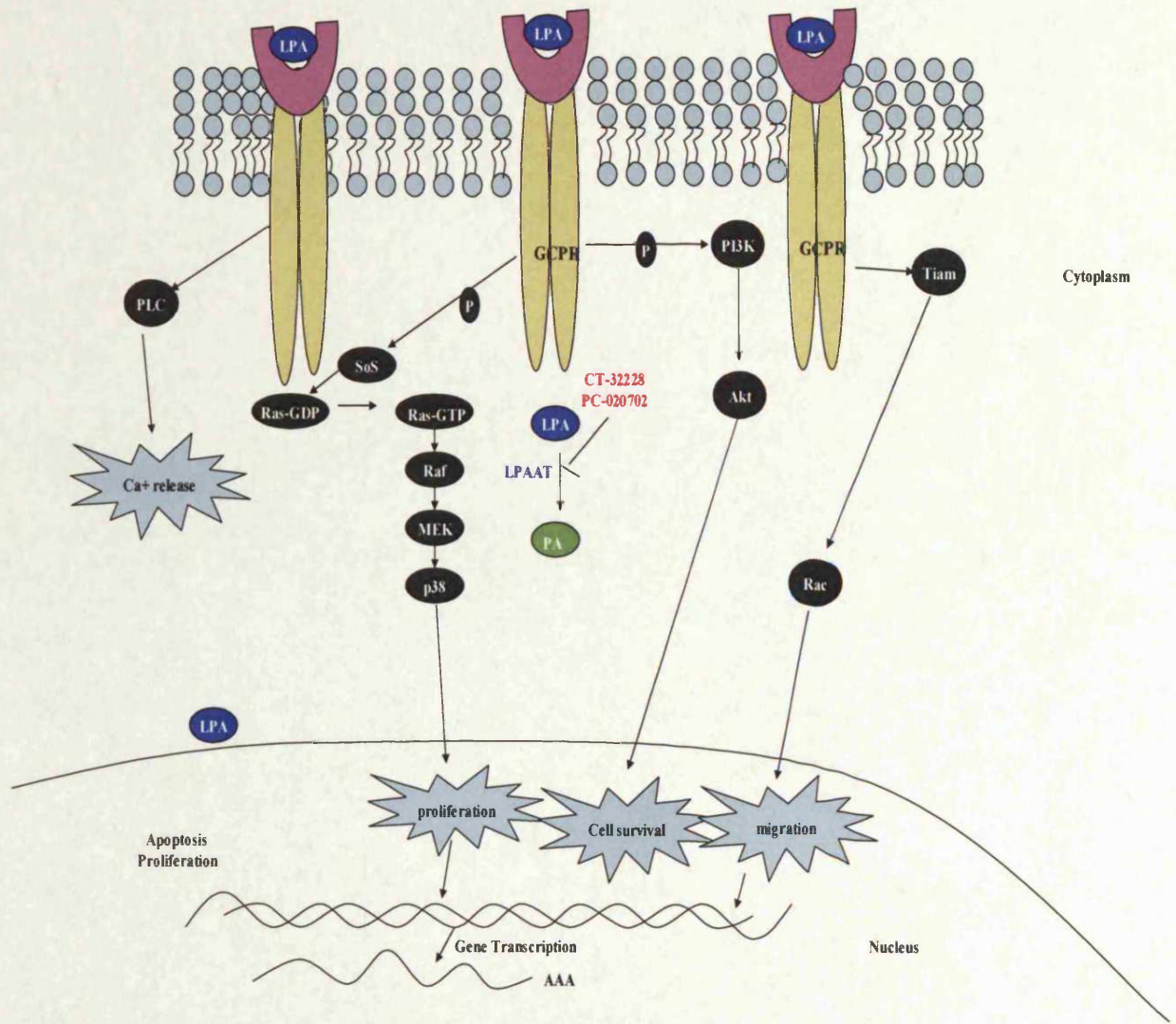
Therefore, taking the consideration of all point countered above, we conclude that LPAAT- β inhibitors may block LPA substrate and consequently block its pathways. LPAAT- β enzyme overexpression is still a matter of debate in AML, however LPAAT- β inhibitors may block LPA and induce toxic effect on AML cells and hence inhibits multiple pathway that can induce apoptosis and cell cycle arrest.

In conclusion, treatment of AML cell lines with LPAAT- β inhibitors were cytotoxic antiproliferative, and induced apoptosis through LPA pathways and not PA pathways. LPA has been proposed as a molecular target for LPAAT- β inhibitors. Therefore, LPAAT- β inhibitors are an attractive and novel target in AML and cancer therapeutics.

7.3 Future Works

To date no studies have found a role of LPA in protecting AML against apoptosis. However, sphingosine 1 phosphate (S1P) a similar like LPA phospholipids, acts both intracellularly and extracellularly to cause pleiotropic biological responses. S1P was found to protect HL60 cells from apoptosis intracellularly without acting on the Edg 1 receptor (Van Brocklyn et al. 1998).

Documentation that LPAAT- β and its substrate LPA are important for the survival of ATRA sensitive and resistant AML cell lines may have significant clinical implications. CT32228 and PC020702 are toxic when given systemically and induce apoptosis. The results presented here form the foundation for exploring the use of these compounds, either alone or in combination with other chemotherapy or differentiation therapy, in the treatment of AML. More importantly, these results for the first time provide an insight of LPAAT- β and LPA as a target of acute myeloid leukaemia therapy. In addition LPAAT- β inhibitors are a specific target for LPA which will open a frame work for the role of LPA in cancer especially intracellular pathways. Interestingly, LPA has been reported to function as a high-affinity ligand for the transcription factor peroxisome proliferating activating receptor- γ (PPAR γ). PPAR γ normally binds fatty acid derivatives and regulates genes that are involved in energy metabolism, cell differentiation, apoptosis and inflammation, but it can also affect cell proliferation and differentiation in various malignances (McIntyre et al. 2003). Therefore the identification of the pathways regulating LPA production and action indicates that therapeutic approaches targeting the LPA cascade might be a realistic addition to the treatment of leukaemia and malignant disease in the near future (Scheme 1).



Scheme 7.1 Major LPA signaling Pathways. LPA signals through its own G-protein coupled receptors via at least three distinct classes of heterotrimeric G proteins leading to activation of multiple downstream effector pathways. Among the main LPA-induced signaling pathways are G_q-mediated activation of phospholipase C (PLC), which leads to hydrolysis of phosphatidylinositol bisphosphate (PIP₂), with consequent calcium mobilization and protein kinase C (PKC) activation; G_i-mediated activation of the RAS-P38 pathways, leading to cell proliferation; G_i-mediated activation of the PI3K-Akt pathway, leading to survival pathway, which suppresses apoptosis; and activation of the RHO And RAC GTPases, which lead to cytoskeletal remodeling and migration. Intracellular signaling of LPA is still not known. LPA may act also on nuclear transcription factor (van Corven et al. 1989; Fang et al. 2000; Fang et al. 2000; Kranenburg & Moolenaar 2001; Takeda et al. 1999; van Corven, et al. 1989; van Corven, et al. 1993; van Leeuwen et al. 2003; McIntyre et al. 2003).

Reference List

- Aguado B, Campbell R D. Characterization of a human lysophosphatidic acid acyltransferase that is encoded by a gene located in the class III region of the human major histocompatibility complex. *J Biol Chem* 1998; (273): 4096-4105.
- Alberts B. *Molecular biology of the cell*. Garland Science, New York 2002.
- Altschul S F, Madden T L, Schaffer A A, Zhang J, Zhang Z, Miller W, Lipman D J. Gapped BLAST and PSI-BLAST: a new generation of protein database search programs. *Nucleic Acids Res* 1997; (25): 3389-3402.
- Andresen B T, Rizzo M A, Shome K, Romero G. The role of phosphatidic acid in the regulation of the Ras/MEK/Erk signaling cascade. *FEBS Lett* 2002; (531): 65-68.
- Anliker B, Chun J. Lysophospholipid G protein-coupled receptors. *J Biol Chem* 2004; (279): 20555-20558.
- Athenstaedt K, Daum G. Phosphatidic acid, a key intermediate in lipid metabolism. *Eur J Biochem* 1999; (266): 1-16.
- Baker D L, Umstot E S, Desiderio D M, Tigyi G J. Quantitative analysis of lysophosphatidic acid in human blood fractions. *Ann N Y Acad Sci* 2000; (905): 267-269.
- Balkham S E, Sargent J M, Elgie A W, Williamson C J, Taylor C G. Comparison of BCL-2 and BAX protein expression with in vitro sensitivity to ARA-C and 6TG in AML. *Adv Exp Med Biol* 1999; (457): 335-340.
- Ballas L M, Bell R M. Topography of glycerolipid synthetic enzymes. Synthesis of phosphatidylserine, phosphatidylinositol and glycerolipid intermediates occurs on the cytoplasmic surface of rat liver microsomal vesicles. *Biochim Biophys Acta* 1981; (665): 586-595.
- Barr F A, Shorter J. Membrane traffic: do cones mark sites of fission? *Curr Biol* 2000; (10): R141-R144.
- Baudhuin L M, Cristina K L, Lu J, Xu Y. Akt activation induced by lysophosphatidic acid and sphingosine-1-phosphate requires both mitogen-activated protein kinase kinase and p38 mitogen-activated protein kinase and is cell-line specific. *Mol Pharmacol* 2002; (62): 660-671.
- Bechoua S, Daniel L W. Phospholipase D is required in the signaling pathway leading to p38 MAPK activation in neutrophil-like HL-60 cells, stimulated by N-formyl-methionyl-leucyl-phenylalanine. *J Biol Chem* 2001; (276): 31752-31759.

- Bell S P, Dutta A. DNA replication in eukaryotic cells. *Annu Rev Biochem* 2002; (71): 333-374.
- Berridge M J, Lipp P, Bootman M D. The versatility and universality of calcium signalling. *Nat Rev Mol Cell Biol* 2000; (1): 11-21.
- Bloch A. Dynamics of interaction between DNA-specific antitumor agents and serum-contained cytokines in the initiation of ML-1 human myeloblastic leukemia cell differentiation. *Leukemia* 1993; (7): 1219-1224.
- Bonham L, Leung D W, White T, Hollenback D, Klein P, Tulinsky J, Coon M, De Vries P, Singer J W. Lysophosphatidic acid acyltransferase-beta: a novel target for induction of tumour cell apoptosis. *Expert Opin Ther Targets* 2003; (7): 643-661.
- Boyle E I, Weng S, Gollub J. GO: TermFinder-open source software for accessing Gene Ontology information and finding significantly enriched Gene Ontology terms associated with a list of genes. *Bioinformatics* 2004; 20(18): 3710-3715.
- Breitman T R, Selonick S E, Collins S J. Induction of differentiation of the human promyelocytic leukemia cell line (HL-60) by retinoic acid. *Proc Natl Acad Sci U S A* 1980; (77): 2936-2940.
- Buhring H J, Herbst R, Kostka G, Bossenmaier B, Bartke I, Kropshofer H, Kalbacher H, Busch F W, Muller C A, Schlessinger J. Modulation of p145c-kit function in cells of patients with acute myeloblastic leukemia. *Cancer Res* 1993; (53): 4424-4431.
- Cai D, Dhe-Paganon S, Melendez P A, Lee J, Shoelson S E. Two new substrates in insulin signaling, IRS5/DOK4 and IRS6/DOK5. *J Biol Chem* 2003; (278): 25323-25330.
- Chakraborty T R, Vancura A, Balija V S, Haldar D. Phosphatidic Acid Synthesis in Mitochondria. Topography of formation and transmembrane migration. *J Biol Chem* 1999; (274): 29786-29790.
- Coffer P J, Woodgett J R. Molecular cloning and characterisation of a novel putative protein-serine kinase related to the cAMP-dependent and protein kinase C families. *Eur J Biochem* 1992; (205): 1217.
- Coleman J. Characterization of the *Escherichia coli* gene for 1-acyl-sn-glycerol-3-phosphate acyltransferase (plsC). *Mol Gen Genet* 1992; (232): 295-303.
- Collins S J, Gallo R C, Gallagher R E. Continuous growth and differentiation of human myeloid leukaemic cells in suspension culture. *Nature* 1977; (270): 347-349.
- Contos J J, Fukushima N, Weiner J A, Kaushal D, Chun J. Requirement for the lpA1 lysophosphatidic acid receptor gene in normal suckling behavior. *Proc Natl Acad Sci U S A* 2000; (97): 13384-13389.

- Contos J J, Ishii I, Fukushima N, Kingsbury M A, Ye X, Kawamura S, Brown J H, Chun J. Characterization of lpa(2) (Edg4) and lpa(1)/lpa(2) (Edg2/Edg4) lysophosphatidic acid receptor knockout mice: signaling deficits without obvious phenotypic abnormality attributable to lpa(2). *Mol Cell Biol* 2002; (22): 6921-6929.
- Coon M, Ball A, Pound J, Ap S, Hollenback D, White T, Tulinsky J, Bonham L, Morrison D K, Finney R, Singer J W. Inhibition of lysophosphatidic acid acyltransferase beta disrupts proliferative and survival signals in normal cells and induces apoptosis of tumor cells. *Mol Cancer Ther* 2003; (2): 1067-1078.
- Cserzo M, Wallin E, Simon I, von Heijne G, Elofsson A. Prediction of transmembrane alpha-helices in prokaryotic membrane proteins: the dense alignment surface method. *Protein Eng* 1997; (10): 673-676.
- Dalton W T, Jr., Ahearn M J, McCredie K B, Freireich E J, Stass S A, Trujillo J M. HL-60 cell line was derived from a patient with FAB-M2 and not FAB-M3. *Blood* 1988; (71): 242-247.
- Darzynkiewicz Z. Apoptosis in anti-tumour strategies: modulation of cell cycle differentiation., *Journal of Cellular Biochemistry* 1995; (58): 151-159.
- Datta S R, Dudek H, Tao X, Masters S, Fu H, Gotoh Y, Greenberg M E. Akt phosphorylation of BAD couples survival signals to the cell-intrinsic death machinery. *Cell* 1997; (91): 231-241.
- Dowhan W. Molecular basis for membrane phospholipid diversity: why are there so many lipids? *Annu Rev Biochem* 1997; (66): 199-232.
- Droin N, Dubrez L, Eymin B, Renvoize C, Breard J, Dimanche-Boitrel M T, Solary E. Upregulation of CASP genes in human tumor cells undergoing etoposide-induced apoptosis. *Oncogene* 1998; (16): 2885-2894.
- Dudek H, Datta S R, Franke T F, Birnbaum M J, Yao R, Cooper G M, Segal R A, Kaplan D R, Greenberg M E. Regulation of neuronal survival by the serine-threonine protein kinase Akt. *Science* 1997; (275): 661-665.
- Duprez E, Ruchaud S, Houge G, Martin-Thouvenin V, Valensi F, Kastner P, Berger R, Lanotte M. A retinoid acid 'resistant' t(15;17) acute promyelocytic leukemia cell line: isolation, morphological, immunological, and molecular features. *Leukemia* 1992; (6): 1281-1287.
- Eberhardt C, Gray P W, Tjoelker L W. Human lysophosphatidic acid acyltransferase. cDNA cloning, expression, and localization to chromosome 9q34.3. *J Biol Chem* 1997; (272): 20299-20305.
- Eder A M, Sasagawa T, Mao M, Aoki J, Mills G B. Constitutive and lysophosphatidic acid (LPA)-induced LPA production: role of phospholipase D and phospholipase A2. *Clin Cancer Res* 2000; (6): 2482-2491.

- Eichholtz T, Jalink K, Fahrenfort I, Moolenaar W H. The bioactive phospholipid lysophosphatidic acid is released from activated platelets. *Biochem J* 1993; (291 (Pt 3)): 677-680.
- Eisen M B, Spellman P T, Brown P O, Botstein D. Cluster analysis and display of genome-wide expression patterns. *Proc Natl Acad Sci U S A* 1998; (95): 14863-14868.
- Elbashir S M, Harborth J, Lendeckel W, Yalcin A, Weber K, Tuschl T. Duplexes of 21-nucleotide RNAs mediate RNA interference in cultured mammalian cells. *Nature* 2001; (411): 494-498.
- English D, Cui Y, Siddiqui R A. Messenger functions of phosphatidic acid. *Chem Phys Lipids* 1996; (80): 117-132.
- Estrov Z, Thall P F, Talpaz M, Estey E H, Kantarjian H M, Andreeff M, Harris D, Van Q, Walterscheid M, Kornblau S M. Caspase 2 and Caspase 3 Protein Levels as Predictors of Survival in Acute Myelogenous Leukemia. *Blood* 1998; (92): 3090-3097.
- Fang X, Gaudette D, Furui T, Mao M, Estrella V, Eder A, Pustilnik T, Sasagawa T, Lapushin R, Yu S, Jaffe R B, Wiener J R, Erickson J R, Mills G B. Lysophospholipid growth factors in the initiation, progression, metastases, and management of ovarian cancer. *Ann N Y Acad Sci* 2000; (905): 188-208.
- Fang X, Schummer M, Mao M, Yu S, Tabassam F H, Swaby R, Hasegawa Y, Tanyi J L, Lapushin R, Eder A, Jaffe R, Erickson J, Mills G B. Lysophosphatidic acid is a bioactive mediator in ovarian cancer. *Biochim Biophys Acta* 2002; (1582): 257-264.
- Fang X, Yu S, Bast R C, Liu S, Xu H J, Hu S X, Lapushin R, Claret F X, Aggarwal B B, Lu Y, Mills G B. Mechanisms for lysophosphatidic acid-induced cytokine production in ovarian cancer cells. *J Biol Chem* 2004; (279): 9653-9661.
- Fang X, Yu S, Lapushin R, Lu Y, Furui T, Penn L Z, Stokoe D, Erickson J R, Bast R C, Jr., Mills G B. Lysophosphatidic acid prevents apoptosis in fibroblasts via G(i)-protein-mediated activation of mitogen-activated protein kinase. *Biochem J* 2000; (352 Pt 1): 135-143.
- Fang Y, Vilella-Bach M, Bachmann R, Flanigan A, Chen J. Phosphatidic acid-mediated mitogenic activation of mTOR signaling. *Science* 2001; (294): 1942-1945.
- Faucheu C, Blanchet A M, Collard-Dutilleul V, Lalanne J L, Diu-Hercend A. Identification of a cysteine protease closely related to interleukin-1 beta-converting enzyme. *Eur J Biochem* 1996; (236): 207-213.
- Faucheu C, Diu A, Chan A W, Blanchet A M, Miossec C, Herve F, Collard-Dutilleul V, Gu Y, Aldape R A, Lippke J A, . A novel human protease similar to the interleukin-1

- beta converting enzyme induces apoptosis in transfected cells. *EMBO J* 1995; (14): 1914-1922.
- Finney R E, Bishop J M. Predisposition to neoplastic transformation caused by gene replacement of H-ras1. *Science* 1993; (260): 1524-1527.
- Fishman D A, Liu Y, Ellerbroek S M, Stack M S. Lysophosphatidic acid promotes matrix metalloproteinase (MMP) activation and MMP-dependent invasion in ovarian cancer cells. *Cancer Res* 2001; (61): 3194-3199.
- Furui T, Lapushin R, Mao M, Khan H, Watt S R, Watt M A, Lu Y, Fang X, Tsutsui S, Siddik Z H, Bast R C, Mills G B. Overexpression of *edg-2/vzg-1* induces apoptosis and anoikis in ovarian cancer cells in a lysophosphatidic acid-independent manner. *Clin Cancer Res* 1999; (5): 4308-4318.
- Gaits F, Fourcade O, Le Balle F, Gueguen G, Gaige B, Gassama-Diagne A, Fauvel J, Salles J P, Mauco G, Simon M F, Chap H. Lysophosphatidic acid as a phospholipid mediator: pathways of synthesis. *FEBS Lett* 1997; (410): 54-58.
- Gallagher R E, Bilello P A, Ferrari A C, Chang C S, Yen R W, Nickols W A, Muly E C, III. Characterization of differentiation-inducer-resistant HL-60 cells. *Leuk Res* 1985; (9): 967-986.
- Ghosh S, Bell R M. Regulation of Raf-1 kinase by interaction with the lipid second messenger, phosphatidic acid. *Biochem Soc Trans* 1997; (25): 561-565.
- Ghosh S, Strum J C, Sciorra V A, Daniel L, Bell R M. Raf-1 kinase possesses distinct binding domains for phosphatidylserine and phosphatidic acid. Phosphatidic acid regulates the translocation of Raf-1 in 12-O-tetradecanoylphorbol-13-acetate-stimulated Madin-Darby canine kidney cells. *J Biol Chem* 1996; (271): 8472-8480.
- Gingras A C, Raught B, Sonenberg N. Regulation of translation initiation by FRAP/mTOR. *Genes Dev* 2001; (15): 807-826.
- Goetzl E J, An S. Diversity of cellular receptors and functions for the lysophospholipid growth factors lysophosphatidic acid and sphingosine 1-phosphate. *FASEB J* 1998; (12): 1589-1598.
- Goetzl E J, Dolezalova H, Kong Y, Hu Y L, Jaffe R B, Kalli K R, Conover C A. Distinctive expression and functions of the type 4 endothelial differentiation gene-encoded G protein-coupled receptor for lysophosphatidic acid in ovarian cancer. *Cancer Res* 1999; (59): 5370-5375.
- Goetzl E J, Lee H, Dolezalova H, Kalli K R, Conover C A, Hu Y L, Azuma T, Stossel T P, Karliner J S, Jaffe R B. Mechanisms of lysolipid phosphate effects on cellular survival and proliferation. *Ann N Y Acad Sci* 2000; (905): 177-187.

- Gong B, Hong F, Kohm C, Bonham L, Klein P. Synthesis and SAR of 2-arylbenzoxazoles, benzothiazoles and benzimidazoles as inhibitors of lysophosphatidic acid acyltransferase-beta. *Bioorg Med Chem Lett* 2004; (14): 1455-1459.
- Gong B, Hong F, Kohm C, Jenkins S, Tulinsky J, Bhatt R, De Vries P, Singer J W, Klein P. Synthesis, SAR, and antitumor properties of diamino-C,N-diarylpyrimidine positional isomers: inhibitors of lysophosphatidic acid acyltransferase-beta. *Bioorg Med Chem Lett* 2004; (14): 2303-2308.
- Gore S D, Weng L J, Jones R J, Cowan K, Zilcha M, Piantadosi S, Burke P J. Impact of in vivo administration of interleukin 3 on proliferation, differentiation, and chemosensitivity of acute myeloid leukemia. *Clin Cancer Res* 1995; (1): 295-303.
- Gotoh T, Ohsumi K, Matsui T, Takisawa H, Kishimoto T. Inactivation of the checkpoint kinase Cds1 is dependent on cyclin B-Cdc2 kinase activation at the meiotic G(2)/M-phase transition in *Xenopus* oocytes. *J Cell Sci* 2001; (114): 3397-3406.
- Guo M, Hay B A. Cell proliferation and apoptosis. *Curr Opin Cell Biol* 1999; (11): 745-752.
- Harris M A, Lomax J, Ireland A, Clark J I. The Gene Ontology Project, in Subramaniam, S., Ed., *Encyclopedia of Genetics, Genomics, Proteomics and Bioinformatics, Part 4. Bioinformatics, 4.7. Structuring and Integrating Data*, John Wiley & Sons, Ltd (2005).
- Harris N L, Jaffe E S, Diebold J, Flandrin G, Muller-Hermelink H K, Vardiman J, Lister T A, Bloomfield C D. World Health Organization Classification of Neoplastic Diseases of the Hematopoietic and Lymphoid Tissues: Report of the Clinical Advisory Committee Meeting Airlie House, Virginia, November 1997. *J Clin Oncol* 1999; (17): 3835-3849.
- Hassan H T, Rees J K. Triple combination of retinoic acid + low concentration of cytosine arabinoside + hexamethylene bisacetamide induces differentiation of human AML blasts in primary culture. *Hematol Oncol* 1989; (7): 429-440.
- Hassan H T, Rees J K. Triple combination of retinoic acid+aclacinomycin A+dimethylformamide induces differentiation of human acute myeloid leukaemic blasts in primary culture. *Anticancer Res* 1989; (9): 647-651.
- Heath R J, Rock C O. A conserved histidine is essential for glycerolipid acyltransferase catalysis. *J Bacteriol* 1998; (180): 1425-1430.
- Hecht J H, Weiner J A, Post S R, Chun J. Ventricular zone gene-1 (vzg-1) encodes a lysophosphatidic acid receptor expressed in neurogenic regions of the developing cerebral cortex. *J Cell Biol* 1996; (135): 1071-1083.

- Hideshima T, Chauhan D, Hayashi T, Podar K, Akiyama M, Mitsiades C, Mitsiades N, Gong B, Bonham L, De Vries P, Munshi N, Richardson P G, Singer J W, Anderson K C. Antitumor activity of lysophosphatidic acid acyltransferase-beta inhibitors, a novel class of agents, in multiple myeloma. *Cancer Res* 2003; (63): 8428-8436.
- Hideshima T, Chauhan D, Ishitsuka K, Yasui H, Raje N, Kumar S, Podar K, Mitsiades C, Hideshima H, Bonham L, Munshi N C, Richardson P G, Singer J W, Anderson K C. Molecular characterization of PS-341 (bortezomib) resistance: implications for overcoming resistance using lysophosphatidic acid acyltransferase (LPAAT)-beta inhibitors. *Oncogene* 2005; (24): 3121-3129.
- Hirst J, Bright N A, Rous B, Robinson M S. Characterization of a fourth adaptor-related protein complex. *Mol Biol Cell* 1999; (10): 2787-2802.
- Ho A, Dowdy S F. Regulation of G(1) cell-cycle progression by oncogenes and tumor suppressor genes. *Curr Opin Genet Dev* 2002; (12): 47-52.
- Hoffbrand A V, Pettit J E, Moss P. *Essential haematology*. Blackwell Science, Oxford 2001.
- Hoffbrand A V, Tuddenham E G D, Lewis S M. *Postgraduate haematology*. Arnold, London 2001.
- Honda A, Nogami M, Yokozeki T, Yamazaki M, Nakamura H, Watanabe H, Kawamoto K, Nakayama K, Morris A J, Frohman M A, Kanaho Y. Phosphatidylinositol 4-phosphate 5-kinase alpha is a downstream effector of the small G protein ARF6 in membrane ruffle formation. *Cell* 1999; (99): 521-532.
- Howard M R, Hamilton P J. *Haematology an illustrated colour text*. Churchill Livingstone, Edinburgh 2002.
- Howell A L, Stukel T A, Bloomfield C D, Davey F R, Ball E D. Induction of differentiation in blast cells and leukemia colony-forming cells from patients with acute myeloid leukemia. *Blood* 1990; (75): 721-729.
- Hsu S M, Raine L, Fanger H. Use of avidin-biotin-peroxidase complex (ABC) in immunoperoxidase techniques: a comparison between ABC and unlabeled antibody (PAP) procedures. *J Histochem Cytochem* 1981; (29): 577-580.
- Hu X, Haney N, Kropp D, Kabore A F, Johnston J B, Gibson S B. Lysophosphatidic Acid (LPA) Protects Primary Chronic Lymphocytic Leukemia Cells from Apoptosis through LPA Receptor Activation of the Anti-apoptotic Protein AKT/PKB. *J Biol Chem* 2005; (280): 9498-9508.

- Hu Y L, Tee M K, Goetzl E J, Auersperg N, Mills G B, Ferrara N, Jaffe R B. Lysophosphatidic acid induction of vascular endothelial growth factor expression in human ovarian cancer cells. *J Natl Cancer Inst* 2001; (93): 762-768.
- Hu Z B, Minden M D, McCulloch E A. Post-transcriptional regulation of bcl-2 in acute myeloblastic leukemia: significance for response to chemotherapy. *Leukemia* 1996; (10): 410-416.
- Ibrado A M, Huang Y, Fang G, Liu L, Bhalla K. Overexpression of Bcl-2 or Bcl-xL inhibits Ara-C-induced CPP32/Yama protease activity and apoptosis of human acute myelogenous leukemia HL-60 cells. *Cancer Res* 1996; (56): 4743-4748.
- Imamura F, Horai T, Mukai M, Shinkai K, Sawada M, Akedo H. Induction of in vitro tumor cell invasion of cellular monolayers by lysophosphatidic acid or phospholipase D. *Biochem Biophys Res Commun* 1993; (193): 497-503.
- Jalink K, Eichholtz T, Postma F R, van Corven E J, Moolenaar W H. Lysophosphatidic acid induces neuronal shape changes via a novel, receptor-mediated signaling pathway: similarity to thrombin action. *Cell Growth Differ* 1993; (4): 247-255.
- Jalink K, van Corven E J, Moolenaar W H. Lysophosphatidic acid, but not phosphatidic acid, is a potent Ca²⁺(+)-mobilizing stimulus for fibroblasts. Evidence for an extracellular site of action. *J Biol Chem* 1990; (265): 12232-12239.
- Jones D, Morgan C, Cockcroft S. Phospholipase D and membrane traffic. Potential roles in regulated exocytosis, membrane delivery and vesicle budding. *Biochim Biophys Acta* 1999; (1439): 229-244.
- Jones D R, Sanjuan M A, Stone J C, Merida I. Expression of a catalytically inactive form of diacylglycerol kinase alpha induces sustained signaling through RasGRP. *FASEB J* 2002; (16): 595-597.
- Kam yoon, Exton J H. Role of phospholipase D1 in the regulation of mTOR activity by lysophosphatidic acid. *FASEB J* 2004; (18): 311-319.
- Kamada S, Kikkawa U, Tsujimoto Y, Hunter T. Nuclear translocation of caspase-3 is dependent on its proteolytic activation and recognition of a substrate-like protein(s). *J Biol Chem* 2005; (280): 857-860.
- Kamada S, Washida M, Hasegawa J, Kusano H, Funahashi Y, Tsujimoto Y. Involvement of caspase-4(-like) protease in Fas-mediated apoptotic pathway. *Oncogene* 1997; (15): 285-290.
- Kanfer J, Kennedy E P. Metabolism and function of bacterial lipids. I. Metabolism of phospholipids in *Escherichia Coli* B. *J Biol Chem* 1963; (238): 2919-2922.

- Kaufmann S H, Karp J E, Svingen P A, Krajewski S, Burke P J, Gore S D, Reed J C. Elevated Expression of the Apoptotic Regulator Mcl-1 at the Time of Leukemic Relapse. *Blood* 1998; (91): 991-1000.
- Ketley N J, Allen P D, Kelsey S M, Newland A C. Modulation of Idarubicin-Induced Apoptosis in Human Acute Myeloid Leukemia Blasts by All-Trans Retinoic Acid, 1,25(OH)₂ Vitamin D₃, and Granulocyte-Macrophage Colony-Stimulating Factor. *Blood* 1997; (90): 4578-4587.
- King K L, Cidlowski J A. Cell cycle and apoptosis: common pathways to life and death. *J Cell Biochem* 1995; (58): 175-180.
- Knutzon D S, Lardizabal K D, Nelsen J S, Bleibaum J L, Davies H M, Metz J G. Cloning of a coconut endosperm cDNA encoding a 1-acyl-sn-glycerol-3-phosphate acyltransferase that accepts medium-chain-length substrates. *Plant Physiol* 1995; (109): 999-1006.
- Kosugi H, Towatari M, Hatano S, Kitamura K, Kiyoi H, Kinoshita T, Tanimoto M, Murate T, Kawashima K, Saito H, Naoe T. Histone deacetylase inhibitors are the potent inducer/enhancer of differentiation in acute myeloid leukemia: a new approach to anti-leukemia therapy. *Leukemia* 1999; (13): 1316-1324.
- Kranenburg O, Moolenaar W H. Ras-MAP kinase signaling by lysophosphatidic acid and other G protein-coupled receptor agonists. *Oncogene* 2001; (20): 1540-1546.
- Kranenburg O, Poland M, van Horck F P, Drechsel D, Hall A, Moolenaar W H. Activation of RhoA by lysophosphatidic acid and Galpha12/13 subunits in neuronal cells: induction of neurite retraction. *Mol Biol Cell* 1999; (10): 1851-1857.
- Kumagai N, Morii N, Fujisawa K, Nemoto Y, Narumiya S. ADP-ribosylation of rho p21 inhibits lysophosphatidic acid-induced protein tyrosine phosphorylation and phosphatidylinositol 3-kinase activation in cultured Swiss 3T3 cells. *J Biol Chem* 1993; (268): 24535-24538.
- Lanotte M, Martin-Thouvenin V, Najman S, Balerini P, Valensi F, Berger R. NB4, a maturation inducible cell line with t(15;17) marker isolated from a human acute promyelocytic leukemia (M3). *Blood* 1991; (77): 1080-1086.
- Lee M L, Kuo F C, Whitmore G A, Sklar J. Importance of replication in microarray gene expression studies: statistical methods and evidence from repetitive cDNA hybridizations. *Proc Natl Acad Sci U S A* 2000; (97): 9834-9839.
- Lee S D, Lee B D, Han J M, Kim J H, Kim Y, Suh P G, Ryu S H. Phospholipase D2 activity suppresses hydrogen peroxide-induced apoptosis in PC12 cells. *J Neurochem* 2000; (75): 1053-1059.
- Leist M. & Nicotera P. The shape of cell death. *Biochemical And Biophysical Research Communications* 1997; (236): 1-9.

- Leung D W. The structure and functions of human lysophosphatidic acid acyltransferases. *Front Biosci* 2001; (6): D944-D953.
- Leung D W, Tompkins C K, White T. Molecular cloning of two alternatively spliced forms of human phosphatidic acid phosphatase cDNAs that are differentially expressed in normal and tumor cells. *DNA Cell Biol* 1998; (17): 377-385.
- Levine A J. p53, the cellular gatekeeper for growth and division. *Cell* 1997; (88): 323-331.
- Lewin T M, Wang P, Coleman R A. Analysis of amino acid motifs diagnostic for the sn-glycerol-3-phosphate acyltransferase reaction. *Biochemistry* 1999; (38): 5764-5771.
- Lin X Y, Choi M S, Porter A G. Expression analysis of the human caspase-1 subfamily reveals specific regulation of the CASP5 gene by lipopolysaccharide and interferon-gamma. *J Biol Chem* 2000; (275): 39920-39926.
- Masui Y. Towards understanding the control of the division cycle in animal cells. *Biochem Cell Biol* 1992; (70): 920-945.
- Matsuda K, Yoshida K, Taya Y, Nakamura K, Nakamura Y, Arakawa H. p53AIP1 regulates the mitochondrial apoptotic pathway. *Cancer Res* 2002; (62): 2883-2889.
- McCulloch E A. Stem cell renewal and determination during clonal expansion in normal and leukaemic haemopoiesis. *Cell Prolif* 1993; (26): 399-425.
- McGall G H, Fidanza J A. Photolithographic synthesis of high-density oligonucleotide arrays. *Methods Mol Biol* 2001; (170): 71-101.
- McGiffert C, Contos J J, Friedman B, Chun J. Embryonic brain expression analysis of lysophospholipid receptor genes suggests roles for s1p(1) in neurogenesis and s1p(1-3) in angiogenesis. *FEBS Lett* 2002; (531): 103-108.
- McIntyre T M, Pontsler A V, Silva A R, St Hilaire A, Xu Y, Hinshaw J C, Zimmerman G A, Hama K, Aoki J, Arai H, Prestwich G D. Identification of an intracellular receptor for lysophosphatidic acid (LPA): LPA is a transcellular PPARgamma agonist. *Proc Natl Acad Sci U S A* 2003; (100): 131-136.
- Mehta A B, Hoffbrand A V. *Haematology at a glance*. Blackwell Science, Malden, MA 2000.
- Milella M, Kornblau S M, Estrov Z, Carter B Z, Lapillonne H, Harris D, Konopleva M, Zhao S, Estey E, Andreeff M. Therapeutic targeting of the MEK/MAPK signal transduction module in acute myeloid leukemia. *J Clin Invest* 2001; (108): 851-859.
- Moolenaar W H. Lysophosphatidic acid, a multifunctional phospholipid messenger. *J Biol Chem* 1995; (270): 12949-12952.

- Moolenaar W H, Kranenburg O, Postma F R, Zondag G C. Lysophosphatidic acid: G-protein signalling and cellular responses. *Curr Opin Cell Biol* 1997; (9): 168-173.
- Moolenaar W H, van Corven E J. Growth factor-like action of lysophosphatidic acid: mitogenic signalling mediated by G proteins. *Ciba Found Symp* 1990; (150): 99-106.
- Moolenaar W H, van der Bend R L, van Corven E J, Jalink K, Eichholtz T, van Blitterswijk W J. Lysophosphatidic acid: a novel phospholipid with hormone- and growth factor-like activities. *Cold Spring Harb Symp Quant Biol* 1992; (57): 163-167.
- Morgan J M. A protocol for preparing cell suspension with formaline fixation and paraffin embedding which minimises the formation of cell aggregates. *Journal of Cellular Pathology* 2001; (5): 171-181.
- Morrison D K, Cutler R E. The complexity of Raf-1 regulation. *Curr Opin Cell Biol* 1997; (9): 174-179.
- Munday N A, Vaillancourt J P, Ali A, Casano F J, Miller D K, Molineaux S M, Yamin T T, Yu V L, Nicholson D W. Molecular cloning and pro-apoptotic activity of ICERell and ICERelll, members of the ICE/CED-3 family of cysteine proteases. *J Biol Chem* 1995; (270): 15870-15876.
- Nagiec M M, Wells G B, Lester R L, Dickson R C. A suppressor gene that enables *Saccharomyces cerevisiae* to grow without making sphingolipids encodes a protein that resembles an *Escherichia coli* fatty acyltransferase. *J Biol Chem* 1993; (268): 22156-22163.
- Niesporek S, Denkert C, Weichert W, Kobel M, Noske A, Sehouli J, Singer J W, Dietel M, Hauptmann S. Expression of lysophosphatidic acid acyltransferase beta (LPAAT-beta) in ovarian carcinoma: correlation with tumour grading and prognosis. *Br J Cancer* 2005; (92): 1729-1736.
- Obaya A J, Sedivy J M. Regulation of cyclin-Cdk activity in mammalian cells. *Cell Mol Life Sci* 2002; (59): 126-142.
- Oda K, Arakawa H, Tanaka T, Matsuda K, Tanikawa C, Mori T, Nishimori H, Tamai K, Tokino T, Nakamura Y, Taya Y. p53AIP1, a potential mediator of p53-dependent apoptosis, and its regulation by Ser-46-phosphorylated p53. *Cell* 2000; (102): 849-862.
- Orkin S H. Hematopoiesis: how does it happen? *Curr Opin Cell Biol* 1995; (7): 870-877.
- Ormerod M G. *Introduction & Instrumentation*. Bios Scientific, Oxford, 1999.
- Osborne B A. Apoptosis and the maintenance of homeostasis in the immune system. *Current Opinion in immunology* 1996; (8): 245-254.

- Pagel J M, Laugen C, Bonham L, Hackman R C, Hockenbery D M, Bhatt R, Hollenback D, Carew H, Singer J W, Press O W. Induction of apoptosis using inhibitors of lysophosphatidic acid acyltransferase-beta and anti-CD20 monoclonal antibodies for treatment of human non-Hodgkin's lymphomas. *Clin Cancer Res* 2005; (11): 4857-4866.
- Palmetshofer A, Robson S C, Nehls V. Lysophosphatidic acid activates nuclear factor kappa B and induces proinflammatory gene expression in endothelial cells. *Thromb Haemost* 1999; (82): 1532-1537.
- Pandolfi P P. Histone deacetylases and transcriptional therapy with their inhibitors. *Cancer Chemother Pharmacol* 2001; (48 Suppl 1): S17-S19.
- Pawelczyk T, Matecki A. Phospholipase C-delta3 binds with high specificity to phosphatidylinositol 4,5-bisphosphate and phosphatidic acid in bilayer membranes. *Eur J Biochem* 1999; (262): 291-298.
- Raff M C. Social controls on cell survival and cell death. *Nature* 1992; (356): 397-400.
- Raynal P, Pollard H B. Annexins: the problem of assessing the biological role for a gene family of multifunctional calcium- and phospholipid-binding proteins. *Biochim Biophys Acta* 1994; (1197): 63-93.
- Reutelingsperger C P, Hornstra G, Hemker H C. Isolation and partial purification of a novel anticoagulant from arteries of human umbilical cord. *Eur J Biochem* 1985; (151): 625-629.
- Rizzo M A, Shome K, Watkins S C, Romero G. The recruitment of Raf-1 to membranes is mediated by direct interaction with phosphatidic acid and is independent of association with Ras. *J Biol Chem* 2000; (275): 23911-23918.
- Santini V, Scappini B, Gozzini A, Grossi A, Villa P, Ronco G, Douillet O, Pouillart P, Bernabei P A, Rossi F P. Butyrate-stable monosaccharide derivatives induce maturation and apoptosis in human acute myeloid leukaemia cells. *Br J Haematol* 1998; (101): 529-538.
- Saulnier-Blache J S, Girard A, Simon M F, Lafontan M, Valet P. A simple and highly sensitive radioenzymatic assay for lysophosphatidic acid quantification. *J Lipid Res* 2000; (41): 1947-1951.
- Sautin Y Y, Crawford J M, Svetlov S I. Enhancement of survival by LPA via Erk1/Erk2 and PI 3-kinase/Akt pathways in a murine hepatocyte cell line. *Am J Physiol Cell Physiol* 2001; (281): C2010-C2019.
- Schmid B, Finnen M J, Harwood J L, Jackson S K. Acylation of lysophosphatidylcholine plays a key role in the response of monocytes to lipopolysaccharide. *Eur J Biochem* 2003; (270): 2782-2788.

- Schmidt A, Wolde M, Thiele C, Fest W, Kratzin H, Podtelejnikov A V, Witke W, Huttner W B, Soling H D. Endophilin I mediates synaptic vesicle formation by transfer of arachidonate to lysophosphatidic acid. *Nature* 1999; (401): 133-141.
- Schulte K M, Beyer A, Kohrer K, Oberhauser S, Roher H D. Lysophosphatidic acid, a novel lipid growth factor for human thyroid cells: over-expression of the high-affinity receptor *edg4* in differentiated thyroid cancer. *Int J Cancer* 2001; (92): 249-256.
- Sergeant S, Waite K A, Heravi J, McPhail L C. Phosphatidic acid regulates tyrosine phosphorylating activity in human neutrophils: enhancement of Fgr activity. *J Biol Chem* 2001; (276): 4737-4746.
- Shahrestanifar M, Fan X, Manning D R. Lysophosphatidic acid activates NF-kappaB in fibroblasts. A requirement for multiple inputs. *J Biol Chem* 1999; (274): 3828-3833.
- Shao W, Fanelli M, Ferrara F F, Riccioni R, Rosenauer A, Davison K, Lamph W W, Waxman S, Pelicci P G, Lo Coco F, Avvisati G, Testa U, Peschle C, Gambacorti-Passerini C, Nervi C, Miller W H, Jr. Arsenic trioxide as an inducer of apoptosis and loss of PML/RAR alpha protein in acute promyelocytic leukemia cells. *J Natl Cancer Inst* 1998; (90): 124-133.
- Shapiro H M. *Overture. Practical flow cytometry*. Wiley-Liss, New York, 1995.
- Shen Y, Xu L, Foster D A. Role for phospholipase D in receptor-mediated endocytosis. *Mol Cell Biol* 2001; (21): 595-602.
- Shen Z X, Chen G Q, Ni J H, Li X S, Xiong S M, Qiu Q Y, Zhu J, Tang W, Sun G L, Yang K Q, Chen Y, Zhou L, Fang Z W, Wang Y T, Ma J, Zhang P, Zhang T D, Chen S J, Chen Z, Wang Z Y. Use of Arsenic Trioxide (As₂O₃) in the Treatment of Acute Promyelocytic Leukemia (APL): II. Clinical Efficacy and Pharmacokinetics in Relapsed Patients. *Blood* 1997; (89): 3354-3360.
- Smits V A, Medema R H. Checking out the G(2)/M transition. *Biochim Biophys Acta* 2001; (1519): 1-12.
- Soignet S L, Maslak P, Wang Z G, Jhanwar S, Calleja E, Dardashti L J, Corso D, DeBlasio A, Gabrilove J, Scheinberg D A, Pandolfi P P, Warrell R P. Complete Remission after Treatment of Acute Promyelocytic Leukemia with Arsenic Trioxide. *N Engl J Med* 1998; (339): 1341-1348.
- Stam J C, Michiels F, van der Kammen R A, Moolenaar W H, Collard J G. Invasion of T-lymphoma cells: cooperation between Rho family GTPases and lysophospholipid receptor signaling. *EMBO J* 1998; (17): 4066-4074.
- Starr R, Willson T A, Viney E M, Murray L J, Rayner J R, Jenkins B J, Gonda T J, Alexander W S, Metcalf D, Nicola N A, Hilton D J. A family of cytokine-inducible inhibitors of signalling. *Nature* 1997; (387): 917-921.

- Takeda H, Matozaki T, Takada T, Noguchi T, Yamao T, Tsuda M, Ochi F, Fukunaga K, Inagaki K, Kasuga M. PI 3-kinase gamma and protein kinase C-zeta mediate RAS-independent activation of MAP kinase by a Gi protein-coupled receptor. *EMBO J* 1999; (18): 386-395.
- Tallman M S, Nabhan C, Feusner J H, Rowe J M. Acute promyelocytic leukemia: evolving therapeutic strategies. *Blood* 2002; (99): 759-767.
- Tanyi J L, Hasegawa Y, Lapushin R, Morris A J, Wolf J K, Berchuck A, Lu K, Smith D I, Kalli K, Hartmann L C, McCune K, Fishman D, Broaddus R, Cheng K W, Atkinson E N, Yamal J M, Bast R C, Felix E A, Newman R A, Mills G B. Role of decreased levels of lipid phosphate phosphatase-1 in accumulation of lysophosphatidic acid in ovarian cancer. *Clin Cancer Res* 2003; (9): 3534-3545.
- Tanyi J L, Morris A J, Wolf J K, Fang X, Hasegawa Y, Lapushin R, Auersperg N, Sigal Y J, Newman R A, Felix E A, Atkinson E N, Mills G B. The human lipid phosphate phosphatase-3 decreases the growth, survival, and tumorigenesis of ovarian cancer cells: validation of the lysophosphatidic acid signaling cascade as a target for therapy in ovarian cancer. *Cancer Res* 2003; (63): 1073-1082.
- Tawhid H, Rees J. Triple combination of retinoic acid + 6-thioguanine + hexamethylene bisacetamide induces differentiation of human AML blasts in primary culture. *Leuk Res* 1990; (14): 109-117.
- Tigyi G, Dyer D L, Miledi R. Lysophosphatidic acid possesses dual action in cell proliferation. *Proc Natl Acad Sci U S A* 1994; (91): 1908-1912.
- Tigyi G, Parrill A L. Molecular mechanisms of lysophosphatidic acid action. *Prog Lipid Res* 2003; (42): 498-526.
- Tokumura A, Fukuzawa K, Tsukatani H. Effects of synthetic and natural lysophosphatidic acids on the arterial blood pressure of different animal species. *Lipids* 1978; (13): 572-574.
- Tokumura A, Miyake M, Nishioka Y, Yamano S, Aono T, Fukuzawa K. Production of Lysophosphatidic Acids by Lysophospholipase D in Human Follicular Fluids of In Vitro Fertilization Patients. *Biol Reprod* 1999; (61): 195-199.
- Topham M K, Prescott S M. Diacylglycerol kinase zeta regulates Ras activation by a novel mechanism. *J Cell Biol* 2001; (152): 1135-1143.
- Towatari M, Iida H, Tanimoto M, Iwata H, Hamaguchi M, Saito H. Constitutive activation of mitogen-activated protein kinase pathway in acute leukemia cells. *Leukemia* 1997; (11): 479-484.
- Van Brocklyn J R, Lee M J, Menzeleev R, Olivera A, Edsall L, Cuvillier O, Thomas D M, Coopman P J P, Thangada S, Liu C H, Hla T, Spiegel S. Dual Actions of

- Sphingosine-1-Phosphate: Extracellular through the Gi-coupled Receptor Edg-1 and Intracellular to Regulate Proliferation and Survival.** *J Cell Biol* 1998; (142): 229-240.
- van Corven E J, Groenink A, Jalink K, Eichholtz T, Moolenaar W H. Lysophosphatidate-induced cell proliferation: identification and dissection of signaling pathways mediated by G proteins. *Cell* 1989; (59): 45-54.
- van Corven E J, Hordijk P L, Medema R H, Bos J L, Moolenaar W H. Pertussis toxin-sensitive activation of p21ras by G protein-coupled receptor agonists in fibroblasts. *Proc Natl Acad Sci U S A* 1993; (90): 1257-1261.
- van der Bend R L, Brunner J, Jalink K, van Corven E J, Moolenaar W H, van Blitterswijk W J. Identification of a putative membrane receptor for the bioactive phospholipid, lysophosphatidic acid. *EMBO J* 1992; (11): 2495-2501.
- van Dijk M C, Postma F, Hilkmann H, Jalink K, van Blitterswijk W J, Moolenaar W H. Exogenous phospholipase D generates lysophosphatidic acid and activates Ras, Rho and Ca²⁺ signaling pathways. *Curr Biol* 1998; (8): 386-392.
- van Leeuwen F N, Olivo C, Grivell S, Giepmans B N, Collard J G, Moolenaar W H. Rac activation by lysophosphatidic acid LPA1 receptors through the guanine nucleotide exchange factor Tiam1. *J Biol Chem* 2003; (278): 400-406.
- Vermes I, Haanen C, Steffens-Nakken H, Reutelingsperger C. A novel assay for apoptosis. Flow cytometric detection of phosphatidylserine expression on early apoptotic cells using fluorescein labelled Annexin V. *J Immunol Methods* 1995; (184): 39-51.
- Vivanco I, Sawyers C L. The phosphatidylinositol 3-Kinase AKT pathway in human cancer. *Nat Rev Cancer* 2002; (2): 489-501.
- Waggoner D W, Gomez-Munoz A, Dewald J, Brindley D N. Phosphatidate Phosphohydrolase Catalyzes the Hydrolysis of Ceramide 1-Phosphate, Lysophosphatidate, and Sphingosine 1-Phosphate. *J Biol Chem* 1996; (271): 16506-16509.
- Wang Z G, Rivi R, Delva L, Konig A, Scheinberg D A, Gambacorti-Passerini C, Gabrilove J L, Warrell R P, Jr., Pandolfi P P. Arsenic Trioxide and Melarsoprol Induce Programmed Cell Death in Myeloid Leukemia Cell Lines and Function in a PML and PML-RARalpha Independent Manner. *Blood* 1998; (92): 1497-1504.
- Warrell R P, Jr., He L Z, Richon V, Calleja E, Pandolfi P P. Therapeutic Targeting of Transcription in Acute Promyelocytic Leukemia by Use of an Inhibitor of Histone Deacetylase. *J Natl Cancer Inst* 1998; (90): 1621-1625.
- Wartmann M, Davis R J. The native structure of the activated Raf protein kinase is a membrane-bound multi-subunit complex. *J Biol Chem* 1994; (269): 6695-6701.

- Wasik M A, Nowak I, Zhang Q, Shaw L M. Suppression of proliferation and phosphorylation of Jak3 and STAT5 in malignant T-cell lymphoma cells by derivatives of octylamino-undecyl-dimethylxanthine. *Leuk Lymphoma* 1998; (28): 551-560.
- Weiner J A, Chun J. Schwann cell survival mediated by the signaling phospholipid lysophosphatidic acid. *Proc Natl Acad Sci U S A* 1999; (96): 5233-5238.
- West J, Tompkins C K, Balantac N, Nudelman E, Meengs B, White T, Bursten S, Coleman J, Kumar A, Singer J W, Leung D W. Cloning and expression of two human lysophosphatidic acid acyltransferase cDNAs that enhance cytokine-induced signaling responses in cells. *DNA Cell Biol* 1997; (16): 691-701.
- Wolf B B, Green D R. Suicidal tendencies: apoptotic cell death by caspase family proteinases. *J Biol Chem* 1999; (274): 20049-20052.
- Xu Q, Simpson S E, Scialla T J, Bagg A, Carroll M. Survival of acute myeloid leukemia cells requires PI3 kinase activation. *Blood* 2003; (102): 972-980.
- Xu Y, Fang X J, Casey G, Mills G B. Lysophospholipids activate ovarian and breast cancer cells. *Biochem J* 1995; (309 (Pt 3)): 933-940.
- Yoshida K, Nishida W, Hayashi K, Ohkawa Y, Ogawa A, Aoki J, Arai H, Sobue K. Vascular remodeling induced by naturally occurring unsaturated lysophosphatidic acid in vivo. *Circulation* 2003; (108): 1746-1752.
- Zhang C, Baker D L, Yasuda S, Makarova N, Balazs L, Johnson L R, Marathe G K, McIntyre T M, Xu Y, Prestwich G D, Byun H S, Bittman R, Tigyi G. Lysophosphatidic acid induces neointima formation through PPARgamma activation. *J Exp Med* 2004; (199): 763-774.
- Zheng Y, Kong Y, Goetzl E J. Lysophosphatidic acid receptor-selective effects on Jurkat T cell migration through a Matrigel model basement membrane. *J Immunol* 2001; (166): 2317-2322.
- Zhu J, Koken M H, Quignon F, Chelbi-Alix M K, Degos L, Wang Z Y, Chen Z, de Thé H. Arsenic-induced PML targeting onto nuclear bodies: Implications for the treatment of acute promyelocytic leukemia. *PNAS* 1997; (94): 3978-3983.
- Zhu Y M, Haynes A P, Keith F J, Russell N H. Abnormalities of retinoblastoma gene expression in hematological malignancies. *Leuk Lymphoma* 1995; (18): 61-67.